UNIVERSITY OF BIRMINGHAM

NEUTROPHIL FUNCTION IN CHRONIC INFLAMMATORY DISEASE STATES

by

Helen Michelle Roberts

A thesis submitted to
The University of Birmingham
for the degree of
DOCTOR OF PHILOSOPHY

School of Dentistry
Institute of Clinical Sciences
College of Medical & Dental Sciences
The University of Birmingham
August 2016

UNIVERSITY OF
BIRMINGHAM

University of Birmingham Research Archive

e-theses repository

This unpublished thesis/dissertation is copyright of the author and/or third parties. The intellectual property rights of the author or third parties in respect of this work are as defined by The Copyright Designs and Patents Act 1988 or as modified by any successor legislation.

Any use made of information contained in this thesis/dissertation must be in accordance with that legislation and must be properly acknowledged. Further distribution or reproduction in any format is prohibited without the permission of the copyright holder.

i Abstract

Inflammation is a central component of the immune response. In its acute form it aids the transition from disease to health via the activation of numerous immune cells, enabling them to reach the site of infection/injury and orchestrate themselves to combat pathogens, facilitating resolution and repair to restore the host to health. However, chronic inflammation is deleterious to the host and differs from the "classical" acute inflammatory process in that the inflammation is not necessarily so readily obvious and is not self-limiting; rather, the immune system is in a constant state of low-grade activation and when challenged by pathogenic or sterile injury the response is heightened, resulting in prolonged tissue damage and a failure of efficient resolution mechanisms.

Neutrophils are important mediators of acquired innate immune responses but may also contribute to the pathogenesis of chronic inflammatory diseases. Neutrophils are heavily involved in antimicrobial defence; their primary role is the localisation and elimination of pathogenic microorganisms. This, combined with their relatively short lifespan, has resulted in a traditional view of them as limited "kamikaze" cells. However, as detailed here, neutrophils have been shown to act with complexity and sophistication, orchestrating the immune/inflammatory response but also inadvertently contributing to tissue damage in different disease states. This thesis includes the study of neutrophil function in acute inflammatory episodes such as gingivitis and more chronic long-term health conditions such as obesity,chronic periodontitis and Papillon-Lefèvre Syndrome. The findings outlined here support the role of neutrophils as important contributors to both acute and chronic disease, showing these cells to be far more sophisticated than previously regarded.

ii Acknowledgements

I thank my wonderful supervisors Dr Melissa Grant and Professor Iain Chapple for their exceptional support and for the opportunities they have given me throughout my PhD. Their encouragement and guidance has given me confidence in my research ability and a true understanding of the nature of determination, particularly with regard to organising clinical trials. I would also like to thank the MRC for funding this work. Thanks to the lab personnel; in particular Dr Naomi Hubber, and Dr Helen Wright who was always on hand with an inappropriate story and a generous supply of gingerbread men on difficult days. Thanks to the porters (in particular Neil) who kept the building open for me, enabling me to process my clinical samples without time constraints. Thanks to all my PhD colleagues who were with me at the beginning, in particular Dr Eisha Comar, Dr Jonathan Robinson, Dr Sonam Kalra, Dr Owen Davies, Rachel Flight, Ilaria Chicca, Cleo White, Nina Vyas, Isabel Lopez-Olivia and Dr Michael Sandholzer (whose endless supply of chocolate and good humour will not be forgotten!) and to those I met later on: Sean Lewin, Hannah Serrage, and Nurul Iman, whom I have been lucky to get to know. A very special mention goes to Dr Phillipa White, who was with me from the very beginning and has become a lifelong friend; she managed to make the PhD both an interesting and socially rewarding experience. I thank my friends who inspired me in ways they may not realise: Dr Elizabeth Marsh, Dr Rebecca Taylor, Faye Lanni, Emily Blackwell, Alexandra Watson and Sarah Facey. Thank you Will Bosworth for always managing to make a bad day good. Thank you John Hunter for helping me see it though til the end.

Lastly, I thank my family: my parents for their unending support, and my siblings Hayley and Kayne who were always patient and full of advice, both academic and personal. I couldn't have done it without you.

CONTENTS

LIST OF TABLES

LIST OF FIGURES

CHAPTER 2 - MATERIALS AND METHODS

CHAPTER 3 RESULTS - OPTIMISATION OF CHEMOTAXIS

CHAPTER 4 RESULTS - NEUTROPHIL FUNCTION IN ACUTE AND CHRONIC INFLAMMATORY ORAL STATES

Abbreviations

AFU	Arbitrary fluorescence units
AMP	Antimicrobial peptide
AMRVL	Adjusted mean resultant vector length
ANOVA	Analysis of variance
ATCC	American type culture collection
ATP	Adenosine triphosphate
BCA	Bicinchoninic acid
BHI	Brain heart infusion
BMI	Body mass index
BOP	Bleeding on probing
BSA	Bovine serum albumin
C	Complement
CAL	Clinical attachment loss
Ca^{2+}	Calcium ions
CAM	Cell adhesion molecule
CG	Cathepsin G
CGD	Chronic granulomatous disease
CI	Chemotactic index
COPD	Chronic obstructive pulmonary disease
CV	Coefficient of variation
CXCL8	Interleukin-8
DAG	Diacylglycerol
DAMP	Damage-associated molecular pattern
DCs	Dendritic cells
DMSO	Dimethyl sulfoxide
DNA	Deoxyribonucleic acid
DNase	Deoxyribonuclease
DPI	Diphenylene iodonium
EDTA	Ethylenediaminetracetic acid
ELISA	Enzyme linked immunosorbent assay
FCγR	Fc-gamma receptor
Fiji	Fiji is just image J
FMI	Forward migration index
fMLP	N-Formylmethionyl-leucyl-phenylalanine
GCF	Gingival crevicular fluid
GI	Gingival index
GM-CSF	Granulocyte-macrophage colony-stimulating factors
GPCR	G-protein-coupled receptor
GSH	Reduced glutathione
GSSG	Oxidised glutathione
GTP	Guanosine triphosphate
H_2O_2	Hydrogen peroxide

HbA1c	Glycated haemoglobin
HDL	High-density lipoproteins
HEPES	4-(2-hydroxyethyl)-1-piperazineethanesulfonic acid
HOCl	Hypochlorous acid
HRP	Horseradish peroxidase
HSP	Heat shock protein
ICAM	Intercellular adhesion molecule
IFNα	Interferon alpha
IgG	Immunoglobulin G
IL-	Interleukin-
IR	Insulin resistance
K^+	Potassium ions
L	Litre
LAP	Localised aggressive periodontitis
LDL	Low-density lipoproteins
LFA-1	Leukocyte function-associated antigen-1
LL-37	Cathelicidin
LLD	Lipid-lowering drugs
LPS	Lipopolysaccharide
LTB_4	Leukotriene B4
M	Molar
Mac-1	Macrophage-1
min	Minutes
MIP1α	Macrophage inflammatory protein-1 alpha
mm	Millimetre
MMP	Matrix metalloproteinase
MNase	Micrococcal nuclease
MOI	Multiplicity of infection
MPO	Myeloperoxidase
MRV	Mean resultant vector
MRVL	Mean resultant vector length
NAC	N-acetyl-cysteine
NADPH	Nicotinamide adenine dinucleotide phosphate
NE	Neutrophil elastase
NETs	Neutrophil extracellular traps
NF-κB	Nuclear factor kappa B
nm	Nanometres
$NO^{\cdot}$	Nitric oxide
NSP	Neutrophil serine protease
$O_2^{\cdot}$	Superoxide
$OCl^{\cdot}$	Hypochlorite ions
$OH^{\cdot}$	Hydroxyl ion
OSA	Obstructive sleep apnoea
PAD	Peptidyl arginine deiminase

PAF	Platelet activating factor
PAMP	Pathogen-associated molecular patterns
PBN	Peripheral blood neutrophil
PBS	Phosphate buffered saline
PKC	Protein kinase C
PI	Plaque Index
PLS	Papillon Lefèvre syndrome
PMA	Phorbol 12-myristate 13-acetate
PMNL	Polymorphonuclear leukocytes
PPD	Probing pocket depth
PR3	Proteinase 3
PRR	Pattern recognition receptor
rcf	Relative centrifugal force
RLU	Relative light units
ROS	Reactive oxygen species
SD	Standard deviation
SEM	Scanning electron microscopy
S.E.M.	Standard error of the mean
SLE	Systemic lupus erythematosus
SOD	Superoxide dismutase
T1/2/3	Time point 1/2/3
TEM	Transendothelial migration
TG	triglyceride
TLR	Toll like receptor
TNF	Tumour necrosis factor
TSA	Tryptone soya agar
TSB	Tryptone soya broth
U	Units
VLCD	Very low calorie diet

CHAPTER 1 - INTRODUCTION

1.1. The neutrophil

1.1.1. Origin and role in the body

The human innate immune system is comprised of various cells, their secreted proteins/peptides and the complement system, providing an effective defence against pathogenic organisms. Neutrophils, along with basophils and eosinophils, are members of the granulocyte family of white blood cells, also known as leukocytes (Ehrlich 1880). These terminally differentiated phagocytic cells amount to 50-60% of all circulating leukocytes; they are short-lived cells with a circulatory lifespan of up to 5.4 days (Pillay *et al.* 2010). In the absence of infection/inflammation, neutrophils in circulation die by a spontaneous apoptosis program (Geering & Simon 2011) and apoptotic bodies are cleared by macrophages (Bratton & Henson 2011). Neutrophils are approximately 12-14μm in diameter and feature a characteristic multi-lobed nucleus which facilitates the elastic nature of the cell, allowing it to rapidly leave the blood circulation when required (Dong *et al.* 1991). Under normal physiological conditions neutrophils are generated in the bone marrow at a rate of 10^{11} cells a day, however this number can increase tenfold upon exposure to injurious agents (Cannistra & Griffin 1988). Mature neutrophils differentiate from haematopoietic stem cells in the bone marrow by a process known as granulocytopoiesis (Borregaard 2010) and the release of neutrophils from the bone marrow is tightly regulated; the small percentage that is constitutively present are confined to the vascular capillaries in the absence of infection/injury. Stimulation of granulopoiesis is a multi-step process culminating in the release of neutrophils into the circulation from the bone marrow and is initiated by the production of the cytokines granulocyte-colony stimulating factor (G-CSF) and granulocyte macrophage-colony stimulating factor (GM-CSF) by immune cells, such as tissue macrophages and mast cells, which become activated upon exposure to an infectious challenge such as pathogenic agents or apoptotic host cell material (Stark *et al.* 2005).

Exposure to G-CSF/GM-CSF alters the expression of particular neutrophil cell-surface receptors, dictating their confinement or release into the circulation; expression of the chemokine receptor CXCR4 ensures neutrophils remain within the bone marrow (Eash *et al.* 2009) whereas CXCR2 allows the cells to be released into the circulation, migrating to a potential site of injury/inflammation (Theilgaard-Mönch *et al.* 2005) in a process known as transendothelial migration (TEM).

1.2. Transendothelial migration (TEM)

Leukocytes can migrate from the circulation to elicit immune responses via two major routes: migration into lymph nodes via venules to the lymphatic system and direct movement into inflamed sites/tissues. TEM, also known as diapedesis, describes the multistep process by which immune cells, including neutrophils, exit the circulatory system to reach the site of inflammation (Figure 1.1). This cascade of events is initiated by resident immune cells such as macrophages or dendritic cells (DCs) at the site of injury/infection, which detect foreign particles such as bacteria, fungi and viruses (and their products) or signals emanating from damaged tissues. Exposure to any of these agents results in the secretion of inflammatory mediators, such as histamine, cytokines and leukotrienes, which in turn activate endothelial cells that line blood vessels (Sadik *et al.* 2011). The activated endothelial cells subsequently release agents known as chemoattractants to attract circulating neutrophils, that under normal physiological conditions flow in the centre of the blood stream in a quiescent state, toward the vessel wall. Changes in the expression of surface molecules such as the intercellular adhesion molecule (ICAM-1/2) and junctional adhesion molecules (JAM-A/B/C) on the activated endothelial cell surface attract and capture neutrophils. This facilitates their exit from the circulation by ligating complementary receptors such as the integrins leukocyte function-associated antigen-1 (LFA-1) and macrophage-1 antigen (Mac-1) on the neutrophil

surface, enabling them to adhere and cross the endothelium and enter inflamed/infected tissues (Huber *et al.* 1991; Borregaard 2010). The passage of neutrophils across vascular walls occurs only at postcapillary venules, where the vessel wall is thin. Neutrophils can cross endothelial cells in two ways: transcellularly, where the cells pass through the endothelial cells themselves (Feng *et al.* 1998), or paracellularly, where cells travel between endothelial cells (Marchesi & Florey 1960). Both types of migration rely on homophilic interactions between adhesion molecules on neutrophil and endothelial cell surfaces and the release of soluble mediators. For example, the release of leukotriene A4 by neutrophils induces changes in the actin cytoskeleton of endothelial cells resulting in cell contraction and loss of barrier integrity (Colgan *et al.* 1993).

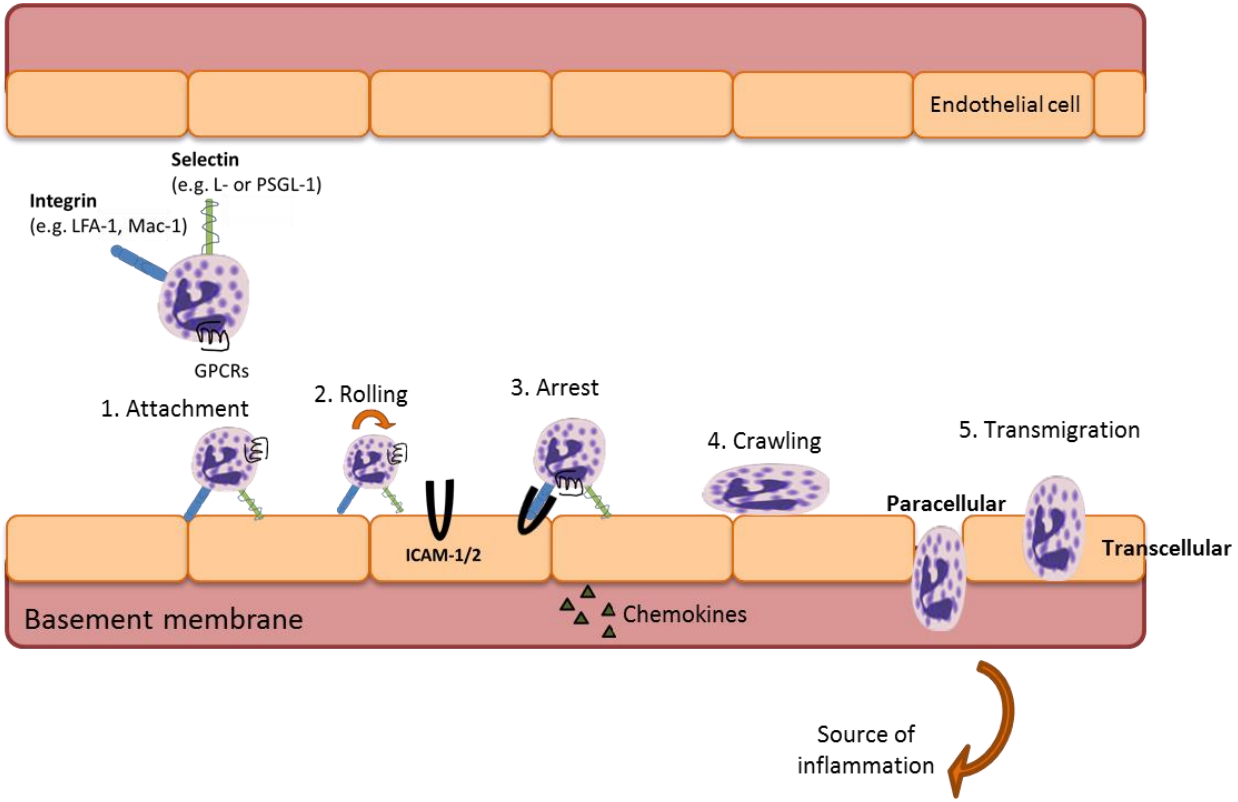

Figure 1.1 Transendothelial migration (TEM) of neutrophils mechanism of action

1. **Neutrophil attachment**: occurs via interaction of P- and L-selectins (Buscher *et al.* 2010) with endothelial ligands expressed as a result of activation by stimuli (e.g. pro-inflammatory cytokines) released from nearby inflamed tissues. **2. Rolling**: low affinity binding of selectins and their receptors results in cell rolling, allowing for sampling of the microenvironment (Steegmaier *et al.* 1997). **3. Arrest**: At the appropriate inflammatory cue, e.g. chemotattractant detection, integrins on the neutrophil surface attach to ICAM-1 and ICAM-2 on the endothelial cell causing arrest. **4. Crawling**: Neutrophil topology studies reveal extensive protrusions and processes on the cells' surface with embedded integrins which bind to the endothelial cell wall, allowing the "flatter" part of the cell to bind and adhere to facilitate transmigration by deciphering an appropriate luminal exit point. **5. Transmigration:** Exit from vessel occurs para- or transcellularly and neutrophils are guided to inflamed tissues via chemoattractants in a gradient-driven manner.

Post TEM neutrophils are functionally distinct from those in circulation, giving evidence for the existence of different subsets based on expression of specific molecular markers such as Olfactomedin 4 (OLFM4) (Liu *et al.* 2012) and CD177 (Hu *et al.* 2009). Neutrophils that leave the circulation are in an activated state, enabling them to react quickly and effectively upon exposure to pathogenic stimuli. Neutrophils have also been shown to revert back into the vascular lumen in a process known as reverse transendothelial endothelial migration (rTEM) (Mathias *et al.* 2006). Neutrophils that have undergone rTEM show high expression of ICAM-1 and low expression of the CXCR1 chemokine receptor (Buckley *et al.* 2006). rTEM is facilitated through interactions between neutrophils and endothelial cells via JAM-C (Woodfin *et al.* 2011). The identified subpopulations have not been shown to display any differences in terms of proneness to undergo apoptosis or ability to phagocytose bacteria, nor in their propensity to transmigrate into tissues in response to inflammatory stimuli (Welin *et al.* 2013). A functional difference between the subsets remains to be found.

1.3. Neutrophil surface receptors

1.3.1. Receptors involved in TEM

The two major groups of neutrophil receptors involved in TEM are selectins and integrins:

a) Selectins are single-chain glycoproteins that recognise carbohydrate moieties and mediate transient interactions between leukocytes and the vessel wall (Sperandio *et al.* 2009). P-selectin is expressed on platelets and endothelial cells, E-selectin is expressed on endothelial cells during inflammatory responses and L-selectin is expressed on leukocytes. Selectins interact with a large number of carbohydrate-containing cell surface molecules including P-selectin glycoprotein protein ligand 1 (PSGL-1) on leukocytes which act as the counter-receptor of P- and E-selectins on endothelial cells (Carlow *et al.* 2009). Selectins and their ligands are required for the rolling phase of TEM (Figure 1.1).

b) Integrins are heterodimeric transmembrane glycoproteins present on virtually all mammalian cells. For neutrophils the most important integrins belong to the β_2 integrin family which are characterised by the β_2 integrin chain and a unique α-chain, such as LFA-1 and Mac-1, which both bind to endothelial ICAM-1 and are involved in different phases of TEM (Schymeinsky *et al.* 2007).

1.3.2. Receptors involved in neutrophil pathogen detection and killing

The three receptor types involved in neutrophil activation to enable pathogen detection and killing include pattern recognition receptors (PRRs), opsonic receptors and G-protein coupled-receptors (GPCRs). These are described below (see also Figures 1.2, 1.3 and 1.4).

a) PRRs recognise pathogen/damage associated molecular patterns (PAMPs/DAMPs) including microbe-specific molecules, such as bacterial DNA and bacterial cell wall components, and host-derived proteins/peptides, such as necrotic cell matter. DAMPs occur during sterile inflammatory episodes such as in burns or hypoxia. Major PRRs that result in ligand (pathogenic or host) internalisation are C-type lectin receptors, such as Dectin-1, which recognises the fungal cell wall component β-glucan, and upon association with the integrin Mac-1, internalises and subsequently eliminates fungal pathogens (Kennedy *et al.* 2007; X. Li *et al.* 2011). Major non-phagocytic PRRs are known as Toll-like receptors (TLRs) which recognise both host-derived and pathogenic molecules including lipids, carbohydrates peptides, DNA and RNA (Trinchieri & Sher 2007). In particular, TLR2 and TLR4 can be stimulated by bacteria and their products, including the bacterial pathogen *Fusobacterium nucleatum* (Wakelin *et al.* 2006; Kikkert *et al.* 2007). Engagement by TLRs activates neutrophils, enabling increased cytokine release and a reduction in the rate of apoptosis (Parker *et al.* 2005). Other PRRs include the cytoplasmic nucleotide-binding oligomerisation domain (NOD-like) receptors, of which NOD2 is expressed in neutrophils and can detect

peptidoglycan-related molecules of bacteria present within the cell cytoplasm, also resulting in cytokine release (Ekman & Cardell 2010).

b) Opsonic receptors are critical for neutrophil-mediated pathogen killing. Engagement of the host-derived complement product C3b or IgG coated pathogenic material with its cognate high affinity Fc Receptors (FcRs), FCγRIIA/FCγRIIIB and FCγRI respectively, facilitates rapid uptake and strong stimulation of neutrophil killing mechanisms (Bruhns 2012).

c) GPCRs have diverse downstream signalling outcomes and ligands that can bind them including bacterial products (such as formyl peptides) and endogenous molecules such as the chemokine interleukin-8 (IL-8/CXCL8) and leukotrienes that results in neutrophil chemotaxis. Other GPCR signalling results in neutrophil activation which endows the cell with the ability to kill invading microbes.

1.3.3. Receptor-independent neutrophil activation

The NADPH oxidase complex can be activated by a number of non-physiological agents including the calcium ionophore ionomycin and the diester phorbol 12-myristate 13-acetate (PMA) (Lundqvist *et al.* 1996; Dahlgren & Karlsson 1999). During PMA stimulation, an assembly of the oxidase occurs not only in the plasma membrane but also in the specific granule membrane, giving rise to intracellular oxygen metabolites. Thus reactive oxygen species (ROS) production occurs both extracellularly and intracellularly (Karlsson *et al.* 2000).

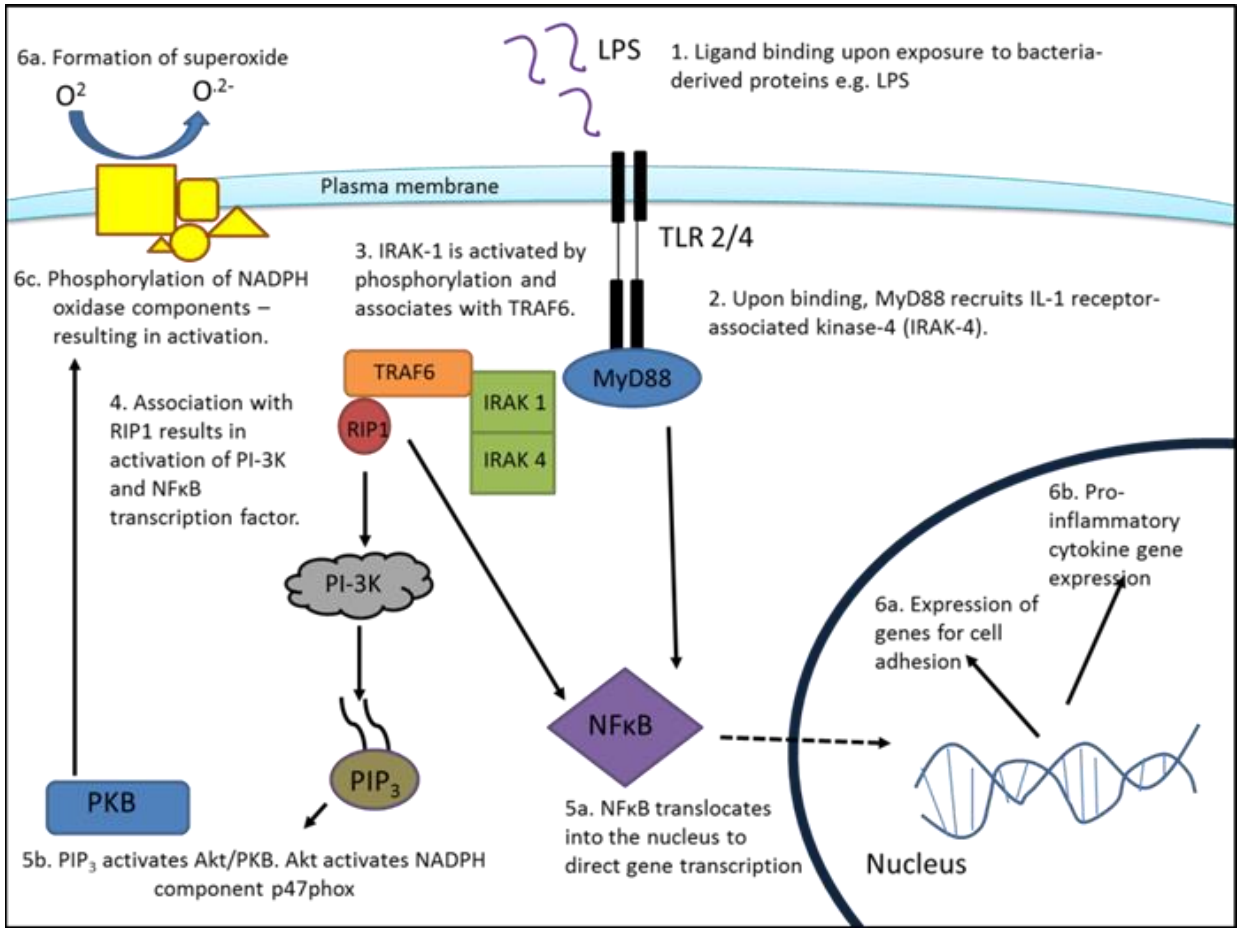

Figure 1.2 Toll-like receptor (TLR) activation pathway.

TLR receptor-ligand pathway results in the activation of the NADPH oxidase complex and subsequent ROS production. Images constructed using several sources (Karlsson *et al.* 2000; Cicchetti *et al.* 2002; Laroux *et al.* 2005; Ichikawa *et al*. 2012; Futosi *et al.* 2013).

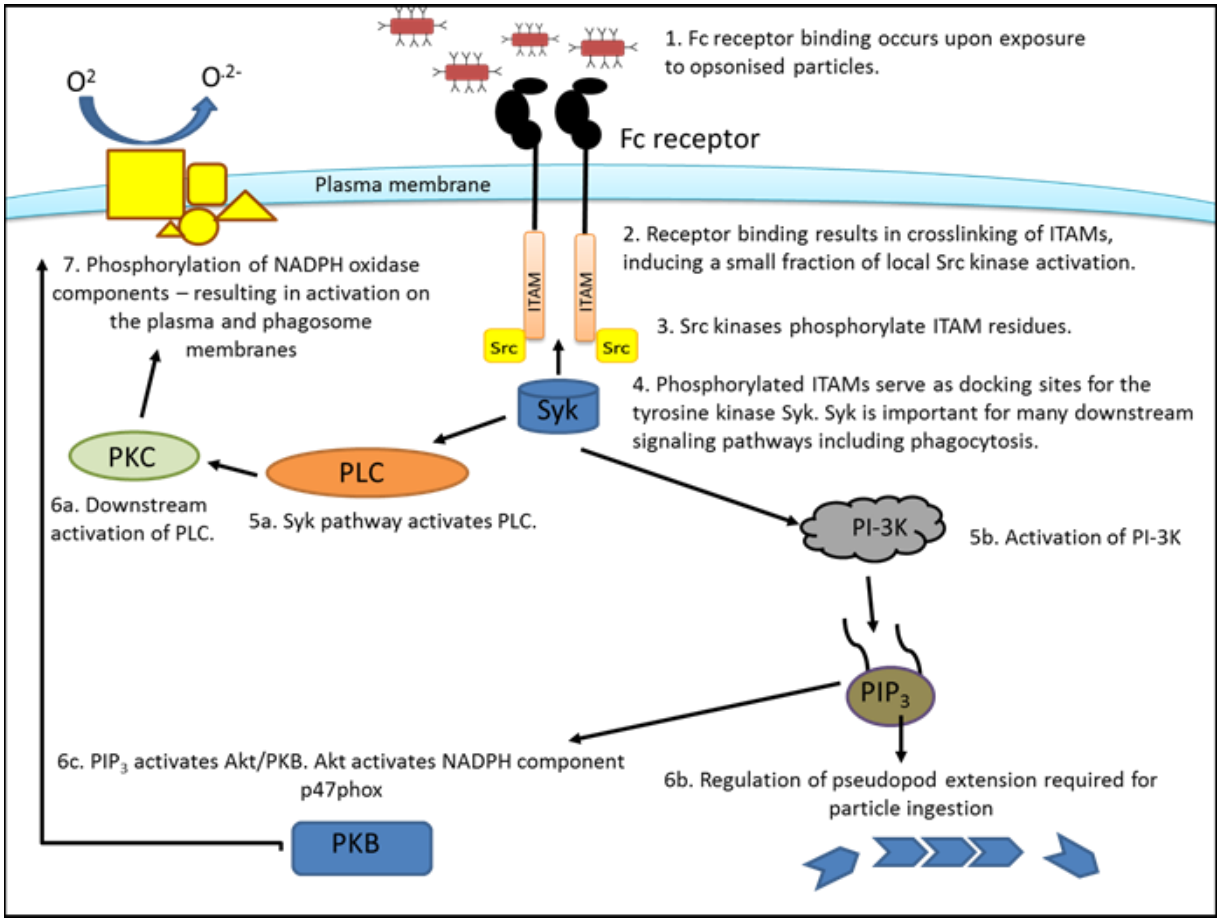

Figure 1.3 Fc-gamma activation pathway

Fc-gamma ligand-receptor pathway can result in neutrophil activation characterised by the activation of the NADPH oxidase complex and subsequent ROS production. Images constructed using several sources (Karlsson *et al.* 2000; Cicchetti *et al.* 2002; Laroux *et al.* 2005; Ichikawa *et al.* 2012; Futosi *et al.* 2013).

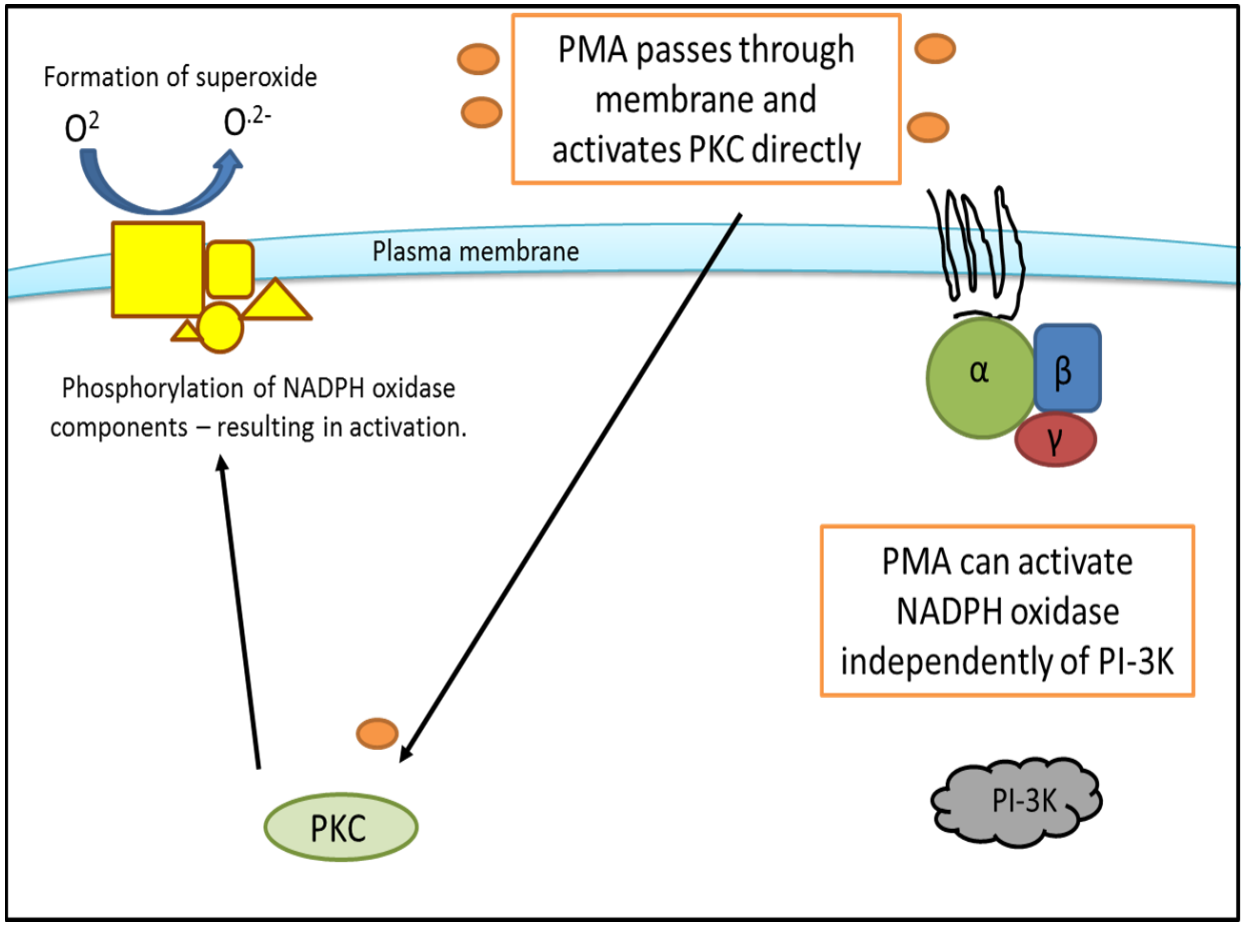

Figure 1.4 Non-receptor activation pathway

Non-receptor routes can result in neutrophil activation characterised by the activation of the NADPH oxidase complex and subsequent ROS production. Images constructed using several sources (Karlsson *et al.* 2000; Cicchetti *et al.* 2002; Laroux *et al.* 2005; Ichikawa *et al.* 2012 Futosi *et al.* 2013;).

1.4. Neutrophil chemotaxis

Chemotaxis is the process by which cell motility is biased along a concentration gradient of soluble factors/extracellular signals known as chemoattractants (Insall 2010). Molecular gradients are required to activate intracellular signalling events and establish directional cues for migrating cells and chemotaxis exists in a large and diverse number of organisms from amoebae to eukaryotes (Van Haastert & Devreotes 2004). For neutrophils, chemotaxis allows the cell to migrate to infection sites along a chemoattractive gradient in order to kill invading microorganisms. This process involves a number of interacting processes resulting in coordinated cell movement including recognition of the chemoattractant, internal signalling to activate the cells' motility centre and gradient detection to influence movement in a persistent direction (Levine & Rappel 2013). Neutrophil movement is achieved by producing actin-rich pseudopods at the leading edge of the cell whilst retracting in other regions (Friedl *et al.* 2001); the orientation of these protrusions towards a chemoattractant determines the direction of migration. In the absence of chemoattractive factors these protrusions occur randomly at all edges of the cell. When a chemoattractant is detected however, the protrusions are directed towards the source of the chemoattractant thereby determining the direction of migration (Andrew & Insall 2007).

1.4.1. Chemoattractants

Neutrophil chemoattractants encompass numerous host and foreign molecules as listed in Table 1.1 that include leukotriene B4 (LTB_4), complement proteins (C5a), cytokine-derived chemoattractants (known as chemokines), formylated peptides from bacteria and lipopolysaccharide (LPS), an integral component of the outer membrane of Gram negative bacteria (Erridge *et al.* 2002). Chemoattractants have different potencies, forming a chemical

hierarchy that serves to recruit neutrophils to the inflammation site. Those that elicit the strongest migration are molecules that emerge from the inflammation/infection source, such as bacterial *N*-formly-methionyl-leucyl-phenyalanine (fMLP), one of the strongest chemoattractants to induce neutrophil chemotaxis (Showell 1976). Intermediary chemoattractants include CXCL8 and LTB_4, which are expressed by epithelial and endothelial cells during neutrophil recruitment from the circulation (Phillipson & Kubes 2011).

Table 1.1 Major neutrophil chemoattractants and their receptors

Adapted from Sadik *et al.* (2011). BLT1 = leukotriene B4 receptor-1, ENA-78 = epithelial neutrophil-activating protein 78, FPR = formylated peptide receptor, GCP = granulocyte chemotactic protein 2, GRO = growth-regulated oncogene, HCC = human CC chemokine, LTB_4 = leukotriene B_4, MCP = monocyte chemotactic protein, MIF = macrophage inhibitory factor, MIP = macrophage inhibitory protein, NAP-2 = neutrophil-activating peptide-2, PAF = platelet activating factor , PGP = proline-glycine-proline, SDF-1α = stromal cell-derived factor 1 alpha.

Chemokines	
Receptor	Ligand
CCR1	MIP-1α, RANTES, MIP-3, MCP-3, HCC-2
CXCR1/2	GROα, GROβ, GROγ, ENA-78, GCP-2, NAP-2, CXCL8
CXCR4	SDF-1α
Peptides/cytokines	
C5aR	C5a
C3aR	C3a
FPR1	Formylated peptides (e.g. fMLF)
CXCR2	PGP
FPR2	LL-37
PAFR	PAF
Other	
CXCR2	MIF, Eicosanoids
BLT1	LTB_4

The host-derived chemokines specifically attract and recruit populations of immune effector cells to sites of injury/infection and thereby shape the development and progression of the inflammatory response (Borish & Steinke 2003). Chemokines are divided into four structurally similar sub-families (CXC, CX3C, CC and C), split according to the spacing of their first two cysteine residues near their amino terminus (Bonecchi *et al.* 2009). Over 44 chemokines have been described in humans, several of which can bind to the 21 described human chemokine receptors (Esche *et al.* 2005). Individual neutrophil chemokine receptors are GPCRs specific for chemokines, and typically from a single chemokine subfamily (Nibbs & Graham 2013). CXC chemokines can be subdivided into two subfamilies; those containing the glutamic acid-leucine-arginine (ELR) sequence and those that do not (Zlotnik & Yoshie 2000). CXC-ELR$^+$ chemokines are the main activators of neutrophil recruitment to sites of inflammation and include CXCL8 and macrophage inhibitory protein alpha (MIP1α) (Rollins 1997). Chemokines selectively recruit discrete cell populations into sites of injury and thereby effectively regulate leukocyte trafficking (Scapini *et al.* 2000). During infection/inflammation, chemokines secreted by activated endothelial cells can induce rapid blood neutrophilia, stimulating neutrophil adhesion and transmigration across the endothelium and direct the migration of neutrophils within the tissue to the site of inflammation (Furze & Rankin 2008; Williams *et al.* 2011). Neutrophils are also a source of chemokines that are chemotactic for a range of other immune cells including neutrophils themselves, monocytes, DCs and natural killer cells (Sadik *et al.* 2011).

1.4.2. Chemotactic signaling pathways

The intracellular events that result in chemotaxis are not fully understood. Chemokines, chemotactic complement products, lipid mediators (such as leukotrienes) and the bacterial formyl peptides can all be sensed by members of the GPCR family that transduce signals via

cytoplasmic G proteins to cytoskeletal proteins which govern the directed movement of neutrophils (Di Gennaro & Haeggström 2012; Sun & Ye 2012; Klos *et al.* 2013). Figure 1.5a-d describes the process of neutrophil recruitment to inflamed periodontal tissues. During infection bacteria and their products, such as fMLP, penetrate the tissues surrounding the tooth and are detected by resident macrophages and epithelial cells that, in turn secrete CXCL8. Both CXCL8 and fMLP attract circulating neutrophils into the affected tissues and signalling pathways are activated following MIP1α, CXCL8 and fMLP exposure. Figure 1.5e describes GPCR resulting in the activation of several of downstream signalling pathways; PLC, PI3K, p38 and RHO G proteins (Camps *et al.* 1992; Stoyanov *et al.* 1995; Brahmbhatt & Klemke 2003; Kim & Haynes 2013) that initiate directional chemotactic neutrophil migration (Gambardella & Vermeren 2013). Activation of GPCRs results in internalisation and conformational changes to facilitate downstream signalling before being recycled and returned to the cell surface or degraded (Forsman *et al.* 2013). The GPCR subunits, G_a and $G_{\beta\gamma,}$ dissociate following internalisation (Gierschik *et al.* 1989) leading to the consequential activation of PI-3K, PLC and activation of small G proteins of the RHO family (RHO, RAC and CDC42) to initiate actin polymerisation and direct chemotactic neutrophil migration (Camps *et al.* 1992; Worthen *et al.* 1994; Stoyanov *et al.* 1995; Verploegen *et al.* 2002; Gambardella & Vermeren 2013). PI-3K phosphorylation catalyses the formation of phosphatidylinositol 3,4,5-triphosphate (PIP_3) from phosphatidylinositol 4,5-biphosphate (PIP_2). PIP_3 acts as a second messenger controlling cell adhesion and cytoskeletal reorganisation (Toker & Cantley 1997). In a cell responding to a chemoattractant, PIP_3 is found at the leading edge of the cell (Bagorda & Parent 2008). At the lagging end of the cell, retraction of the cell membrane is mediated by the phosphatase and tensin homolog (PTEN). Downstream of receptor signaling the MAPK and nuclear factor (NF)-κB signalling pathways are also activated. Cellular changes that result from chemoattractant binding

include polymerisation of F-actin, the formation of new pseudopods at the leading edge, and retraction at the posterior edge of the cell. Calcium ions are also released from the endoplasmic reticulum via the ryanodine receptor to elicit cell signalling (Kurihara *et al.* 1993; Berridge *et al.* 2003; Clapham 2007). Other additional processes are activated as a consequence of GPCR-agonist binding, including activation of the respiratory burst, degranulation and upregulation of surface molecules (Sandborg & Smolen 1988; Horuk 1996).

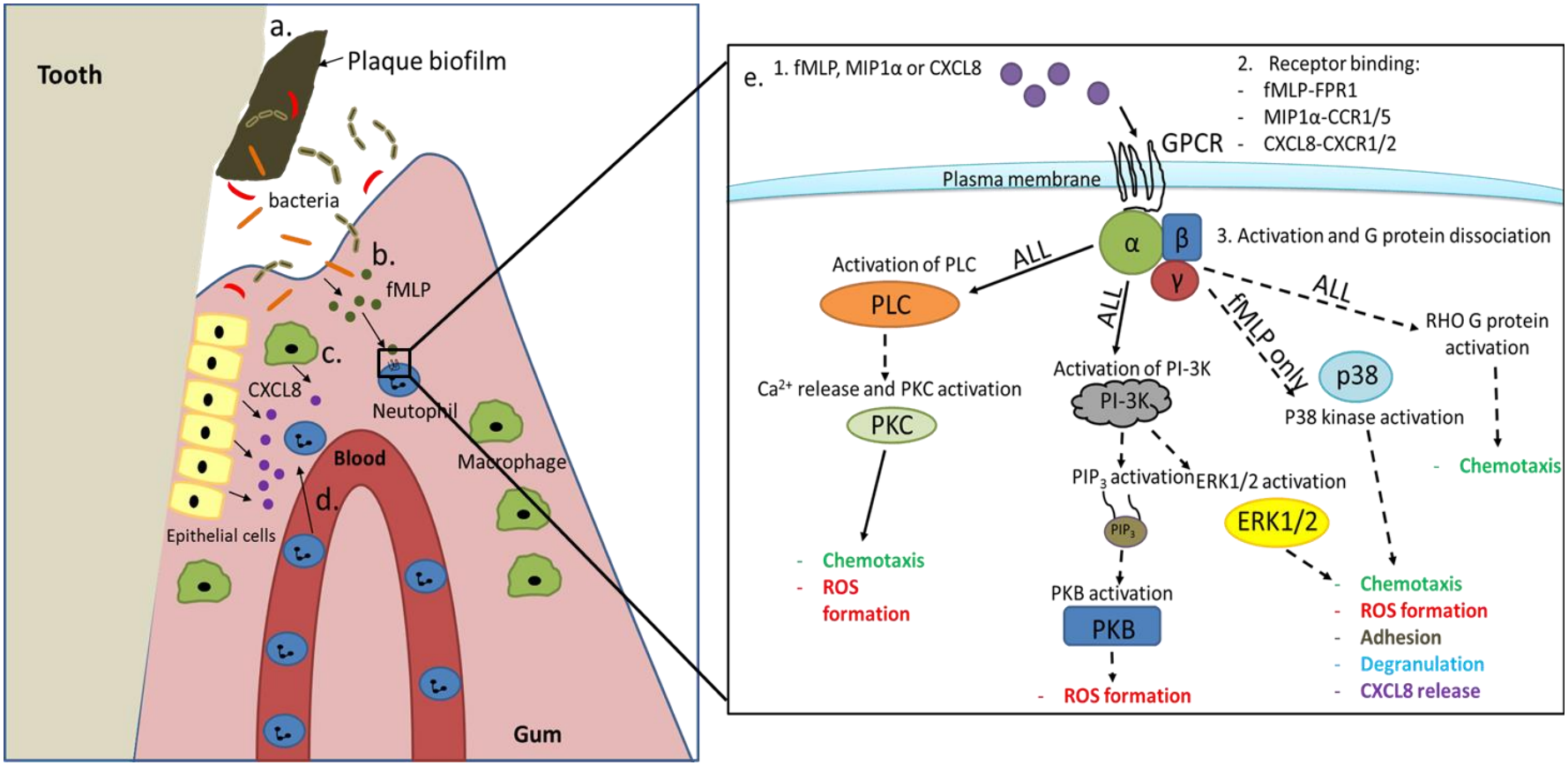

Figure 1.5 Neutrophil recruitment to inflamed periodontal tissues

Plaque biofilm is formed of diverse bacterial species (a). During infection bacterial degradation products (fMLP) are released (b). Following bacterial exposure resident macrophages and epithelial cells secrete CXCL8 (c). CXCL8 and fMLP attract circulating neutrophils into the affected tissues (d). GPCR binding results in the activation of downstream signalling pathways resulting in directional chemotactic neutrophil migration (e). Image devised from several sources (Nick *et al.* 1997; Herlaar & Brown 1999; Cicchetti *et al.* 2002;O ttonello *et al.* 2005; Futosi *et al.* 2013).

Though some chemoattractants share the same receptors and other chemoattractants share the same signalling cascade, the resulting chemotaxis isn't necessarily the same, for example, LTB_4 is a significantly weaker inducer of chemotaxis compared to CXCL8. Furthermore, neutrophils have been shown to prioritise when they encounter multiple signals in favour dominant chemoattractants over secondary ones, which aids cell mobilisation in the correct orientation (Kim & Haynes 2012).

The two signaling pathways involved in neutrophil chemotaxis are detailed in Figure 1.5e: the PI3-K/PTEN pathway that is activated following exposure to weaker chemoattractants such as CXCL8 and LTB_4 and the p38 mitogen-activated pathway, which is activated after exposure to stronger chemoattractants such as C5a and fMLP (Foxman *et al.* 1997; Foxman *et al.* 1999). Activation of the respective signaling pathways is dependent on the chemoattractant present; inhibition studies of the p38 pathway have been shown to prevent the migration of neutrophils towards fMLP and C5a, but not towards CXCL8 or LTB_4 (Khan *et al.* 2005).

The p38 pathway dominates the PTEN pathway and becomes activated, even in the presence of weaker chemoattractants, after exposure to stronger chemoattractants which are located at the infection/inflammation source (Heit *et al.* 2002). The switch to prioritise the cell towards more potent chemoattractants appears to require PTEN, as *Pten-/-* neutrophils exposed to opposing gradients are unable to preferentially migrate towards the stronger chemoattractants (Heit *et al.* 2008).

1.4.3. Measuring neutrophil chemotaxis

Chemotaxis has been a focus of research for more than a century due to its involvement in several important physiological and pathological processes including TEM (section 1.2), tumour metastasis and angiogenesis. The study of chemotaxis allows the behaviour of cells to

be observed *in vitro* when subjected to a linear gradient of chemoattractant most often via microscopy.

Most chemotaxis assays employ a two-well design whereby cells are seeded between the wells, one containing a control or buffer substance and the other with a chemoattractant, and cells are able to migrate between them. The first system to measure chemotaxis *in vitro* was the Boyden chamber (Boyden 1962) and derived assays that work with either thick filters or thin porous membranes which the cells are placed on. In response to a concentration gradient of chemotactic agent, the cells migrate through the membrane and are counted, but the information obtained is limited and gradients are steep and undefined. Furthermore, the counting of migrated cells can be time consuming, tedious and subject to error. The Boyden assays do not assess the cells' path or locomotion and persistent chemotaxis cannot be distinguished from random migration. Advantages of the Boyden chamber include employing fluorescence detection of cells and semi-high throughput application using 96 well plates.

Another chemotaxis assay type are direct visualisation chambers, these allow cells to be observed migrating using time-lapse microscopy and are considered the gold standard for investigating true chemotaxis (Wells 2000). Bridge chambers provide a visualisation platform for observing the behaviour of cells between the two wells; cells are plated onto coverslips which are inverted leaving a gap between the chamber and coverslip for the addition of desired chemoattractant. These chambers provide gradients for cells to accelerate toward rather than exposure of the cells to absolute concentrations alone. Examples include the Zigmond, Dunn and Insall chambers and are described briefly below.

1. The Zigmond chamber was first described in 1977 for the study of polymorphonuclear cells (Zigmond 1977). The chamber permits the generation of shallow gradients at a near steady state linear gradient. It has a variable gap between the bridge and coverslip which can

result in unpredictable variations in the chemotactic gradient (Zicha *et al.* 1991). Furthermore, the chamber is not designed for inverted microscopes, which modern time-lapse microscopy commonly employ.

2. The Dunn chamber is derived from the Zigmond chamber and achieves stability by being a sealed, rigid, glass enclosure entirely filled with incompressible medium using thick (0.25-0.35 mm) coverslips. The circular bridge design can result in variable chemoattractant gradient orientation and changing the gradient in Dunn chambers is inefficient (Muinonen-Martin *et al.* 2010).

3. The Insall chamber, derived in turn from the Dunn chamber (Muinonen-Martin *et al.* 2010), is designed to ensure better stability between the gap between the bridge and coverslip. The bridge structure has a square arrangement with two linear bridges of differing widths on opposite sides whilst the other two sides are large coverslip supports. The Insall Chamber has been recently referenced in several studies, mainly observing cell movement in *Dictostelium discoidium* (Phillips & Gomer 2012; Choi *et al.* 2013; Kaul *et al.* 2013; Herlihy, Pilling, *et al.* 2013; Herlihy, Tang, *et al.* 2013). The chamber is made from nonpolarising polymethyl methacrylate (PMMA) blanks and allows the use of thin cover slips because of the supports within the bridges, which is not possible for Dunn and Zigmond chambers because the cover slips bend and occlude the chamber. Furthermore, the cover slip can easily be sealed in place avoiding the need for cover slip springs, unlike the Zigmond chamber, which can potentially deform the chamber and distort the gradient.

Though other more advanced options exist for the study of chemotaxis, including microfluidic devices and transmigrational models (Toetsch *et al.* 2009), the ease and simplicity of a bridge chamber enables chemotaxis measurements under time restrictive conditions, such as when working with clinical samples.

1.5. Neutrophil priming

During the process of TEM, neutrophils are exposed to stimuli such as cytokines, chemokines and growth factors, which lead to partial activation of the cell that in turn enhances its ability to respond to a secondary stimulus (Hallett & Lloyds 1995). This effect, known as priming, allows for maximal neutrophil activation characterised by the killing of pathogenic agents via several mechanisms (as outlined in section 1.6) as well as the increased potential of the cell to release cytokines which further contribute to the inflammatory process (Gustafsson *et al.* 1997; Dias *et al.* 2011). Neutrophil priming has been demonstrated both *in vitro* and *in vivo* (Condliffe *et al.* 1998) and the signal transduction processes involved in priming utilise calcium dependent and independent pathways (Thelen *et al.* 1993).

Neutrophil priming in chemotaxis is required for the cell to respond to other chemokines, such as MIP1α, allowing for maximal recruitment to the site of inflammation. Release of GM-CSF at inflammatory sites, documented in diseases such as rheumatoid arthritis and glomerulonephritis (Xu *et al.* 1989; Matsuda *et al.* 1996), can prime neutrophils to activate receptors present on the cell surface, such as CCR5.

1.6. Neutrophil killing mechanisms

Neutrophils action antimicrobial killing via several major mechanisms as outlined below.

1.6.1. Phagocytosis and Reactive Oxygen Species (ROS) generation

Phagocytosis is the process of pathogen engulfment by the host cell and its subsequent destruction. Internalisation is achieved through the binding of two different receptor classes; Fcγ receptors and complement receptors (Witko-Sarsat *et al.* 2000). Bacteria that have been opsonised by antibody or complement molecules bind to FcγRII or complement receptors

respectively, which aggregate on the cell surface (Wilson *et al.* 1995) leading to the intracellular activation of Src-tyrosine kinases, which in turn trigger various signalling pathways that coordinate to phagocytose the bacterial particle, forming a structure known as a phagosome (Greenberg *et al.* 1996; Nordenfelt & Tapper 2011). The phagocytosed bacterium is destroyed by the merging of vesicles with the phagosome that contain microbicidal molecules such as proteolytic enzymes and binding proteins such as lactoferrin, which are contained within granules formed from the Golgi apparatus. The formation and release of Reactive Oxygen Species (ROS) also occurs within the phagosomal space within the cell, in what is commonly known as the "respiratory burst", killing the engulfed microbes (El-Benna *et al.* 2008) and activating granule proteins from their pro-forms.

ROS are powerful oxidizing agents formed endogenously as bi-products in metabolism in addition to being a form of defence against invading pathogens (Dröge 2002). Reduction of molecular oxygen to water results in a large free energy release giving rise to ROS. The ROS-generating system is composed of cytosolic and membrane subunits to generate ROS at the expense of NADPH known as the NADPH oxidase. NADPH components include membrane components $gp91^{phox}$, $g22^{phox}$, and the GTPase Rac1 and cytosolic components $p47^{phox}$, $p67^{phox}$, and $p40^{phox}$, which when assembled become the functional oxidase. The NADPH-oxidase initiates the electron transfer to oxygen resulting in superoxide ($O_2^{\cdot}$), an anion that can activate other ROS-generating enzymes as outlined in Figure 1.6. $O_2^{\cdot}$ is acted on by such enzymes which add more electrons forming other ROS species: $O_2^{\cdot}$ is converted to hydrogen peroxide (H_2O_2) either spontaneously or by the enzyme superoxide dismutase (SOD-2) and finally H_2O_2 can be converted to hypochlorous acid (HOCl) by myeloperoxidase or to water by the enzyme catalase (Harrison & Schultz 1976; Chapple 1996; Battino *et al.* 1999; Robinson 2008). HOCl is a powerful antimicrobial (Klebanoff 2005) that elicits bactericidal activity by chlorinating bacteria (Winterbourn 1985).

In addition to the NADPH oxidase system creating ROS, nitric oxide synthase present in primary granules can produce nitric oxide ($NO^{\cdot}$) when the neutrophil is activated, for example, by stimulation by cytokines (Evans *et al.* 1996) or during bacterial infection (Wheeler *et al.* 1997).

During attempted neutrophil phagocytosis of large foreign particles, ROS and cytolytic content release into the extracellular environment may occur. This process is known as "frustrated phagocytosis" and can cause damage to other cells (Sheppard *et al.* 2005). Yet despite the potential to cause damage, ROS formation in immune defence is vital, as evident in people with severe impairments in this pathway. For example, sufferers of chronic granulomatous disease (CGD) – a hereditary condition occurring in 1 in every 250,000 births (van den Berg *et al.* 2009) in which defects in the NADPH-oxidase enzyme system result in the inability to generate ROS – are vulnerable to recurrent bouts of severe infections (Curnutte 1993).

As well as acting as powerful microbicidal weapons, ROS are also generated by chemoattractant stimulation and play a role in signal transduction of cell movement (Dickinson & Chang 2011). One study demonstrated ROS produced by NADPH oxidase activity could regulate pseudopod formation and chemotactic migration in neutrophils via actin glutathionylation and polymerisation (Sakai *et al.* 2012). Furthermore, inhibition of NADPH oxidase-dependent ROS formation within healthy neutrophils led to diminished chemotaxis efficiency when exposed to a chemoattractive gradient. Hydrogen peroxide, a membrane-permeable ROS that can travel across cell membranes via aquaporins (Bienert & Chaumont 2014), is able to direct cell movement in a gradient driven manner (Niethammer *et al.* 2009). This finding was further supported by another study in which ROS were found to deactivate PTEN resulting in the build-up of PIP_3 at the leading edge of the migrating cell which is necessary for chemotaxis (Kuiper *et al.* 2011).

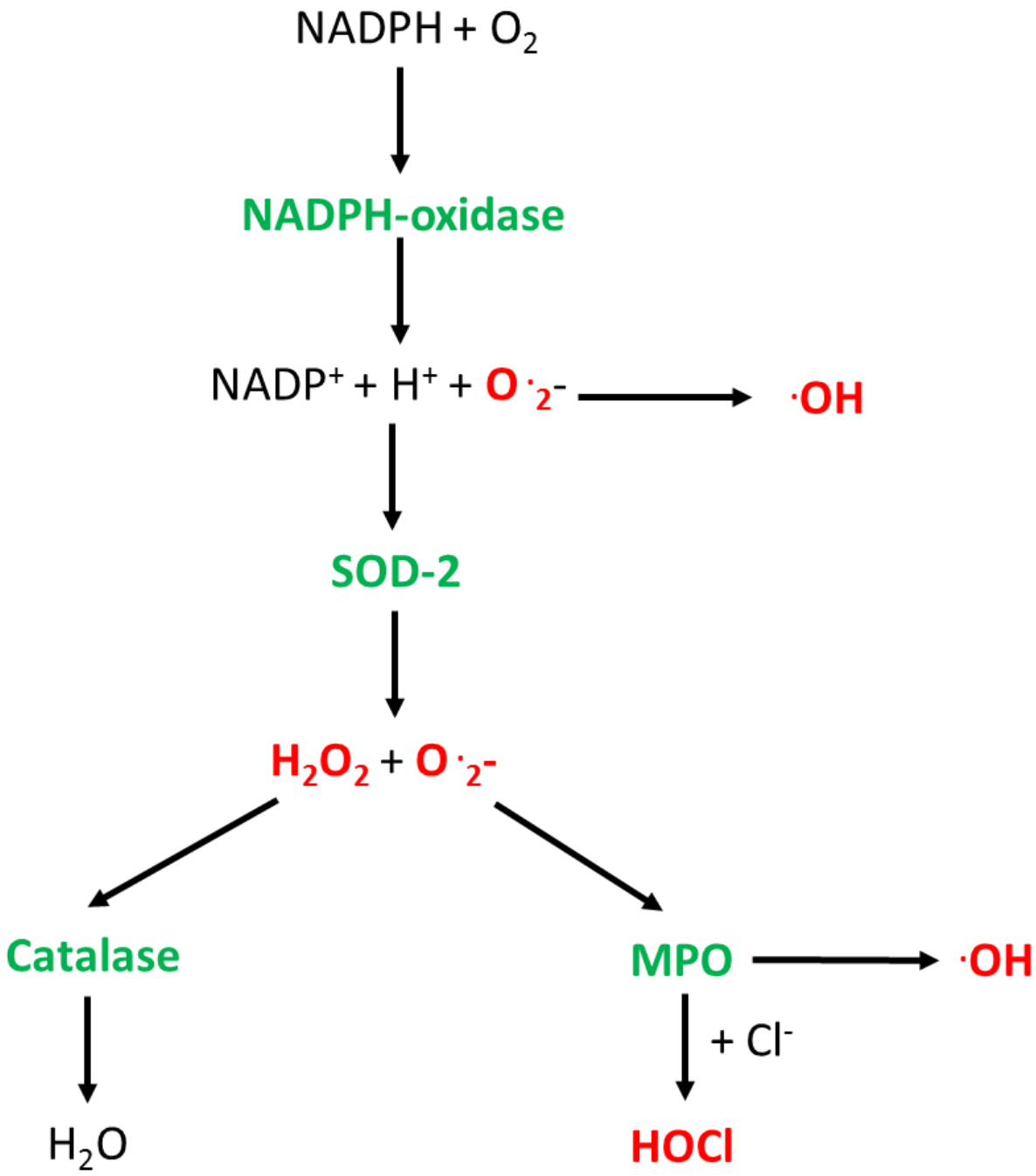

Figure 1.6 NADPH-mediated ROS generation

Neutrophil activation results in NADPH-oxidase assembly. Reduction of oxygen yields superoxide ($O_2^{\cdot}$) which is converted to hydrogen peroxide (H_2O_2) by superoxide dismutase (SOD-2). H_2O_2, in combination with chloride ions (Cl^-), is subsequently converted to hypochlorous acid (HOCl) by myeloperoxidase (MPO). The hydroxyl radical ($^{\cdot}OH$) is also produced during superoxide and HOCl generation.

1.6.2. Degranulation and Neutrophil Serine Proteases (NSPs)

Neutrophils produce an array of microbicidal proteins including hydrolytic enzymes and antimicrobial peptides (AMPs) capable of digesting pathogens and their products via non-oxidative pathways. These are stored within specialised compartments known as granules within the cytosol and there are four types: azurophilic (primary), which contain myeloperoxidase (MPO), a haem containing protein which catalyses the formation of hypochlorous acid from hydrogen peroxide (Faurschou & Borregaard 2003) and defensins as well as neutrophil serine proteases (NSPs); specific (secondary) and gelatinase (tertiary) granules include lactoferrin, metalloproteinases and lysozyme; and secretory vesicles which can kill bacteria and fungi (Faurschou & Borregaard 2003). The granules are formed during promyelocyte maturation (Häger *et al.* 2010) by aggregation of immature transport vesicles that bud off from the trans-Golgi network (Sossin *et al.* 1990). Granules fuse with the phagosome during pathogen uptake and with the plasma membrane for extracellular content release, however the latter usually only involves tertiary and secretory vesicles – leakage of products of primary and secondary granules occurs due to leakage from the phagosome, which is common during frustrated phagocytosis. Extracellular secretory vesicle content release results in the presentation of adhesion and chemotactic receptors that promote neutrophil transmigration.

1.6.2.1. Granule-associated proteins: Neutrophil Serine Proteases

Neutrophil serine proteases (NSPs) include neutrophil elastase (NE), cathepsin G (CG), proteinase 3 (PR3) (de Haar *et al.* 2004) and the recently described neutrophil serine protease 4 (NSP4) (Perera *et al.* 2012). NSP synthesis is regulated at the transcriptional level during granulocyte development and also at the post-translational level. They are stored in their proteolytically active mature form within azurophilic granules until they fuse with the

phagololysosome or undergo limited exocytosis upon exposure to specific stimuli (Owen & Campbell 1999; Kobayashi *et al 2005*). The lysosomal signal peptidase cathepsin C (CTSC) activates NSPs via N-terminal dipeptide removal (McGuire *et al.* 1993; Adkison *et al.* 2002) as they leave the Golgi complex (Pham 2006). In the absence of CTSC the pro-forms of the NSPs are either constitutively secreted (Garwicz *et al.* 2005) or degraded (Pham & Ley 1999). NSPs have many bacterial and fungal targets which include components of cell walls and virulence factors (Belaaouaj *et al.* 2000; Reeves *et al.* 2002; Weinrauch *et al.* 2002). NSPs released extracellularly can bind to the external cell surface in active form, acting on a variety of host chemokines, cytokines, growth factors and cell surface receptors, contributing to both pro- and anti-inflammatory and immune processes. For example, PR3 has been shown to cleave the pro-inflammatory cytokines CXCL8 (Padrines *et al.* 1994), IL-1β (Coeshott *et al.* 1999) and membrane bound tumour necrosis factor alpha (TNFα) (Robache-Gallea *et al.* 1995; Armstrong *et al.* 2009) resulting in their activation. Other targets of NSPs demonstrate anti-inflammatory effects, such as inactivation of MIP1α (Ryu *et al.* 2005) and CXCL8 (Leavell *et al.* 1997). In addition, NSPs have been shown to inactivate IL-6 at inflammatory sites (Bank *et al.* 2000), thus NSPs appear to play a key role in orchestrating immunostimulatory signals. NSPs are known to be associated with neutrophil extracellular traps (NETs) (Brinkmann *et al.* 2004), furthermore, NE has been shown to be fundamental to NET release (Papayannopoulos *et al.* 2010) and cathelicidin (hCAP18/LL-37) is cleaved by PR3, forming LL-37, which is also known to facilitate NET formation (Neumann *et al.* 2014).

1.6.2.2. Granule-associated proteins: LL-37

One well-described NSP target is human cathelicidin antimicrobial protein (hCAP18), a member of the *α*-helical cathelicidin protein family expressed in several cell types including

neutrophils (Yang *et al.* 2009), NK cells (Büchau *et al.* 2010), mast cells (Di Nardo *et al.* 2003) and epithelial cells (Vandamme *et al.* 2012). Activation of TLRs (Liu *et al.* 2006) and/or alteration in the cytokine milieu, such as increased TNFα (Kim *et al.* 2009) as a result of infection/tissue damage, can cause degranulation and subsequent release of the inactive hCAP18 precursor, which is stored in specific granules. Release of hCAP18 precursor into the extracellular environment/entry into the phagosome results in exposure to PR3, and subsequent cleavage to yield the bactericidal 37-amino-acid peptide LL-37 (Sørensen *et al.* 2001).

LL-37 can interact with negatively charged membrane components of pathogens including bacteria, fungi and enveloped viruses, resulting in membrane disruption and cell lysis (Sood *et al.* 2008; Dean *et al.* 2011; Wong, Ng, *et al.* 2011; Wong, Legowska, *et al.* 2011). LL-37 can also stimulate neutrophil chemotaxis, induce chemokine receptor stimulation, suppress neutrophil apoptosis and can also interact and potentiate the actions of other immune cells such as DCs (Lande *et al.* 2007). In addition, LL-37 has been shown to have immunomodulatory functions (Nijnik & Hancock 2009). For example, soluble LL-37 can enter host cells via endocytosis without damaging the cytoplasmic membrane (Sandgren *et al.* 2004), whereas LL-37 can disrupt the nuclear membrane, thereby facilitating the formation of neutrophil extracellular traps (NETs; section 1.6.3) during innate immune responses (Neumann *et al.* 2014).

The far-ranging effects of LL-37 are thought to be attributed to its ability to activate multiple receptors (De Yang *et al.* 2000) including CXCR2 receptor (Zhang *et al.* 2009), and TLR receptors (Liu *et al.* 2006). Furthermore, LL-37 can induce macrophages to release CXCL8, indirectly attracting more immune cells to the inflammatory site (Montreekachon *et al.* 2011). LL-37 has also been found to be implicated in wound and bone healing, as blood monocytes are stimulated by LL-37 to migrate to the site of bone fracture and differentiate

into bone-forming cells known as mono-osteophils (Zhang *et al.* 2010). LL-37 can also recruit endothelial progenitor cells to the site of wound healing, inducing their proliferation and thereby inducing angiogenesis (Pfosser *et al.* 2010).

1.6.2.3. Granule-associated proteins: Matrix metalloproteinases (MMPs)

Matrix metalloproteinases (MMPs) are contained within gelatinase granules and are synthesised during the late maturation process in the bone marrow. Neutrophils are the dominant sources of particular MMPs, including MMP-8 and MMP-9 within the circulation (Jönsson *et al.* 2011) and are responsible for the rapid release of MMPs that occur in blood upon stimulation with endotoxin or pro-inflammatory cytokines (Borregaard & Cowland 1997; Claesson *et al.* 2002). The release of MMP-9 is assumed to serve as a sensitive and early marker of neutrophil activation (Pugin *et al.* 1999). MMPs, of which 24 are found in mammals, are secreted or anchored to the cell surface to exert their effects in the extracellular space; MMP-8, 9 and 12 are all secreted. MMPs are not typically expressed in healthy tissues whilst by contrast MMPs can be detected in repair/remodelling processes, in diseased/inflamed tissues and in cell cultures. MMPs are responsible for the turnover, degradation, catabolism and destruction of the extracellular matrix (Pilcher *et al.* 1997). Thus increased or dysregulated levels of many MMPs are observed in any disease characterised or associated with inflammation (Nathan 2002). MMPs can proteolyse many endogenous molecules resulting in their deactivation, such as the chemokines CXCL5 (ENA78) and CXCL6 (GCP2), as well as their activation, such as CXCL8, leading to a marked increase in chemotactic activity (Van den Steen *et al.* 2000; Van den Steen *et al.* 2003) and can cleave the pro-inflammatory cytokine IL-1β, activating it (Schönbeck *et al.* 1998). MMP-9 also targets the serine protease inhibitor α1-antitrypsin, a potent inhibitor of NE, enabling it to carry out its antimicrobial function (Liu *et al.* 2000).

1.6.3. Neutrophil extracellular traps (NETs)

Neutrophil extracellular traps (NETs) are strand-like extrusions of de-condensed nuclear chromatin complexed with histones and granule proteins, released by neutrophils following dissolution of the nuclear and granule membranes into the extracellular space. NETs are believed to function as an active and terminal defence mechanism to immobilise pathogens (Brinkmann *et al.* 2004; Fuchs *et al.* 2007). NETs firstly trap pathogens, including fungi (McDonald *et al.* 2012), bacteria (Urban *et al.* 2006) and viruses (Jenne *et al.* 2013), preventing their dissemination and aiding subsequent phagocytosis by other immune cells. Pathogens are also exposed to high concentrations of antimicrobial peptides and enzymes trapped within the chromatin which include MPO, NE and LL-37 (Urban *et al.* 2009; Scott & Krauss 2012). In addition, histones within the chromatin backbone have also been shown to have significant antimicrobial activity (Papayannopoulos & Zychlinsky 2009; Papayannopoulos *et al.* 2010; Phillipson & Kubes 2011;).

The process of NET formation (NETosis) is not yet fully understood but there appear to be two methods of NET release. One involves the release of NETs from dying neutrophils known as ‘suicidal NETosis’ that occurs within 2-3 hours of exposure to stimuli including phorbol myristate (PMA). The second form, termed ‘vital NETosis', involves NET extrusion from intact neutrophils, which can occur within 60 minutes upon exposure to TLR-signaling stimuli such as LPS, platelets or pathogenic bacteria (Clark et al. 2007; Pilsczek *et al.* 2010; Kaplan & Radic 2012; Yipp & Kubes 2013). During vital NETosis, the neutrophil plasma membrane remains intact and the process is not dependent upon MPO, elastase or NADPH oxidase (Urban *et al.* 2009) and the NETosis neutrophils have been shown to be capable of other cellular functions including chemotaxis (Clark *et al.* 2007). Suicidal NETosis requires ROS production through NADPH oxidase (Keshari *et al.* 2013), MPO (Metzler *et al.* 2011)

and HOCl (Palmer *et al.* 2012). During NET formation chromatin is completely de-condensed, a process regulated by histone citrullination (Wang *et al.* 2009) catalysed by the nuclear enzyme peptidylarginine deiminase 4 (PAD4) (Wang *et al.* 2004). Knockout mice lacking PAD4 have impaired NETosis and reduced host defences to infection (Li *et al.* 2011). Stimulation by microbial products requires NADPH oxidase activity (Bianchi *et al.* 2011) but stimulation by host immune complexes does not require ROS production (Chen *et al.* 2012). Opsonisation of several oral bacteria with complement has also been shown to promote NET formation (Palmer *et al.* 2015).

NET formation has been liked to various neutrophil-mediated pathologies including sepsis (Clark *et al.* 2007) and systemic lupus erythematosus (SLE) nephritis (Hakkim *et al.* 2010). Excessive NET formation and endothelial cell activation are also associated with pre-eclampsia in pregnancy (Gupta *et al.* 2010). NETs have been seen in an experimental *in vivo* model of dysentery as well as human appendicitis samples (Brinkmann *et al.* 2004).

1.6.4. Other contributions of neutrophils/neutrophil proteins

1.6.4.1. Cytokine production

Cytokines represent an integral component of the signalling network among various cells and many are essential for the development and regulation of innate and adaptive immune responses. Cytokines regulate the responsiveness and maturation of particular cell populations, modulate the balance between cellular and humoral immune reactions and are important determinants of health and disease (O'Shea & Murray 2008). They constitute a large family of small proteins produced by both immune and non-immune cells that act within their local environment to direct biological processes involving neighbouring cells such as inflammation, immunity, repair and angiogenesis (Feldmann 2008). Cytokines are released by neutrophils constitutively or upon activation by local stimuli (Cassatella 1999)

contributing to both physiological and pro-inflammatory processes. The receptors that induce cytokine production in neutrophils include the Fcγ-, complement, GPCR- and PRR receptors (Benelli *et al.* 2002). Transcriptional activation of the corresponding genes in neutrophils is dependent on several transcription factor families including NF-κB (McDonald *et al.* 1997; Cloutier *et al.* 2007; Cloutier *et al.* 2009). Neutrophils express cytokines belonging to various families including pro-inflammatory cytokines (such as IL-1β and IL-6), chemokines (such as CXCL8 and MIP1α) and colony stimulating factors (such as G-CSF and GM-CSF) (Tecchio *et al.* 2014). At sites of infection neutrophils can release IL-17, which acts upon neutrophils indirectly by increasing their number through G-CSF production (Gaffen 2008), thereby increasing their recruitment to the affected area. IL-17 can also attract macrophages (Sergejeva & Lindén 2009); in turn these activated macrophages can prolong the lifespan of neutrophils via the release of cytokines including IL-1β, TNFα and GM-CSF (Lee *et al.* 1993; Hume *et al.* 2002).

1.6.4.2. Cell-cell cross-talk

Neutrophils can communicate with other immune cells including lymphocytes, macrophages and DCs through direct cell-cell contact or via production of soluble mediators in response to intracellular pathogens and viruses. Cross talk occurs through the ability of neutrophils to secrete host cytokines and express cell surface molecules that interact with other immune cells (Mantovani *et al.* 2011). For example, neutrophil products such as the chemokine MIP1α can recruit DCs to sites of infection (Charmoy *et al.* 2010) and the release of LL-37 can induce maturation of immature DCs (Bandholtz *et al.* 2006). Neutrophil/DC binding has been shown to promote DC maturation into effective antigen presenting cells (APCs) (Boudaly 2009). Neutrophils can traffic to lymph nodes in response to infection (Abadie *et al.* 2005) and have been shown to act as APCs to T-cells within lymph nodes (Beauvillain *et*

al. 2011). Neutrophils are a major source of the cytokine B-cell-activating factor (BAFF) that is required for B-cell survival and activation (Scapini *et al.* 2008). At the site of inflammation neutrophils contribute to monocyte influx by secreting chemokines including CCL2, CCL3 and CCL20.

Neutrophil membrane microparticles derived from activated neutrophils have also been shown to exhibit immunomodulatory properties. Microparticles are small membrane fragments (<1μm) released by blebbing during cellular activation and contain cell surface proteins. In the case of neutrophils, these include CD11b, CD62 and CD66 and have been shown to exhibit immune-activating properties on platelets and endothelial cells as well as immunosuppressive functions on macrophages (Pluskota *et al.* 2008; Dalli *et al.* 2008).

1.6.4.3. Calgranulins

Calgranulins constitute a subgroup of calcium-binding proteins including S100A8, S100A9 and S100A12, all of which are highly abundant within neutrophils: S100A8 and 9 comprise ~45% of cytosolic proteins (Edgeworth *et al.* 1991) and are constitutively produced (Hessian *et al.* 1993). When stimulated, large amounts of S100A8 and 9 can be excreted by neutrophils (>100 μM from 1 x 10^6 neutrophils) (Test & Weiss 1986). These proteins are found in high concentrations in inflamed tissues (Odink *et al.*1987) and can activate neutrophils as demonstrated by their ROS-inducing capabilities (Grimbaldeston *et al.* 2003). Both S100A8 and 9 homodimers and the heterodimer S100A8/9 (which forms in the presence of calcium and is subsequently known as calprotectin), are all chemotactic for neutrophils (Ryckman, McColl, *et al.* 2003; Ryckman, Vandal, *et al.* 2003). S100A8, S100A9 and S100A8/9 are examples of DAMPs (Bianchi 2007) that can exhibit both intra- and extra-cellular activities; they are regulators of NADPH oxidase and can activate the transcription of pro-inflammatory genes (Vogl *et al.* 2007) inside the cells and can act as

proinflammatory factors once secreted (Kessel *et al.* 2013), such as by promoting phagocyte migration (Ryckman, Vandal, *et al.* 2003; Vandal *et al.* 2003).

1.7. Neutrophil-related diseases

Individuals with defects in neutrophil function have helped define and explain the different roles neutrophil proteins have in overall neutrophil function and how this affects individuals as a whole. Infections arising as a consequence of disorders of neutrophil function typically involve the skin, mucosa, gums, lungs or cause deep tissue abscesses. Table 1.2 details diseases in which neutrophil defects cause systemic problems. Papillon-Lefèvre Syndrome (PLS) is covered in more detail in section 1.10.2.

Table 1.2 Disorders of neutrophil function

Area affected	Disorder	Cause	Neutrophil defect	Effects	References
Homeostasis	Severe congenital neutropenia (SCN)	25% of cases caused by defects in the *ELA2* gene	No neutrophil elastase (NE). Failed neutrophil maturation.	Endoplasmic reticulum stress and neutrophil apoptosis	Grenda et al. 2007;Zeidler et al. 2009
Recruitment	Leukocyte adhesion deficiency (LAD): I, II and III	Integrin mutations: LAD I = mutations in CD18 LAD II = fucose transferase LAD III = Kindlin-3	Failure of neutrophils to undergo trans-endothelial migration (TEM)	Recurrent infections and severe periodontal disease	Abram & Lowell 2009; Hanna & Etzioni 2012
Chemotaxis	Job's syndrome	Mutations in the *STAT3* gene	Defective chemotaxis	Recurrent infections with opportunistic organisms e.g. *S. aureus*	Hill et al. 1974
	Localised aggressive periodontitis (LAP)	Associated with IL-17 polymorphisms	Defective chemotaxis	Severe periodontitis	Daniel et al. 1993; Chaudhari et al. 2016
Pathogen killing	Chronic granulotomous disease	defects in NADPH-oxidase assembly	Inability to form NETs or generate ROS	Chronic intestinal inflammation, recurrent systemic infections	Fuchs et al. 2007; Berg et al. 2009; Casanova & Abel 2009; Bianchi et al. 2009;
	Chédiak-Higashi syndrome	mutations in the lysosomal trafficking regulator (*LYST*) gene	decrease in phagocytosis	Ulceration of the oral mucosa, severe gingivitis and periodontal disease	Introne et al. 2015
	Specific granule deficiency (SGD)	Mutations in the CCAAT/enhancer binding protein (CEBPE) transcription factor	Neutrophils lack secondary and tertiary granules	Ulceration of the oral mucosa and severe periodontal disease	Khanna-Gupta et al. 2007
	Papillon-Lefèvre Syndrome (PLS)	Mutation in cathepsin C gene	deficiency in NSPs	Skin disorder (palmoplantar keratoderma) and severe periodontitis	Hart et al. 1999; Toomes et al. 1999 Nakano et al. 2001; Korkmaz et al. 2010; Perera et al. 2012;
	Myeloperoxidase (MPO) deficiency	Mutations in MPO gene	Deficiency of MPO	Increased risk of systemic *candida albicans* infections	Mauch et al. 2007

1.8. Characteristics of chronic inflammation

Inflammation is a feature of the biological response to harmful stimuli/agents. There are two major types: acute, which usually features a fast-onset (minutes or hours), a self-limiting "classical" response reflecting the body's response to infection or injury with neutrophils as the major cell type involved (Hotamisligil 2006); and chronic, characterised by a slow, severe progression (weeks and beyond) involving cells of the adaptive immune system and the simultaneous destruction and healing of the tissue from the inflammatory process. A state of chronic inflammation can cause inappropriate responses, such as in the absence of pathogenic stimuli which can lead to autoimmunity. The inflammatory response, if not adequately regulated, can lead to excessive tissue damage and spill-over into normal tissues. Underlying causes of chronic inflammation include the persistent presence of an injurious agent, prolonged exposure to a toxic agent or autoimmune disease.

A component of chronic inflammation at the cellular level is the imbalance between the production of ROS and physiological antioxidant defences (Hold & El-Omar 2008), a condition known as oxidative stress. The release of MPO and the diffusion of ROS extracellularly, such as during frustrated phagocytosis, enables extraphagosomal oxidation. If cellular antioxidant systems do not inactivate ROS, they can react with cellular macromolecules and enhance the process of lipid peroxidation, cause DNA damage and/or induce protein carbonylation and nucleic acid modifications (Yu 1994; Dean *et al.* 1997). Carbonyl groups can be generated on proteins through oxidation of arginine, proline and lysine residues or by direct reaction of these amino acids with oxidants such as HOCl and chloramines (Vissers & Winterbourn 1991; Requena *et al.* 2001. Protein carbonyls can also result from covalent attachment of electrophilic aldehydes produced during lipid peroxidation, such as 4-hydroxynonenal (HNE) to cysteine, lysine and histidine residues

(Uchida & Stadtman 1993). These oxidised products generally have decreased biological activity, for example, HNE modification of calprotectin inhibits the bacteriostatic properties of the protein (Harrison *et al.* 1999; Lusitani *et al.* 2003; Wilkie-Grantham *et al.* 2015), leading to metabolic dysregulation and alterations in cell signalling and other cellular functions implicated in the pathogenesis of various inflammatory diseases states (Ames *et al.* 1993; Wiseman & Halliwell 1996). Oxidative stress occurs frequently in conditions characterized by immune activation and inflammation and can occur in diseases including Alzheimer's disease, RA, diabetes, sepsis, chronic renal failure, respiratory distress syndrome and periodontitis (Basu *et al.* 2009).

1.9. Role of neutrophils in chronic inflammatory diseases

As neutrophils represent a large proportion of the leukocyte population, investigating their role in chronic inflammatory diseases is of interest and, furthermore, the contribution neutrophils make to the progression of chronic inflammatory pathologies is increasingly evident. Below are some examples of chronic inflammatory diseases that demonstrate how the presence of neutrophils and their products may contribute to disease progression:

1.10. Chronic inflammatory disorders

1.10.1. Gingivitis and periodontitis

Oral tissues are constantly exposed to bacteria and their products; the exposed surface of soft and hard (tooth enamel) tissues in close association create a niche in which bacteria can survive, multiply and colonise forming plaque biofilms (Bolstad *et al.* 1996). More than 400 bacterial species have been cultured from periodontal pockets and plaque biofilms and 1,200 phylotypes have been identified by molecular methods (Dewhirst *et al.* 2010), however few are implicated in disease (Signat *et al.* 2011). Characteristics of pathogenic periodontal

bacteria include the ability to colonise and form plaque biofilms, evade the host immune system and release virulence factors that induce an inflammatory response. Saliva, gingival crevicular fluid (GCF) and epithelial keratinocytes of oral mucosa protect the underlying tissues of the periodontium. In addition, immune cells are ever present, infiltrating tissues from the blood stream in response to endogenous and exogenous chemoattractants as described earlier (section 1.4.1) (Gamonal *et al.* 2001). Neutrophils are the major primary defence cell mobilised during an immune response against bacterial pathogens within the periodontal tissues (Scott & Krauss 2012), concentrated in the GCF, a fluid exudate flowing from the crevice between the tooth and gingival tissues (Brill 1962; Kinane *et al.* 1991), of the periodontium (Cooper *et al.* 2013). They comprise 50% of the inflammatory cell infiltrate within the junctional epithelium and 90% of the infiltrate within gingival extracellular fluid (Kowashi *et al.* 1980). As stated earlier, upon exposure to pathogenic stimuli neutrophils can release AMPs, MMPs and ROS, excessive production of which can cause collateral host tissue damage within the periodontal tissues (Shin *et al.* 2008; Scott & Krauss 2012).

Gingivitis is an inflammatory disorder characterised by infiltration of the connective tissues adjacent to the crevicular and junctional epithelia by inflammatory-immune cells, where neutrophils are dominant. The inflammation is caused by the accumulation of plaque at the gingival margin (Page & Schroeder 1976). In susceptible patients with gingivitis, the inflammatory response can progress to involve the periodontal attachment apparatus, leading to destruction of the periodontal ligament and alveolar bone loss, a condition known as periodontitis (Listgarten 1986). Periodontitis is initiated by bacteria within the subgingival biofilm, but progresses due to abnormal host inflammatory-immune responses to the biofilm organisms that fail to re-establish a “health-associated” biofilm, eventually resulting in bone resorption and receding gingival epithelium (Graves & Cochran 2003). During the course of infection, there is a characteristic shift in the bacteria that exist in the gingival plaque biofilm

that causes dysbiosis. Early colonisers are Gram positive bacteria that create favourable conditions for some of the more fastidious and virulent species of Gram negative bacteria strongly implicated in the development of periodontitis such as *Porphymonas gingivalis* and *Fusobacterium* species (Haffajee *et al.* 1998), which eventually replace them (Socransky & Haffajee 2005). The tissue destruction evident in periodontal disease results for the most part from the actions of the immune system and in particular the pro-inflammatory effects of cytokines and the induction of tissue degrading proteinases (Gemmell *et al.* 1997).

Of the different types of periodontal disease, chronic periodontitis develops in individuals later in life with a slow rate of progression and can serve as a risk factor for other inflammatory diseases including type 2 diabetes (Herring & Shah 2006), rheumatoid arthritis (Pischon *et al.* 2008) and cardiovascular diseases (Pihlstrom *et al.* 2005; Dietrich *et al.* 2013). Risk factors for periodontitis include smoking (Palmer *et al.* 2005), obesity, age, gender (males over females), socioeconomic status, an individual's oral microflora and underlying genetic factors (Michalowicz *et al.* 1991). The multifaceted nature of these risk factors makes assessment of the magnitude of the effect of a particular risk factor being more relevant than another difficult.

Chronic inflammatory conditions such as periodontitis are associated with increased systemic oxidative stress (Morel *et al.* 1991; Noguera *et al.* 2001; Chapple & Matthews 2007; Chapple *et al.* 2007; D'Aiuto *et al.* 2010; Dias *et al.* 2013a). As explained earlier (section 1.6.1), neutrophils produce ROS as a method of killing pathogenic organisms, however, excessive ROS production can also cause detrimental effects to host cells. Reduced glutathione (GSH) is an important intracellular anti-oxidant; it is reversibly converted to its oxidised form (GSSG) by donating electrons to ROS. Thus neutralising them. In the absence of sufficient GSH, ROS can oxidise a number of structurally important host macromolecules including proteins, lipids and carbohydrate resulting in irreversible cellular damage

(Gutteridge *et al.* 1981; Halliwell & Cross 1994; Waddington *et al.* 2000) and oxidatively stressed cells.

Peripheral blood neutrophils from chronic periodontitis sufferers have been shown to generate significantly higher levels of ROS in the absence of any stimulating agent and also after *in vitro* FcγR stimulation compared with gender- and age-matched healthy controls (Asman *et al.* 1986; Gustafsson & Åsman 1996; Matthews *et al.* 2007a; Matthews *et al.* 2007b;). The hyper-responsive neutrophil phenotype in chronic periodontitis could be an innate property of the neutrophils (hyperactivity) or involve sensitising or priming (section 1.5) by cytokines or bacterial components (hyper-reactivity) (Matthews *et al.* 2007a). A study by Matthews *et al.* (2007b) showed that non-surgical periodontal therapy in patients with chronic periodontitis resulted in a reduction but not a complete removal of the hyper-reactive neutrophil phenotype with elevated extracellular ROS release remaining in patients versus controls. This suggests the role of peripheral priming of neutrophils may underlie the hyper-reactive neutrophil phenotype exhibited by patients with chronic periodontitis, but the neutrophil hyperactivity (ROS release in the absence of a stimulus) may remain independent of priming. Effects of both a hyperactive and hyper-reactive neutrophil phenotype with regard to enhanced ROS generation results in an altered GSH:GSSG balance with a reduction in the antioxidant capacity of blood, saliva, plasma and GCF in chronic periodontitis patients compared to healthy controls (Grant *et al.* 2010; Konuganti *et al.* 2012; Biju *et al.* 2014; Baser *et al.* 2015). In addition, increased ROS release correlates with intracellular GSH depletion in neutrophils from chronic periodontitis patients (Dias *et al.* 2013b).

Periodontal tissue damage may also arise due to premature neutrophil activation during migration, extracellular release of microbicidal products (e.g. NE and ROS) during the killing of some microbes (such as frustrated phagocytosis), or failure to resolve acute inflammatory responses (Smith 1994). There is also evidence of ROS production by

phagocytes activating osteoclasts, one of the major subtypes of cells found in bone involved in bone resorption (Galli *et al.* 2011).

Neutrophil behaviour has been shown to be dysfunctional in specific types of periodontal disease. Localised aggressive periodontitis (LAP), previously known as localised juvenile periodontitis (LJP) (Kantarci *et al.* 2003) is a disease of adolescence with a genetic basis demonstrated by high incidence rates in individuals from the same family. LAP differs from chronic periodontitis, which largely occurs in adults and develops at a slower rate of progression. There are distinct differences in LAP sufferers compared to other forms of periodontitis including variations in the periodontal microflora and the specific involvement of first molar and incisor teeth. LAP patients otherwise appear to be systemically healthy individuals (Genco *et al.* 1986). A significant number (65-75%) of LAP sufferers have been shown to exhibit defective neutrophil chemotaxis (Lavine *et al.* 1979; Genco *et al.* 1980; Van Dyke *et al.* 1985; Page *et al.* 1985).

1.10.2. Papillon-Lefèvre Syndrome

Papillon-Lefèvre Syndrome (PLS) is a rare inherited autosomal recessive disease characterised by diffuse palmoplantar keratosis and severe precocious periodontitis (Papillon and Lefèvre 1924), in which tissue damage ensues during the eruption of the primary dentition causing severe inflammation of the periodontal tissues, destruction of collagen fibres of the periodontal ligament and alveolar bone loss that results in the loss of both the primary and secondary dentition (Battino *et al.* 2001; Dhanrajani 2009). Signs and symptoms appear between 1 and 4 years of age, typically resulting in permanent tooth loss during adolescence. The prevalence of PLS is estimated to be 1-4 cases per million and whilst there is no predominant racial or gender predilection, a third of reported cases involve parental consanguinity (Hart & Shapira 1994). Systemic immunodeficiency in PLS is relatively mild,

with 15-20% being pre-disposed to recurrent infections (Pham *et al.* 2004), yet local periodontitis is profoundly aggressive.

PLS is caused by mutations in the gene encoding cathepsin C, (CTSC), also known as dipeptidyl peptidase I, (DPPI), resulting in loss of activity. The CTSC gene is located on chromosome 11 and spanning 4.7 kb and over 50 mutations in the gene have been reported as responsible for PLS with phenotypes ranging from specific loss of function (resulting in a deficiency) to complete absence of the enzyme (Hart *et al.* 1999; Toomes *et al.* 1999 Nakano *et al.* 2001; Korkmaz *et al.* 2010; Perera *et al.* 2012). In neutrophils, CTSC is responsible for the activation of granule-derived neutrophil serine proteases (NSPs) and its loss causes the subsequent cessation of NSP activity (Pham & Ley 1999; de Haar *et al.* 2004). NSP deficiency results in a failure to eliminate periodontal bacteria and is thought to be the underlying cause of the severe periodontal disease in PLS patients but comprehensive and systematic characterisation of neutrophil function in PLS has been hampered by the rarity of the disease and case studies limited to individual patients.

1.10.3. Obesity

Obesity is a condition characterised by abnormal or excessive fat accumulation that poses a risk to general health; an individual with a body mass index (BMI) exceeding 30 kg/m^2 is regarded as obese (WHO 2013). Obesity was classified as a disease by the American Medical Association in 2013 (Frellick 2013). Worldwide obesity has nearly doubled since 1980 with the highest numbers of obese individuals residing in Western countries including the USA and Europe (Pengelly & Morris 2009) and approximately 3.4 million adults a year die from obesity-related complications (WHO 2013). Obesity involves a complex pathological process arising as a consequence of environmental and genetic interactions, certain medical disorders such as Cushing's and Prader-Willi Syndromes (Farooqi & O'Rahilly 2006; Han *et al.* 2010)

as well as lifestyle factors including inactivity and poor dietary habits (Kumanyika *et al.* 2002).

Direct adverse effects of obesity include altered blood pressure, insulin resistance and a low grade chronic inflammatory state (Aguirre *et al.* 2002; Hotamisligil 2006) that contributes to obesity-related diseases. Obese individuals have a more than ten-fold risk of developing type-2 diabetes compared with normal weight individuals (Kopelman 2007) and 90% of diabetes patients are overweight or obese (Bray 2004). Furthermore, obesity is strongly associated with stroke incidence, respiratory disorders and osteoarthritis (O'Rourke 2009), with disease severity correlating with the extent of obesity (Suvan *et al.* 2011). The inflammatory state induced by metabolic surplus features a subclinical inflammatory response with few or no symptoms, characterised by increased circulating levels of pro-inflammatory proteins and leukocytes (Bastard *et al.* 2006). Obesity may influence the risk of acquiring an infection or the outcome of an infection once it is established. Possible mechanisms include immune system dysregulation, reduced cell-mediated immune responses, obesity-related co-morbidities and pharmacological issues (Huttunen & Syrjänen 2013; Falagas *et al.* 2009). Obesity has been shown to increase mortality rates in influenza (Louie *et al.* 2011; Yu *et al.* 2011), increase the incidence of urinary tract infections (Semins *et al.* 2012) and nosocomial infections (Choban *et al.* 1995; Kaye *et al.* 2011), and has positive associations with periodontitis (Suvan *et al.* 2015).

1.10.3.1. Adipose tissue biology

Adipose tissue is the major source of fatty acids in mammals and there are two types; brown adipose tissue (BAT) and white adipose tissue (WAT). BAT is a source of energy for non-oxidative phosphorylation, which generates heat to aid adaptation to cold environments (Redinger 2009). WAT is the major source of total body fat and the source of fatty acids that

are used to generate adenosine trisphosphate (ATP) via oxidative phosphorylation in order to supply the body's energy requirements. WAT is distributed all over the body with the major depots being subcutaneous, intra-abdominal, omental and visceral tissues (Gesta *et al.* 2007). WAT (which will subsequently be referred to as adipose tissue) functions include: 1) the storage of triglycerides under conditions of excess calorie consumption and their release during fasting periods, 2) thermoregulation, 3) insulin sensitivity and 4) mechanical organ protection. The cell types that comprise adipose tissue include adipocytes, macrophages, fibroblasts and endothelial cells. Adipocytes have a unique ability to change size in accordance with the body's metabolic needs and without changing their cellular phenotype. Immune cells present in adipose tissue have been shown to have both anti-inflammatory and pro-inflammatory roles. For example, the macrophage M2 anti-inflammatory subtype is involved in immunosuppression and tissue repair, new blood cell formation and removal of necrotic adipocytes (Cursiefen *et al.* 2004; Cinti *et al.* 2005), whereas the M1 pro-inflammatory subtype is characterised by cytokine release that drives immune responses (Zeyda & Stulnig 2007; Reilly & Saltiel 2014). In lean individuals' adipose tissue the M2 macrophage phenotype dominates, thus maintaining a non-inflammatory adipose tissue state (Lumeng *et al.* 2007).

1.10.3.2. Effects of obesity on metabolic and immune function

Many hormones, cytokines, signalling factors, transcription factors and other bioactive molecules have roles in both metabolic and immune pathways. Both systems regulate each other; the inflammatory response to infectious/injurious agents requires metabolic support such as lipid mobilisation and energy redistribution during immune responses (Khovidhunkit *et al.* 2004).

In the obese state, the presence of heightened circulating levels free fatty acids (FFA) occurs, which act as ligands for TLR-4 and therefore may contribute to systemic inflammation (Shi *et al.* 2006; Kim *et al.* 2007) by activation of down-stream pro-inflammatory kinases including protein kinase C (PKC; Capurso & Capurso 2012). In addition, circulating FFA can activate macrophages, triggering a cytokine-driven inflammatory cascade and insulin resistance via TNFα, IL-6 and IL-1β (Saberi *et al.* 2009; Chawla *et al.* 2011). Oxidative stress is another major mechanism by which inflammation in obesity is initiated. This can occur as a result of elevated glucose levels within adipose tissues being taken up by resident endothelial cells and stimulating ROS generation within the cell, which in turn activates inflammatory signalling cascades (Brownlee 2001). Circulating levels of endothelial activation markers such as E-selectin, P-selectin and plasminogen activator inhibitor-1 are increased in obesity indicating an activation of endothelial cells (Vázquez *et al.* 2005).

As body weight increases, adipose tissue changes its mass, distribution, cellular composition and function resulting in impaired tissue function. During sustained adipocyte hypertrophy the vasculature fails to adequately perfuse the expansion of adipose tissue resulting in tissue, hypoxia and apoptotic cell death. The cellular debris left behind causes the recruitment of M1 macrophages and T cells via chemokines such as monocyte chemotactic protein-1 (MCP-1) from the circulation (Kim *et al.* 2007; Rausch *et al.* 2008). Recruited macrophages change in terms of M1:M2 macrophage ratio; with an increase in the M1 resulting in elevated tissue and systemic levels of pro-inflammatory cytokines (Esposito *et al.* 2003; Lehrke *et al.* 2004; Wellen & Hotamisligil 2005; Skurk *et al.* 2007) such as TNFα and IL-6 that inhibit adipocyte differentiation (Sethi & Vidal-Puig 2007). M1 macrophage cytokine release also recruits neutrophils to adipose tissue (Mraz & Haluzik 2014). The adipocyte-derived pro-inflammatory cytokines, also known as adipokines, spill over into systemic circulation, contributing to a low-grade state of chronic inflammation. The adverse production of

adipokines is thought to be the key factor in obesity, giving rise to obesity associated diseases (Klöting & Blüher 2014) including cardiovascular disease and the metabolic syndrome, a disorder associated with abnormal carbohydrate and lipid metabolism (Molica *et al.* 2015). Metabolic syndrome encompasses a range of metabolic disorders including high blood pressure, inflammation, oxidative stress, insulin resistance, visceral obesity and impaired glucose regulation (Bjorntorp 1991; Lemieux *et al.* 2001; Eckel *et al.* 2005; Van Guilder *et al.* 2006). One underlying reason for the development of metabolic syndrome can include genetic pre-disposition to insulin resistance, however lifestyle factors such as diet and exercise might also lead to insulin resistance (DeFronzo & Ferrannini 1991).

1.10.3.3. Adipokines

Adipose tissue has been shown to function as an endocrine organ that can secrete numerous factors that, in excessive adiposity, can cause disease through dysregulated immune responses (Ouchi *et al.* 2011) as adipose tissue is a source of more than 600 adipokines (Lehr *et al.* 2012). The overlapping functions of macrophages and adipocytes demonstrate the definite link between metabolic and immune pathways. In fact, adipocyte precursors (pre-adipocytes) have the potential to differentiate into macrophages after exposure to particular conditions (Charrière *et al.* 2003). In addition to macrophages, adipocytes produce a number of bioactive molecules that influence and communicate with other organ systems and can contribute to systemic inflammation. These adipokines have been found to make a significant contribution to chronic low-grade systemic inflammation characteristic of the obese state.

Adipokines are soluble proteins that include chemokines, complement components, pro-inflammatory and anti-inflammatory cytokines (Li *et al.* 2011). Upon receptor-binding they initiate intracellular signalling cascades resulting in phenotypic changes to the cell through altered gene expression and regulation. They are involved in a number of homeostatic

processes including food intake, lipid metabolism, insulin sensitivity, glucose metabolism, insulin secretion, immunity and inflammation (Blüher & Mantzoros 2015). They are effective at low concentrations and usually act on cellular receptors expressed by tissues within the surrounding environment of the cells they are produced by. Table 1.3 details well-known and recently discovered adipokines. Adipokines, like other cytokines, are able to influence the secretion of other adipokines in networks, for example, IL-1β and TNFα can act synergistically in stimulating IL-6 secretion by human gingival fibroblasts (Kent *et al.* 1998). Conversely, the secretion of some adipokines can be inhibited by others, for example, IL-6 and TNFα secreted by adipocytes inhibit the anti-inflammatory adiponectin from being released by adipocytes (Fasshauer *et al.* 2003; Bruun *et al.* 2003).

The functions of many adipokines have been elucidated from the study of gene knockout animals. For example, knockout mice for the *ob* gene, which codes for leptin, are immunodeficient (Kimura *et al.* 1998) as characterised by impaired phagocytosis and abnormal cytokine gene expression (Loffreda *et al.* 1998). For some of the adipokines their function is only noticeable when the knockout animal is placed under certain conditions. Loss of the gene that codes for adiponectin has no dramatic effect on the normal diet of mice for example, but when fed on a high sucrose diet they develop insulin resistance and high fat accumulation in muscle tissue compared to control animals (Whitehead *et al.* 2005). TNFα is constitutively expressed in adipose tissue and provides a direct link between obesity and insulin resistance, demonstrated by the improved responsiveness of obese rats to insulin when treated with a TNFα receptor antibody (Hotamisligil *et al.* 1993).

Table 1.3 Characteristics of well-known adipokines

(Adapted from Ouchi et al. 2011). IR = insulin resistance

Adipokine	Primary source	Binding partner/ receptor	Function	References
Adiponectin	Adipocytes	Adiponectin receptors 1 and 2	Anti-inflammatory; Induces M1 to M2 switching in macrophages and reduces TNFα expression in adipose tissue. Decreases gluconeogenesis in liver.	Wulster-Radcliffe *et al.* 2004; Ohashi et al. 2010; Maeda et al. 2002; Ouchi et al. 2000; Lago et al. 2007
IL-1β	Stromal vascular fraction cells	IL-1 receptor	Pro-inflammatory	Dinarello 2009
IL-6	Adipocytes, stromal vascular fraction cells, liver and muscle	IL-6 receptor	Pro-inflammatory; stimulates angiogenesis and release of acute phase proteins	Blanchard *et al.* 2009
Leptin	Adipocytes	Ob-Ra (neutrophils) and Ob-Rb (monocytes) leptin receptors	Regulates appetite, energy homeostasis and immune and inflammatory processes	Otero *et al.* 2006; Matarese *et al.* 2005; Mantzoros et al. 2011; Eder 2009; Zarkesh-Esfahani et al. 2004
Resistin	Neutrophils and macrophages	Unknown	Promotes insulin resistance (IR) and inflammation through IL-6 and TNF secretion from macrophages	Patel *et al.* 2003; Telle-Hansen et al. 2013
TNFα	Stromal vascular fraction cells and adipocytes	TNF Receptors 1 and 2	Pro-inflammatory, increases expression of cell adhesion molecules on endothelial cells	Ware 2008; Locksley et al. 2001; Bradley 2008

1.10.3.4. Neutrophils and obesity

Neutrophils are the key initial responder to infectious agents and hence the impact of obesity on neutrophil function is attracting further study. The presence of neutrophils within adipose tissue has been demonstrated early in the course of weight gain in mice fed a high fat diet for 90 days, peaking at 1.5% of the total stromal vascular fraction cells (Talukdar *et al.* 2012). Neutrophil infiltration via M1 macrophages results in a coordinated inflammatory response that includes the recruitment of and crosstalk between B- and T-cells, (Gerhardt *et al.* 2001) via the secretion of cytokines such as CXCL8 (Bruun *et al.* 2004; Mraz & Haluzik 2014) and CXCL2 (Rouault *et al.* 2013). These cytokines further mobilise neutrophil migration into the tissues; both are over-expressed in obese compared to lean individuals (Nijhuis *et al.* 2009).

Neutrophils recruited to adipose tissue appear to promote the M2 to M1 macrophage phenotype switch (Elgazar-Carmon *et al.* 2008) that results following their exposure to interferon (IFN)-γ and/or TLR ligands (Mosser & Edwards 2008). Furthermore, neutrophils have been shown to participate in adipose tissue vascular inflammation (Leik & Walsh 2004; Shah *et al.* 2010). The levels of neutrophil elastase (NE) are raised in the adipose tissue of high fat diet-fed mice compared to normally-fed mice, inhibition of which resulted in improved glucose tolerance and insulin sensitivity and a reduction in neutrophil recruitment into the adipose tissue (Talukdar *et al.* 2012). In addition, NE has been found to degrade insulin receptor substrate 1 (Houghton *et al.* 2010). Neutrophils are thought to play important roles in obesity-related diseases such as during the development and progression of atherosclerotic plaques (Naruko *et al.* 2002; Ionita *et al.* 2010). In models examining thrombus formation, a complication of cardiovascular diseases, neutrophils were found to be the first cell type to adhere to endothelial cells at vessel injury sites (von Brühl *et al.* 2012), which was shown to precede platelet activation (Darbousset *et al.* 2012). Furthermore, NETs

have been shown to trigger platelet activation and thrombus formation *in vitro* (Fuchs *et al.* 2007).

1.10.4. Association between periodontitis and obesity

Many chronic systemic inflammatory diseases associate with each other. The root cause of such associations is thought to be due to the shared presence of inflammatory markers/proteins that feature in the respective diseases and include CRP, inflammatory cytokines and leukocytes. Examples of inflammatory disease associations include rheumatoid arthritis with systematic lupus erythematosus (SLE; Bencze 1970), cardiovascular disease and diabetes (Kannel 1979), cancer with diabetes (Wolf *et al.* 2005; Richardson & Pollack 2005; Pannala *et al.* 2009) and notably, periodontitis with obesity.

Obesity is associated with systemic inflammation that in turn is associated with increased susceptibility to chronic infectious diseases such as periodontitis (Falagas & Kompoti 2006). Many epidemiological studies have demonstrated an association between obesity and periodontitis in humans (Saito *et al.* 2001; Saito *et al.* 2005; Chaffee & Weston 2010; Nibali *et al.* 2013) and also the reverse, i.e. that maintaining a normal weight by regular exercise is associated with lower periodontitis prevalence (Wakai *et al.* 1999; Merchant *et al.* 2003 Karjalainen *et al.* 2009). A meta-analysis study reported that the odds of having periodontitis increased by 27% and 81% for overweight and obese patients respectively relative to normal-weight patients (Suvan *et al.* 2011). The periodontitis-obesity association can also be demonstrated across the life course (Dalla Vecchia *et al.* 2005; Saito *et al.* 2005; Ekuni *et al.* 2008; Khader *et al.* 2009).

The recently established relationship between obesity and periodontitis is consistent with a well-established paradigm of the relationship between obesity-associated type 2 diabetes and the incidence of periodontitis (Preshaw *et al.* 2012). This relationship appears to be bi-

directional, i.e. having type 2 diabetes increases susceptibility to periodontitis and an individual suffering from periodontitis has an increased risk of developing obesity-related diseases including insulin resistance (Matsuzawa-Nagata *et al.* 2008). As obesity and type 2 diabetes are highly interrelated, both are therefore thought to contribute to the development and progression of periodontal diseases; thus a three-way relationship has been suggested with each condition influencing the other two (Zhu & Nikolajczyk 2014).

The link between obesity and periodontitis was first shown in 1977 using a ligature-induced periodontitis in obese Zucker rats, demonstrating bone resorption and periodontal inflammation were more severe in the obese cohort compared with controls (Perlstein & Bissada 1977). The underlying mechanisms for the association between obesity and periodontal disease are not well known and many studies reporting upon the association are cross-sectional in nature making a cause-and-effect relationship difficult to establish. Pro-inflammatory adipokines and other bioactive substances are thought to be the major link, however, which may affect the periodontal tissues directly or indirectly (Ylöstalo *et al.* 2008). Obesity could increase an individuals' susceptibility to periodontitis by altering the host immune responses (Falagas & Kompoti 2006) via systemic oxidative stress as a result of the dysregulated production of pro-inflammatory cytokines, such as TNFα and IL-6 (Ando & Fujita 2009). One example of the hallmarks of periodontitis is the resorption of alveolar bone, caused by the increased expression of RANKL (receptor-activator of nuclear factor-κB ligand) which binds osteoclast pre-cursors and causes them to differentiate into bone resorbing cells (Cochran 2008); RANKL expression can be induced by the adipokines TNFα and IL-1β (Nagasawa *et al.* 2007). GCF and serum levels of some adipokines, notably leptin and IL-6, are altered in individuals who are obese and/or have periodontitis compared to normal weight, periodontally healthy controls (Zimmermann *et al.* 2013). Oxidative stress might be a major mechanism underlying obesity-related complications; in obese individuals

GSH concentrations were lower than those of normal weight individuals (Albuali 2014). In addition, GSH levels are reduced in periodontitis patients (Chapple *et al.* 2002; Grant *et al.* 2010; Tsai *et al.* 2005) and the GSH level is inversely related to the severity of periodontal disease (Biju *et al.* 2014). The mechanism for this may relate to alterations in the redox balance and a systemic increase in ROS following obesity that may trigger gingival oxidative damage, which may lead to the progression of periodontal inflammation (Tomofuji *et al.* 2009; Azuma *et al.* 2011). Another potential mechanism linking the two diseases is homotolerance, in which pre-exposure to TLR2 agonists LPS or FFA in macrophages causes a de-sensitisation to LPS re-stimulation, characterised by an inhibition of TNFα stimulation (Dobrovolskaia *et al.* 2003; Zelkha *et al.* 2010; Amar & Leeman 2013). Obesity has been shown to cause attenuated immune responses to *P. gingivalis* in mice, when, after infection with the bacteria, diet-induced obesity mice featured greater alveolar bone loss and higher levels of *P. gingivalis* compared to lean controls (Amar *et al.* 2007). Furthermore, macrophages isolated from diet-induced obesity mice secreted reduced levels of pro-inflammatory cytokines following infection with *P. gingivalis* compared to lean mice, showing that obesity can interfere with the ability of the immune system to appropriately respond to infectious bacteria (Zhou *et al.* 2009).

1.11. Project aims

Understanding the extent to which neutrophils contribute to the pathogenesis of chronic inflammatory diseases remains to be fully elucidated. Neutrophils are well-known in host defences against acute, infectious episodes and their involvement in more long-term conditions is gaining momentum. Recent studies of their activity repertoire reveal greater lifespan potential than previsouly thought and the ability to perform a broader range of activities outside of direct pathogen-killing. Therefore, the overall aim of this thesis was to

contribute to the current understanding of the role of neutrophil functions in different diseases associated with chronic inflammation. In order to achieve these aims, the work described in this thesis had the following specific objectives:

1. **To optimise a method for the study of neutrophil chemotactic accuracy *ex vivo.***
2. **To assess neutrophil function in acute and chronic oral disease states.**
3. **To assess neutrophil function in obese patients pre- and post-bariatric surgery.**

CHAPTER 2 - MATERIALS AND METHODS

2.1. Study volunteer donors

2.1.1. Selection of healthy volunteers

With the exception of clinical study work, all volunteers for blood sample donations were staff and students recruited from The School of Dentistry. The volunteers' ages ranged 19-37 years of age and were selected if they had no remarkable medical histories. All participants had BMI's ranging 18-25, were non-smokers and were not taking any medication. Ethical approval was obtained from South Birmingham Research Ethics Committee (LREC 2004/074) and written consent was gained from all participants.

2.1.2. Gingivitis study - volunteer selection

A 21 day model of experimental gingivitis (Löe *et al.* 1965) was conducted by the Periodontology Department of the School of Dentistry, as previously described by Chapple *et al.* (1996). Ethical approval was obtained from South Birmingham Research Ethics Committee (LREC 2004/074) and all volunteers gave written informed consent. Fifteen volunteers with no current or historic periodontal disease, not undergoing any orthodontic/prosthetic dental treatment and with unexceptional medical histories were enrolled.

2.1.3. Chronic periodontitis - volunteer selection

Two patient cohorts sre described here. The first cohort was used for the study of chemotaxis in chronic periodontitis as part of a larger clinical study in which GCF was collected, but was to be used for other experimental assays. Therefore GCF was collected from an additional set of chronic periodontitis patients to use in the assays described in this thesis.

2.1.3.1. Periodontitis patient cohort 1

Periodontitis patients were recruited from the Periodontology Department within the School of Dentistry along with gender- and age-matched healthy controls. Ethical approval for the

study was obtained from the West Midlands Research Ethics Committee (10/H1208/48) and all 20 volunteers provided written informed consent. Exclusion criteria for both patient and control subjects included diabetes, pregnancy, smokers and use of vitamin supplements.

2.1.3.2. Periodontitis patient cohort 2

GCF samples were collected from a cohort of 10 chronic periodontitis patients and ethical approval was obtained from the West Midlands Research Ethics Committee (14/SW/1148) and all gave written consent. Patient ages ranged between 30-60 years; gender: 5 female and 5 male. Exclusion criteria for the patients included diabetes, pregnancy, smokers and use of vitamin supplements. GCF collection took approximately 30 seconds using paper strips (Lamster *et al.* 1986).

2.1.4. Papillon-Lefèvre Syndrome (PLS) - volunteer selection

Five Papillon-Lefèvre Syndrome (PLS) patients (age range 9-14 years) from different families were recruited by Professor Iain Chapple following a specialised clinic run by Dermatological and Periodontal specialists at the Birmingham Children's Hospital (BCH). Ethical approval for the study was obtained from the West Midlands Research Ethics Committee (14/WM/1175) and all volunteers provided written informed consent. Prior to study commencement, all patients had been genotyped and their dermatological and periodontal status determined by clinical specialists from within the BCH. Healthy gender-matched controls (aged 19-21) were recruited from undergraduate students within the School of Dentistry as described in section 2.1.1. Exclusion criteria for the healthy volunteers included diabetes and those taking medication. Control selection criteria included unremarkable medical histories and no evidence of periodontal disease.

2.1.5. Obese patient - volunteer selection

Twenty-three patients (ages ranged 27-65) undergoing gastric band surgery were recruited from Heartland's Hospital Community Weight Management Service by Mr Paul Super. Ethical approval for the study was obtained from the North West Research Ethics Committee (15/NW/07) and patients provided written informed consent. Patient exclusion criteria included pregnancy and smoking. Gender- and age-matched controls were also recruited from staff within the School of Dentistry. Exclusion criteria for the controls included a BMI over 27, pregnancy, smoking, and evidence of systemic disease and use of medications/vitamin supplements.

2.2. Neutrophil isolation

The following section details the isolation of neutrophils from whole blood using a discontinuous gradient (Pertoft *et al.* 1978) for use in further assays. Venous blood samples were collected in lithium heparin vacutainers (Greiner, Bio-One); the amount of blood collected depended on the experiment but did not exceed 30ml.

2.2.1. Reagents for neutrophil isolation

2.2.1.1. Percoll gradients

Percoll (1.13g/ml, 8ml; GE Healthcare 17-0891-01), 1.098g/ml density was layered underneath Percoll (8ml) 1.079g/ml density in a 25ml centrifuge tube (Sarstedt). The composition of the Percoll gradients, which includes distilled water and sodium chloride (NaCl) (S9625 Sigma) dissolved in distilled sterile water, is documented in Table 2.1. The layered Percoll densities were stored at 4^{o}C prior to use.

Table 2.1. Percoll density composition

Component	Density 1.079g/ml	1.098g/ml
Percoll	19.708ml	24.823ml
Water	11.792ml	6.677ml
NaCl	3.5ml	3.5ml

2.2.1.2. Lysis buffer

Lysis buffer was made by adding NH_4Cl (8.3g; Sigma, A9434), $KHCO_3$ (1g; Sigma, P9144), Na_2 EDTA $2H_2O$ (0.04g; Sigma, E5134) and bovine serum albumin (2.5g; BSA; Sigma, A4530) sequentially to 1 litre of distilled water and stored 4^oC prior to use.

2.2.1.3. Phosphate buffered saline (PBS)

PBS was made by adding NaCl (7.75g; Sigma, S9625), KH_2PO_4 (0.2g; Sigma, P5379) and K_2HPO_4 (1.5g; Sigma, P8281) to distilled water, the solution was adjusted for pH (7.3) and made up to 1 litre. The solution was subsequently autoclaved and stored at 4^oC prior to use.

2.2.1.4. Glucose supplemented phosphate buffered saline (gPBS)

gPBS was made weekly using 1 litre of sterile PBS to which glucose (1.8g; Sigma G8270), $CaCl_2$ (0.15g; Sigma C1016) and $MgCl_2$ (1.5ml; 1M, Sigma M1028) was added sequentially and stored at 4^oC.

2.2.2. Neutrophil isolation method

Whole blood (approximately 8ml) was layered on top of the pre-prepared Percoll gradients (Section 2.2.1.1). The tubes were then centrifuged (IEC Centra, CL3R) for 8 minutes (min) at 150 relative centrifugal force (rcf), followed by 10 min at 1,200 rcf. The different cell layers that formed after centrifugation are shown in Figure 2.1.

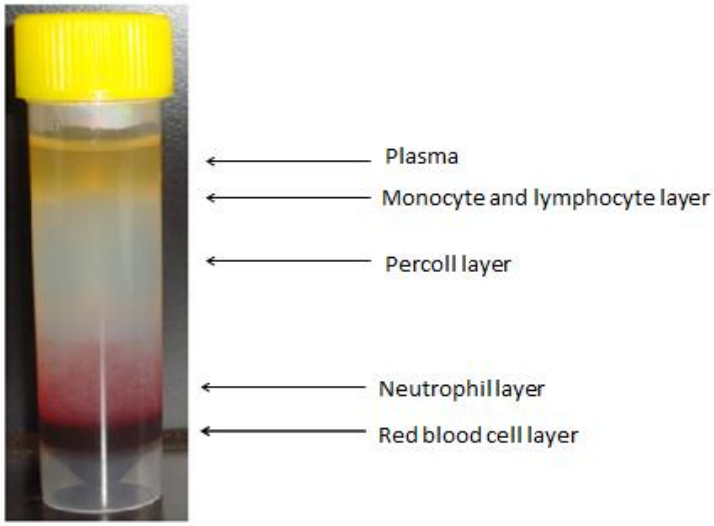

Figure 2.1 Separation of blood by differential Percoll gradients

After the two initial centrifugation steps the blood layers separate within the Percoll; the neutrophil layer sits above the red blood cell layer.

Plasma, monocyte and Percoll layers were removed by manual aspiration using a Pasteur pipette (Appleton Woods, KC230). The neutrophil layer, located at the top of the red blood cell layer, was aspirated and transferred to a 50ml centrifuge tube (Kartell) containing lysis buffer (35ml) (section 2.2.1.2). The tube was gently inverted and incubated for ten min at room temperature to lyse the red blood cells and subsequently centrifuged (6 min, 500 rcf). The supernatant was discarded and the pellet re-suspended in lysis buffer (5ml), incubated for 5 min at room temperature prior to re-centrifugation as before. The supernatant was removed and the cells were suspended in PBS (3ml) (2.2.1.3) and centrifuged again to remove any remaining lysis buffer and re-suspended in PBS (3ml). The cells were counted using a haemocytometer (Neubauer, Reichart) as explained in Figure 2.2 and viability (typically >97%) was checked using trypan blue dye exclusion (Sigma, T8154). Briefly, cells were mixed 1:1 with trypan blue and visualised by light microscope (Leitz Laborluxs). Neutrophils were re-suspended at concentrations required and used immediately in the assays detailed in subsequent sections.

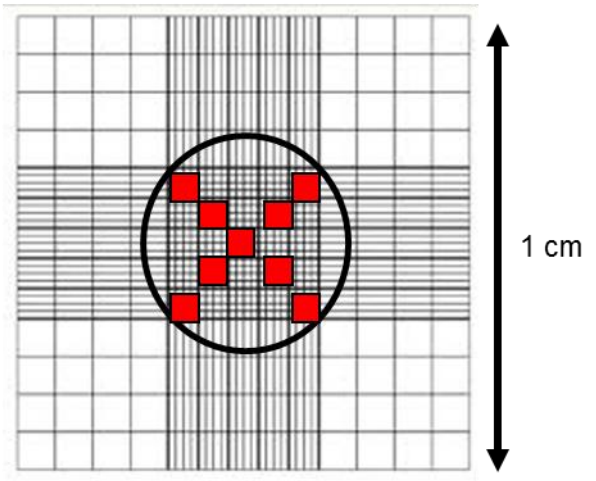

Equation:

1. **(Cell count /9) x 25 = no. of cells in the entire grid.**

2. **No. of cells in the grid x 10^4 = no. of cells per ml.**

Figure 2.2. Haemocytometer for calculating cell concentration

Nine squares (shown in red) were the designated regions for counting neutrophils. The entire grid has a surface area of $1mm^2$ and a depth of 0.1mm, this represents a total volume of 10^{-4} cm^3. As 1 cm^3 = 1ml, the second part of the equation scales the cell count up to per ml.

2.3. Collection of plasma

Plasma was isolated from blood collected into 6ml lithium heparin anticoagulant tubes by centrifugation (30 min, 1000rcf, 4°C; IEC Centra, CL3R), aliquoted (500µl) into cryotubes and stored at -80°C.

2.4. Enhanced chemiluminescence assay for ROS

2.4.1. Reagents prepared for use in the ROS assay

2.4.1.1. Blocking buffer (PBS 1% BSA)

BSA (10g; Sigma, A4503) was dissolved in 1 litre PBS to give 1% BSA in PBS. The solution was aliquoted into 20ml working volumes and stored at -20°C until use.

2.4.1.2. Luminol and isoluminol

A stock solution (30mM) was made by dissolving luminol (0.5g; Sigma, A8511) or isoluminol (0.5g; Sigma A8264) in 94.05ml 0.1M NaOH and stored at 4°C. The working solution was made by diluting 1ml stock luminol or isoluminol with 9ml PBS and the pH adjusted to 7.3 with dilute HCl. The final well concentrations for use in the ROS assays were 0.45mM for luminol and 0.9mM for isoluminol respectively.

2.4.1.3. Lucigenin

A stock solution (1mg/ml) of lucigenin (Sigma. B49203) in PBS was prepared and stored at 4°C. The working solution (0.33mg/ml) was made by diluting the stock solution 1:3 in PBS. The final well concertation was 0.05mg/ml.

2.4.1.4. Horseradish peroxidase (HRP)

HRP (Sigma, P8415) was diluted in PBS to give a working concentration of 100 Units (U)/ml which was stored at -20°C until use. When used in the ROS assay the final well concentration was 1.5U/well.

2.4.1.5. Plate preparation for ROS assays

Blocking buffer (2.4.1.1) was defrosted to room temperature and 200µl was added to each well of a white 96 well microplate (Costar, 3915) and incubated at 5°C overnight. Before use in ROS/NET assays the plates were washed five times with PBS using a microplate washer (BioTek, ELx50).

2.4.2. Enhanced chemiluminescence assay for ROS

Neutrophils were prepared as previously described (2.2.2) and cells (100µl, $1x10^6$ cells/ml) in gPBS (2.2.1.4) were added to white 96-well plates blocked as previously described (2.4.1.5). To detect total ROS generation luminol (30µl, final concentration 0.45mM) (2.4.1.2) was added. To detect extracellular radical generation, isoluminol (60µl, final concentration 0.9mM) (2.4.1.2) in addition to HRP (15µl, 1.5 units) (2.4.1.4) were added. To detect superoxide generation, lucigenin (30µl, final concentration 0.05mg/ml) (2.4.1.3) was added. The total volume of each well was made up to 175µl using PBS and the light output was recorded for 1 second per well in relative light units (RLU) using a microplate luminometer (LB96v Bethold Technologies U.K. Ltd.) at 37°C cycling around the plate over the course of the experiment. The plate was read for 30 min before 25µl of stimuli were added to give a total volume of 200µl per well and read for a further 120 min. For experiments including a priming stage, in which neutrophils were exposed to a priming agent for 30 min prior to stimulation, the agent or control (10µl) were added to the relevant wells.

2.4.3. Stimuli/priming agents used to induce ROS

2.4.3.1. Priming

GM-CSF (Sigma SRP3050) was diluted in PBS to give 200ng/ml working solution in which 10µl was added to the relevant wells giving a final concentration of 10ng/ml in the well.

2.4.3.2. Stimuli for induction of ROS

The range of stimuli used for *ex vivo* stimulation of peripheral neutrophils for the assay of ROS formation is listed in Table 2.2. All bacteria used are known periodontal pathogens grown as described later (2.8).

Table 2.2 Stimuli used to induce neutrophil ROS production

Bacterial strain (ATCC number)/other stimulus	**ATCC number/ Supplier and Cat No.**	**Concentration per well**
Fusobacterium nucleatum subsp. *Polymorphum* (*F. nucleatum*)	10953	3×10^7
Aggregatibacter actinomycetemcomitans serotype *b* (*A. actino*)	43728	3×10^7
Opsonised *Staphylococcus aureus* (Ops *S. aureus*)	9144	1.5×10^7
Phorbol 12-myristate 13-acetate (PMA)	Sigma P8139	25µM

2.5. Assays of NET release

2.5.1. Micrococcal nuclease (MNase) assay of NET release

Neutrophils (100µl, $1x10^6$ cells/ml) were suspended in RPMI (Sigma R8758) and added to blocked white 96 wells plates previously described as for the ROS assay (2.4.1.5). Additional RPMI was added to give a final volume of 175µl after consideration of any additional agents. After a 30 min initial incubation (37°C), stimuli or RPMI (25µl/well) were added and the

plate was incubated for up to 3 hours (37°C). After stimulation NET-DNA was digested: MNase (Worthington, LS004797; 15µl, 1 unit/ml) was added per well and re-suspended by pipette aspiration. The plate was incubated at room temperature for 20 min. After centrifugation (10 min, 1800 rcf) to pellet the cells, supernatant (150µl) was removed and added to a black 96 well plate (Costar 3912) and fluorescent green nucleic acid stain, SYTOX® (Invitrogen, S7020; 15µl, 10nM diluted in RPMI) was added. Fluorescence was recorded from each well in arbitrary fluorescent units (AFU) using a fluorometer (Twinkle LB970, Berthold Technologies) with an excitation wavelength of 485nm and an emission wavelength of 525nm.

2.5.2. Visualisation assay of NET release

NET visualisation, a qualitative means of assessing NET production, was performed using 24-well plates (Costar 3524) which were blocked with PBS containing 1% BSA (500µl) and incubated at 4ºC previously overnight. The blocking buffer was removed by vacuum aspiration and neutrophils (1 x 10^5/ml, 200µl suspended in RPMI) were added to each well. After an initial incubation (30 min, 37°C), stimulus (50µl) and additional RPMI (50µl) were added and the plate was incubated for a further 2 hours at 37°C. Post incubation fluorescent green nucleic acid stain SYTOX® (Invitrogen, S7020; 100nM, 25µl diluted in RPMI) was added to each well. Cells were visualised using a fluorescence microscope (Nikon Eclipse TE300, Surrey, UK) using a x20 objective lens and images captured by digital camera (Nikon CoolPix 450, Surrey, UK).

2.5.3. Stimuli used to induce NETs

The stimuli listed in Table 2.3 were used for *in vitro* stimulation of peripheral neutrophils for the assay of NET production. All stimuli were diluted in RPMI to their respective concentrations.

Table 2.3. Stimuli used to induce neutrophil NET formation

Bacteria/other stimulus	ATCC number/ Supplier and Cat N^{o}	Concentration per well
Staphylococcus aureus (*S. aureus*, opsonised)	9144	3 x 10^7
Phorbol 12-myristate 13-acetate (PMA)	Sigma P8139	50nM
Hypochlorous acid (HOCl)	Sigma	0.75mM

2.6. Chemotaxis assay

2.6.1. Chemotaxis assay protocol

Neutrophils (1 x 10^6/ml) were suspended in RPMI supplemented with BSA (Sigma, A8412; 1.5µl/ml 7.5%). Coverslips (22mm x 22mm; VWR International, VWRI631-0125) were washed in HCl (0.2M) followed by sterile water and dried on filter paper. The coverslips were coated in BSA (400µl at 7.5%; Sigma A8412) and excess fluid was removed by aspiration. Immediately after aspiration, neutrophil suspension (400µl) was added and the coverslips were incubated for 30 min at room temperature. The Insall chamber (Muinonen-Martin *et al.* 2010) was used to study chemotaxis (Figure 2.3). The chamber was washed 3 times with RPMI (400µl). A large droplet of RPMI was left on the chamber after washing. After the 30 min incubation, the coverslip with the cell suspension was inverted and placed at the top of the chamber ensuring that the pipette loading bays were exposed. Excess fluid surrounding the coverslip and within the chemoattractant wells was removed using filter paper. Finally, desired chemoattractant or RPMI (70µl) were injected into the

chemoattractant well and cell movement analysed by microscopy. The chamber was viewed using a Zeiss Primovert microscope at x20 magnification and images were captured using a Q Imaging Retiga 2000R camera. Images were processed using Q proimaging software (Surrey, Canada) and generated every 30 seconds for a total of 40 frames creating a stack of 40 images.

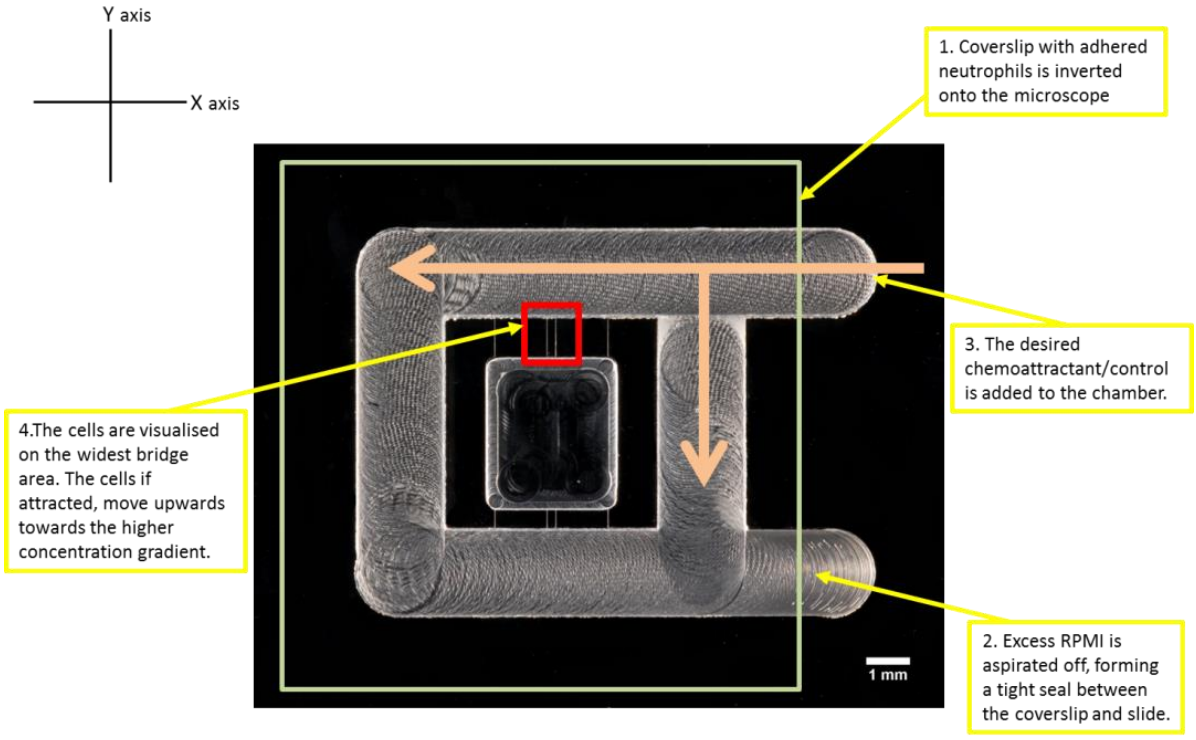

Figure 2.3. Schematic representation of the Insall Chamber

Aspiration of excess fluid from the inverted coverslip forms a seal allowing for the introduction of chemoattractant through the exposed wells.

2.6.2. Chemotaxis image analysis

The image stacks were analysed further using Image J 1.45SR software (Maryland, USA). The manual tracking plug-in MtrackJ (Meijering *et al.* 2012) was used and for each set of images and unless otherwise stated, 15 cells were chosen and tracked through the stack. The numerical data generated was then exported into excel and used to calculate cell speed, cell velocity and chemotactic index (CI) per experiment, which are defined in Figure 2.4. These measurements have been calculated using formulas derived by Sapey *et al.* (2011) and Muinonen-Martin *et al.* (2013) as shown in Figure 2.4. Statistical analysis of each parameter was calculated using Prism 5.0 software (GraphPad, USA).

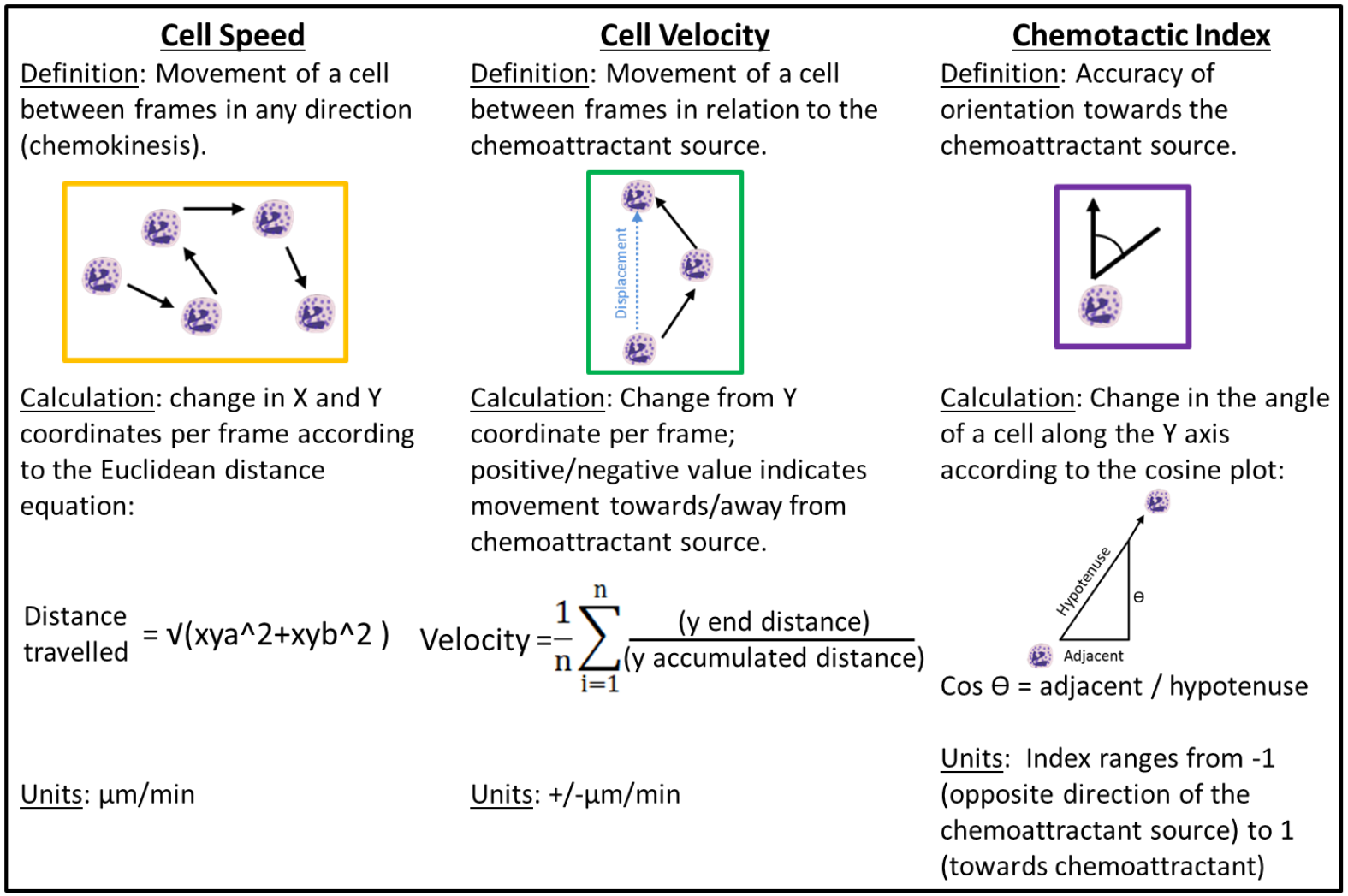

Figure 2.4 Chemotaxis parameters

Speed, velocity and chemotactic index (CI) were all used to provide an accurate profile of cell chemotaxis.

2.6.3. Circular statistics

The XY coordinates of the cell tracks were further analysed using the circular statistics (CircStat) toolbox from MATLAB software (Mathworks, USA) to ascertain the significance of the directionality of cell movement over the time course on an angular scale. Data was processed to yield circular rose plots, angle histograms and the mean resultant vector, which is a measure of the distribution of the cells on a quantifiable scale.

2.6.4. Stimuli used to induce chemotaxis

Table 2.4 shows all the chemoattractants, both bacteria and host-derived, used for the different studies outlined in this thesis. All were diluted in PBS (2.2.1.3) to their respective working concentrations. In addition, Cathepsin G (CG 25µg/ml; Sigma C4428) was pre-incubated (30 min at room temperature) with MIP1α (100ng/ml) in a particular study to demonstrate the effect of cleavage of the chemokine to induce chemotaxis.

Table 2.4. Chemoattractants used to induce neutrophil chemotaxis

Stimuli	Supplier/Cat No.	Concentration in chamber
Interleukin 8 (CXCL8)	Sigma SRP3098	200ng/ml
fMLP	Sigma F3506-5MG	10nM
MIP1α	R&D Systems 270-LD-010	100ng/ml
GM-CSF	Sigma SRP3050	20pg/ml

2.7. Neutrophil cell culture method for cytokine release

2.7.1. Supplemented RPMI for cell culture assay

RPMI (34.5ml; Sigma, R8758) was supplemented with glutamine (0.3g/l), foetal calf serum (20ml; Sigma, F4135 diluted to 10% in RPMI), HEPES (2.23g; Sigma, H4034 diluted in 20ml RPMI and adjusted for pH to 7.3) and streptomycin (100µg/ml; Sigma, P4333). The solution was filter sterilised using 0.22µm syringe filters (Millipore SLGVV255F) and the solution was stored for up to a week at 4°C prior to use.

2.7.2. Overnight culture of stimulated neutrophils

Neutrophils (100µl, 2.5 x 10^6 per well) were suspended in supplemented RPMI (2.7.1). An additional 300µl of supplemented RPMI was added to each well. After a 30 min incubation step at 37°C, stimuli/RPMI control (100µl) was added to the relevant wells and incubated for 18 hours at 37°C (Hatanaka *et al.* 2006). Post incubation viability was assessed using Trypan Blue exclusion (1:1 dilution) and cell counting. Cells were pelleted by centrifugation (10 min, 2000 rcf; SciSpin micro, Geneflow). The supernatants were collected and stored at -80°C for subsequent future measurements.

2.7.3. Stimuli used for overnight culture assay

Table 2.5 describes the various stimuli used to stimulate cytokine release from the neutrophils. LPS derived from *E. coli* (Sigma, L5543) was diluted with supplemented RPMI containing AB plasma (10% v/v; Sigma, H4522). All handling of LPS was done so using siliconized tips (Sigma, Z719595) and eppendorfs (Sigma, T3281). All other bacterial stimuli were diluted in RPMI to desired concentrations.

Table 2.5. Stimuli used during overnight cell culture.

Multiplicity of infection (MOI) respresents the number ratio of bacteria to neutrophils.

Bacteria/ other stimulus	ATCC number/ Supplier and Cat No.	Concentration per well	Anaerobic / aerobic	Bacteria/ ml if OD_{600}=1	Multiplicity of infection (MOI)
E. coli LPS	Sigma, L5543	5µg/ml	-	1.62×10^9	-
F. nucleatum	10953	3×10^7	Anaerobic	6.80×10^9	300:1
A. actinomycetemcomitans b	43146	3×10^7	Anaerobic	1.69×10^8	300:1
Opsonised *S. aureus*	9144	1.5×10^7	Aerobic	1.69×10^9	150:1

2.8. Storage and preparation of bacterial stimuli.

For use as neutrophil stimuli, anaerobic and aerobic periodontal bacteria were originally obtained from the Forsyth Institute (Boston, USA) or purchased from the American Type Culture Collection (ATCC: *F. nucleatum*) with the exception of *T. forsythia* which was provided by Mike Milward. All bacteria were stored at -80^{o}C in 2ml cryovials containing 1.5ml tryptone soya broth supplemented with DMSO 10% v/v.

To grow the bacteria, the frozen aliquots were defrosted at room temperature, inoculated (100µl) and spread onto agar plates using a sterile loop. After 3-5 days of growth subsequent cultures were grown by inoculating broths by scraping a single colony using a sterile loop. Broth cultures were incubated overnight in order to reach stationary growth phase (approx. 10^9/ml). Broth concentration was monitored using additional agar plates inoculated from broth cultures. The bacterial broth suspensions were pelleted and then washed twice with PBS by centrifugation (3,000 rcf, 10 min) and, heat-killed (60 min at 85^{o}C) whilst suspended in sterile PBS. A portion of the suspension was also re-inoculated onto agar plates to ensure the bacteria were dead. Bacterial numbers were estimated from the PBS suspension using a

spectrophotometer (Jenway 6300) at optical density 600nm (OD_{600nm}). The OD_{600nm} values used to estimate bacterial growth were calculated by the Forsyth Institute, Boston and are listed in Table 2.6. All bacteria were stored at -20°C.

Table 2.6. Bacteria used in neutrophil assays

Bacterial strain	ATCC number	Anaerobic/ aerobic	Bacteria/ml if OD_{600}=1	Multiplicity of infection (MOI)
F. nucleatum subsp. *polymorphum*	10953	Anaerobic	1.62×10^9	300:1
A. actinomycetemcomitans b	29523	Anaerobic	6.80×10^9	300:1
Opsonised *S. aureus*	9144	Aerobic	1.69×10^8	150:1
Streptococcus constellatus	27823	Anaerobic	1.69×10^9	500:1
Actinomyces viscosus	43146	Anaerobic	8.30×10^8	300:1
Tanerella forsythia	43037	Anaerobic	8.30×10^8	300:1

2.8.1. Preparation of anaerobic bacteria

Agar and broths were used as described in Table 2.7. Bacteria were grown on blood agar plates in an anaerobic chamber (Don Whitley Scientific, Modular Atmosphere Controlled System, CAL-3200, Shipley, UK) with carbon dioxide (9.97%), hydrogen (9.92%) with nitrogen balance at 37°C. Colonies were subsequently picked off the plates and grown in brain heart infusion (BHI) broth, aliquoted into 10ml batches and autoclaved (121°C, 15min). Broths not immediately used were stored at 4°C for up to three weeks.

2.8.2. Preparation of Opsonised *S. aureus*

S. aureus was grown aerobically in a 5% CO_2 chamber (Gallenkamp Plus II Incubator) at 37°C on tryptone soya agar (TSA) plates which were autoclaved at 121°C for 15min. After cooling to approximately 40°C the liquid was poured into petri dishes (Sterilin 101/IRR) and

allowed to set. The plates were stored at 4^{o}C for up to 3 weeks when not in use. Plate colonies of *S. aureus* were subsequently grown overnight in tryptone soya broth (TSB) which was separated into 10ml aliquots and autoclaved. Broths not immediately used were stored at 4^{o}C for up to three weeks. After washing in PBS, bacterial density was determined spectophotometrically (section 2.8). For opsonisation the suspension was further diluted in sterile PBS to give a suspension of 1x10^{9} bacteria per ml. The bacteria were heat treated by incubation at 80°C for 20 min prior to the addition of 33µl Vigam liquid (5mg/ml IgG; Bio Products Laboratory) per ml of bacteria and incubated overnight at room temperature with constant agitation to allow opsonisation. Following incubation the bacteria were again washed twice in sterile PBS by centrifugation and re-suspension, and stored at -80°C. Bacterial numbers were again estimated by spectrophotometry to allow resuspension in PBS to give 6x10^{8}/ml prior to use.

Table 2.7. Preparation of agar and broths for bacterial growth

Bacteria	Growth media	Supplier/Cat No.	Preparation
Anaerobic	Blood agar	Oxoid, CM2071	Ready to use
	Brain Heart Infusion (BHI) broth	Oxoid, CM1135	37g in 1 L dH_2O
Aerobic	Tryptone Soya Agar (TSA)	Oxoid, CM0131	20g in 500ml dH_2O
	Tryptone Soya Broth (TSB)	Oxoid, CM0129	10g in 1 L dH_2O

2.8.3. Identification of bacteria by Gram stain

Bacterial colonies were picked off agar plates using a sterile loop and emulsified in a droplet of distilled water on a microscope slide. The slide was then passed several times through a flame to evaporate the liquid and fix the bacteria. Crystal violet (2g in 20ml 95% ethanol;

Sigma, C0775), mixed 1:1 with ammonium oxalate (1%, 0.8g in 80ml distilled water; Sigma A8545) was added for 30 seconds followed by the addition of Lugol's iodine (Sigma, L6146) for another 30 seconds after which the slide was rinsed with distilled water. Acetone was added and immediately rinsed with water. Finally the slide was treated with carbol fuchsin (1ml diluted with 9ml distilled water; BDH, 351874U) for 30 seconds and rinsed with distilled water. After blotting dry, the slide was viewed under oil immersion microscope (Leitz Dialux 22). Images were captured using a digital camera (Nikon Coolpix 990) and are shown in Figure 2.5.

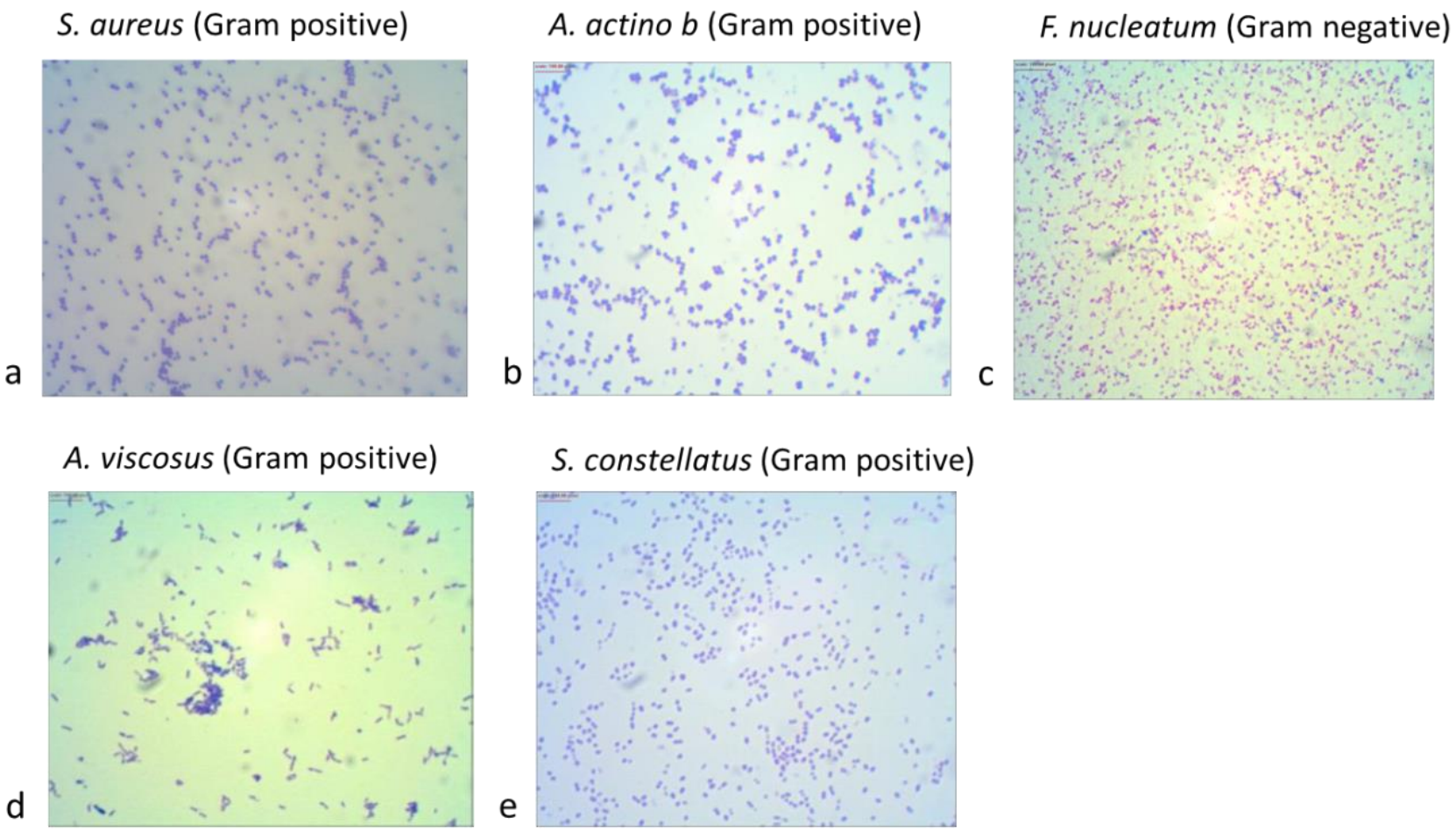

Figure 2.5. Photographs of cultured bacteria used as neutrophil stimuli

Gram stains of grown bacteria: a = *S. aureus* (Gram positive), b = *A. actinomycetemcomitans b* (Gram positive), c = *F. nucleatum* (Gram negative,), d = *A. viscosus* (Gram positive), e = *S.constellatus* (Gram positive). x20 magnification.

2.9. Protein quantification from biological samples

The protein content of collected GCF and plasma samples were measured using the bicinchoninic acid (BCA) protein assay as previously described (Smith *et al.* 1985).

2.9.1. Bicinchoninic acid (BCA) assay preparation

Plasma samples were diluted 1:100 with distilled water. GCF samples were used neat. Standards (ranging 0-1mg/ml) were made using BSA (Sigma, P0834) diluted in PBS.

2.9.2. BCA assay protocol

BCA reagent (Sigma, B9643) was added to copper (II) sulphate solution (Sigma, B9643) at a 1:50 dilution and 200µl was added to each well of a 96 well microplate (Corning, 3591). Standard/sample (10µl) was added to their corresponding well and incubated (30 min, 37^{o}C). Absorbance was measured immediately after in a microplate reader (BioTek ELx800) at a wavelength of 570nm.

2.10. Cytokine/protein quantification from oral health and disease samples

2.10.1.IL-1β and TNFα detection by ELISA

2.10.1.1. IL-1β and TNFα ELISA reagent preparation

TNFα and IL-1β were quantified from GCF samples using commercially available kits (Thermo Scientific, EH3TNFA and KHC0011 respectively). All GCF samples were diluted 1:6 with sterile PBS. Standrards (ranging 0-250pg/ml for IL-1β and 0-1,000 pg/ml for TNFα) were diluted 1:2 using provided reagent diluent.

2.10.1.2. IL-1β and TNFα ELISA protocol

Standard/pre-diluted test samples (50µl) were added in duplicate to relevant wells. Biotinylated anti-IL-1β/ TNFα solution (100µl) was added per well and the plate was sealed and incubated at room temperature for 2 hours. After a manual wash step (400µl per well, aspirated and repeated x4) using wash buffer, streptavidin-HRP (100µl) was added and the plate was sealed and incubated for 30 min at room temperature. After a repeat wash step chromogen substrate (100µl) was added to each well. The plate was incubated in darkness at room temperature for 30 min after which Stop Solution (100µl) was added. Absorbance was immediately measured using a microplate reader (BioTek ELx800) at 450nm.

2.10.2.LL-37 detection by ELISA

2.10.2.1. LL-37 ELISA reagent preparation

LL-37 was quantified from plasma and cell culture supernatant samples using a commercial ELISA kit (Hycult Biotech, HK321). Plasma samples were diluted 1:100 with diluent buffer and cell culture supernatants were used neat. Standards, ranging 0-100ng/ml were diluted serially (1:2) using diluent buffer.

2.10.2.2. LL-37 ELISA protocol

Standard/pre-diluted test sample (100µl) was added in duplicate to relevant wells. The plate was covered with an adhesive seal and incubated for 1 hour at room temperature with mild agitation (Luckham R11/TW, speed 2), after which the plate was washed 4x using wash buffer (300µl per well). Tracer solution (100µl) was added and the plate was incubated again for 1 hour at room temperature. After a repeat wash step, strepavidin-peroxidase solution (100µl) was added to each well and incubated again for 1 hour at room temperature. Post

incubation the plate was washed and 3,3',5,5'-Tetramethylbenzidine (TMB; 100µl) substrate was added to each well and the plate was wrapped in aluminium foil to exclude light and incubated for 30 min at room temperature. Finally oxalic acid stop solution (100µl) was added and absorbance was read immediately using a microplate reader (BioTek ELx800) at 450nm.

2.10.3. Neutrophil elastase (NE) detection by ELISA

2.10.3.1. NE ELISA preparation

Neutrophil elastase (NE) was quantified from plasma and cell culture supernatants using a platinum ELISA kit (eBioscience, BMS269). All plasma samples were diluted 1:100 using sample diluent and cell culture supernatants were used neat in the assay. Standards (ranging 1-10ng/ml) were diluted with reagent diluent.

2.10.3.2. NE ELISA protocol

Standard/pre-diluted test sample (100µl) was added to the relevant wells (in duplicate) of the provided antibody-coated microwell plate, covered with an adhesive film and incubated on a microplate shaker (set to 400rpm) at room temperature for an hour. Post incubation the plate was washed 4 times with wash buffer (300µl), after which HRP-Conjugate anti-α_1-PI polyclonal antibody (150µl) was added per well and the plate was covered and incubated again at room temperature for an hour with agitation (Luckham R11/TW, speed 2). After another wash step, TMB (200µl) substrate solution was added to all wells, the plate was wrapped in aluminium foil to exclude light and incubated at room temperature for up to 20 min. Stop solution (50µl; 2M HCl) was subsequently added to all well and absorbance was read immediately using a microplate reader (BioTek ELx800) at 450nm.

2.10.4. Protein carbonyl detection by ELISA

2.10.4.1. Protein carbonyl ELISA reagent preparation

Plasma carbonylation, was measured in samples as previously described (Carty *et al.* 2000) and recently reviewed (Augustyniak *et al.* 2015). Oxidised BSA standards were kindly provided by Dr Irundika Dias (Aston University). BSA (Sigma P0834) (40mg/ml) was reduced with ascorbic acid (25mM) and ferrous ammonium sulphate (0.1mM) diluted in PBS containing EDTA (1mM). Plasma samples were all diluted to give 20µg/ml as measured by the BCA assay (2.9.2). The samples were diluted in sodium carbonate buffer (50mM; 1.59g Na_2CO_3 with 2.93g $NaHCO_3$/L distilled water; pH 9.2) and used immediately. 0.05% and 1% Tween-20 (Sigma, P2287) were prepared by diluting 1:2000 and 1:100 with PBS respectively. Di-nitrophenol hydrazine (DNPH; Sigma, D199303; 10mM) was prepared by diluting in 2M HCl. OPD substrate was prepared by adding a 20mg o-phenylenediamine tablet (Sigma, P5412) to 10ml of citrate buffer (0.15M; 49ml of 21g/l citric acid added to 51ml 35.6g/l Na_2HPO_4; pH 5) with 10µl 8.8M hydrogen peroxide (Sigma, 516813) immediately before use.

2.10.4.2. Protein carbonyl ELISA protocol

Oxidised BSA standard or diluted plasma sample (50µl at 20mg protein/ml) was added in duplicate to a clear Nunc-Immuno 96 well microplate (Sigma, M5785); the plate was covered with aluminium foil and incubated for 1 hour at 37^{o}C. The plate was washed 3 x using PBS containing 0.05% Tween-20 (200µl/well), after which di-nitrophenol hydrazine (50µl/well) was added to derivitise the standards/sample and the plate was incubated covered at room temperature for 1 hour. After a repeat wash the plate was blocked with PBS Tween-20 1% (200µl/well) and incubated overnight at 4^{o}C. Post incubation the plate was washed as before, and antiserum mouse IgE antibody (Sigma, D8406; 50µl/well; diluted 1:2000 in PBS Tween-

20 1%) was added and the plate was incubated covered at 37^{o}C for 2 hours. After re-washing the plate, peroxidase labelled rat anti-mouse IgE secondary antibody (50µl; diluted 1:500 in PBS Tween-20 1%; Sigma, A9044) was added, and the plate was covered and incubated for 1 hour at 37^{o}C. Post incubation the OPD substrate (50µl/well) was added and the plate was incubated covered at room temperature for 15 min. H_2SO_4 (25µl; 2M) stop solution was added per well and the plate was immediately read at 490nm on a microplate reader (BioTek ELx800).

2.10.5. S100A-8/9 detection by ELISA

2.10.5.1. S100A-8/9 ELISA reagent preparation

S100A-8 and S100A-9 proteins were quantified from plasma and cell culture samples using Duoset Sandwich ELISA kits (R&D Systems, DY4570 and DY5578 respectively). All additional reagents required were from the DuoSet Ancillary Reagent Kit 2 (R&D Systems, DY008). All plasma and culture supernatants were used neat. Standards (ranging 31.3-2000pg/ml) were diluted 1:2 in PBS 1% BSA (section 2.4.1.1).

2.10.5.2. S100A-8/9 ELISA protocol

Capture antibody (100µl; 4µg/ml diluted with PBS 1% BSA) was added to each microplate well. The plate was sealed and incubated overnight at room temperature. After incubation the fluid was aspirated from each well and washed 3 x with wash buffer (300µl). The plate was blocked with ELISA plate-coating buffer (200µl) and incubated at room temperature for 1 hour. After a repeat wash step the plate was ready to use.

Sample/standards (100µl/well) were added to the appropriate wells. The plate was sealed and incubated for 2 hours at room temperature. After a repeat wash step detection antibody (100µl/well; 500ng/ml diluted with PBS 1% BSA) was added and the plate was incubated for

2 hours at room temperature. After a repeat wash, streptavidin-HRP (100µl/well; diluted in PBS 1% BSA) was added and the plate was incubated for 20 min at room temperature. Post-washing, substrate solution (100µl/well) was added per well and the plate was incubated foil-wrapped for up to 20 min. Stop solution (50µl/well; 2M H_2SO_4) was added and absorbance was immediately read using a microplate reader (BioTek ELx800) at 450nm.

2.10.6. Cytokine detection by Luminex assay

2.10.6.1. Luminex assay reagent preparation

Procartaplex™ multiplex immunoassays (Affymetrix eBioscence) were used to quantify the cytokines IL-1β (EPX010-10224-901), CXCL8 (EPX010-10204), IL-6 (EPX010-10213-901), TNFα (EPX010-10223-901), MIP1α (EPX010-12029-901) and the enzyme MMP-9 (EPX010-12016-901) from patient and control plasma, and cell culture supernatants. For cytokine quantification both plasma and cell culture supernatants were used neat. For MMP-9, plasma was diluted 1:50 with universal assay buffer and cell culture supernatants were used neat. Standards were re-constituted in supplemental RPMI (2.7.1) for cell culture supernatants and universal assay buffer for plasma samples (50µl). Each separate standard type was then vortexed for 30 seconds and after centrifugation (2000 rcf for 10 seconds) the standards were incubated on ice for 10 min to ensure complete reconstitution. The entire contents of each standard were pooled and after a repeat vortex and centrifugation step was diluted 4-fold serially using the appropriate diluents.

2.10.6.2. Luminex assay protocol

All antibody magnetic beads for the respective analytes were pooled; the pool was vortexed and 50µl was added to each microplate well after which the plate was immediately inserted into a hand-held magnetic plate washer and incubated at room temperature for 2 min. The

plate was then washed with wash buffer (150µl/well) and removed from the magnetic plate. For plasma sample analysis, universal assay buffer (25µl) was added to wells followed by plasma (25µl). For cell culture supernatants, only samples (50µl) were added to their respective wells. Standard (50µl) were added to relevant wells; plasma standards were pre-diluted 1:2 with universal assay buffer. The plate was sealed, covered with a black microplate lid and incubated at room temperature with agitation (Luckham R11/TW, speed 2) for 2 hours. After a repeat washing step using the plate within the magnetic plate washer, each detection antibody (25µl/well) was added to every well, sealed and covered, and incubated with agitation at room temperature for 30 min. After two repeat wash steps, streptavidin-PE (50µl/well) was added to each well and the plate was incubated with agitation for 30 min. After two repeat washes, reading buffer (120µl/well) was added to each well and the plate was sealed and incubated with agitation for 5 min. Mean fluorescence intensity (MFI) was then measured on a Luminex 100/200 (USA) in the Clinical Immunology labs at the University of Birmingham. Data was recorded and processed using xPONENT® software (USA).

2.11. Neutrophil function in inflammatory states

2.11.1.Neutrophil function in gingivitis

Section 2.1.2 details the volunteers recruited for the study of neutrophil function in gingivitis. For each volunteer moulds of their upper mandible were taken in order to construct a soft vinyl mouth guard (Figure 2.6) to cover the maxillary left 4-6 teeth to be worn during brushing to shield the area from mechanical or chemical cleaning. The maxillary right 4-6 teeth (undergoing normal hygiene practices) were used as control teeth. For the entirety of the study volunteers were asked to refrain from chewing gum or using mouthwashes. The study period (Figure 2.7) consisted of an initial pre-baseline assessment (day -14) in which

impressions were taken for mouth guard construction and the teeth were professionally cleaned. Two weeks following (baseline, day 0), the mouth guard was worn during brushing for 3 weeks (up to day 21). At day 21 plaque was removed by prophylaxis and normal hygiene practices resumed. Participants were assessed again after resolution of inflammation (day 35). Gingivae were assessed throughout the study (days 0, 7, 14, 21 and 35).

Figure 2.6. Photograph of an example mould and mouth guard

These were prepared for each volunteer.

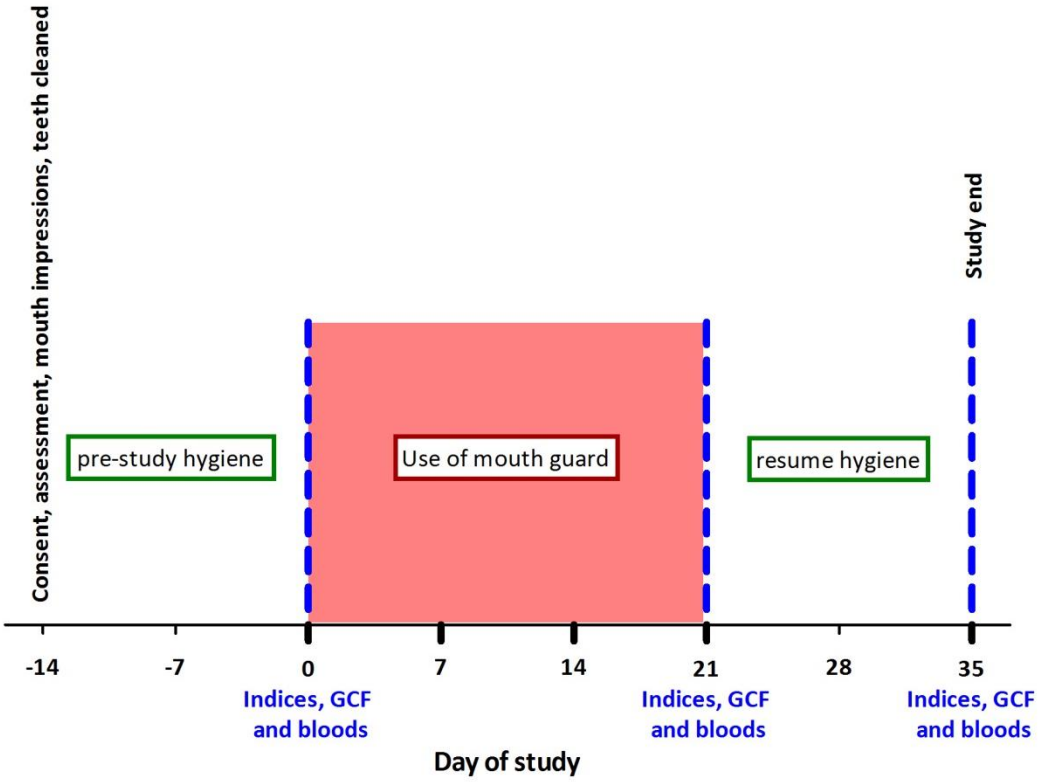

Figure 2.7 Schematic diagram of gingivitis study time frame

2.11.1.1. Clinical gingival inflammation measurements in 21-day gingivitis

The progression of gingival inflammation over the course of the study was measured by gingival index (GI) scores 0-3 (Löe *et al.* 1967), plaque index (PI) using a modified Quigley-Hein index, scores 0-5 (Lobene *et al.* 1982) as outlined in Figure 2.8 and Table 2.8 respectively. GCF volume was measured using a Periotron 8000™ (Oraflow, USA). Gingival and plaque scores were recorded by Dr Martin Ling and GCF volume by Professor Iain Chapple.

Table 2.8 Gingival Index (GI)

(Löe *et al.* 1967)

Gingival Index		
Score	Bleeding	Appearance
0	None	Normal
1	None	Mild edema
2	Bleeding on probing	Redness, edema
3	Spontaneous bleeding	Marked redness, edema, ulceration

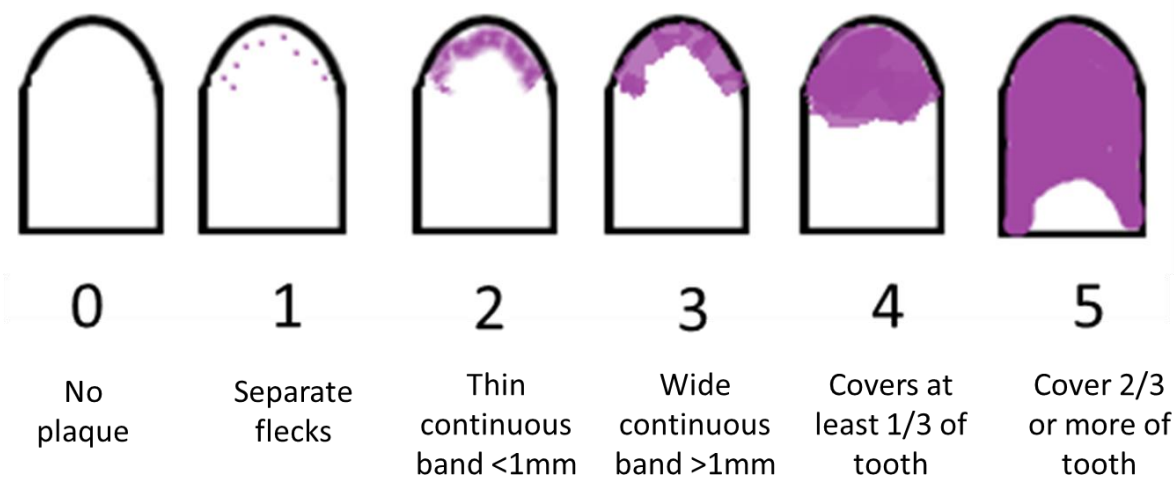

Figure 2.8. Quigley-Hein Plaque Index and description

Taken from (Lobene *et al.* 1982).

2.11.1.2. Gingival crevicular fluid (GCF) sampling and processing

GCF samples were collected from the volunteers using Periopaper strips (OraFlow, USA) inserted into the mesio-buccal gingival crevices of both test and control sites for 30 seconds as originally reported by Chapple *et al.* (2007). GCF strips from each control/test site (3 from each side) were pooled into Eppendorf tubes containing PBS supplemented with BSA (0.05%, 200µl; 50mg/L). The tubes were incubated at room temperature for 30 min to allow GCF to elute, after which the strips were trapped within the lid of each tube. After centrifugation (10 min, 2000 rcf; SciSpin micro, Geneflow, UK), the lid and strips were removed and the GCF diluent was filter sterilised using 0.22µm syringe filters (Gilson Scientific, ANV1322) to remove any cell debris/microbes and stored at -80°C prior to further use.

2.11.2. Neutrophil chemotaxis in chronic periodontitis

Section 2.1.3 details the volunteers recruited for the study of neutrophil chemotaxis in chronic periodontitis. Chronic periodontitis was defined by the European Federation of Periodontology (Tonetti & Claffey 2005) as a minimum of 2 non-adjacent sites per quandrant with probing pocket depths exceeding 4mm and radiographic bone loss above 30%. Whole blood (48ml) was collected in lithium heparin vacutainers (Greiner, Bio-One) at baseline (prior to treatment) and after treatment. Patient treatment involved tailored oral hygiene instruction, non-surgical scaling and root surface debridement of periodontal pockets exceeding 4mm. 3 months post-treatment, attended a second therapy appointment. At the same time (before and after treatment), a blood sample was also taken from age and sex-matched periodontally healthy controls using the same exclusion criteria. The healthy control group showed no interproximal attachment loss, a low mouth bleeding score (less than 10%) and no probing pocket depths exceeding 3mm.

2.11.2.1. Clinical measures of gingival inflammation in chronic periodontitis

The severity to which patient cohort 1 (as outlined in section 2.1.3.1) suffered periodontitis was measured by Dr Martin Ling using several parameters including gingival index, plaque index, clinical attachment loss (CAL) probing pocket depth (PDD) and bleeding on probing (BOP). PI and GI were also measured as outlined in section 2.11.1.1. Periodontal health of volunteers was also confirmed by Dr Martin Ling. All clinical parameters were measured immediately prior to blood collection for neutrophil assays.

The additional 10 chronic periodontitis patients in cohort 2 (outlined in section 2.1.3.2) were all confirmed as having generalised chronic periodontitis by an experienced examiner.

GCF was collected from all periodontitis patients using periopapers and volume was measured using a pre-calibrated Periotron 8000TM (Chapple *et al.*, 1999).

2.11.3. Neutrophil function in Papillon-Lefèvre Syndrome

Section 2.1.4 details the volunteers recruited for the study of neutrophil function in Papillon-Lefèvre Syndrome (PLS). Whole blood (18ml) was collected from each volunteer patient/control in lithium heparin vacutainers on the same day.

2.11.4. Neutrophil function in chronic inflammation: morbid obesity

Section 2.1.5 details the volunteers recruited for the study of neutrophil function in morbid obesity. Initial patient awareness to the study involved the use of a PowerPoint slide (Figure 2.9) during patient attendance at a seminar run by dieticians at Heartlands Hospital. Patients indicated verbally if they would be interested in taking part in the study at the seminar. Written consent was taken upon meeting with the surgeon Mr Paul Super, several weeks after their attendance at the dietician's seminar.

Blood samples were taken at three different time points (Figure 2.10.) during patient attendance at bariatric clinical appointments. The first blood sample was taken prior to commencement of a very low calorie diet, involving 500 calories a day intake for up to 8 weeks before surgery (time point 1). A second blood sample was taken at the patient pre-operative assessment (time point 2) and a final blood sample was taken 3 months following surgery (time point 3). At each time point, whole blood (~30ml) was collected per patient and control in lithium heparin vacutainers at the same time as coordinated between the two hospitals. Blood samples from Heartlands Hospital were transported, at ambient temperature with minimal disturbance, firstly to the Human Biomaterials Resource Centre (HBRC) at the University of Birmingham to be anonymised and then immediately on to the School of Dentistry where all experimentation took place. In the interim (up to 4 hours) the control blood samples were incubated at room temperature without agitation.

2.11.4.1. Blood chemistry measurements

Glycated haemoglobin (HbA1c) was measured using a HemoCue® HbA1c 501 blood analyser (HemoCue, Sweden) from collected whole blood at all three sample donations. Blood lipids high density lipoprotein (HDL), low density lipoprotein (LDL), cholesterol and triglycerides (TG) were also measured from whole blood using a CardioChek PA Blood Analyser (BHR Pharma, UK).

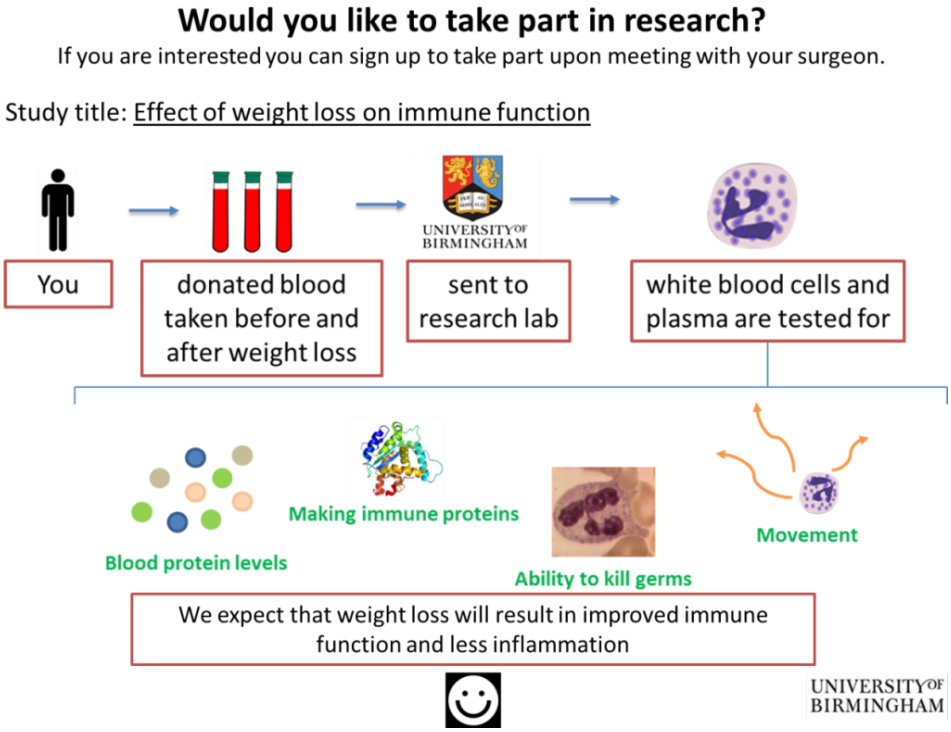

Figure 2.9. Information supplied to patients during seminar

The slide was presented to prospective patient volunteers by dietitians at Heartlands hospital.

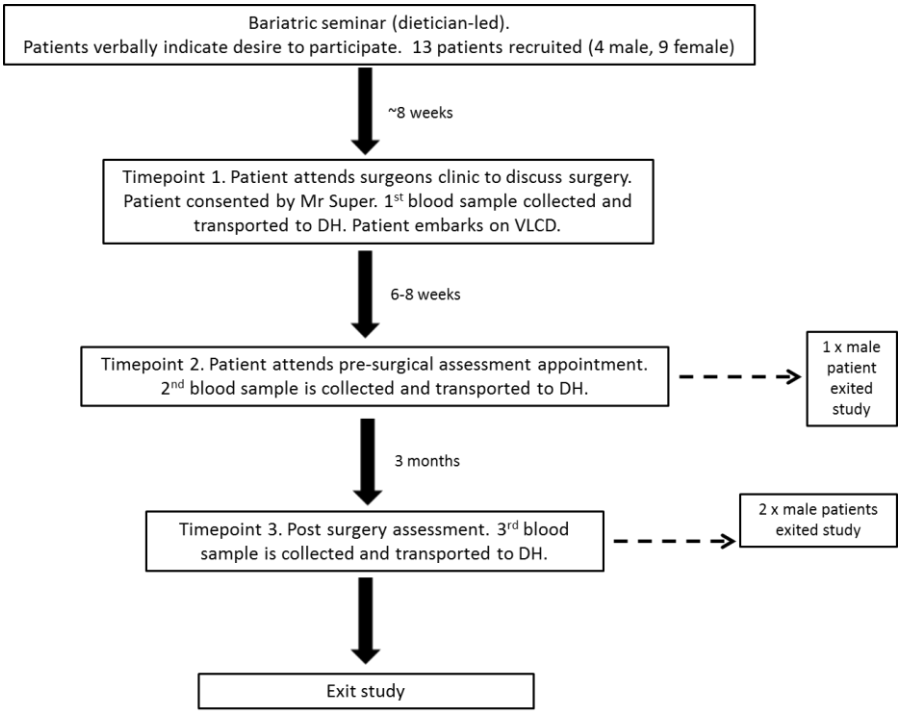

Figure 2.10. Flow diagram of bariatric patient study

VLCD = very low calorie diet, DH = dental hospital.

2.12. Statistical analysis

All data was processed using Microsoft Excel and statistically evaluated using Graphpad Prism 5.0 (GraphPad Software Inc, California, USA). The distribution of datasets (parametric or non-parametric) was initially assessed using the Kolmogorov-Smirnov test for normality. For paired datasets that featured parametric distribution, a paired T test was used; multiple datasets used ANOVA with Tukey post-test. Paired datasets with non-parametric distribution used Wilcoxon test; multiple datasets used Friedman test with Dunn's post-test. Unpaired datasets with non-parametric distribution used Mann-Whitney test; multiple datasets used Kruskal-Wallis test with Dunn's post-test. $P \leq 0.05$ was deemed significant for all data sets.

2.13. Summary of experiemtnal assays per study

Table 2.9 Assays used per clinical study

Assay	Experimental gingivitis	Chronic Periodontitis	PLS	Obesity
ROS assay	✔		✔	✔
NETs assay	✔		✔	✔
Chemotaxis assay	✔	✔	✔	✔
Cell culture			✔	✔
Cytokine ELISA	✔	✔		
LL-37/NE/protein carbonyl/S100A-8/9 ELISA			✔	
Luminex assay			✔	✔

CHAPTER 3 RESULTS - OPTIMISATION OF CHEMOTAXIS

3.1. Introduction

The Insall chamber was chosen for the study of neutrophil chemotaxis. Originally developed to study the movement of *Dictyostelium discoideum* (Phillips & Gomer 2012; Choi *et al.* 2013; Kaul *et al.* 2013; a Herlihy, Tang, *et al.* 2013; Herlihy, Pilling, *et al.* 2013; Muinonen-Martin *et al.* 2010), this bridge chamber can be adapted to study fast moving cells making it appropriate to study neutrophils. The chamber was chosen because of the potential to provide detailed information regarding the kinetics of neutrophil movement in an easy, efficient and reproducible manner. A particular focus was on clinical samples for which additional assays of neutrophil function were employed simultaneously. The optimisation of this technique for use with neutrophils is detailed in this chapter.

3.2. Determination of cell viability over time

Neutrophil viability post-isolation from whole blood was determined to ensure cells retained relevant functional capacity for analysis in the chemotaxis assay. Initial incubation on the coverslip was for 20 minutes and each video was captured for up to 20 minutes in length. As one assay preceded another, pilot data demonstrated that cells not utilised immediately could be incubated at room temperature for up to four hours (Figure 3.1). Neutrophils isolated initially from whole blood were typically >98% trypan blue-free. There was a significant difference in viability between immediate, one, and two hours post-isolation compared with 4 hours post-isolation, showing that beyond 3 hours post isolation, cell viability was compromised, however over 90% of the cells remained viable beyond this time as loss of viability relative to "immediate" use was $\leq$5%. Therefore a limit of four hours was imposed on future assays to balance the logistics of running multiple assays within acceptable cell viability.

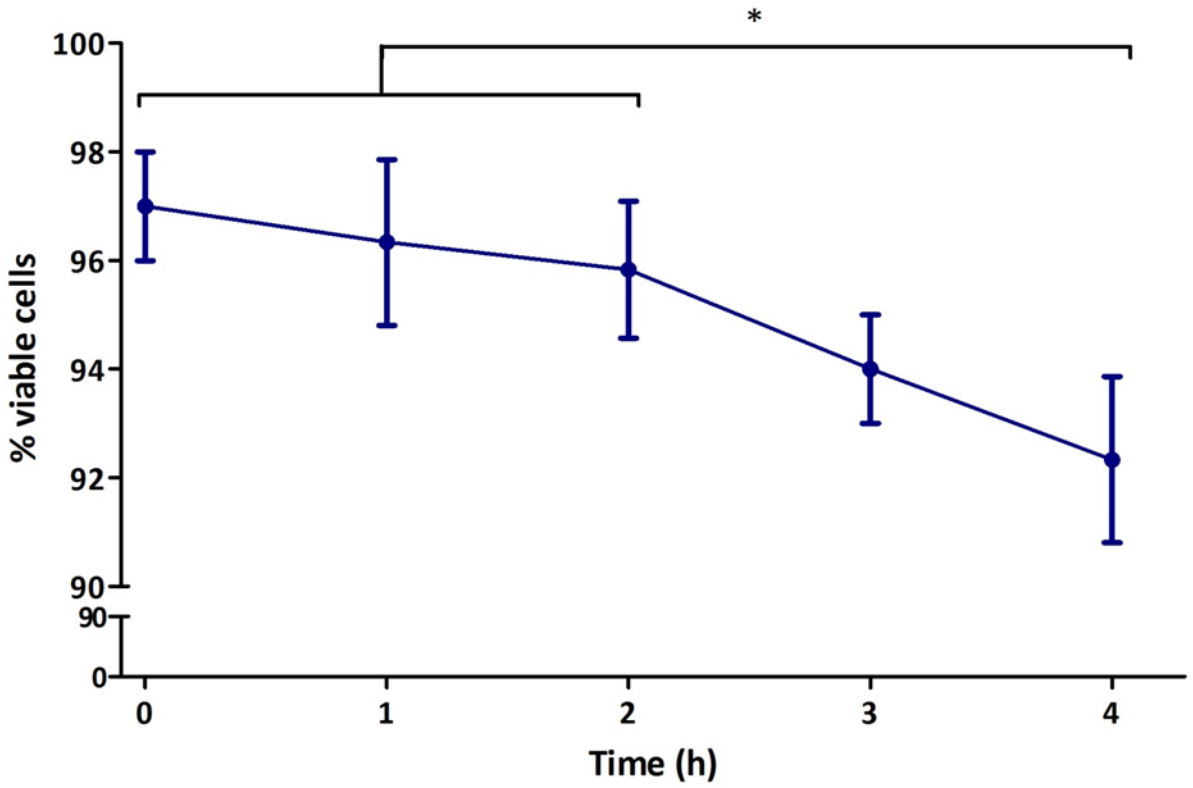

Figure 3.1 Neutrophil viability over time post-isolation

Neutrophils were isolated (section 2.2) and viability (section 2.2.2) over time was assessed over 4 hours. Data expressed as mean ± standard deviation (SD). Statistical test: One Way ANOVA and Tukey's multiple comparisons test (n = 3 neutrophil isolations). * = ($p < 0.05$).

3.3. Cell magnification employed in chemotaxis assays

The fastest average recorded speed for neutrophil movement is approximately 10μm/min using the strong chemoattractant N-Formylmethionyl-leucyl-phenylalanine (fMLP) at 10nM (Worthen *et al.* 1994). With a time course of 20 minutes, a cell could therefore potentially travel 200μm. The microscope employed to film cell movement featured magnification settings of x10, x20 and x40. Figure 3.2 illustrates the extent to which a neutrophil may travel if positioned within the centre of the microscope frame using the three different magnifications. The images demonstrate that a cell viewed with an objective lens at a x20 magnification would be unlikely to leave the frame, whereas for a x40 the cell would be more likely to leave the frame. The potential length a cell could travel when visualised using a x10 objective lens represents only a small area of the whole image. In addition, the small size of the cells at this magnification is such that ensuring the centre of each cell is selected for movement tracking is more difficult, potentially increasing the likelihood of tracking errors when analysing resultant videos. Thus a magnification of x20 was chosen for all future assays.

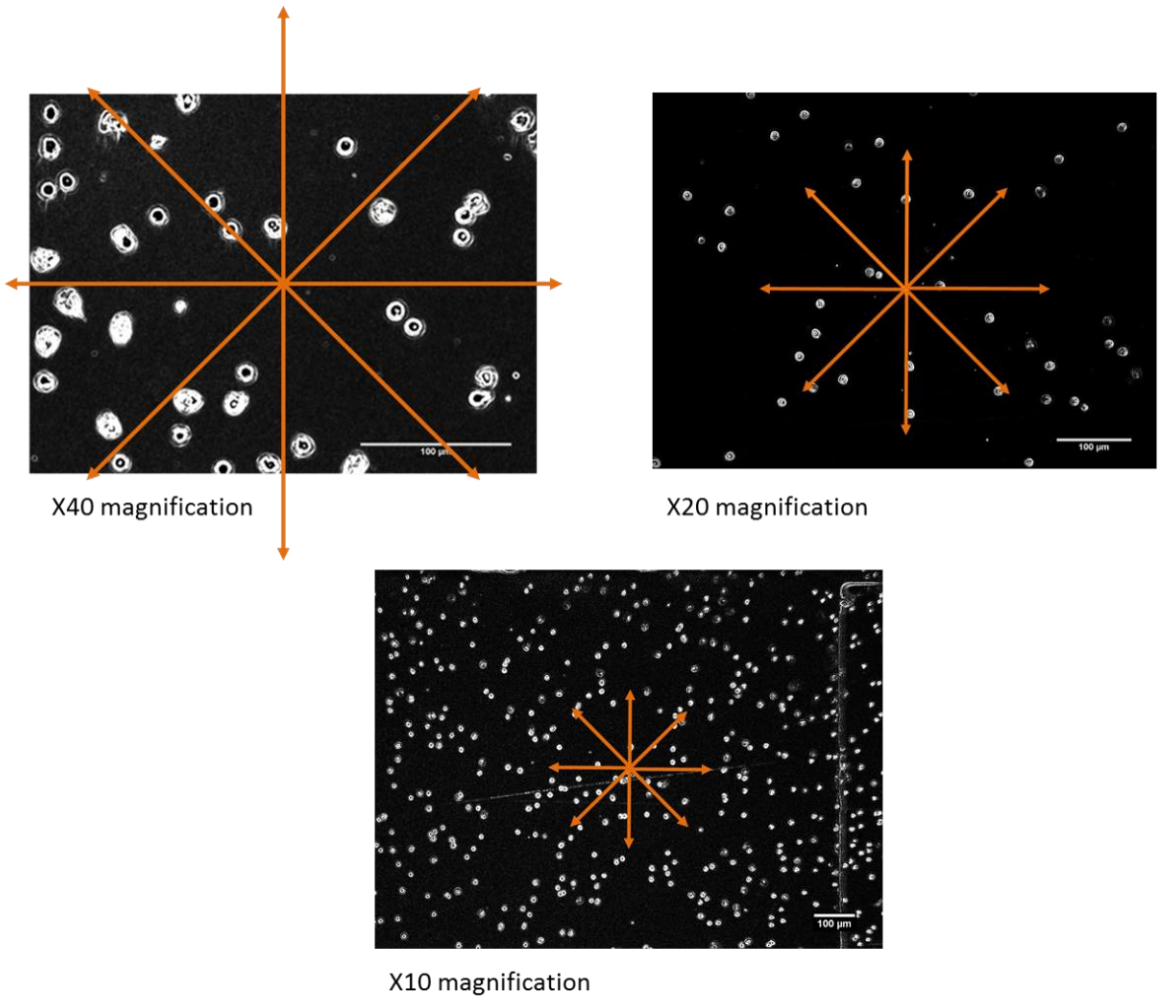

Figure 3.2 Cell magnification for chemotaxis assay

The images detail the extent to which neutrophils could travel (orange arrows) in 20 minutes within the frame of different objective lenses after exposure to the strongest chemoattractant fMLP (10nM). Bars (white) represent 100µm.

3.4. Visualisation and circular statistics to analyse neutrophil chemotaxis

Figure 3.3a-c illustrates the tracking of selected cells in response to a chemoattractant using the Insall chamber. One type of image output, “spider diagrams”, provides a simple visual summary of the tracks of selected cells. Circular statistics provide the opportunity to analyse datasets on an angular scale, providing information about the average direction of movement within a group of cells, in the form of “polar plots” and “angle histograms” (descriptive statistics). Figure 3.4 shows example graphs using the Circular Statistics Toolbox of MATLAB for RPMI (negative control) and the chemoattractant fMLP (10nM). Polar plots (Figure 3.4a and b) detail the mean angle of the data points, known as the mean resultant vector (MRV). MRV length (MRVL) denotes the strength of the mean angle (red line): the longer the line the more data there is to support the angle reported. The MRVL quantifies the measurement of circular spread of the samples on the angular scale; it ranges from 0 to 1, the closer to 1 the more concentrated the data points are around the mean direction (Berens 2009). Dashed lines represent MRV confidence intervals (95%). A mean angle close to 90 degrees is in the direction of the chemoattractant (which is at the 12 O’clock position on these representations). Angle histograms (Figure 3.4c and d) show the distribution of values grouped in angle bins (5 angle bins) reflecting their numeric range. For RPMI the cells are distributed widely, thus the MRVL is short; clearly showing the distribution of cells is random. For fMLP (10nM) the MRVL is in the direction of the chemoattractant and its length is very close to 1 indicating the cells are angled in a similar orientation.

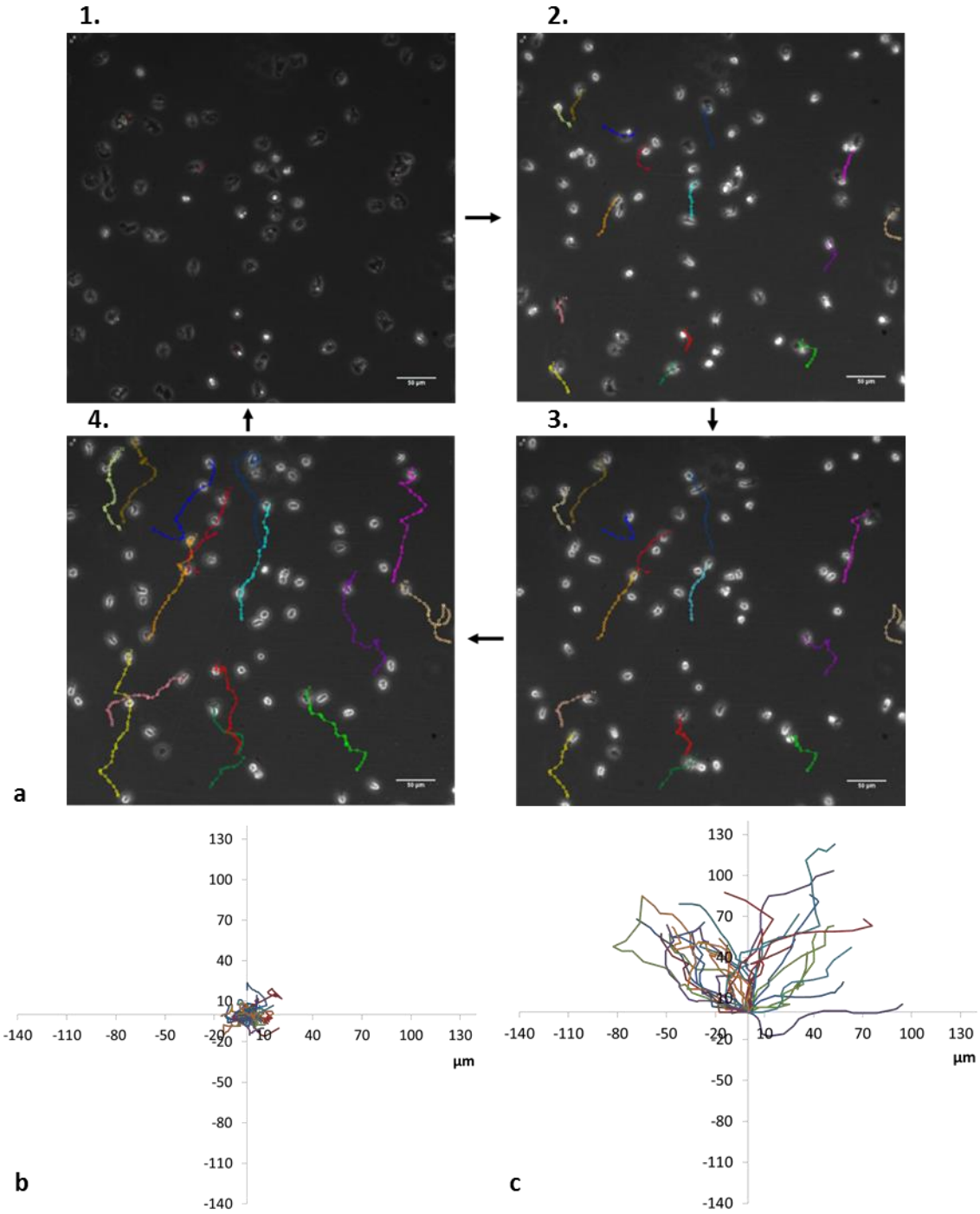

Figure 3.3 Cell track paths of cells

The cell track image sequences (a) demonstrate cell movement from image 1 to 4 at sequential time points (0, 10, 15 and 20 min) with coloured "tails" for the cells selected for tracking; bars (white) represent 50µm. The tracks are then plotted on "spider diagrams" such as demonstrated at the 20 min time point for RPMI control (b) and when the cells are exposed to a chemoattractant such as fMLP after 20 min (c).

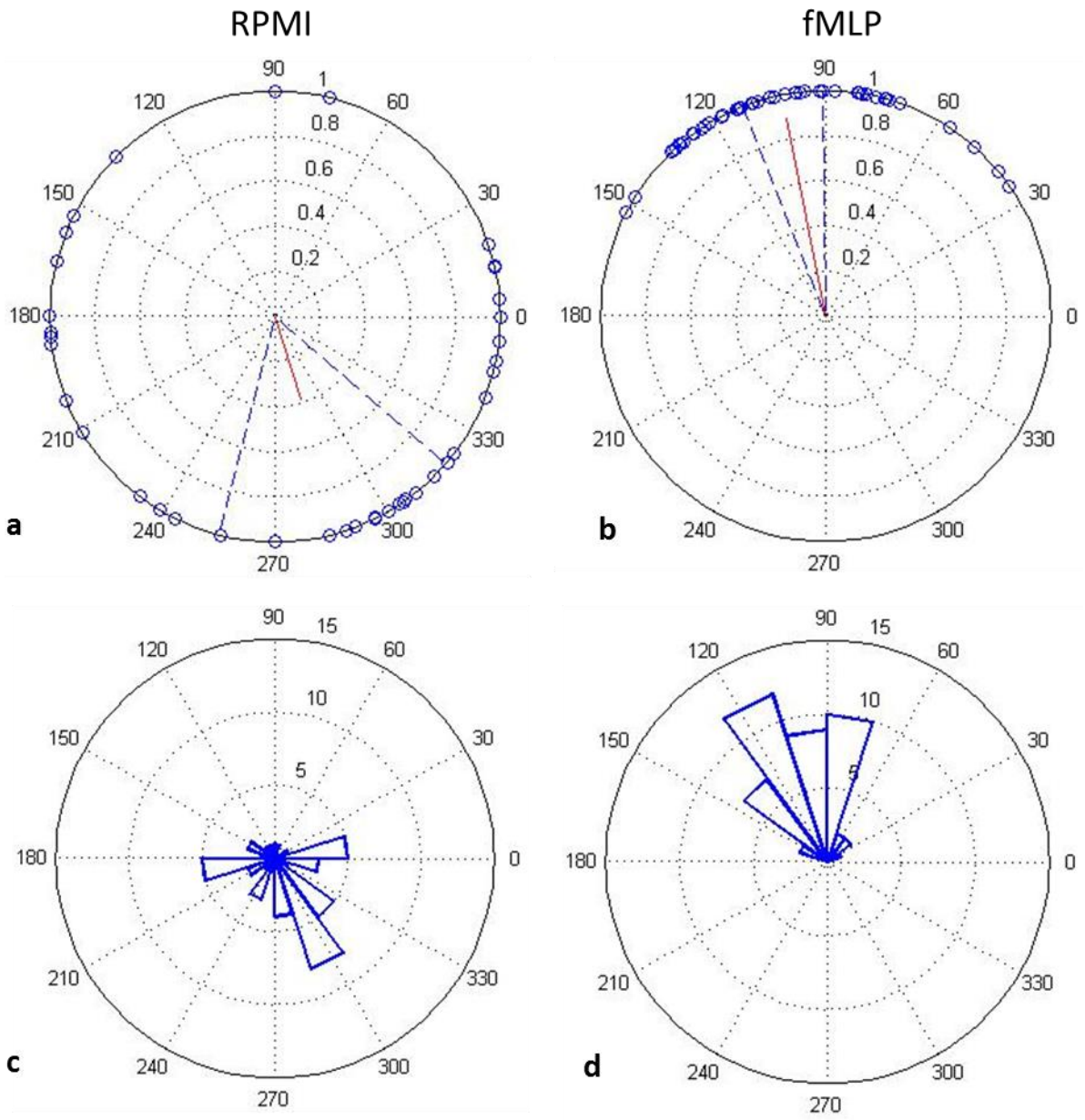

Figure 3.4 Example circular statistics graphs

Neutrophils were isolated (section 2.2) and chemotaxis was performed (section 2.6) using RPMI and fMLP (10nM), after which the cells were analysed (section 2.6.2) and the tracked information was used to generate circular statistical diagrams. "Polar plots" (a) and (b); the red line represents the mean resultant vector (MRV), MRV length (MRVL) is proportional to the number of cells close to the mean (each cell is represented as a blue circle on the edge of the diagrams), indicating cell directional uniformity. Blue dotted lines represent 95% C.I. "Angle histograms" (c) and (d) present the number of cells at a particular angle range, the height of the bins (here ranging 0-15) represent the number of cells present per bin (n = 3 neutrophil isolations; 45 cells tracked per diagram).

3.4.1. Using MRVL to indicate orientational accuracy

MATLAB software generates the MRVL from XY co-ordinates of cells tracked using the MtrackJ plugin supplied by Fiji (ImageJ). The MRVL shows similarities to the chemotactic index (CI), which is generated by the excel spreadsheet supplied by the Insall group (Muinonen-Marten *et al.* 2013); MRVL indicates how clustered the cells are in a particular orientation (regardless of how far the cells have travelled) and makes use of an arbitrary numerical scale (ranging 0-1). Unlike the CI, the MRVL, in the absence of graphical format, does not show the orientation in relation to the chemoattractant source. This can create a significant misrepresentation of the strength of directionality towards the chemoattractant when analysing the numerical value of the MRVL alone and in isolation from the graphs. Figure 3.5 highlights the dilemma when using the MRVL as a standalone value; it is clear that the cells in the RPMI example (Figure 3.5a) are not orientated in the direction of the chemoattractant (towards 90°), and should cell speed be taken into account, the cells would be shown to move very little, however the angle of the cells is such that the MRVL is high – similar to that of fMLP indicating the orientation of cells to be the same (10nM) (Figure 3.5b), yet when observing the graph of the cells exposed to fMLP the orientation of the MRV is in the direction of the chemoattractant source. The use of the MRVL to determine orientational accuracy of a cell is therefore of no value and was not employed here. These graphs also illustrate the importance of speed and velocity as parameters for the study of chemotaxis as speed of the cells is not taken into account in circular statistics and speed may be in a random direction, rather than towards a chemoattractant.

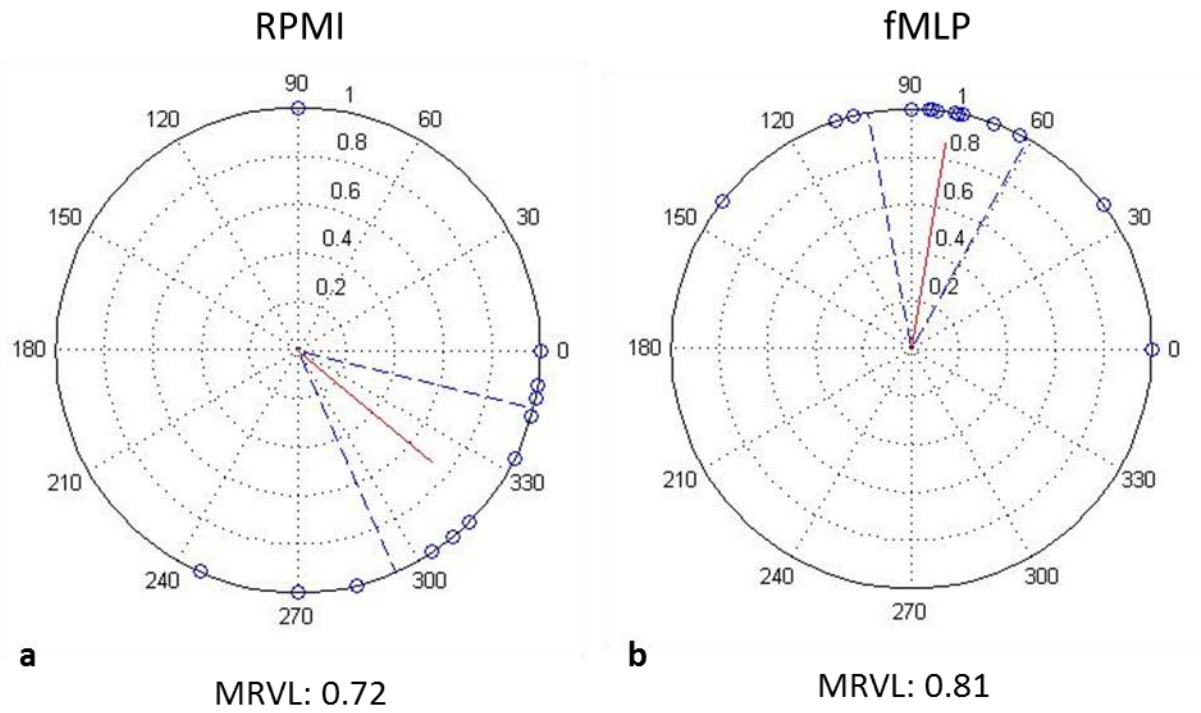

Figure 3.5 Polar plots of RPMI versus fMLP

Neutrophils were isolated (section 2.2) and chemotaxis was performed (section 2.6) using RPMI (a) and fMLP (b; 10nM), after which the cell tracks were analysed (section 2.6.2) and tracked information was used to generate polar plots. The red line represents the mean resultant vector (MRV), MRV length (MRVL) is proportional to the number of cells close to the mean; dotted lines represent 95% C.I.

3.4.2. Accounting for the mean angle and measurement

Circular Statistics provide additional information regarding the polar plot diagrams; the mean angle of all the cells provides information regarding the directionality of the cells on the circular axis. CI and MRVL produce similar results when analysing the same data sets. Figure 3.6 shows the MRVL (a) and CI (b) for 15 cells plotted over a 20 minute time-course as previously described (section 3.5) using control buffer (RPMI) and the chemoattractants interleukin-8 (CXCL8; 200ng/ml) and fMLP (10nM). Whilst the pattern of the results is similar, the spread of data is greater for MRVL than for CI. CI, as a chemotaxis measurement parameter, was published during the course of these studies (Sapey *et al.* 2011). To assess the similarity between both CI and MRVL, the two sets of values were compared by correlation and also by Bland-Altman analysis (Figure 3.6c and d). The linear regression result shows that while a positive interchangeable relationship exists between the CI and the MRVL, the strength, as shown by the coefficient of determination (R^2 = 0.55), is only moderate, moreover according to Bland-Altman, in order for one method to be reliably replaced by another method,, 95% of data points should lie within the limits of agreement (Figure 3.6d), this is not the case for CI and MRVL indicating that one value could not reliably be interpreted as the other. If the MRVL was adjusted to incorporate the mean angle then the result would be expected to be closer to the CI than the MRVL alone. In order to achieve this, the angle quadrants of generated polar plots were given a number designation ranging -1 to 1 as shown in Figure 3.7. The vector length for a given result (i.e. one sample averaging 15 cells) would then be divided by the angle quadrant value to give the Adjusted MRVL (AMRVL). The resulting value would then be plotted in the same manner as the CI value.

When compared to CI, the AMRVL (Figure 3.8a and b) similarities are stronger than for CI and MRVL alone. When the two sets of values were further analysed by Bland-Altman plots

(Figure 3.8c and d) the coefficient of determination was higher (R^2 = 0.85) indicating a more positive interchangeable relationship, also >95% of data points lie within the limits of agreement on the Bland-Altman plot Figure 3.8d). The degree of similarity between AMRVL and CI was such that only the CI result will be utilised in all further chemotaxis assays. The circular statistics diagrams will be presented for visual qualitative purposes only.

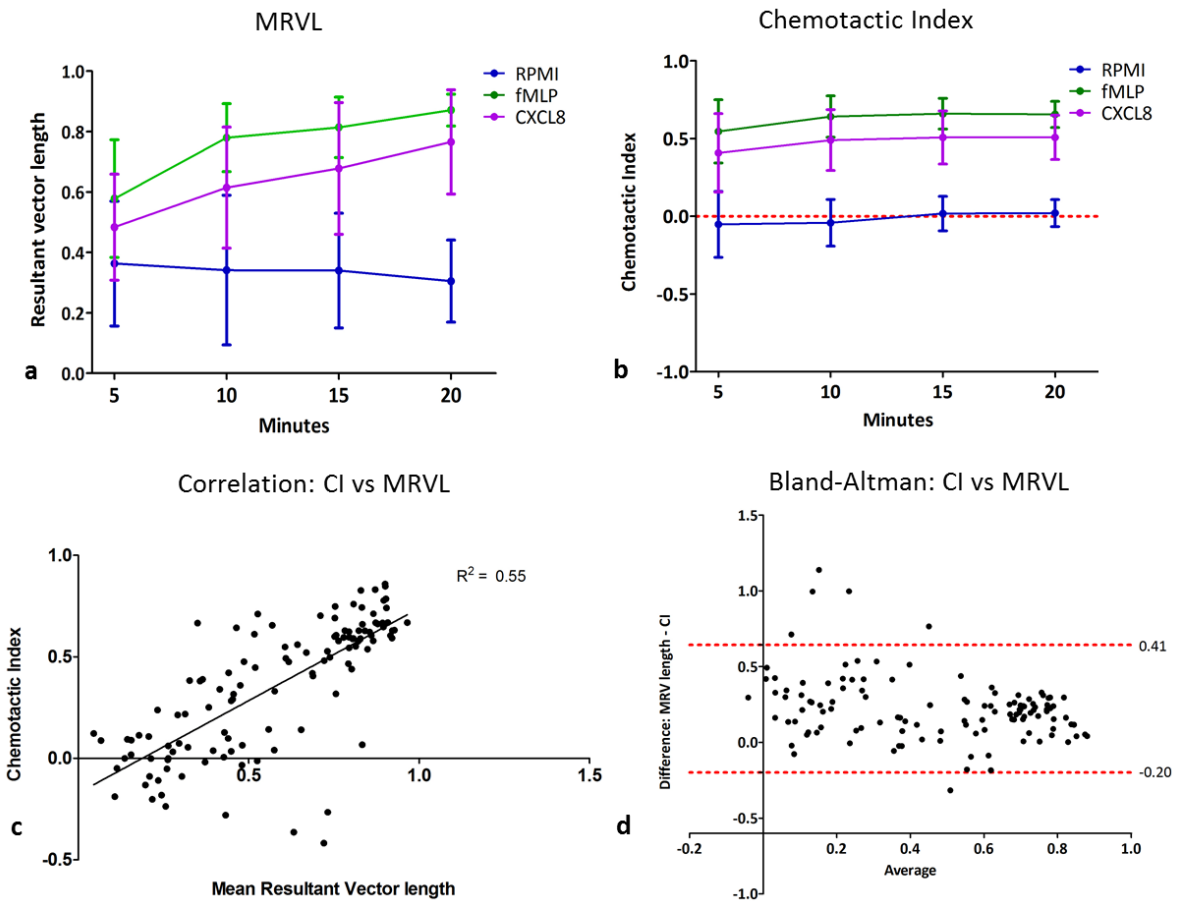

Figure 3.6 Similarities between mean resultant vector length (MRVL) and chemotactic index (CI)

Neutrophils were isolated (section 2.2) and chemotaxis was performed (section 2.6), after which the cells were analysed (section 2.6.2) and tracked information was used to calculate the MRVL (a) and CI (b) from the same set of chemotaxis experiments using RPMI and the chemoattractants CXCL8 (200ng/ml) and fMLP (10nM). Data are expressed as mean ± standard error of the mean (SEM). Correlation and Bland-Altman analysis (c and d); horizontal red lines indicate the limits of agreement which are defined as the mean difference plus and minus 1.96 times the standard deviation of the differences (75 cells, n = 5 neutrophil isolations).

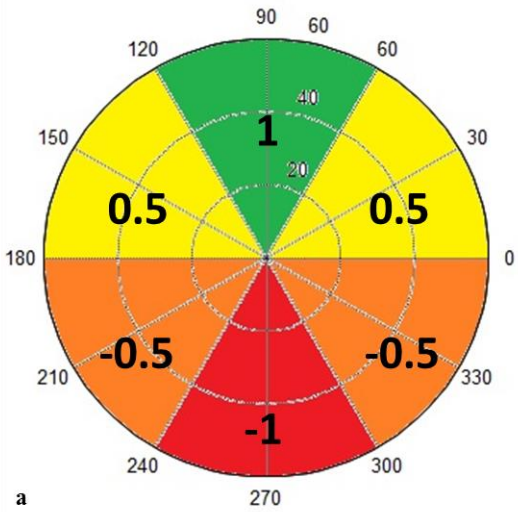

a

RPMI				
Cell no.	MRVL	Mean angle	Quadrant angle designation	MRVL/Quadrant angle designation = AMRVL
1	0.11	310	-1.0	-0.11
2	0.56	1	0.5	0.28
3	0.53	337	-0.5	-0.26
4	0.26	325	-0.5	-0.13
5	0.14	354	-0.5	-0.07

fMLP				
Cell no.	MRVL	Mean angle	Quadrant angle designation	MRVL/Quadrant angle designation = AMRVL
1	0.41	98	1.0	0.41
2	0.87	81	1.0	0.87
3	0.49	101	1.0	0.49
4	0.44	156	0.5	0.22
5	0.33	107	1.0	0.33

b

Figure 3.7 Calculating the adjusted mean resultant vector length (AMRVL)

Calculated polar plot quadrants (a) were given a number designation; 1 is the quadrant with the directionality closest to the supposed chemoattractant source. The further around the circle, the lower the given value (0.5 for yellow, -0.5 for orange and -1 for red) as the cells' orientation is further away from the chemoattractant source. The AMRVL (b) was calculated from the MRVL and the quadrant angle designation was derived from the mean angle value (5 cells shown as an example).

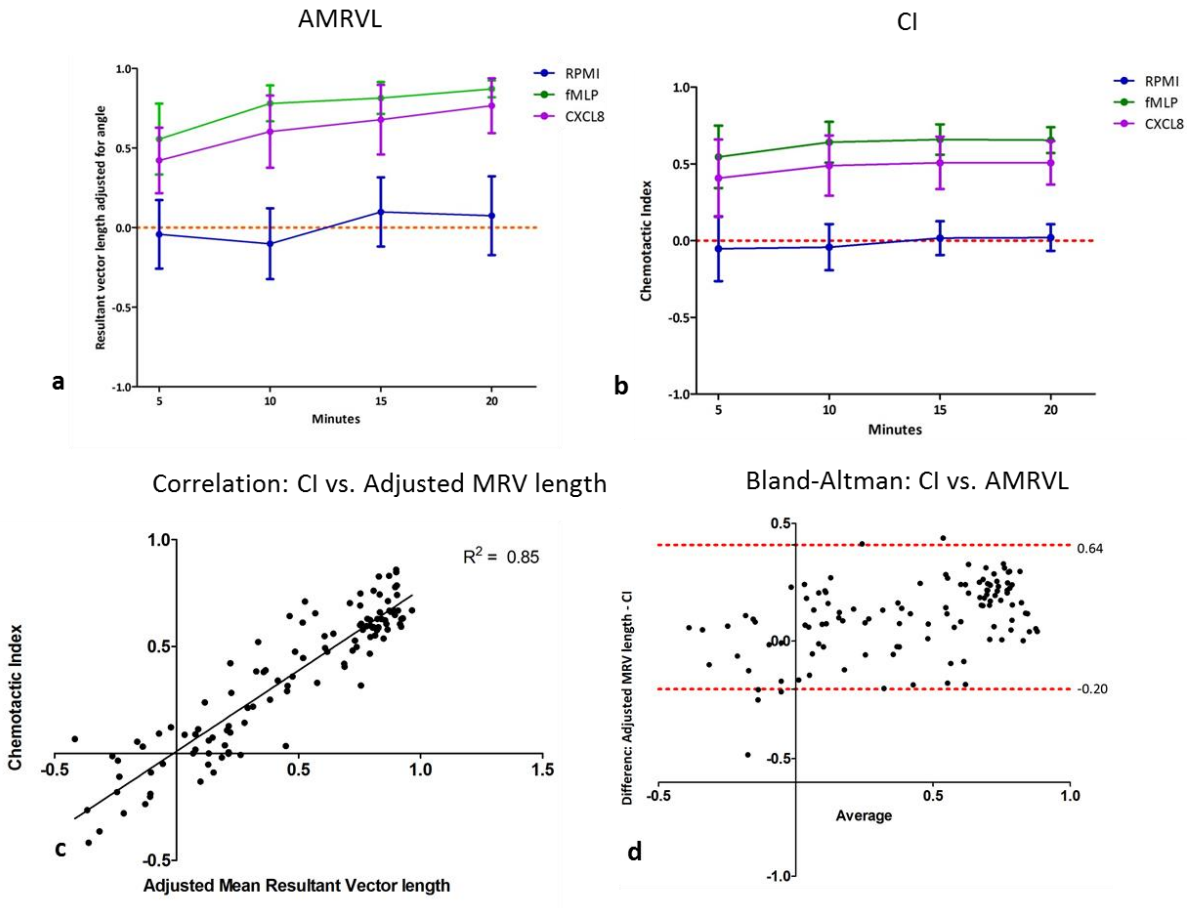

Figure 3.8 Comparing the adjusted mean resultant vector length (AMRVL) to chemotactic index (CI)

AMRVL (a) and CI (b) plotted from the data yielded in Figure 3.7. Chemotaxis experiments employing RPMI and the chemoattractants CXCL8 (200ng/ml) and fMLP (10nM). Data expressed as mean ± standard error of the mean (SEM). Correlation (c) and Bland-Altman analysis (d): horizontal red lines indicate the limits of agreement which are defined as the mean difference plus and minus 1.96 times the standard deviation of the differences (75 cells, n = 5 neutrophil isolations).

3.5. Chemotaxis assay time length

Whilst the most reliable and representative result for the measurement of chemotaxis is likely achieved using the maximum observation and recording time, limitations exist for the study of neutrophils using the Insall chamber. The rapid responsivity of chemotaxing neutrophils is such that unlike experiments involving *Dictostelium* in which a time course of 72 hours in length is typical and the Insall chamber is sealed to prevent evaporation, there is no need to seal the chamber when studying neutrophil movement after 20 minutes. The fast-moving immediate responses of neutrophils to the chemoattractants employed in this project eliminates the need to seal the chamber, a consequence of which is the potential evaporation of chemoattractant/negative control. Beyond 20 minutes under the heat/intensity of the light microscope, evaporation occurs making it unsuitable to measure neutrophil chemotaxis. The maximal video length for cell tracking was therefore set at 20 minutes. In order to identify the optimal filming time, a range of 5-20 minutes was evaluated.

Figure 3.9 illustrates the speed, velocity and CI for the allotted time points. At 5 minutes the cells responded as expected to the chemoattractants fMLP and CXCL8, however as observation length increased, speed and velocity increased, reaching an apparent plateau between 15 and 20 minutes. Significant differences were seen between 5 minute and 20 minute time points for optimal concentrations of CXCL8 and fMLP and the negative control RPMI, with speed and velocity measurements ($p < 0.05$). There was no significant difference in CI throughout the time course; indicating that this measure of chemotaxis was not dependent upon recording length. A time limit of 20 minutes was therefore used in all future experiments.

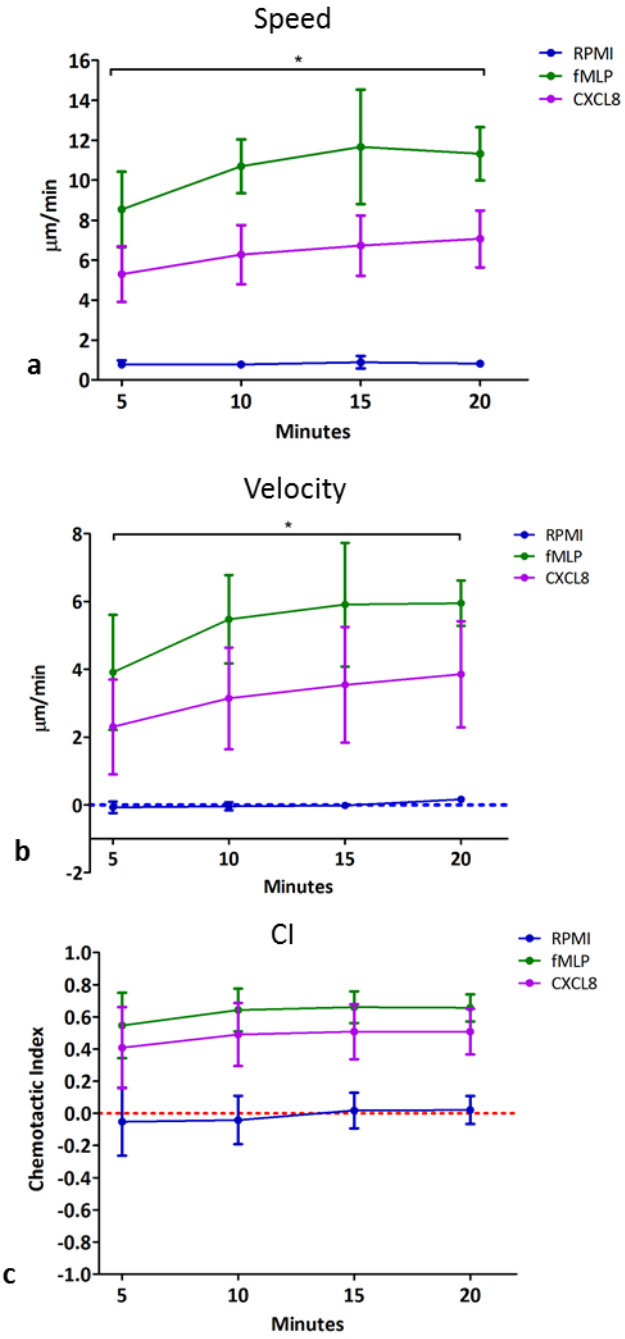

Figure 3.9 Chemotaxis at different time points

Neutrophils were isolated (section 2.2) and chemotaxis was performed (section 2.6), after which the cells were analysed (section 2.6.2) and tracked information was used to generate speed (a), velocity (b) and CI (c) measurements over a 20 minute time course using RPMI (negative control) and the chemoattractants CXCL8 (200ng/ml) and fMLP (10nM). Data is expressed as mean ± standard error of the mean (SEM). The blue/red dotted lines for velocity and CI mark 0 as a reference point. (n = 10 different blood donors; 15 cells tracked per chemoattractant/RPMI). Statistical test: One Way ANOVA and Tukey's post-test. * = (p < 0.05).

3.6. Chemoattractant concentrations

The bacteria-derived peptide fMLP and the host derived chemokines CXCL8 and macrophage inflammatory protein-1-alpha (MIP1α) are among the most physiologically important chemoattractants for neutrophils. A range of chemoattractant concentrations were tested to identify the most effective for use in the Insall chamber.

3.6.1. fMLP and CXCL8 concentrations

Figure 3.10 shows the effect of different concentrations of CXCL8 and fMLP on neutrophil chemotaxis using the Insall Chamber. Chemokinesis with fMLP (utilising the Boyden chamber) can be initiated at concentrations as low as 10pM, however preliminary studies using the Insall chamber induced no directed neutrophil movement, therefore the lowest concentration utilised was 10nM (Iizawa *et al.* 1995). Speed and velocity were significantly lower at increased fMLP concentrations (50nM and 100nM) compared to the lowest concentration (10nM). By contrast CXCL8 showed increased speed and velocity with increasing concentration, and significance was reached at 200ng/ml for velocity only. CI for both chemoattractants was not significantly affected by the concentration used. fMLP at 10nM and CXCL8 at 200ng/ml were therefore chosen as optimal concentrations for future chemotaxis studies as they demonstrated the greatest directional and overall movement. For all subsequent analyses of chemotaxis RPMI was anticipated to be significantly different from assays using chemoattractants ($p < 0.001$) and was thus employed as the negative control.

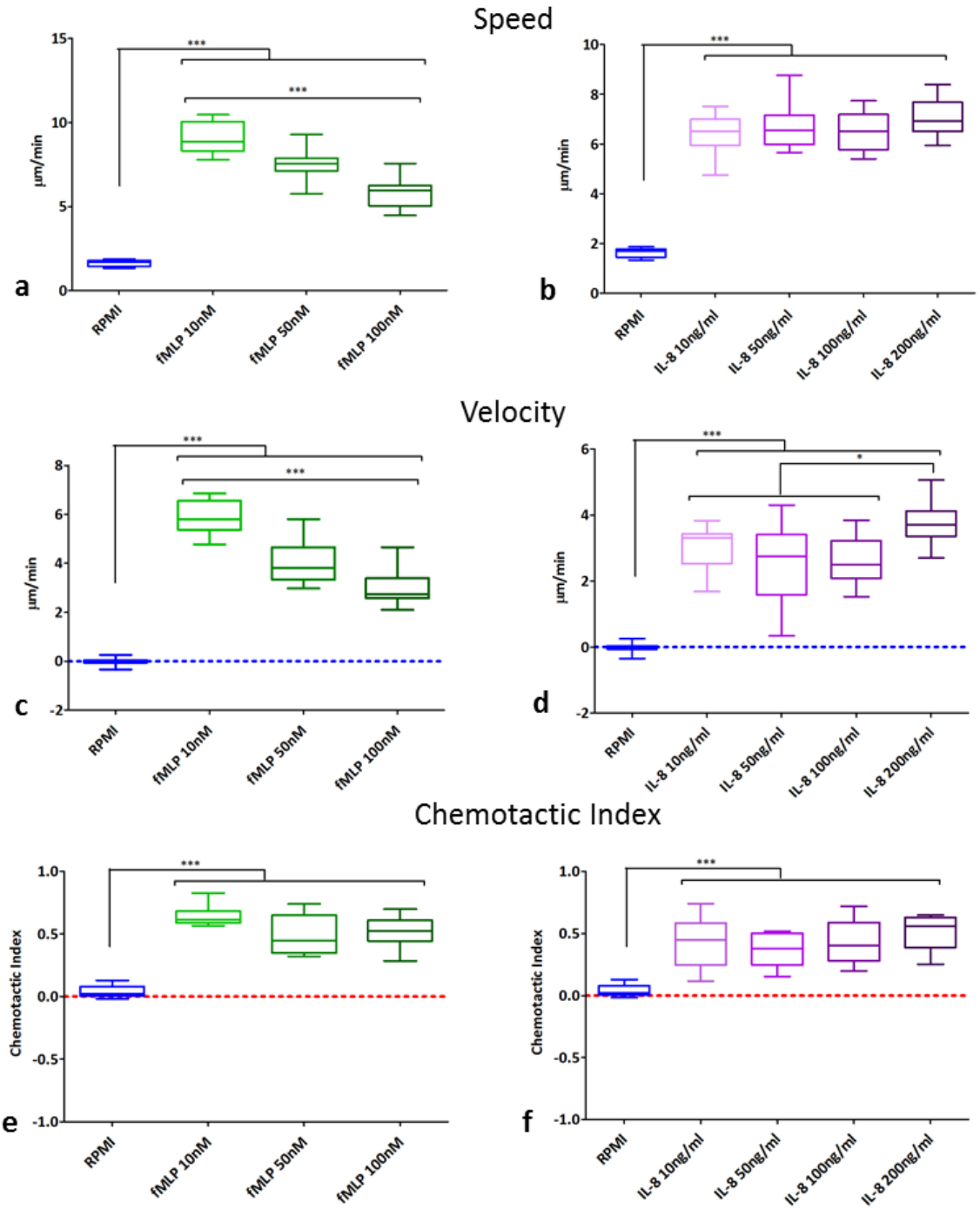

Figure 3.10 Optimisation of CXCL8 and fMLP concentrations

Neutrophils were isolated (section 2.2) and chemotaxis was performed (section 2.6), following which the cells were analysed (section 2.6.2) and tracked information was used to generate speed (a and b), velocity (c and d) and CI (e and f) measurements for concentration ranges of fMLP and CXCL8 respectively. Box and whisker plots (the band within the box represents the median, surrounded by the 1st and 3rd quartiles, the ends of the whiskers represent the minimum and maximum data points). (n = 10 different blood donors; 15 cells tracked per chemoattractant/RPMI). Statistical test: One Way ANOVA and Tukey's multiple comparisons test. * = ($p < 0.05$), *** = ($p < 0.001$).

3.6.2. MIP1α and GM-CSF concentrations

Neutrophil chemotaxis towards MIP1α requires pre-incubation with GM-CSF to enable the constitutively expressed MIP1α cell surface receptor CCR5 to bind to and respond to the chemoattractant (Ottonello *et al.* 2005). **Error! Reference source not found.**3.11 shows the peed, velocity and CI of a range of GM-CSF and MIP1α concentrations (0.2-200pg/ml and 10-100ng/ml respectively). The effect of GM-CSF priming was also measured following subsequent exposure to fMLP (10nM), and at increasing GM-CSF concentrations (20 and 200pg/ml) the neutrophil responses to MIP1α were heightened compared to fMLP alone. As expected, chemotaxis with MIP1α was not as effective as fMLP, but was clearly evident when compared with RPMI negative control. There were significant differences between 0.2pg/ml GM-CSF with all MIP1α concentration ranges and all other GM-CSF concentrations ($p < 0.001$) for all chemotaxis parameters (Figure a-c). In addition, there were significant increases in speed, velocity and CI between 2pg and 20pg/ml GM-CSF priming concentrations. There were no differences between 20pg/ml and 200pg/ml GM-CSF. With regard to MIP1α concentrations, 100ng/ml was the optimal concentration yielding the greatest speed, velocity and CI score, significance was only evident between 10ng/ml and 100ng/ml with MIP1α when 20pg/ml GM-CSF was used ($p < 0.001$). Thus MIPα at a concentration of 100ng/ml and a GM-CSF priming concentration of 20pg/ml were used in all relevant future chemotaxis experiments.

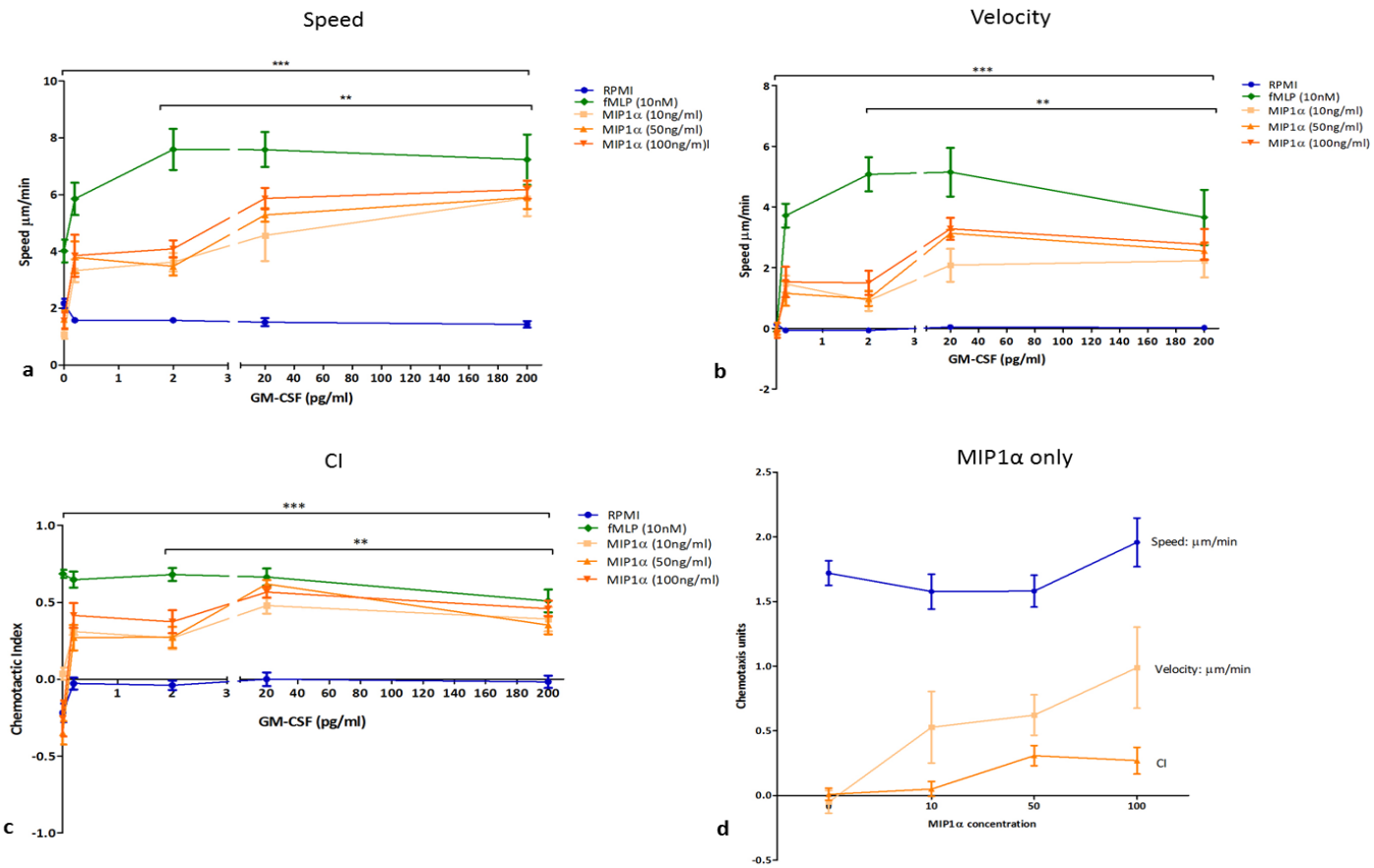

Figure 3.11 Optimisation of MIP1α neutrophil priming concentration

Neutrophils were isolated (section 2.2) and chemotaxis was performed (section 2.5), after which the cells were analysed (section 2.5.2) and tracked information was used to generate speed (a), velocity (b) CI (c) plots for concentration ranges of MIP1α with different ranges of GM-CSF. Measuremnts were also done of MIP1α in the absence of GM-CSF priming (d). Data is expressed as mean ± standard error of the mean (SEM). (n = 10 different blood donors; 15 cells tracked per chemoattractant/RPMI). Statistical test: One Way ANOVA and Tukey's multiple comparisons test. * = ($p < 0.05$), ** = ($p < 0.01$), *** = ($p < 0.001$).

3.7. Number of cells tracked

The optimal number of neutrophils selected to measure chemotaxis (speed, velocity and CI) was identified by comparing 5, 10, 15 and 20 cells. Figure 3.12 shows the calculated speed, velocity and CI with increasing numbers of cells tracked. There were no statistical differences with increasing numbers of cells for any of the parameters addressed; however average velocity and CI demonstrated an increasing trend with more cells present. 15 cells per visual field were selected as the standard number to track in future assays to ensure reliable results and an achievable cell quantity available for selection within the given time frames.

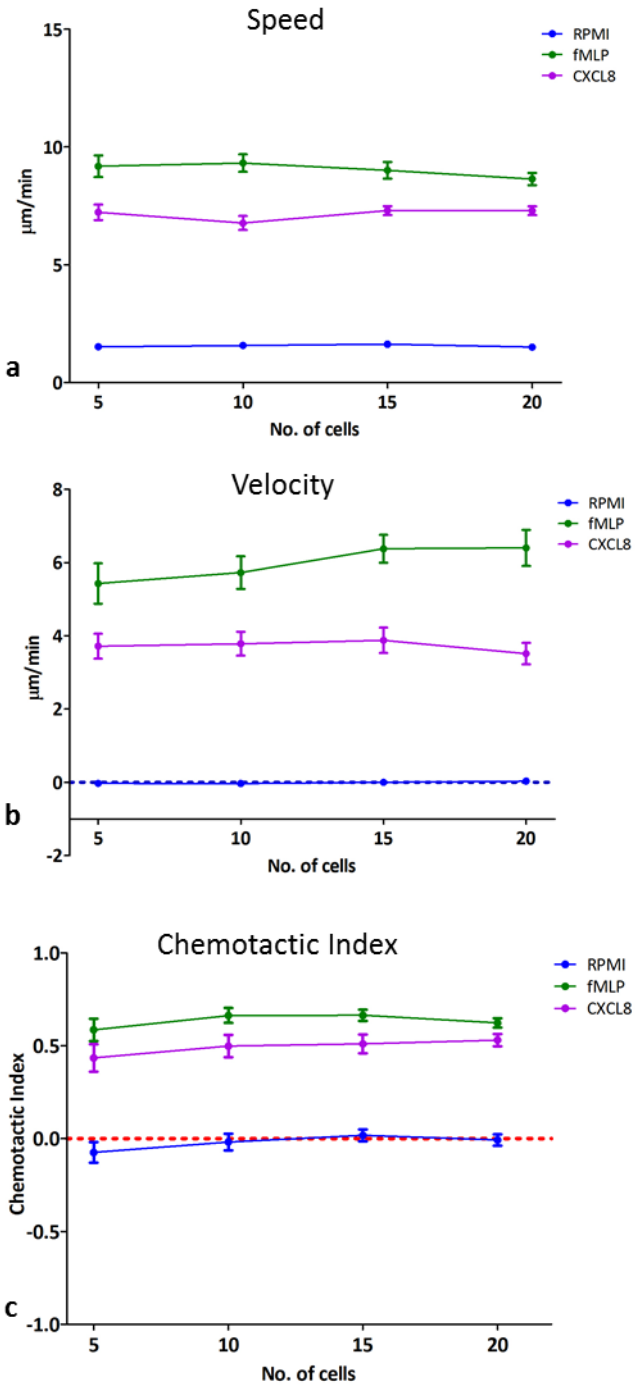

Figure 3.12 Impact of cell numbers tracked per assay

Neutrophils were isolated (section 2.2) and chemotaxis was performed (section 2.6), after which the cells were analysed (section 2.6.2) and tracked information was used to generate speed (a), velocity (b) and CI (c) plots with increasing cell numbers using RPMI and the chemoattractants CXCL8 (200ng/ml) and fMLP (10nM). Data expressed as mean ± standard error of the mean (SEM). (n = 10 different blood donors). Statistical test: One Way ANOVA and Tukey's multiple comparisons test.

3.8. Effects of cell density

Different cell densities were investigated to assess potential inaccuracies evident with increased numbers of cells present within the video frames. To optimise the number of cells required for the chemotaxis assay, ten videos utilising fMLP (10nM) as the chemoattractant from 10 healthy donor neutrophil isolates at three different densities were analysed. Figure 3.13a-c shows still photo micrographs of each of the movies recorded at the different densities: low; 1×10^5, medium; 1×10^6 and high; 2×10^6 cells/ml respectively. Figure 3.13d-f shows the effect of increasing cell densities on speed, velocity and CI. The medium cell density video (1×10^6 cells/ml) demonstrated greater overall speed, which was significantly higher compared with low ($p < 0.05$) and high ($p < 0.001$) cell density. This may be the result of optimum visuals for the operator – the number of cells does not overwhelm the tracking process (which may be the case for the high density video) yet the operator is not constrained by the lack of cells (as could be the case for the low density video). Velocity and CI demonstrated no significant differences. All further chemotaxis assays therefore utilised cells at medium density (1×10^6 cells/ml).

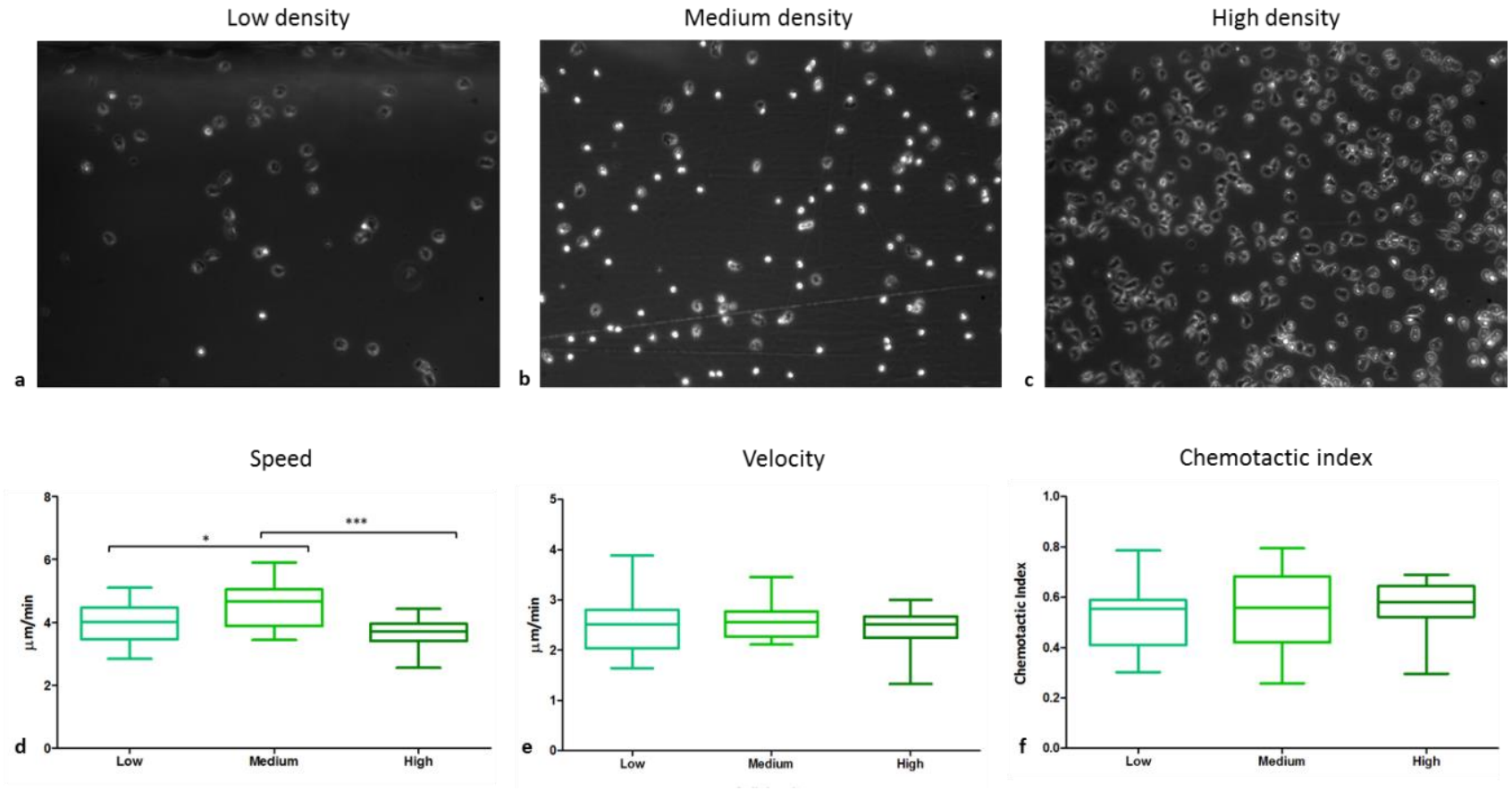

Figure 3.13 Differing cell densities for manual tracking

Neutrophils were isolated (section 2.2) and chemotaxis was performed (section 2.6) using fMLP (10nM), after which the cells were analysed (section 2.6.2) using three different cell densities: Low; 5 x 10^6 cells/ml (a), medium; 1 x 10^6 cells/ml (b) and high; 2 x 10^6 cells/ml (c). Tracked information was used to generate speed (d), velocity (e) and CI (f). Box and whisker plots (the band within the box represents the median, surrounded by the 1st and 3rd quartiles, the ends of the whiskers represent the minimum and maximum data points). n = 10 different blood donors; 15 cells tracked per analysis. Statistical test: One Way ANOVA and Tukey's multiple comparisons test. * = ($p < 0.05$), *** = ($p < 0.001$).

3.9. Intra-individual manual tracking validation

The manual tracking plugin, MtrackJ, generates information regarding changes in the XY co-ordinates of selected cells, which when further processed using Microsoft Excel yields the speed, velocity and CI, thus quantifying the movement of neutrophils in different states, such as in health and disease or after exposure to particular agents. Manual tracking is the gold standard technique with regard to monitoring different cells; it requires the observer to click on a reference point within a chosen cell for each frame of the stack. In order to ensure the use of MtrackJ was not biased by the author of this thesis, who was the sole operator for all chemotaxis tracking analyses, ten videos of fMLP (10nM) were repeatedly analysed blindly on three separate occasions; a minimum of one week separated each re-analysis. Figure 3.14a-c shows the average speed, velocity and CI per repeat analysis. The coefficient of variation for each parameter was also calculated (Figure 3.14d). There were no statistically significant differences between repeat analyses for any chemotaxis parameter. The coefficient of variation was greatest between the three analyses for CI (29%), indicating the sensitivity of this particular parameter.

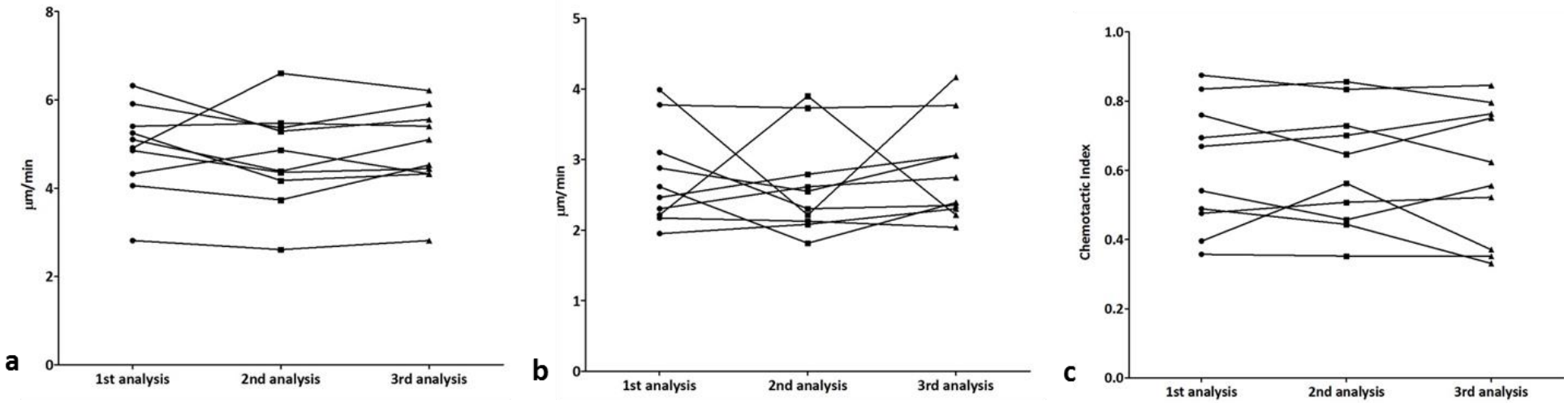

d

	Speed	Velocity	CI
Average	4.53	2.54	0.55
St. Dev.	0.69	0.35	0.16
% C.V.	15	14	29

Figure 3.14 Variation in cell tracking with repeated analyses

Neutrophils were isolated (section 2.2) and chemotaxis was performed (section 2.6) using fMLP (10nM), after which the cells were analysed (section 2.6.2) on three separate occasions using the same videos. The cell density used was 1 x 10^6 cells/ml. Tracked information was used to generate speed (a), velocity (b) and CI (c). Data is expressed as line graphs denoting individual analyses. The coefficient of variation for each respective parameter was also calculated (d). n = 10 different blood donors; 15 cells tracked per analysis. Statistical test: One Way ANOVA and Tukey's multiple comparisons test.

3.10. Donor variation in chemotactic responses

To assess the potential impact of day to day variation within donors on the neutrophil chemotaxis assay, healthy volunteers (n = 16) were bled on two different days; at least 2 weeks apart from each other. The entire experiment spanned 2 months. Isolated neutrophils were exposed to fMLP (10nM) and speed, velocity and CI (Figure 3.15a, b and c respectively) were measured. No statistically significant differences were found between the chemotaxis parameters of neutrophils from repeat isolates. The response to fMLP varied between donors, however the coefficient of variation was within acceptable limits (Figure 3.15d). These results indicate that day-to-day variation in neutrophil behaviour creates only subtle differences when measuring chemotaxis using the present method and does not appear to be a confounding factor when measuring chemotaxis from the same donor at different times, e.g. before and after therapeutic intervention.

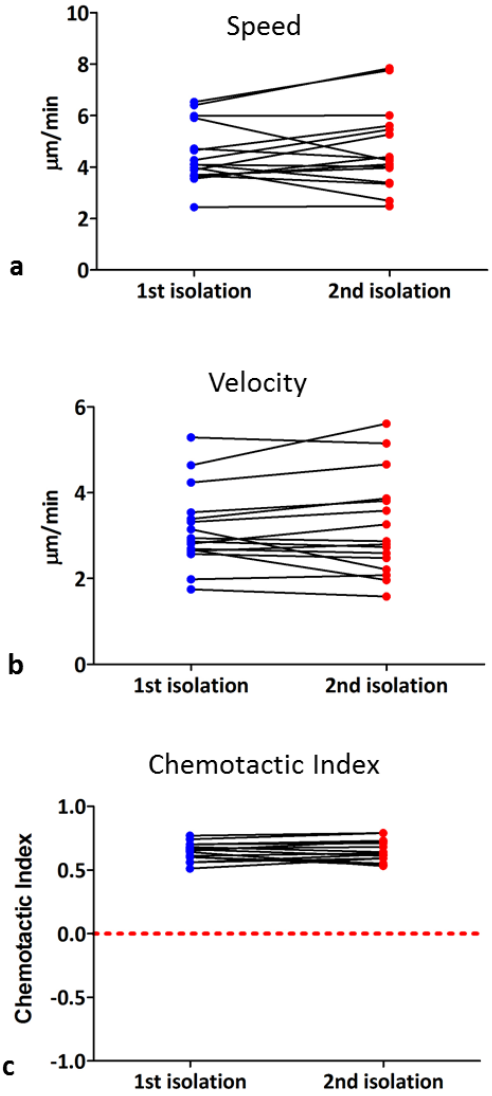

	Speed	Velocity	Chemotactic Index
Avergae	4.61	3.18	0.65
St. Dev.	0.53	0.24	0.03
d % C.V.	11.50	7.74	5.11

Figure 3.15 Repeat donor chemotaxis assay

Neutrophils were isolated (section 2.2) and chemotaxis was performed (section 2.6), after which the cells were analysed (section 2.6.2) and tracked information was used to generate speed (a), velocity (b) and CI (c) measurements using fMLP (10nM) using the same volunteers donating blood on two separate occasions. Averages from each of the cells tracked from the 1st and 2nd isolations were used to calculate the coefficient of variation from each parameter (d). Data is expressed as line graphs, each dot represents a donor at first (blue) and second (red) isolation. (n = 16 different blood donors; 15 cells tracked per isolation). Statistical test: paired t test.

3.11. Discussion

Live cell real-time microscopy is a powerful approach to study the characteristics of cell movement. The Insall chamber was selected for the study of neutrophil chemotaxis in several clinical studies in this thesis because of the ease of use and relatively short application time. This enabled the use and re-use of the assay with several different neutrophil preparations isolated in tandem, with different chemoattractants or a negative control. As the Insall chamber is a recently developed form of bridge chamber, few studies are available reporting its use, and of those, only three specifically reference neutrophils (Sapey *et al.* 2011; Herlihy, Tang, *et al.* 2013; Sapey *et al.* 2014). Table 3.1 describes the outcome of the different parameters measured in this chapter in order to optimise the use of this chamber for the study of neutrophil movement in the remainder of this thesis.

Table 3.1 Optimal parameters for neutrophil chemotaxis with the Insall chamber

Optimisation experiment	Experimental outcome future assays
Cell incubation prior to assay	Up to 4 hours
Cell Density	1 x 10^6/ml
Magnification	x20
Time course	20 minutes
Chemoattractant concentration	fMLP (10nM), CXCL8 (200ng/ml), MIP1α (100ng/ml) with GM-CSF (20pg/ml) incubation.
No. of cells tracked/video	15 cells
Quantitative measures	Speed, velocity and CI
Qualitative measures	Spider diagrams, polar plots and angle histograms

The ability of neutrophils to undergo chemotaxis was not impeded for several hours post-isolation, with viability dropping only marginally up to four hours following isolation (section 3.2). Neutrophils have recently been shown to survive in the body beyond 5 days (Pillay *et al.* 2010); far longer than previously thought. Thus neutrophils appear to be far more than just the 'kamikaze-like' cells they were once considered to be and appear capable of subtle protein/peptide synthesis and cell signaling activity. In order to optimise conditions for their use in the Insall chamber, image magnification and length of video recording (section 3.3), were considered for the assay itself and also for subsequent quantification of movement using manual tracking software.

The wealth of information that can be acquired using the Insall chamber is not limited to processing by ImageJ or Microsoft Excel. Circular statistics can be employed to generate quantitative and qualitative data regarding the orientational accuracy of cell movement. The Circular Statistics Toolbox, used by Muinonen-Martin *et al.* (2013) provides additional visual and numerical data to test for uniformity of cell movement in a particular condition. When comparing the MRV with the CI the similarities between the two values was apparent (section 3.4.1), and when adjusted to include the direction as well as the length of movement (the AMRVL), the degree of similarity was such that CI could be substituted for AMRVL according to the Bland-Altman analysis (section 3.4.2). The plot diagrams generated from MATLAB provide additional visual values to the study of chemotaxis using this chamber.

It was necessary to optimise the concentrations of chemoattractants used with the Insall chamber. Within the literature, fMLP has been shown to have a concentration-dependent effect on neutrophils; the results reported in this thesis demonstrated that concentrations beyond 10nM impaired chemotaxis. fMLP has been shown to elicit ROS production at concentrations above 10nM, reaching peak ROS production at 1mM, such a peak in ROS generation may provide insight into the disruption of chemotaxis at higher concentrations of

this chemoattractant (Iizawa *et al.* 1995). The most effective chemoattractant concentration of fMLP using a modified two-chamber chemotaxis assay, such as the Boyden chamber, was previously reported to range between 0.1-10nM (Kohidai *et al.* 2003). Results presented here (section 3.6.1) confirm that concentrations above 10nM impaired speed and velocity, however no significant differences were evident with regard to CI, demonstrating that at different concentrations the chemoattractants have no effect on the orientation of the neutrophil movement, but do effect cell speed towards the chemoattractant. fMLP was expected to elicit a stronger chemotactic response in neutrophils than host-derived chemoattractants as it activates more signalling pathways (Figure 1.5). Differing CXCL8 concentrations employed in the chemotaxis assay demonstrated that the maximal CXCL8 concentration yielded the most effective chemotactic response in agreement with Lin *et al.* (2004). Jeon *et al.* (2002) reported that increases in CXCL8 were accompanied by enhanced neutrophil chemotaxis using a microfabricated device. The authors used a maximum concentration of 50ng/ml, however their chemotaxis time course was 90 minutes, an inappropriate length of time for use with the Insall chamber, which is not sealed to enable its re-use. Thus a higher concentration (200ng/ml) was found to be most appropriate for chemotaxis with the Insall Chamber.

The chemoattractant MIP1α used in the absence of any other agent will not induce neutrophil migration, as demonstrated by Zhang *et al.* (1999), even at high concentrations (up to 1μM). Ottonello *et al.* (2005), using the Boyden chamber, showed that acute incubation with GM-CSF enabled neutrophils to migrate in response to MIP1α. GM-CSF has been shown to induce mRNA expression for CCR1, one of the MIP1α receptors, allowing responsiveness to the chemoattractant upon exposure to it (Cheng *et al.* 2001). GM-CSF is a powerful priming agent for neutrophils, allowing them to respond effectively to subsequent stimuli (e.g. pathogens) (Gasson 1991).

Although the MIP1α receptor, CCR5, is constitutively expressed on neutrophils, the absence of priming will not allow for stimulation of downstream signalling pathways that lead to an alteration in cell movement. Signal transduction by host chemoattractants such as MIP1α is MAPK-pathway dependent (Lehman *et al.* 2001), inducing ERK-2 phosphorylation, however host chemoattractants cannot induce ERK-1 phosphorylation in the absence of priming and the locomotion of unprimed/naïve neutrophils cannot be triggered due to dependence on ERK-1. Pre-treatment with GM-CSF results in ERK-1 activation thereby allowing induction of CCR5 competence to MIP1α. The p38 kinase signaling pathway is more important upon fMLP-receptor binding (Heit *et al.* 2002; Heit, Liu, *et al.* 2008). The combination of both p38 and ERK-1/2 activation in fMLP is most likely the underlying reason for its greater potency (Figure 1.5).

To ensure the reliability of a particular chemotaxis result it was necessary to track a suitable number of cells. Other groups that have used the Insall chamber to study chemotaxis track varied numbers ranging from 10-30 cells (Sapey *et al.* 2011; Herlihy *et al.* 2013). The data presented here (section 3.7, Figure 3.12) did not show a significantly different effect from increasing the number of cells tracked, however the cells were taken from healthy donors and the chemoattractants used were known to have a potent effect on the cells; thus the number of cells tracked may be of greater importance under different conditions using the same chemoattractants e.g. health versus disease states. Furthermore, the magnitude of error in data quantification would be lower the greater the number of cells analysed.

Manual tracking is commonly employed for quantifying cell chemotaxis, yet several drawbacks to the technique have been identified (Cordelières *et al.* 2013): firstly defining the reference point of the cell (often the centre of the nucleus is used); secondly, precision can be a problem as clicking the correct pixel can influence the result of the cells movement; thirdly, consistency with clicking (one sample for processing requires 15 cells chosen over a period

of 40 frames requires 600 separate clicks), fourthly, there is difficulty in achieving consistency between operators. In addition, the process is extremely time-consuming with operator fatigue leading to the possibility of inaccurate tracking. To address these potential problems, the reference point was designated as the centre of the cell mass, ensuring the variance setting was the same for all videos (i.e. to provide a black and white image by which clicking would be visually easier). Cell density was assessed in order to achieve the optimal number of cells present in any one frame (section 3.8). Tracking 15 cells per video takes approximately 6 minutes, therefore a limit of 5 videos for tracking at any one time (total time approximately 30 minutes) was set to ensure fatigue did not influence tracking capabilities. Finally, the same operator was used for all chemotaxis assays and intra-individual variability was assessed (section 3.9) which demonstrated no significant difference with repeat analysis of videos. In order to explore the possibility of day-to-day variation affecting neutrophil chemotaxis, the same donors were bled at two different times (section 3.10) and although variation was evident the differences were not significant, thus data collected from further studies, i.e. before and after therapeutic intervention, was not normalised for comparative analysis.

Automated tracking systems are an attractive, alternative method for acquiring quantitative data regarding cell movement. As cell detection is based on identifying differences between the cell itself and the background, automated tracking using phase-contrast microscopic videos is difficult to achieve because of the lower contrast between the background and the cells. An alternative method, by which cells can be tracked by automated software analysis, uses fluorescently labelled cells. The differential between cell and background is easier to achieve with this technique (Debeir *et al.* 2008), however light excitation/emission wavelengths can have a toxic effect on cells due to the generation of free radicals and specifically singlet and triplet forms of oxygen, reducing their ability to migrate (Magidson

& Khodjakov 2013). Automated tracking provides an opportunity to reduce the subjectivity of results to yield high-throughput analysis of time-lapse microscopic images. However, several challenges have impeded the development of such software for neutrophils, including the rapidly changing cell shape, high cell densities and cells moving in and out of the focal plane of the microscope. More recently automated segmentation and tracking algorithms have been developed to provide a framework for high-throughput tracking of cells in time-lapse microscopy videos (Brandes *et al.* 2015) that do not rely upon fluorescent cell labelling. The technique involves taking static images within each frame into account allowing the distinction between background and cell, based upon temporal and spatial image variation, allowing their detection independent of their morphology and image illumination. Automated tracking is therefore being developed as an increasingly attractive alternative to manual tracking.

The Insall chamber, like many of its predecessors, employs simplified environments such as static buffer conditions or a single chemoattractant gradient (Nelson *et al.* 1975; Brown 1982; Zigmond 1977; Zicha *et al.* 1991; Hopkins *et al.* 1984; Inoue & Meyer 2008; Heit, Robbins, *et al.* 2008) which cannot reflect the complex chemical signalling events *in vivo*. In an attempt to address this challenge, the field of microfluidics has emerged. Microfluidic chambers allow the formation of competing gradients of two chemoattractants whilst monitoring the behaviour of individual neutrophils. The 2-dimensional (2-D) μ-slide chemotaxis chamber (IBIDI, 80302) was tested with isolated neutrophils (section 8.1) as an alternative to the Insall chamber for the study of chemotaxis. Despite the obvious advantages of the μ-slide (more advanced gradient formation application and the ease of which the chamber can be sealed to provide longer-term chemotaxis videos), there were some significant drawbacks. These included: gradient formation taking several hours to form (Zengel *et al.* 2011), the chamber is only fit for single use and is technically difficult to use

(Irimia 2010). The Insall chamber assay was therefore preferred because of its simplicity, its ability to be re-used and its time-effectiveness.

3.12. Chapter 3 Summary

This chapter has investigated the optimisation of a neutrophil chemotaxis assay that provides ease-of-use and good replicability within a short time frame. The data that can be generated using the Insall chamber provides a wealth of novel information regarding the overall movement of cells from individuals with different health states and under different chemoattractant conditions. Optimisation of this assay provides an opportunity to assess chemotaxis in neutrophils from clinical samples alongside other measures of neutrophil function.

CHAPTER 4 RESULTS - NEUTROPHIL FUNCTION IN ACUTE AND CHRONIC INFLAMMATORY ORAL STATES

4.1. Introduction

Chronic periodontitis and chronic gingivitis are among the most common inflammatory disorders in humans. Gingivitis does not necessarily always lead to periodontitis, but it is regarded as a necessary pre-requisite. As gingivitis is a reversible periodontal disease and gingival inflammation is a key driver of periodontitis itself, gingivitis represents a suitable model disease to study in order to better understand the pathogenic mechanisms underlying periodontitis. Understanding the effects of the chronic inflammation on neutrophils may shed light upon how periodontitis can act as a risk factor for other chronic inflammatory diseases.

This chapter presents results from the assessment of neutrophil ROS, NET formation and chemotactic behaviours in a 21-day experimental gingivitis model, to assess the potential systemic effects of gingival/periodontal inflammation. In addition, gingival crevicular fluid (GCF) was collected to assess the chemoattractive potential of healthy and inflamed sites. Neutrophil chemotaxis was also examined in chronic periodontitis patients prior to and following non-surgical periodontal therapy. Again, GCF was collected from inflamed and non-inflamed sites and measured as for its chemoattractive properties.

The data collected adds to current understanding of the systemic effects of short-term, localised inflammation.

4.2. Volunteer information

Section 2.1.2 describes the volunteer selection for the experimental gingivitis study; section 2.1.3.1 and 2.1.3.2 details the selection process for the periodontitis patient cohorts 1 and 2 respectively. Table 4.1 describes the age and gender of the experimental gingivitis study volunteers and the two periodontitis patient cohorts. For cohort 1, two patients were not

included in the chemotaxis assays, one due to withdrawal from the study and the other because they were neutropenic.

Table 4.1 Gingivitis and periodontitis patient demographics

	Gingivitis study	Periodontitis cohort 1		Periodontitis cohort 2	
		Control	Patient	Control	Patient
No. of participants	15	18	18	10	10
Gender (% females)	60	39		50	
Mean age ± SD (range)	22 ±3 (20-29)	52 ±11 (40-75)		46 ±8 (37-61)	46 ±8 (32-62)
% >60 yrs.	0	3		1	1

4.3. Clinical measures for 21-day gingivitis study and chronic periodontitis patients

To determine the extent of experimental gingival inflammation and the severity of periodontitis (patient cohort 1), gingival and plaque indices were taken and GCF was collected by Dr Martin Ling at both control/healthy and inflamed/diseased sites. In addition, for the chronic periodontitis patients (cohort 1), clinical attachment loss (CAL), periodontal probing depths (PPD) and bleeding on probing (BOP) were recorded before and after non-surgical treatment (Appendix II) alongside healthy controls that were assessed simultaneously at each time point. CAL, PPD and BOP were measured immediately prior to blood collection for neutrophil assays by Dr Martin Ling, who also confirmed periodontal health in the healthy controls. Figure 4.1 shows the gingival and plaque indices for the 21-day gingivitis volunteers and chronic periodontitis patients (cohort 1) with matched healthy controls displayed as the percentage of sites above health. The gingival index (GI) ranges 0–3 (Löe et al. 1967); 0 is deemed as optimal plaque control. The modified Quigley-Hein

plaque index ranges 0 to 5; 0 and 1 are deemed to be healthy. The gingival index (GI) scores demonstrated the induction of inflammation for the experimental gingivitis study volunteers of day 7 with significant increases at test sites by day 21 (**** = $p < 0.0001$) but not at control sites during plaque accumulation; these returned to baseline levels at day 35 following a professional prophylaxis and resumption of normal brushing at day 21 (Figure 4.1a). For the chronic periodontitis patients, GI (Figure 4.1c) was significantly higher before treatment ($p < 0.001$) compared with the healthy controls and with post-periodontal treatment values; there was no significant difference between control measurements. In the case of gingivitis the plaque index (PI) values show that plaque accumulates significantly at the test sites following cessation of normal tooth brushing but not the control sites, ($p < 0.001$), its removal at day 21 triggered a return to baseline levels, as reflected in the scores for both control and test sites at day 35 (Figure 4.1b). For the periodontitis patients (cohort 1), treatment lowered the PI to a level no longer significantly different to pre-treatment levels or to healthy control levels (Figure 4.1d).

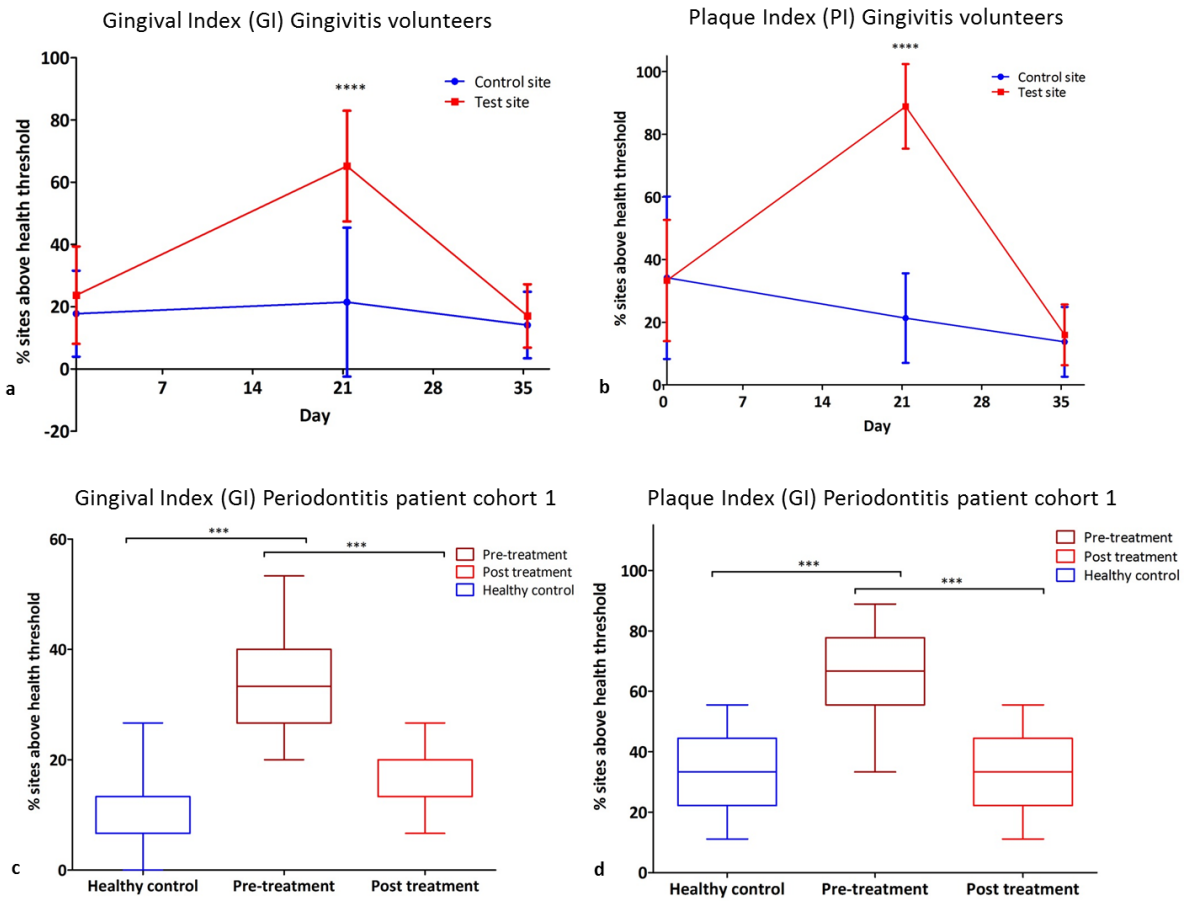

Figure 4.1 Gingival index (GI) and plaque index (PI) in 21-day experimental gingivitis model and in chronic periodontitis (cohort 1) volunteers pre and post periodontal treatment

Percentage of sites above healthy threshold (designated value of 0) for both GI (a and c) and PI (b and d) for gingivitis and periodontitis conditions. Data presented as line graphs (a and b) and box and whisker graphs (c and d); the band within the box represents the median, surrounded by the 1st and 3rd quartiles; the ends of the whiskers represent the minimum and maximum data points. n = 15 for gingivitis, n = 18 for periodontitis cohort 1. Statistical test: one way ANOVA and Tukey's test.*** = ($p < 0.001$).**** = ($p < 0.0001$).

4.4. Gingival crevicular fluid (GCF) volume and protein quantity: 21-day experimental gingivitis cohort and chronic periodontitis group

GCF was collected from the control and test sites of the experimental gingivitis study volunteers, the chronic periodontitis patient cohort 1 (diseased and matched-healthy control sites), and also from an inflamed area and a non-inflamed area from periodontitis patient cohort 2. Figure 4.2 shows the GCF volumes for gingivitis (Figure 4.2a) and chronic periodontitis patients cohort 1 and 2 (Figure 4.2b and c respectively). For the gingivitis volunteers, the volume of GCF collected was significantly higher at day 21 than at baseline ($p < 0.05$). For periodontitis patient cohort 1, significantly higher volumes of GCF were collected pre-treatment compared with post-treatment ($p < 0.05$) and controls ($p < 0.01$). When compared with healthy controls the volume post-treatment remained significantly higher than controls ($p < 0.01$).

Although all chronic periodontitis patients were clinically diagnosed, systemic clinical measurement data was available for patient cohort 1 only. Figure 4.3 shows the positive correlation between PPD and GCF volumes for pre- and post-treatment for cohort 1 and healthy controls. The data indicates that GCF volumes are associated with disease severity, a finding reported in other studies involving GCF (Sanikop *et al.* 2012; Bhadbhade *et al.* 2012; Subrahmanyam & Sangeetha 2003), and may even act as a more reliable marker of disease than other clinical markers of gingival inflammation such as BOP and PPD (Oh *et al.* 2015). Although systematically collected clinical measurement data was not available for cohort 2, the collected GCF volumes for periodontitis patient cohort 2 healthy sites (0.14µl, SD = ±0.06) were significantly lower than for diseased sites (0.27 SD = ±0.12) ($p < 0.05$).

The protein content of GCF samples from gingivitis study volunteers and chronic periodontitis cohort 2 patients was determined for subsequent quantification of the pro-

inflammatory cytokines TNFα and IL-1β and for the ability of GCF to induce chemotaxis in neutrophils collected from periodontally and systemically healthy donors. Figure 4.4 shows the protein concentration of the GCF collected after processing (section 2.11.1.2). The trend in both gingivitis and periodontitis (cohort 2) shows an increased protein concentration from GCF at test/diseased sites with significance ($p < 0.01$) reached between healthy sites (91μg/ml SD = ±14) versus diseased sites only (102μg/ml SD = ±17) in periodontitis volunteers.

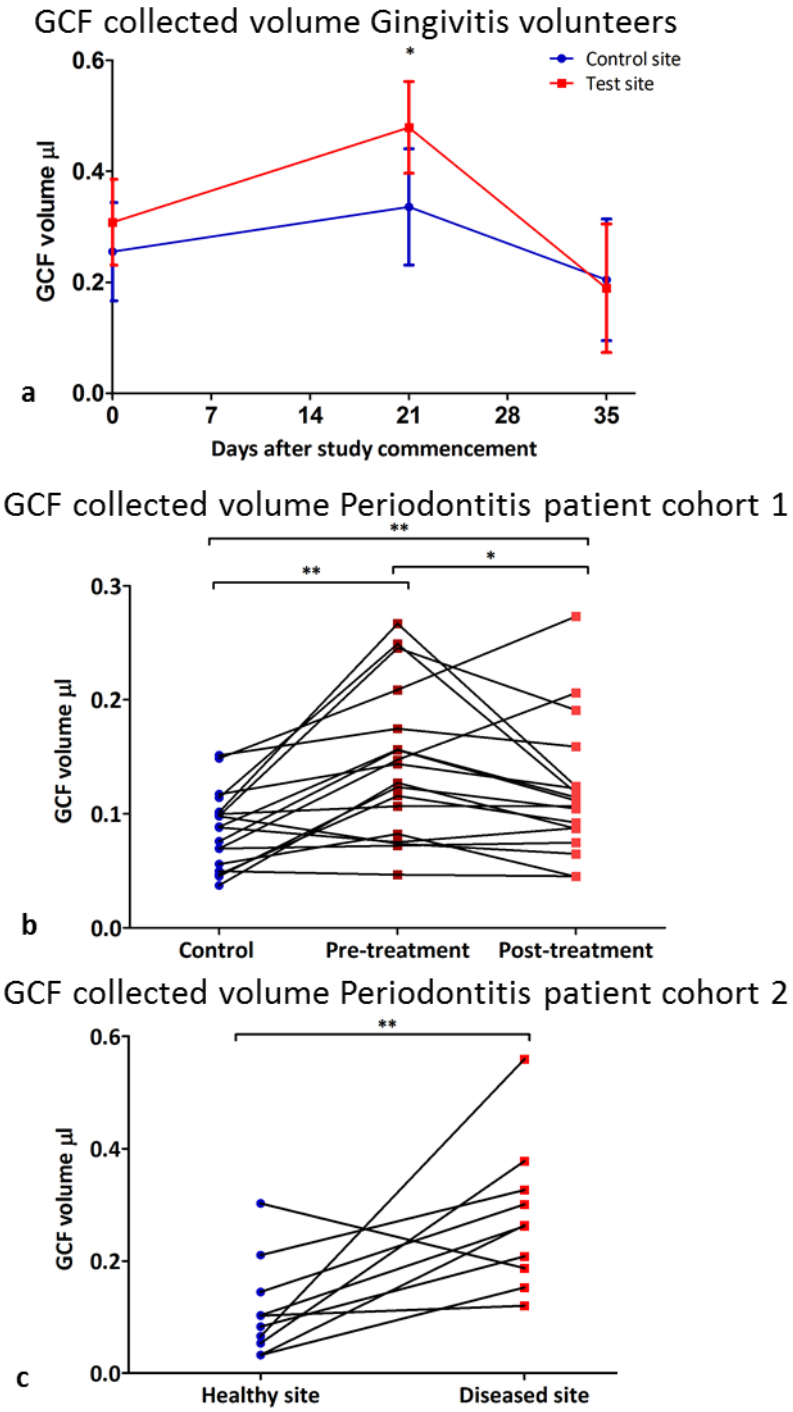

Figure 4.2 GCF volumes collected in experimental gingivitis and chronic periodontitis

GCF was collected (section 2.11.1.2) at control and test sites and non-inflamed (control) and inflamed (test) sites in gingivitis study volunteers (a) and chronic periodontitis patient cohort 1 (b) and cohort 2 (c). Data is presented as line graphs; each dot represents an individual control/healthy (blue) and test/diseased (red) collection site. n = 15 for gingivitis, n = 18 and n = 10 for chronic periodontitis patients cohort 1 and 2 respectively. Statistical test: paired t-test test. * = ($p < 0.05$) and ** = ($p < 0.01$).

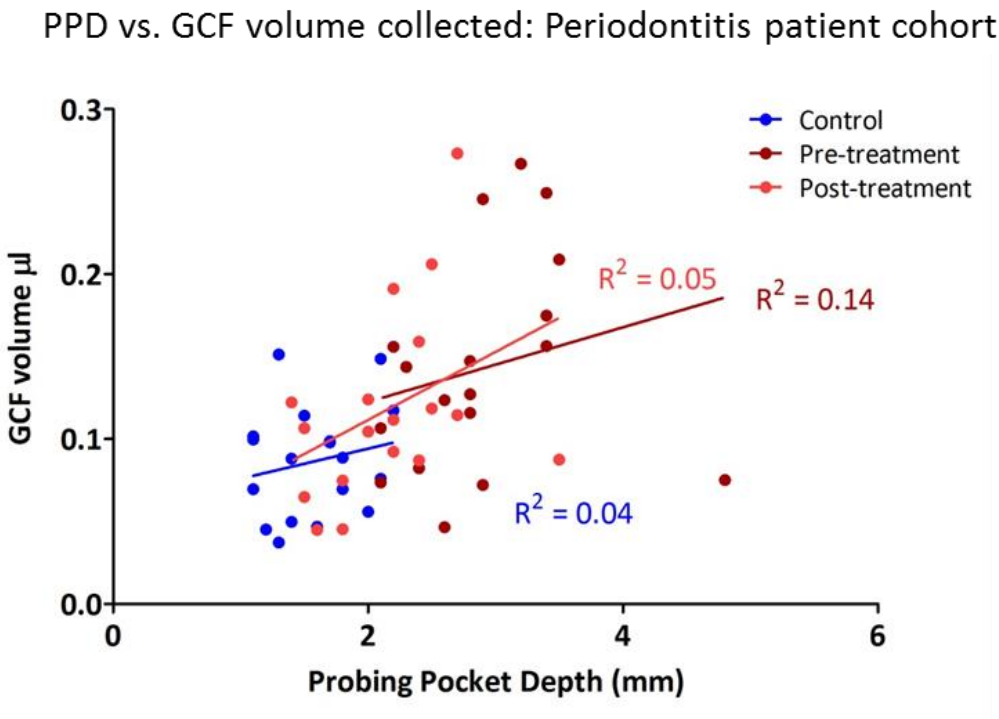

Figure 4.3 GCF concentrations and relation to probing pocket depth (PPD) in chronic periodontitis

Pre-, post-treatment and healthy control site probing pocket depths were correlated with collected GCF volumes for chronic periodontitis patient cohort 1, data presented as correlation analysis. n = 18. * = ($p < 0.05$). Statistical test: unpaired t-test test.

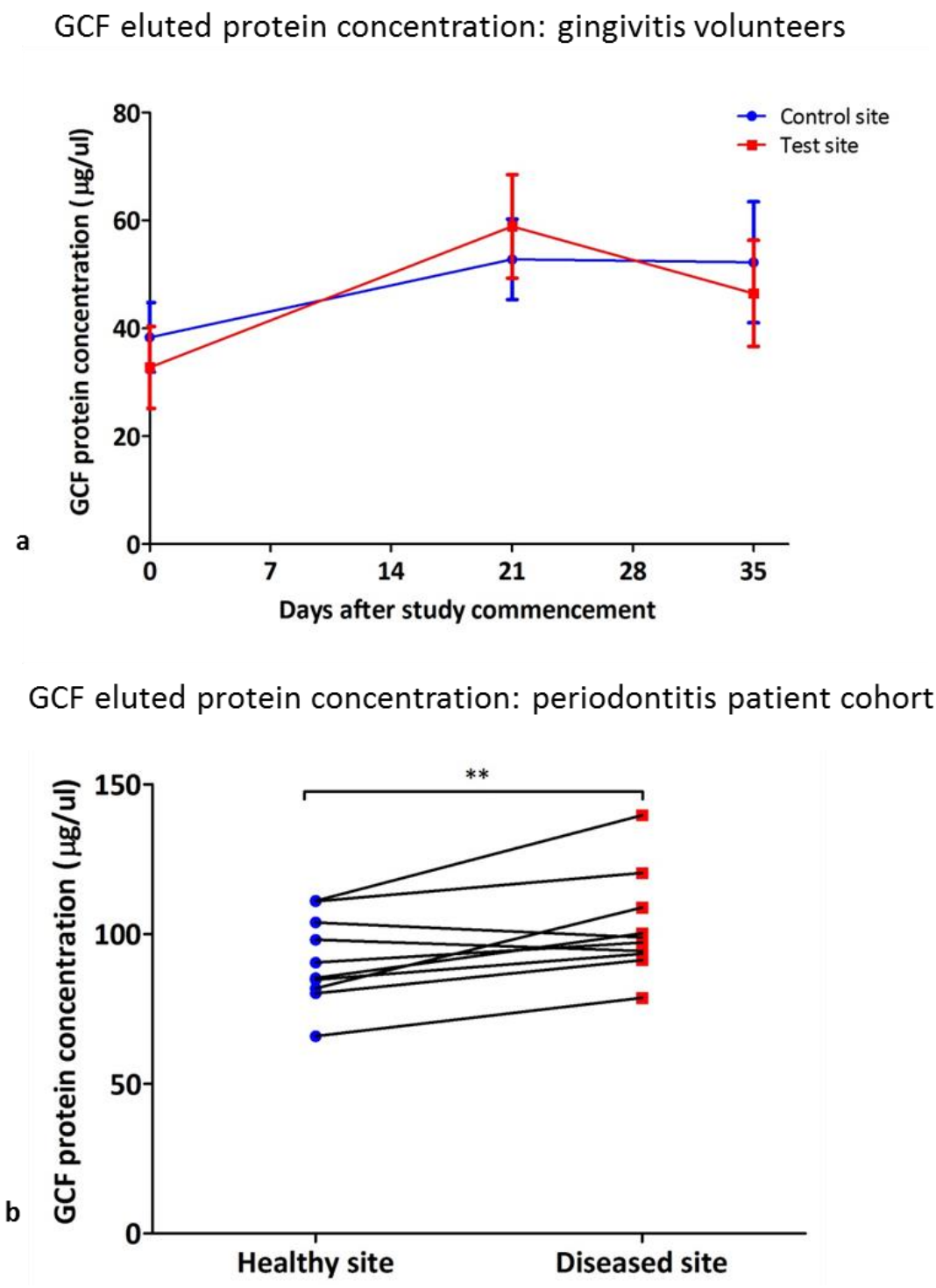

Figure 4.4 Protein concentration of GCF in gingivitis and periodontitis

Collected GCF samples were processed (section 2.11.1.2) and the protein concentration was determined (section 2.9) in gingivitis (a) and chronic periodontitis cohort 2 samples (b). Data is presented as line graphs; each dot represents an individual control/healthy (blue) and test/diseased (red) collection site. n = 15 for gingivitis, n = 10 for chronic periodontitis (cohort 2). Statistical test: paired t-test. * = ($p < 0.05$) and ** = ($p < 0.01$).

4.5. NET formation in gingivitis and chronic periodontitis

NET formation during experimental gingivitis was also assessed for the first time (Figure 4.5). Fluorometric quantification revealed few differences in NET production. However, significance was identified between day 21 (height of inflammation) and day 35 (inflammation resolution) with HOCl ($p < 0.05$) (Figure 4.5c), indicating NET production to be higher at day 21; a similar trend was seen with PMA, despite no significant differences.

NET production in chronic periodontitis patient cohort 1 has already been reported (White 2015). In summary, neutrophils isolated from cohort 1 pre- and post-treatment were compared with age and gender-matched controls using the stimuli PMA and HOCl. Significant increases in NET formation were identified between patient pre-treatment and control samples after exposure to PMA (Wilcoxon test; $p=0.021$) but not for an HOCl stimulus. When presented as a ratio to the matched healthy controls, NET production by patients significantly decreased following treatment in response to PBS, PMA and HOCl (Wilcoxon test; $p=0.007$, $p=0.004$, $p=0.012$ respectively) (White et al. 2015; data not shown here).

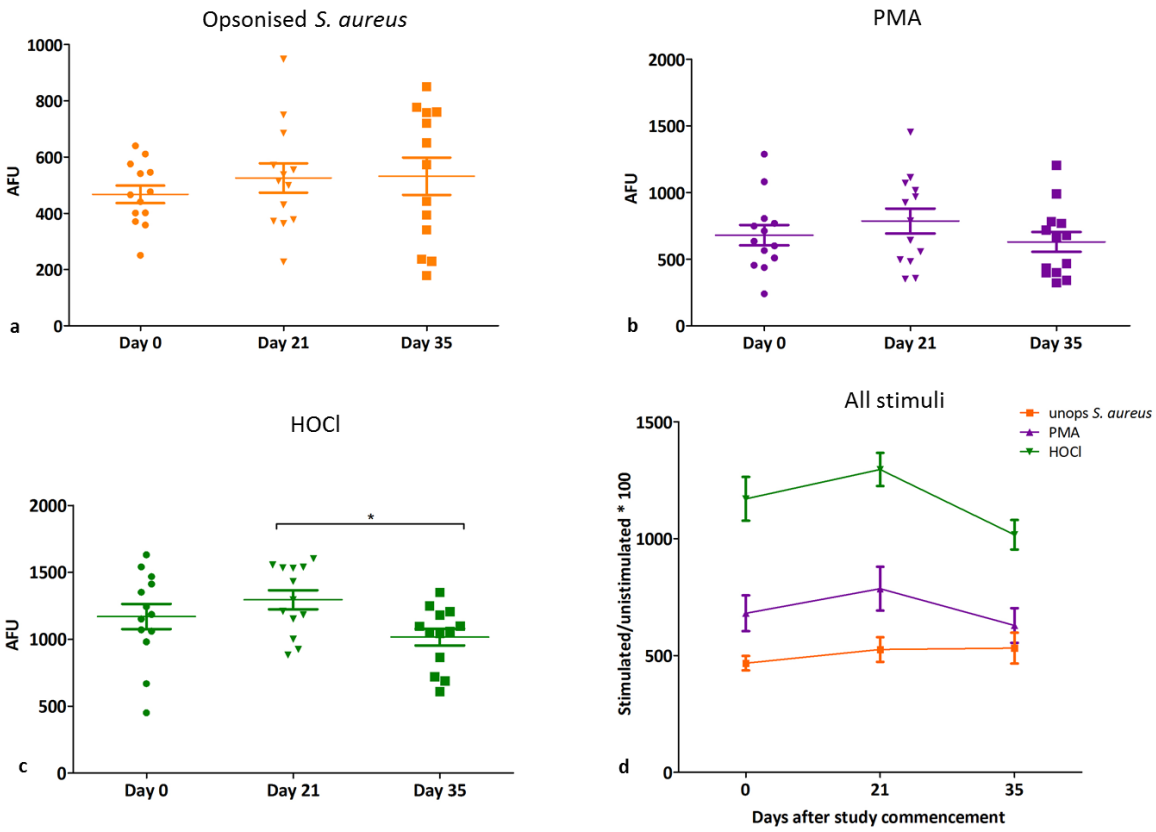

Figure 4.5 NET quantification in gingivitis

Neutrophils were isolated (section 2.2) and NETs were quantified in response to opsonised *S. aureus* (MOI 1 in 150; a), PMA (50nM; b) and HOCl (0.75 mM; c) (section 2.5). All data is shown together (d). Averaged AFU readings were normalised by dividing all values by the respective gPBS control for a given time point x 100. n = 15 volunteers. Statistical test: ANOVA with Tukey's post-test. * = ($p < 0.05$).

4.6. Neutrophil ROS generation in experimental gingivitis and periodontitis

To assess for potential differences in ROS release from peripheral blood neutrophils with induced gingivitis, total ROS production was determined using the chemiluminescent reagent luminol (Figure 4.6). The stimuli used activated the three different signalling pathways as previosuly described (section 1.3.2). The effect of GM-CSF (10ng/ml) priming (section 1.5) was also measured. In the absence of priming, ROS generation revealed minimal differences between baseline (day 0), day 21 and inflammation resolution (day 35) following exposure to opsonised *S. aureus* and *F. nucelatum* (Figure 4.6a and b respectively). However significant differences were evident at day 21 with PMA (Figure 4.6c) compared to baseline (day 0; $p < 0.05$) and inflammation resolution (day 35; $p < 0.001$). The effect of priming was only significant with PMA stimulation between days 21 and 35 ($p < 0.01$).

ROS generation in chronic periodontitis patient cohort 1 has already been reported (Ling *et al.* 2016). In summary, neutrophils isolated pre- and post-treatment were compared with age and gender-matched controls using lucigenin ($O_2^{\cdot}$ detection). Prior to stimulation $O_2^{\cdot}$ release was significantly higher in patients pre-treatment than controls (Wilcoxon test; p=0.011) and differences were lost following periodontal treatment when compared with controls. In the presence of stimuli, significantly more $O_2^{\cdot}$ was released pre-treatment with *P. gingivalis* (Wilcoxon test; p=0.0266) and *F. nucleatum* (Wilcoxon test; p=0.0064) and again significance was lost when comparing patients post-treatment to control values.

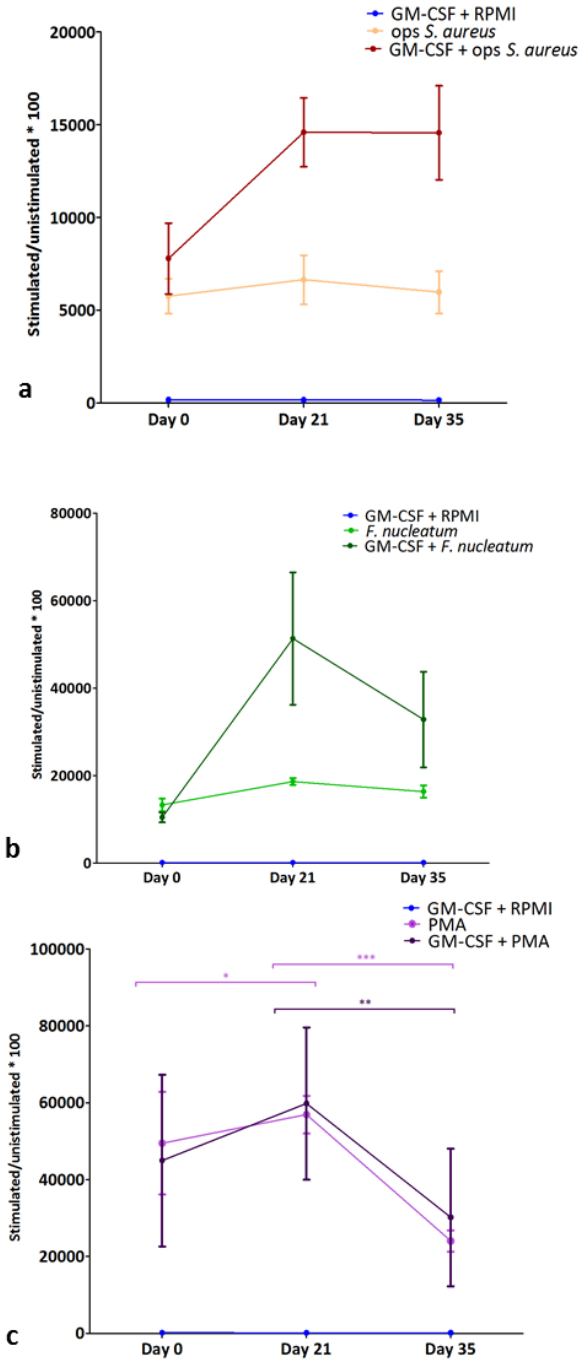

Figure 4.6 ROS production in gingivitis

Neutrophils were isolated (section 2.2) and peak values for ROS generation were measured in the presence of PBS, opsonised *S. aureus* (MOI 1 in 150) (a), *F. nucleatum* (b) (MOI 1 in 300) and PMA (25 nM) (c) (section 2.4.3). Three different stimulation pathways were assayed: Fcγ receptors (using opsonised *S. aureus*); TLR's (*F. nucleatum*); and direct receptor-independent stimulation of PKC by PMA. The effect of priming was also measured using GM-CSF (10ng/ml) (section 2.4.3.1) Total ROS was detected using luminol (n = 15). Peak data was normalised by dividing all values by the respective gPBS for a given time point x 100. Statistical test: ANOVA with Tukey's post-test. * = ($p < 0.05$), ** = ($p < 0.01$) and *** = ($p < 0.001$). The colour of the lines denoting significance reflect the respective colour of the stimulus used.

4.7. Chemotaxis in gingivitis and chronic periodontitis

Neutrophil speed, velocity and chemotactic index (CI) were measured over time in the presence of buffer or chemoattractant (fMLP or CXCL8) in neutrophils from experimental gingivitis study volunteers (Figure 4.7) and chronic periodontitis patient cohort 1 before (Figure 4.8) and after (Figure 4.9) non-surgical periodontal treatment. Tracked cell paths, polar plots and angle histograms were generated illustrating the differences in the course of cell movements for gingivitis volunteers (Figure 4.10) and periodontitis patients pre- (Figure 4.11) and post-treatment (Figure 4.12). Neutrophils isolated from gingivitis volunteers showed increased speed at day 21 compared to day 0 for both chemoattractants ($p < 0.001$) and day 35 with fMLP only ($p < 0.001$). No significant differences were noted with velocity, but for CI a small but significant decrease was seen comparing days 21 to the other days for fMLP only ($p < 0.001$).

For chronic periodontitis patients (cohort 1), pre-treatment neutrophils demonstrated significantly lower speed, velocity and CI than neutrophils from healthy volunteers for both fMLP ($p < 0.01$) and CXCL8 ($p < 0.05$). Following treatment, patient neutrophils still exhibited a significantly lower value for all three parameters after exposure to fMLP, however with the exception of speed, patient neutrophils were not significantly different in their response to CXCL8. Patients' pre- and post-treatment results were analysed separately due to high inter-individual variation that can arise when neutrophils are isolated on different days (which was explored in section 3.10).

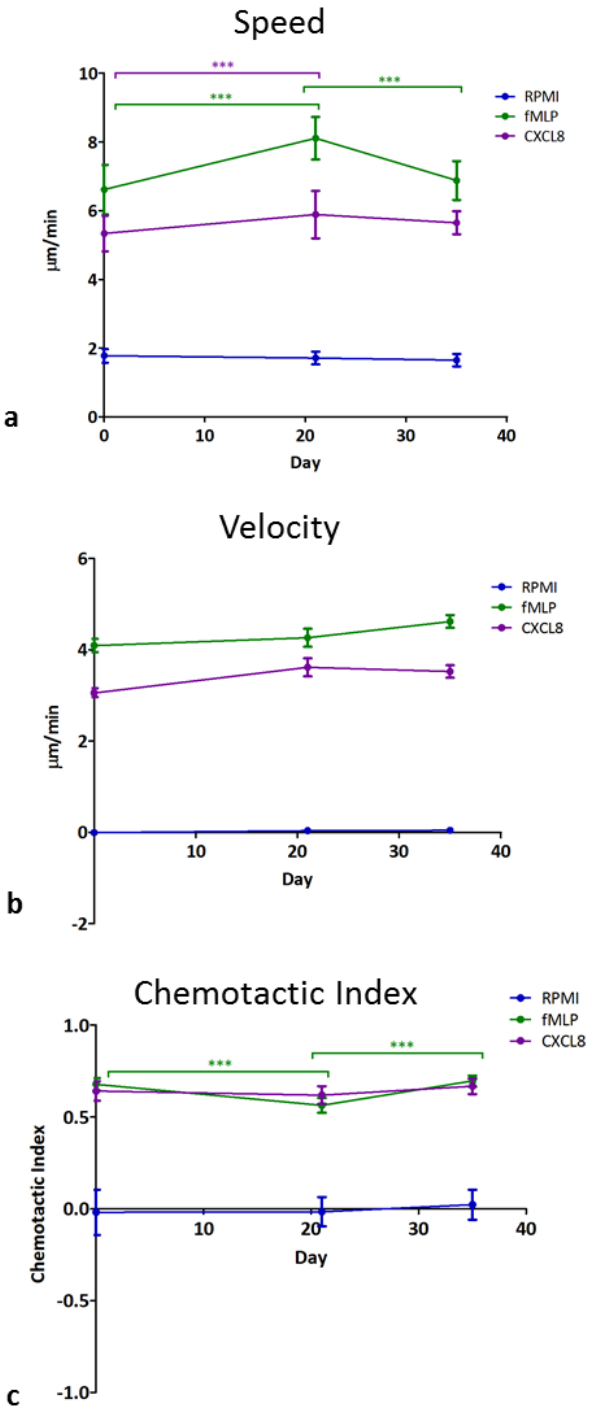

Figure 4.7 Chemotaxis in gingivitis

Neutrophils were isolated (section 2.2) and chemotaxis was performed (section 2.6), after which the cell moments were analysed (section 2.6.2) and tracked information was used to generate average speed (a), velocity (b) and CI (c) for neutrophils from gingivitis study volunteers in the presence of RPMI (negative control), fMLP (10nM) and CXCL8 (200ng/ml) chemoattractants. (n = 15; 15 cells tracked per chemoattractant/RPMI). Statistical test: ANOVA with Tukey's post-test. *** = ($p < 0.001$).

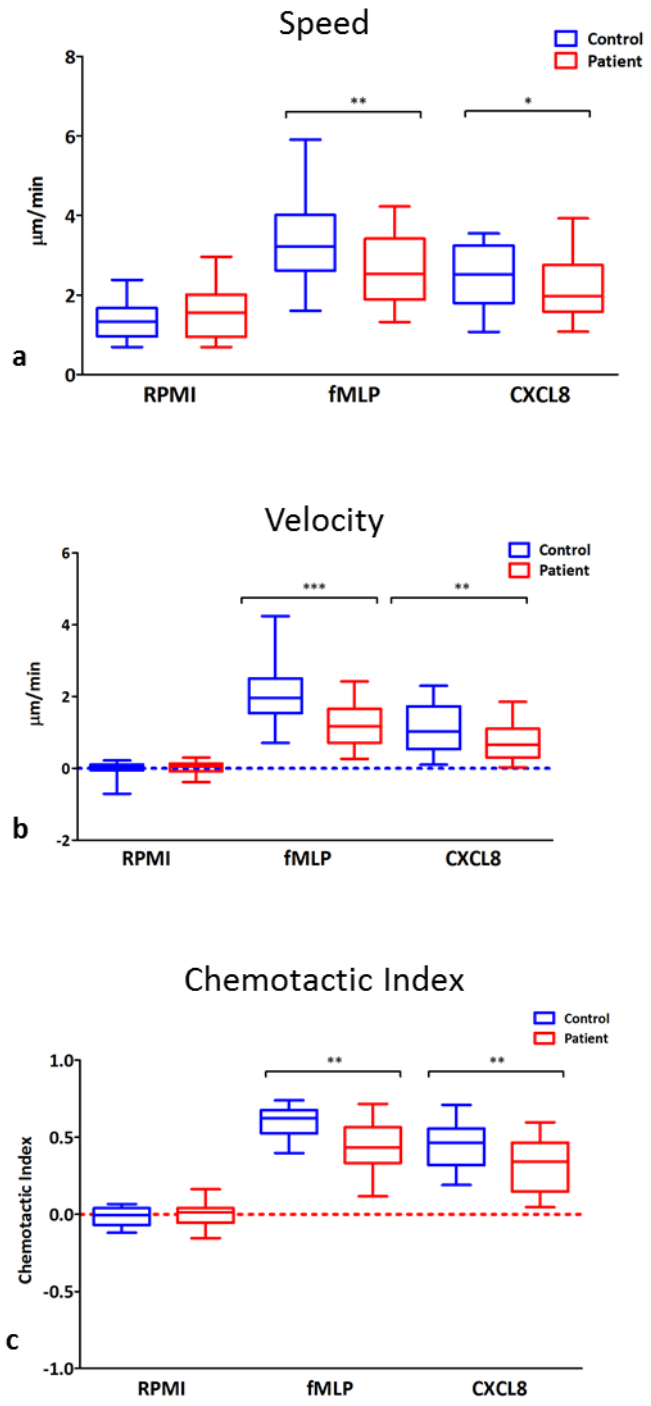

Figure 4.8 Chemotaxis in chronic periodontitis (patient cohort 1) pre-treatment

Neutrophils were isolated (section 2.2) and chemotaxis was performed (section 2.6), after which the cell moments were analysed (section 2.6.2) and tracked information was used to generate average speed (a), velocity (b) and CI (c) for neutrophils from chronic periodontitis patients (cohort 1) pre-treatment compared to healthy controls in the presence of RPMI (negative control), fMLP (10nM) and CXCL8 (200ng/ml) chemoattractants. (n = 15; 15 cells tracked per chemoattractant/RPMI). Statistical test: Wilcoxon test. ** = ($p < 0.01$). *** = ($p < 0.001$).

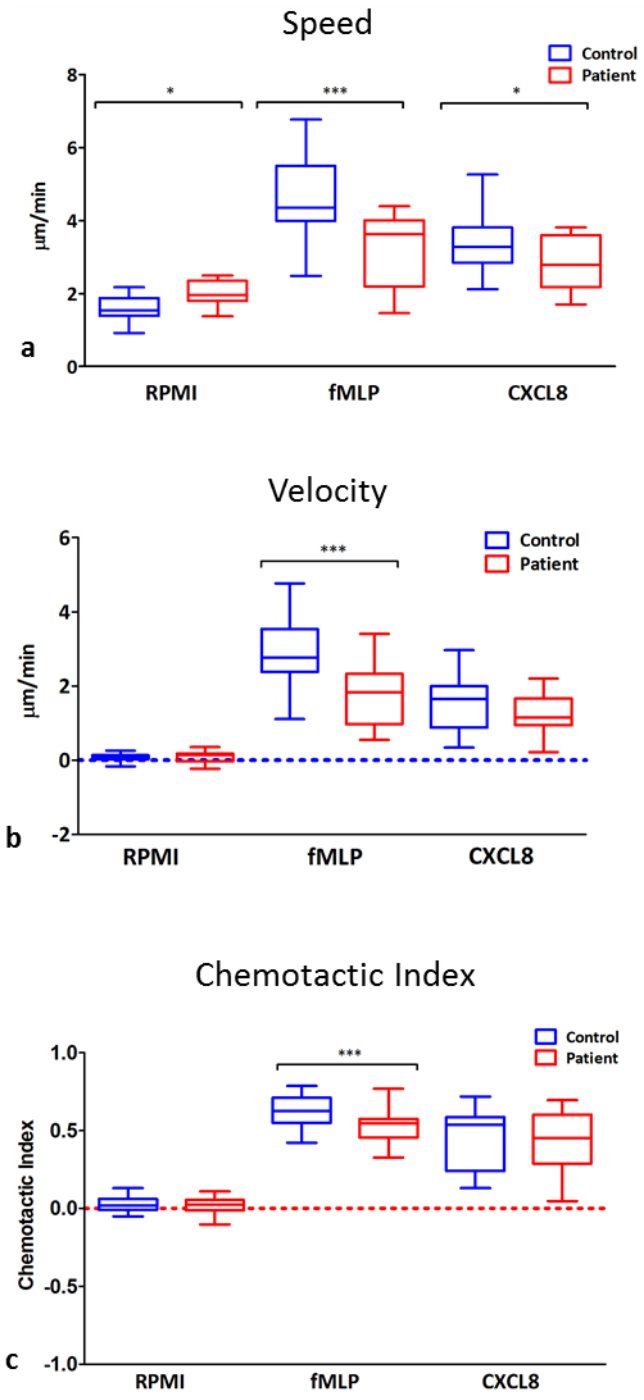

Figure 4.9 Chemotaxis in chronic periodontitis (patient cohort 1) post-treatment

Neutrophils were isolated (section 2.2) and chemotaxis was performed (section 2.6), after which the cell moments were analysed (section 2.6.2) and tracked information was used to generate average speed (a), velocity (b) and CI (c) for neutrophils from chronic periodontitis patients (cohort 1) post-treatment compared to healthy controls in the presence of RPMI (negative control), fMLP (10nM) and CXCL8 (200ng/ml) chemoattractants. (n = 15; 15 cells tracked per chemoattractant/RPMI). Statistical test: Wilcoxon test. * = ($p < 0.05$), *** = ($p < 0.001$).

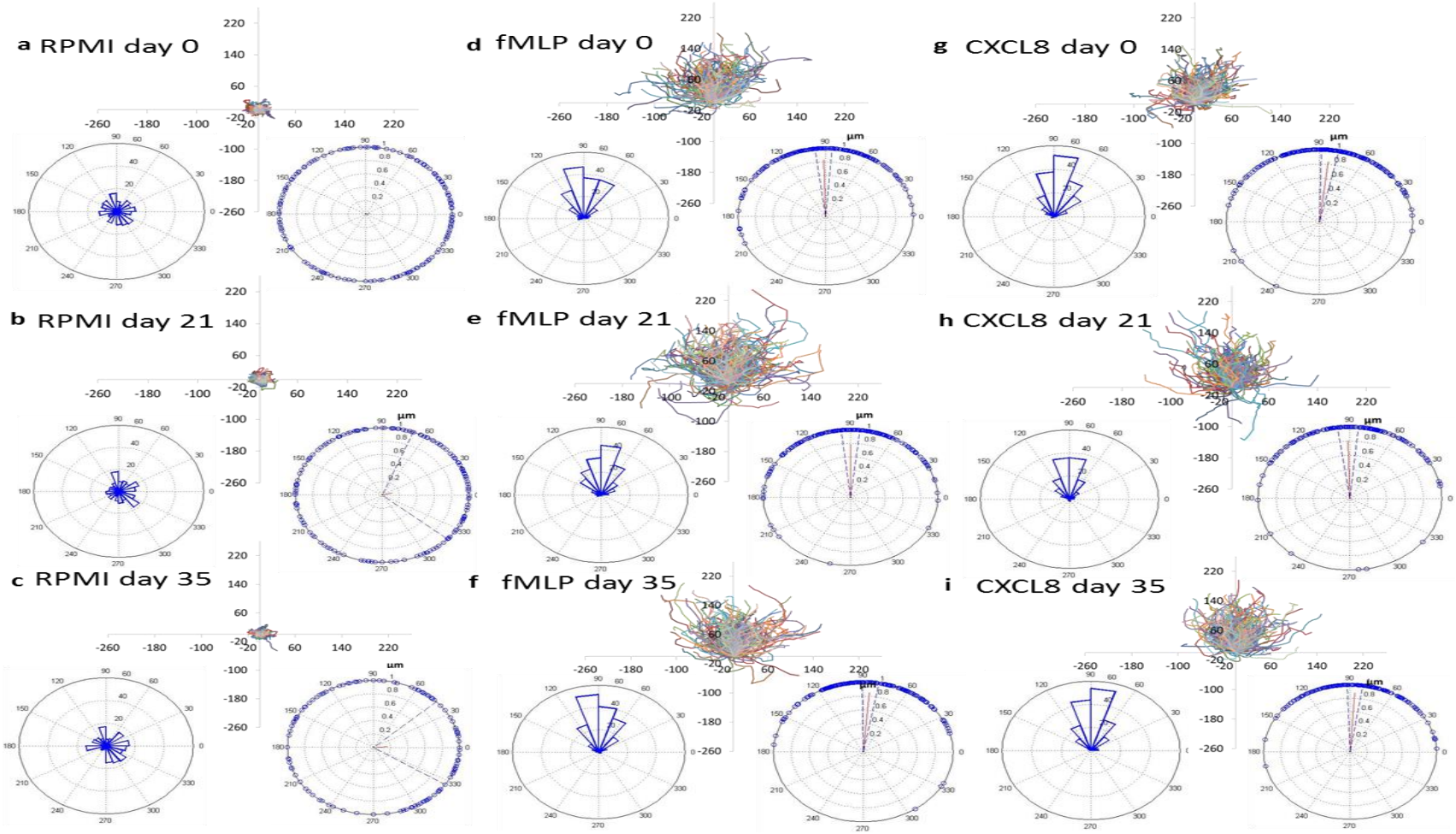

Figure 4.10 Gingivitis cell tracks
Cell tracks, polar plots and angle histograms overlayed for neutrophils isolated at days 0, 21 and 35 neutrophils were generated to give a qualitative overview of chemotaxis using RPMI (negative control; a-c), fMLP (d-f) and CXCL8 (g-i) chemoattractants respectively.

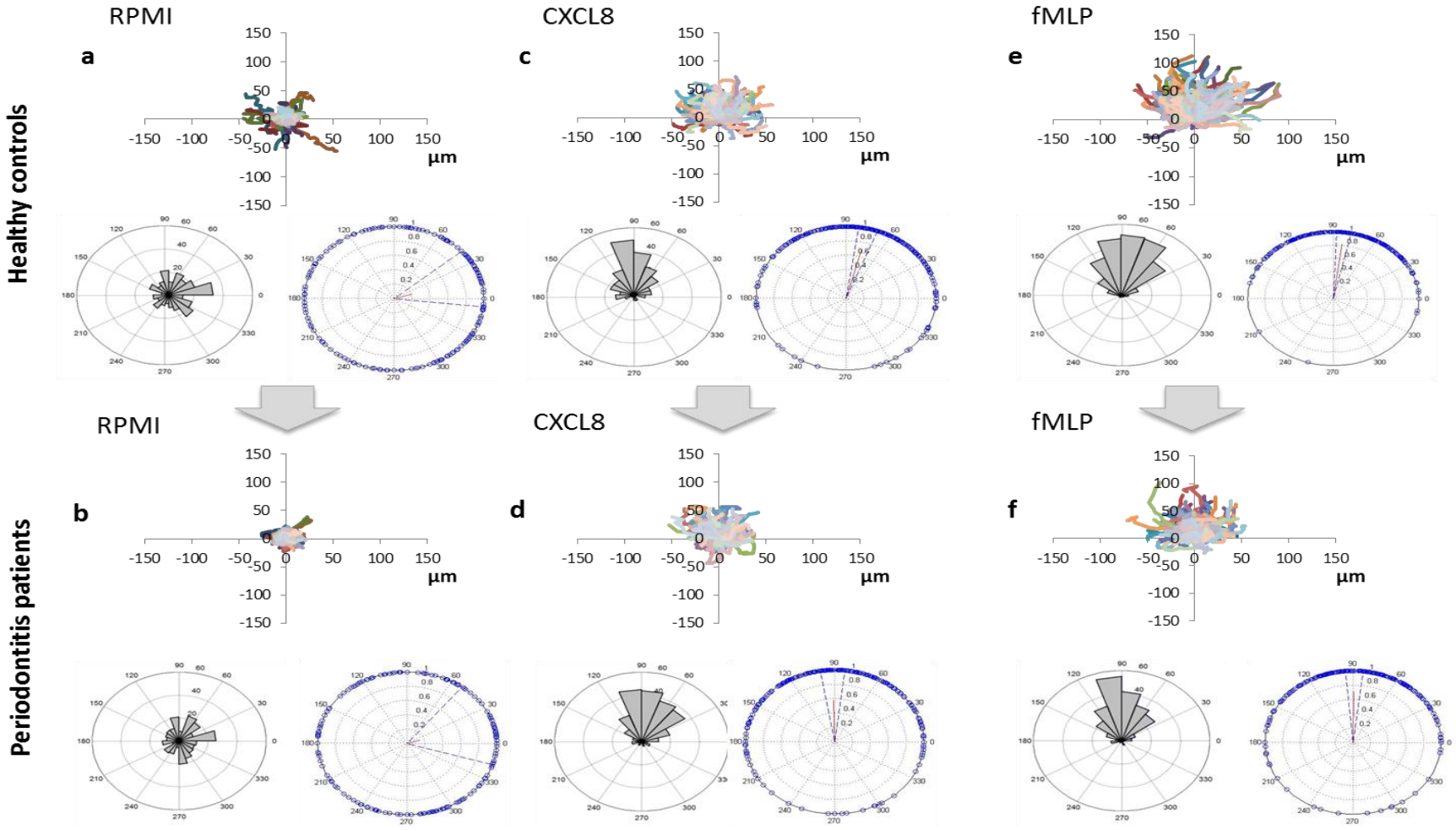

Figure 4.11 Chronic periodontitis (cohort 1) pre-treatment cell tracks
Cell tracks, polar plots and angle histograms overlayed for control (a,c,e) and patient (b,d,f) neutrophils were generated to give a qualitative overview of chemotaxis using RPMI (negative control), fMLP and CXCL8 chemoattractants respectively.

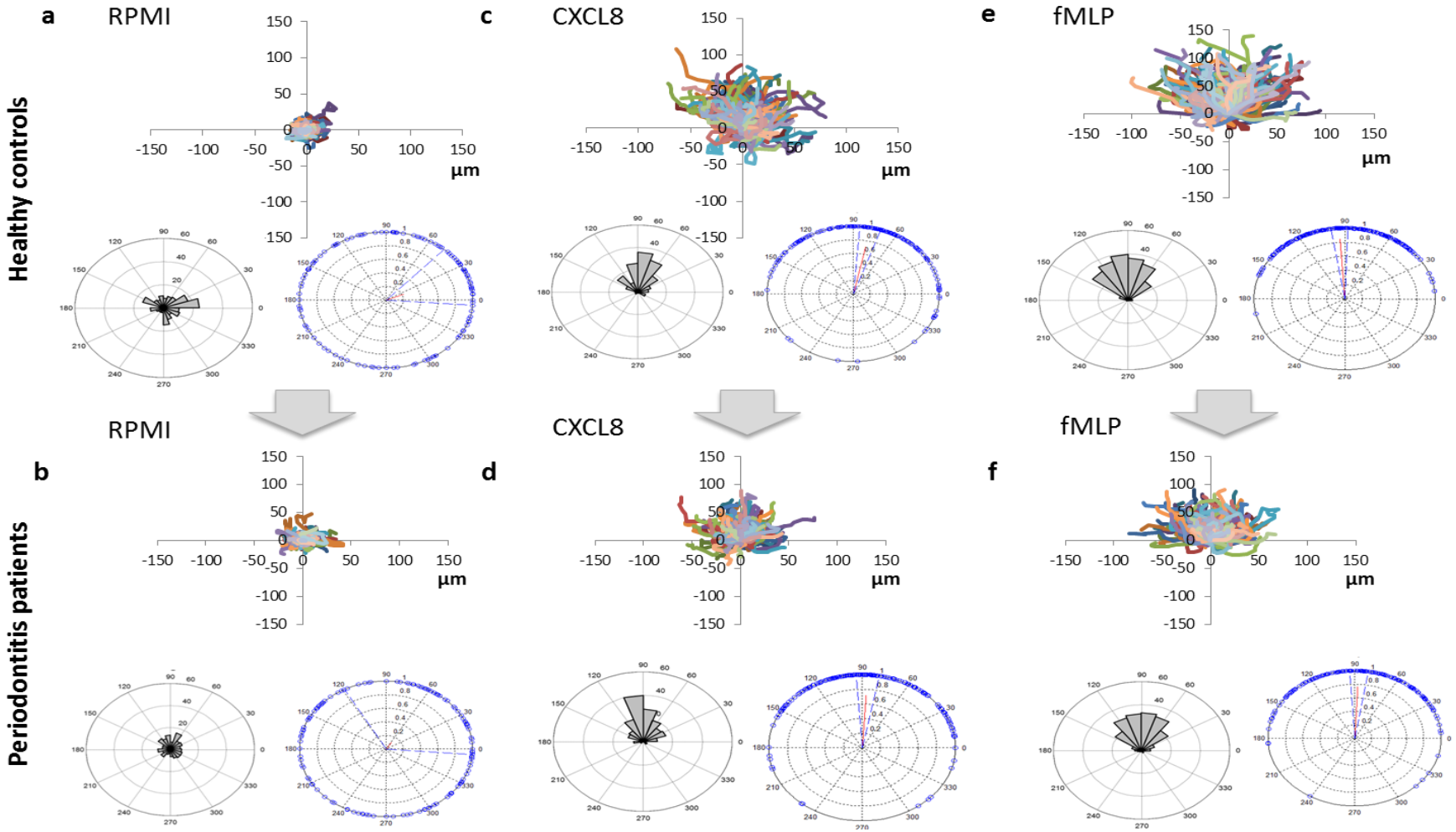

Figure 4.12 Chronic periodontitis (cohort 1) post-treatment cell tracks
Cell tracks, polar plots and angle histograms overlayed for control (a,c,e) and patient (b,d,f) neutrophils were generated to give a qualitative overview of chemotaxis using RPMI (negative control), fMLP and CXCL8 chemoattractants respectively.

4.8. Chemotactic capabilities of GCF in gingivitis and chronic periodontitis

GCF collected from test/diseased and control/healthy sites of experimental gingivitis volunteers and chronic periodontitis patients (cohort 2) respectively was analysed for chemoattractive properties. Neutrophils were isolated from periodontally and systemically healthy blood donors (section 2.1.1) and exposed to GCF after which chemotaxis was measured. Figure 4.13 shows the speed, velocity and CI for the 21-day gingivitis study volunteer GCF samples at day 0, 21 and 35; GCF protein content was normalised to the same levels for all samples. There were no differences at day 0 between the two sites, however at day 21 (the height of inflammation) GCF from test sites caused a significant increase in all three parameters ($p < 0.0001$) compared with their corresponding control sites. At day 35 significance was still evident for velocity ($p < 0.05$) and CI ($p < 0.01$) between control and test sites. For the chronic periodontitis GCF samples (Figure 4.14), there was a consistently significant increase in all three parameters with GCF collected from diseased sites compared with healthy sites ($p < 0.0001$).

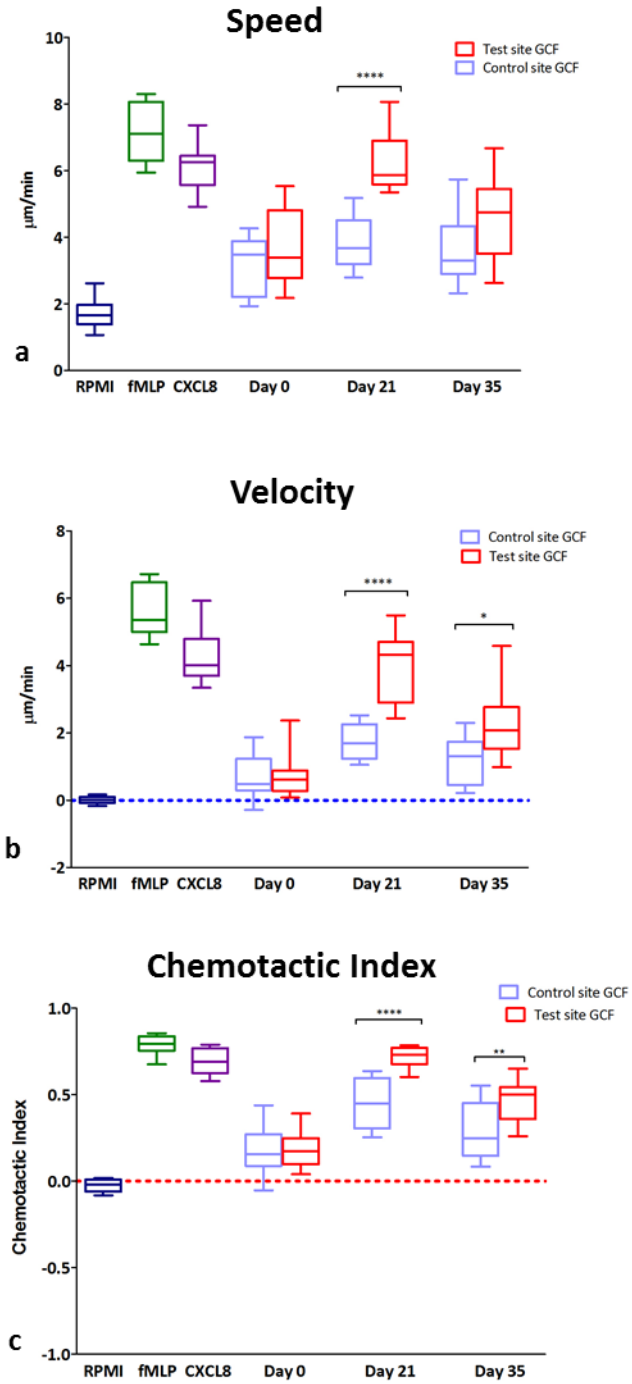

Figure 4.13 Chemotaxis using GCF from experimental gingivitis volunteers

Neutrophils were isolated (section 2.2) and chemotaxis was performed (section 2.6), after which the cell moments were analysed (section 2.6.2) and tracked information was used to generate average speed (a), velocity (b) and CI (c) for neutrophils from healthy blood donors in the presence of RPMI (negative control), fMLP (postive control; 10nM), CXCL8 (positive control; 200ng/ml) and GCF collected and processed (section 2.11.1.2) from test and control sites of the gingivitis study volunteers. (n = 10; 15 cells tracked per chemoattractant/RPMI/GCF sample). Statistical test: Wilcoxon test. * = $p < 0.05$, ** = $p < 0.01$, **** = $p < 0.0001$.

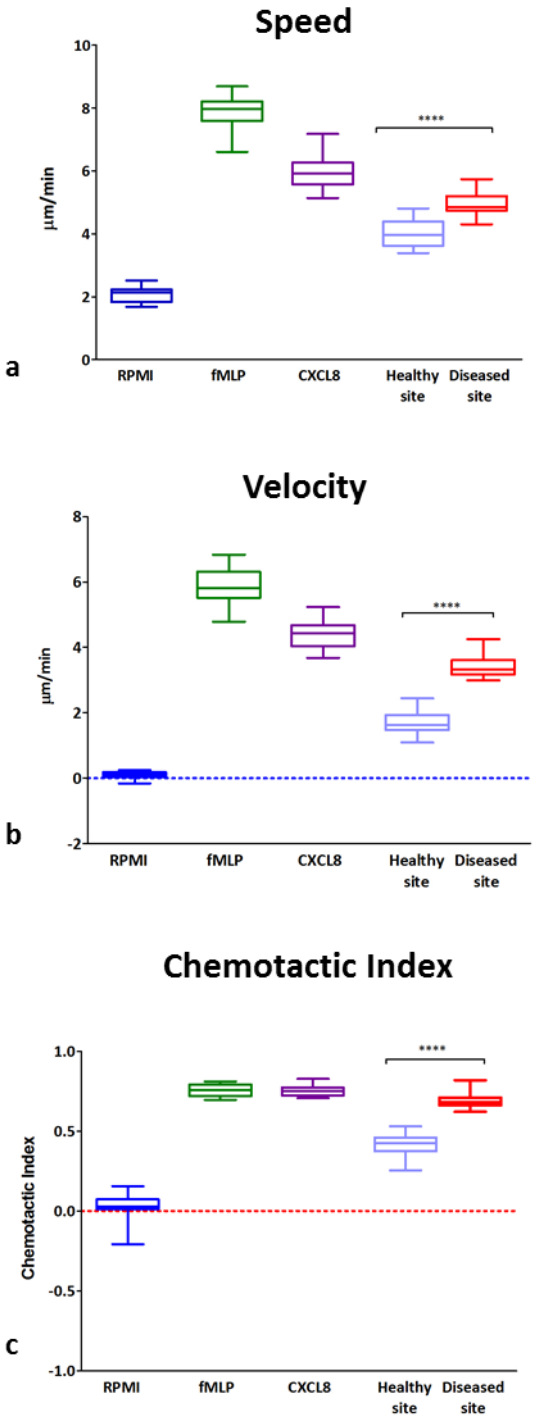

Figure 4.14 Chemotaxis using GCF from chronic periodontitis patients (cohort 2)

Neutrophils were isolated (section 2.2) and chemotaxis was performed (section 2.6), after which the cell moments were analysed (section 2.6.2) and tracked information was used to generate average speed (a), velocity (b) and CI (c) for neutrophils from healthy blood donors in the presence of RPMI (negative control), fMLP (positive control; 10nM), CXCL8 (positive control; 200ng/ml) and GCF collected and processed (section 2.11.1.2) from diseased and healthy sites of chronic periodontitis patients (cohort 2). (n = 10; 15 cells tracked per chemoattractant/RPMI/GCF sample). Statistical test: Wilcoxon test. * = $p < 0.05$, ** = $p < 0.01$, **** = $p < 0.0001$.

4.8.1. Cytokine quantification in GCF during gingivitis and chronic periodontitis

The pro-inflammatory cytokines IL-1β and TNFα were quantified by ELISA from the GCF collected from control/healthy and test/diseased sites of experimental gingivitis study volunteers and chronic periodontitis patients (cohort 2) respectively. Previous experiemental work have found both cytokines to be measurable by ELISA in GCF (data unpublished) whereas other cytokines, notably CXCL8, are below the detection limit. Furthermore, the small collected sample volumes restricted the number of cytokines that could be quantified. Figure 4.15 show the results for IL-1β and Figure 4.16 for TNFα, the data is expressed as amount (pg) per 30 second sample time as previsouly described (Chapple et al. 1999). For GCF from gingivitis sites there was a clear increase in both IL-1β and TNFα at day 21 compared with baseline (day 0) and inflammation resolution (day 35) (Figure 4.15d and Figure 4.16d respectively) which was significant between test and control sites at day 21 ($p < 0.05$). For chronic periodontitis (cohort 2), the test sites had significantly greater concentrations of both cytokines in diseased sites over healthy ($p < 0.01$) (Figure 4.15e and Figure 4.16e). It is interesting to note that the concentrations of both IL-1β and TNFα are far greater than respective gingivitis control and test sites at the height of inflammation (day 21).

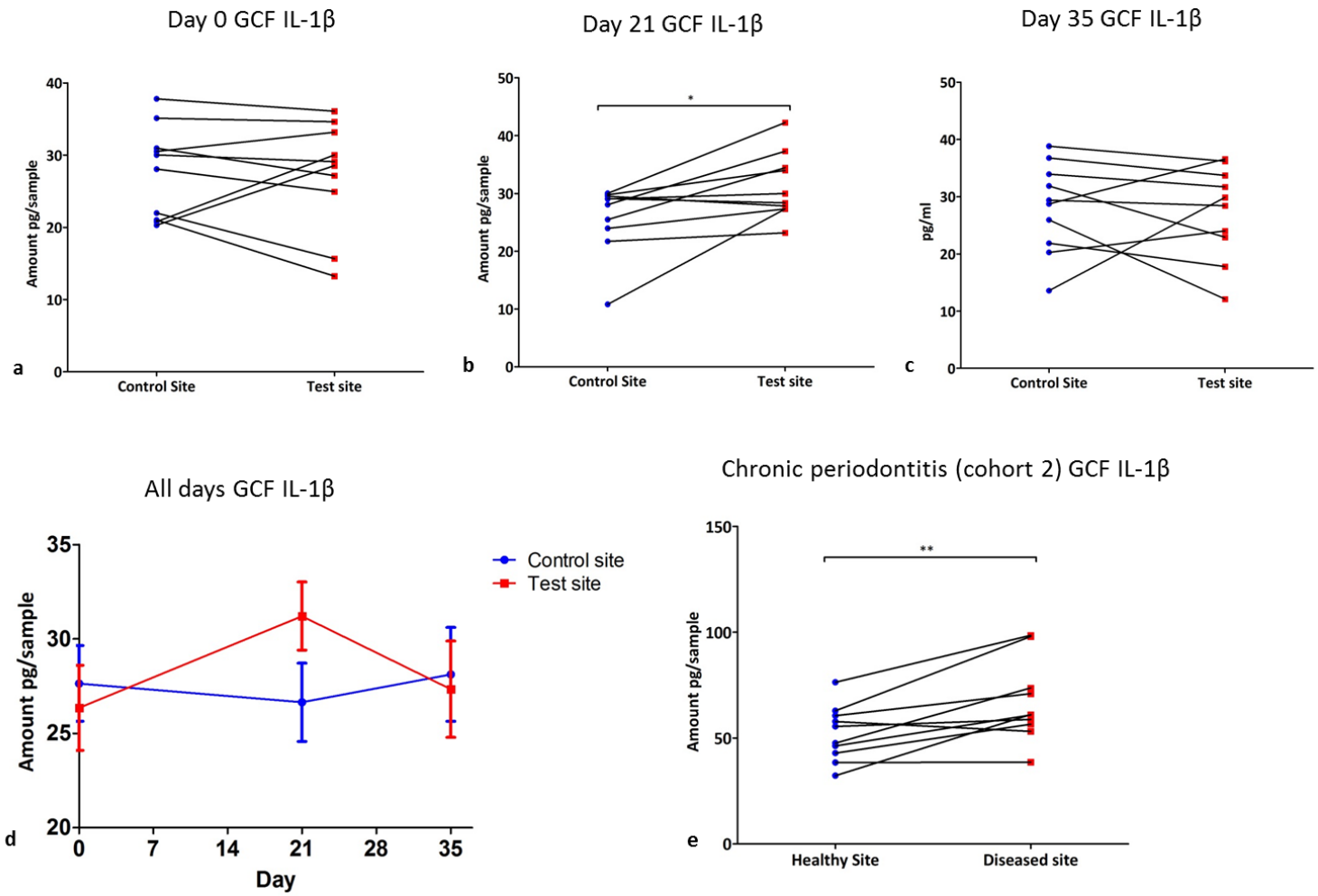

Figure 4.15 IL-1β ELISA in GCF samples

GCF was collected and processed (2.11.1.2) after which IL-1β was quantified from control/healthy and test/diseased sites for days 0, 21 and 35 of the gingivitis study and in chronic periodontitis patients (cohort 2). n = 10. Statistical test: paired t-test. * = $p < 0.05$, ** = $p < 0.01$.

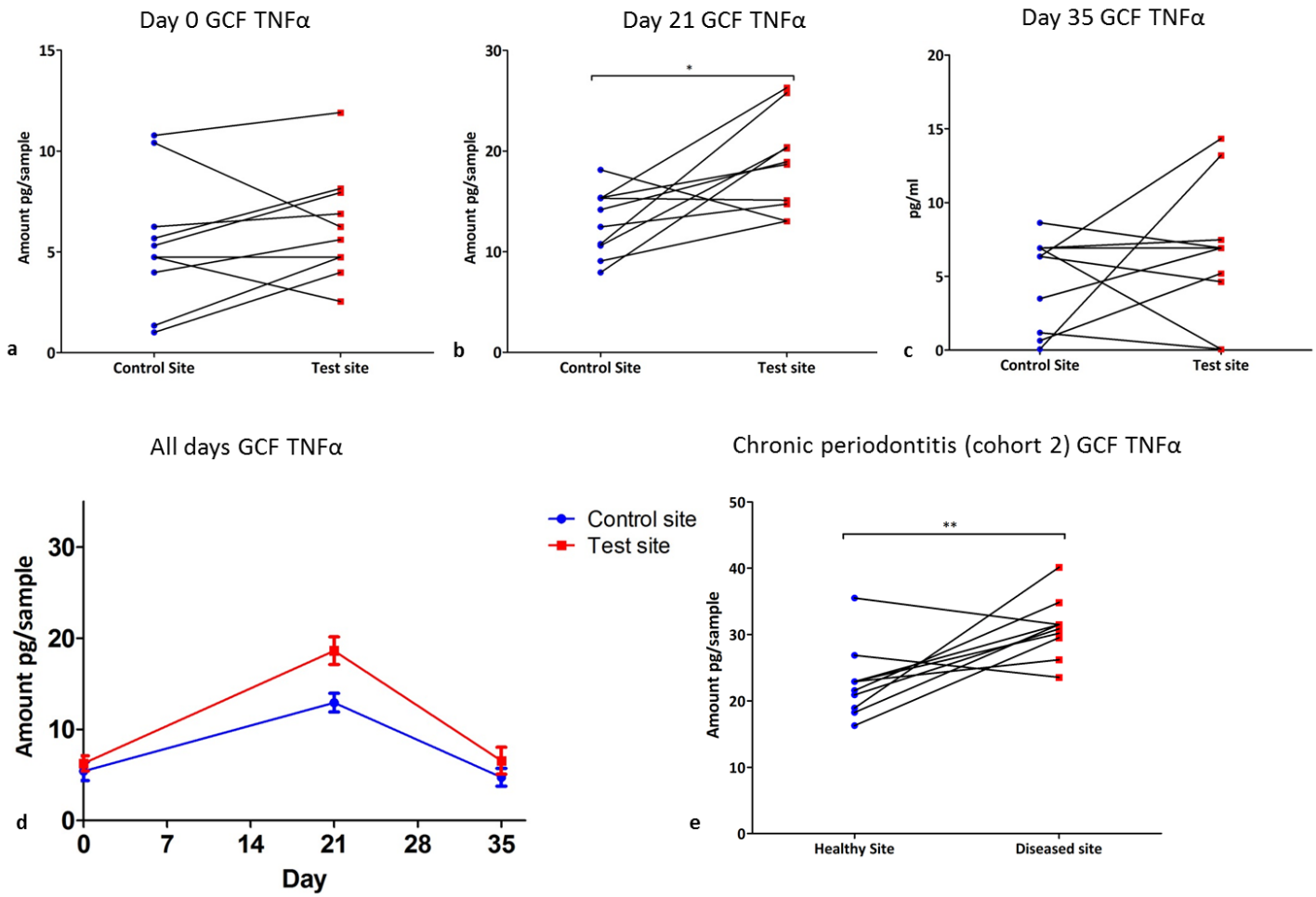

Figure 4.16 TNFα ELISA in GCF samples

GCF was collected and processed (2.11.1.2) before TNFα was quantified from control/healthy and test/diseased sites for days 0, 21 and 35 of the gingivitis study and in chronic periodontitis patients (cohort 2). n = 10. Statistical test: paired t-test. * = $p < 0.05$, ** = $p < 0.01$.

4.9. Discussion

The chemotaxis results for chronic periodontitis presented here have now been published (Roberts *et al.* 2015) and are detailed in Appendix II.

Neutrophil ROS and NET production and chemotactic accuracy were assessed in a 21-day experimental gingivitis model in which healthy volunteers were prevented from brushing specified oral sites in order to induce reversible gingivitis. Neutrophils were isolated and the assays were performed at three time points representing baseline, the height of inflammation, and resolved inflammation. Neutrophil chemotactic accuracy was also measured in neutrophils isolated from a group of chronic periodontitis patients (cohort 1) alongside healthy gender- and age-matched controls prior to and following treatment, representing a longitudinal study. Finally, GCF was collected from the gingivitis study volunteers and a second cohort of chronic periodontitis patients (cohort 2). Two different sites were sampled representing health or disease/inflammation in order to measure pro-inflammatory cytokine release from GCF and to investigate its potential chemoattractive properties.

The 21-day experimental gingivitis model provides an opportunity to investigate the induction and resolution of inflammation after a short period (35 days in total) of increased exposure to accumulating bacteria in a precisely controlled inflammatory process (Löe and Theilade 1965; Chapple *et al.* 1996; Wright *et al.* 2003). Other reported uses of this model include assessing the effects of compounds in drugs (Heasman *et al.* 1993) and environmental toxins such as tobacco smoke (Bergstrom & Preber 1986; Giannopoulou *et al.* 2003) on the progression of gingival inflammation. As expected, the cessation of plaque removal by brushing resulted in increased gingival and plaque indices for the gingivitis volunteers. For the chronic periodontitis patients (cohort 1) both GI and PI were significantly

higher pre-treatment compared to both post-treatment and periodontally healthy controls; however any significant differences were lost following treatment.

Gingival crevicular fluid (GCF) is a serum transudate/exudate that can be collected at the gingival margin or from the gingival crevice and represents a non-invasive method of measuring the inflammatory state of the periodontal tissues. GCF volume is expected to increase during inflammation (Löe *et al.* 1965), thereby demonstrating the induction/presence of gingivitis and periodontitis (Wright *et al.* 2003). In the study of chronic periodontitis, two cohorts of patients were studied due to the impossibility of accessing GCF from cohort 1. Cohort 2 did not have systematically collected clinical data and thus further details describing the extent of their periodontal disease could not be described in detail, but both cohorts had GCF volumes measured. Although GCF volume increases with increasing inflammation it may not correlate to disease severity but the levels of IL-1β in GCF have been postulated to be a marker of disease severity and activity (Baser *et al.* 2014) and were measured in the GCF of cohort 2 as discussed below.

ROS production over the course of the 21-day gingivitis study showed an increase at the height of inflammation (day 21) and in the presence of the priming agent GM-CSF. Significance was only reached with a PMA stimulus in both the absence/presence of priming at the height of inflammation (day 21) compared to the other two time points (day 0 and 35) although increases from day 0 to day 21 were visible with the other stimuli used. These results demonstrate the potential for localised acute inflammation to have a systemic impact (because neutrophils were collected from peripheral blood), potentially enhancing the responsiveness of neutrophils to stimuli such as bacteria or their products or to priming agents, but following inflammation resolution the effect on ROS production was reversible. ROS generation from chronic periodontitis patient cohort 1 has previously been reported (Ling 2015) with results demonstrating a higher level of $O_2^{\cdot}$ generation pre-stimulation in

neutrophils prior to periodontal treatment (Ling *et al.* 2016), an indication of hyperactivity which has also previously been reported in periodontitis (Matthews *et al.* 2007a), but which was no longer detectable following successful periodontal treatment. In the presence of stimulation, neutrophils from pre-treatment patients exhibited enhanced ROS generation, indicating a hyper-reactive neutrophil phenotype (Matthews *et al.* 2007b), which was also lost following treatment. The plasma-derived stimulants implicated in neutrophil hyperactivity and hyper-reactivity included GM-CSF, CXCL8 and Interferon alpha (IFNα) (Dias *et al.* 2011). Elevated IFNα levels have been identified in periodontitis patients relative to healthy controls (Wright *et al.* 2008); the gene expression profile of periodontitis patient neutrophils revealed differential expression of 163 genes, in particular increased expression of a number of type-1 IFN-responsive genes (Wright *et al.* 2008). The constitutively reactive nature of the hyperactive neutrophil phenotype may also be due to an altered intracellular redox state (GSH:GSSG ratio) reported in chronic periodontitis patient neutrophils leading to cellular stress and resultant relocation of NADPH oxidase to the outer cell membrane (Dias *et al.* 2013a) and supporting the contribution of ROS as a significant contributor to the systemic oxidative stress reported to characterise periodontitis.

NET formation was also measured in the gingivitis study volunteers, with all stimuli increasing NETs at day 21 which then normalised/decreased by day 35. Significance was reached with HOCl at day 21 compared with day 35. Neutrophils and NET-associated proteins have been identified within the supragingival plaque of individuals partaking in the experimental gingivitis model, demonstrating that biofilms are composed of both microbial and host immune cells (Hirschfeld *et al.* 2015). NET measurements were previously reported in periodontitis patient cohort 1 (White 2015), in which no differences in NET production were observed patients following treatment when compared with age and gender- matched controls. When expressed as a ratio of patient NETs to control NETs pre- and post-treatment

in order to accommodate day-to-day variability of neutrophil assays, the decrease in NET production was more pronounced. NET formation has been shown to be upregulated in other disorders of chronic inflammation such as in COPD patient sputum when compared with healthy controls (Grabcanovic-Musija *et al.* 2015), pre-eclampsia (Gupta *et al.* 2005) and small-vessel vasculitis (Kessenbrock *et al.* 2009). However, there is no data to date on peripheral blood neutrophil NET production in periodontitis patients in comparison with controls other than unpublished data (White *et al.* 2016 in press), the results of which demonstrated no overall NET differences relative to matched controls, though NET production was significantly decreased in patients when comparing pre and post-treatment. Chemotactic accuracy was measured in both experimental gingivitis and chronic periodontitis (cohort 1). Neutrophils from the gingivitis cohort exhibited greater overall speed at day 21, but lower CI compared with baseline and resolution. These effects were mainly seen with the chemoattractant fMLP. The chronic periodontitis patients (cohort 1) demonstrated an overall reduced chemotactic accuracy prior to treatment with both CXCL8 and fMLP chemoattractants and following treatment only significance with fMLP remained compared to healthy controls. Defective neutrophil chemotaxis has been shown in individuals with chronic inflammatory conditions including rheumatoid arthritis (Biemond *et al.* 1986; Miesel *et al.* 1996; Bostan *et al.*2002; Cedergren *et al.* 2007) and COPD (Rahman *et al.* 1997; Yoshikawa *et al.* 2007; Sapey *et al.* 2011), however few studies have examined chemotaxis in chronic periodontitis (Kumar & Prakash 2012). Numerous studies have reported chemotaxis in localised aggressive periodontitis (LAP), a condition associated with a strong genetic pre-disposition occurring in otherwise systemically healthy individuals (Nibali *et al.* 2008). Despite the differences between LAP and chronic periodontitis, which includes differences in the oral microflora of these patients (Fu *et al.* 2002), reports of defective chemotaxis in LAP help to characterise the defects in the ability of neutrophils to

chemotax towards stimuli in a gradient-driven manner. Several studies have reported a diminished capacity of fMLP to bind to neutrophils from LAP patients, indicating a reduction in receptor numbers on the cell surface, the receptors themselves appearing fully-functional (Van Dyke *et al.* 1981; Van Dyke *et al.* 1986). Such a finding could explain the diminished responsiveness of these cells to a chemoattractive gradient. Furthermore, LAP neutrophils have been shown to express reduced levels of the glycoprotein gp110 (ADRM1 or hRpn13) (Van Dyke *et al.* 1987; Van Dyke *et al.* 1990), and studies in which gp110 function is attenuated resulted in diminished neutrophilic responses from healthy individuals in response to fMLP (Cotter *et al.* 1981). LAP neutrophils are also reported to have reduced expression of CD38, another receptor required for chemotaxis via fMLP (Fujita *et al.* 2005). Downstream signalling upon chemoattractant-receptor binding results in the activation of numerous signalling pathways; the PI3-K mediated activation of phosphoinositide dependent kinase-1 (PDK-1) is an essential regulator of chemotaxis and has reduced expression and activity in LAP neutrophils (Yagi *et al.* 2009). The PKC activator diacylglycerol (DAG) functions as a second messenger in a variety of neutrophil cellular processes including $O_2^{\cdot}$ production and chemotaxis (Nishizuka 1986; Harvath *et al.* 1987; Lambeth 1988), and has been shown to be elevated in LAP neutrophils. This offers an attractive option for the identification of such an abnormality in chronic periodontitis neutrophils, to support the potential that neutrophils are kept in a primed state for subsequent enhanced activity following exposure to an appropriate stimulus. However, cross-correlation between the defects witnessed in LAP and those reported here remains to be elucidated. The in-depth identification of deficiencies in LAP neutrophils provides an attractive avenue for further work to identify any commonalities between the different clinical definitions of periodontitis.

GCF represents a convenient, non-invasive, and efficient means to sample biomarkers of inflammation in the oral cavity. GCF collected from gingivitis volunteers and chronic

periodontitis patients (cohort 2) was used in two assays as detailed in this chapter: first as a chemoattractant to measure the ability to induce chemotaxis in neutrophils isolated from healthy individuals; and second to quantify the pro-inflammatory cytokines IL-1β and TNFα. This chemotaxis data demonstrated the inability of GCF from control/healthy sites to have a potent chemotactic effect, conversely, at the height of inflammation (day 21 in experimental gingivitis) and in periodontitis samples, all chemotaxis parameters were greater than their respective controls, showing a similar effect to CXCL8 and fMLP. GCF carries proteins from the gingival tissues and fluid via the crevice, which may provide insights into the immunological processes occurring within the gingival tissues (Adonogianaki *et al.* 1994; Gonzáles *et al.* 2001; Wright *et al.* 2003). Proteomic analysis of GCF detected temporal changes in numerous proteins during the course of experimental gingivitis, such as neutrophil defensins, which were elevated at day 35 in test sites (Grant *et al.* 2010) and which may reflect the role of neutrophils in maintaining a healthy state upon resolution of inflammation (Bostanci *et al.* 2010); cytokines were not detected due to low sub-attomole concentrations. The IL-1β and TNFα ELISA results showed a significant increase in both cytokines at the height of inflammation in the gingivitis volunteer test sites and in the diseased sites of chronic periodontitis patients (cohort 2). Interestingly the concentrations of both cytokines were greater in chronic periodontitis healthy sites in comparison to control sites of the experimental gingivitis GCF samples, indicating a different level of overall immune activation in chronic periodontitis compared to gingivitis. For gingivitis significance was lost by day 35. Cytokines can potentially serve as biomarkers of disease; dysregulation of the relative balance of cytokines can often be the earliest marker of a pathologic response (Bozza *et al.* 2007; Chun *et al.* 2007). Numerous studies have reported raised levels of cytokines in experimental gingivitis which include LTB_4 (Heasman *et al.* 1993), transforming growth factor beta (TGFβ) (Wright *et al.* 2003) and IL-1α (Offenbacher *et al.* 2010). The potent pro-

inflammatory cytokines IL-1β and TNFα both exhibit bone-resorbing activty (Tani-Ishii *et al.* 1999). Enhanced levels during gingivitis alongside expectedly high levels in chronic periodontitis provides a more detailed understanding of the conditions to which neutrophils within the oral cavity are exposed, which may underly any hyper-reactive responses, particularly with regard to ROS generation, a factor known to result in host-collateral tissue damage. Increases in IL-1β concentrations have previosuly been reported in experimental gingivitis (Gonzales *et al.* 2001; Offenbacher et a. 2010; Scott & Krauss 2012) and are associated with increasing gingival inflammation (Buduneli & Kinane 2011; Boronat-Catalá *et al.* 2014).

4.10. Chapter 4 summary

The mechanisms underlying the progression of gingivitis to periodontitis in susceptible individuals are poorly understood. Neutrophils are key immune cells involved in protecting the host from bacterial challenge. Disruption to neutrophil functions such as ROS, NETs and chemotaxis may pre-dispose an individual to further infection and inflammation, exacerbating disease pathogenesis. Reduced neutrophil chemotactic accuracy may affect the ability of neutrophils to efficiently exit the circulation in order to reach the site of infection, potentially allowing periodontal pathogens to colonise in the periodontal tissues with a reduced host-immune threat. Moreover increased tissue transit times coupled with enhanced ROS generation (Matthews *et al.* 2007a) and NET production (White *et al.* 2016), as a result of underlying increases in pro-inflammatory cytokines (Ling *et al.* 2015), may result in enhanced collateral host tissue damage contributing to the inflammatory burden. These findings add to the current understanding of the effects of acute and chronic inflammatory states on the functional abilities of neutrophils and how they in turn may contribute to disease progression via host-mediated tissue damage (Grossi *et al.* 1994).

CHAPTER 5 RESULTS - AN ASSESSMENT NEUTROPHIL FUNCTION IN PAPILLON-LEFÈVRE SYNDROME

5.1. Introduction

Papillon-Lefévre Syndrome (PLS) is a rare inherited autosomal recessive disease affecting 1 in 250,000-1 million people and is characterised by palmoplantar keratosis and severe pre-pubertal periodontitis leading to premature loss of all teeth. The underlying mutation(s) in PLS is in the cathepsin C (CTSC) gene, resulting in loss of activity and subsequent failure to activate neutrophil serine proteases (NSPs) and therefore immune response proteins. The NSP deficiency has been postulated by many to be the underlying cause for the severe pre-pubertal periodontitis in PLS as a result of NSP deficiencies failing to eliminate pathogenic bacteria. However, the severe inflammation and bone destruction evident in these patients indicates a far more complex picture and a more comprehensive assessment of neutrophil function in PLS seems likely to reveal a greater depth of understanding of the mechanisms that culminate in the destructive localised chronic periodontal inflammation that characterises PLS.

This chapter presents results from a cross-sectional assessment of neutrophil ROS and NET production as well as chemotaxis and cytokine release from individuals with PLS compared with healthy gender-matched controls. The data collected will add to current understanding of aetiology of PLS, in particular the influence of NSPs on neutrophil functionality.

5.2. Patient background information

As described in 2.1.4, adolescent patients and young adult control volunteers were recruited specifically for this study. Table 5.1 provides summary patient demographics and CTSC mutation analyses. Controls were gender-matched, ages ranged from 19-21 and BMI ranged ~18-23. All volunteers had severe pre-pubertal periodontitis and mutation analysis was by direct sequencing by Professor Nalin Thakker and Dr Ratna Veeramachaneni. Patient 1 was a compound heterozygote and had the mildest clinical phenotype, but also had a very low

neutrophil count at the time of venepuncture and was thus only involved in the study of NET quantification. Volunteer 2 had a Y294C mutation (maternal allele) and is thus heterozygous for this mutation. The paternal allele was not detected and is probably within the intronic region that was not subject to analyses. Figure 5.1 illustrates the palmoplantar keratosis and periodontal destruction in one of the patients recruited.

Table 5.1 Characteristics of patients recruited in PLS study

Patient no.	Age	Gender	Ethnicity	BMI	PLS type	Mutation
1	12	Male	Caucasian	18.93	Heterozygous	1/2 G139R; 1/2 N427T
2	14	Female	Indian	19.90	Heterozygous	1/2 Y294C; 1/2 not detected
3	14	Female	Pakistani	20.04	Homozygous	2/2 R272P
4	9	Male	Pakistani	22.83	Homozygous	2/2 R272P
5	15	Male	Pakistani	18.15	Homozygous	2/2 R272P

Figure 5.1 PLS patient clinical characteristics

Hyperkeratosis of the plantar surfaces of the feet (a) and palmar surfaces of the hands (b) in one of the patients (left) and the patient's father (right) who also has PLS (**a**). Intraoral radiograph and photograph showing generalized recession and severe periodontal destruction of the patient at aged 5-years (**c**). Images courtesy of Professor I. Chapple.

5.3. Analysis of NETs and NET-related proteins ion PLS

5.3.1. Quantification of neutrophil elastase (NE) and cathelicidin (LL-37)

NE and LL-37 (the active form of cathelicidin) were quantified in plasma (Figure 5.12a-b) and cultured neutrophil supernatants both unstimulated and following TLR- (*A. actino*) and FcγR- (opsonised *S. aureus*) stimulation (Figure 5.12c-d). Both proteins are activated by CTSC; NE is activated by CTSC directly and LL-37 is activated via PR3 (Sørensen *et al.*, 2001), following PR3 activation by CTSC. NE was almost completely absent in both plasma and neutrophil supernatants from PLS patients, and when compared to controls (figure a and c). LL-37 was absent in plasma from PLS patients but was present at low concentrations in cultured neutrophil supernatants following stimulation (figure 5.2b and d), suggesting minimal CTSC activity or an alternative processing pathway. These results indicate a local and systemic NSP deficiency in the patients.

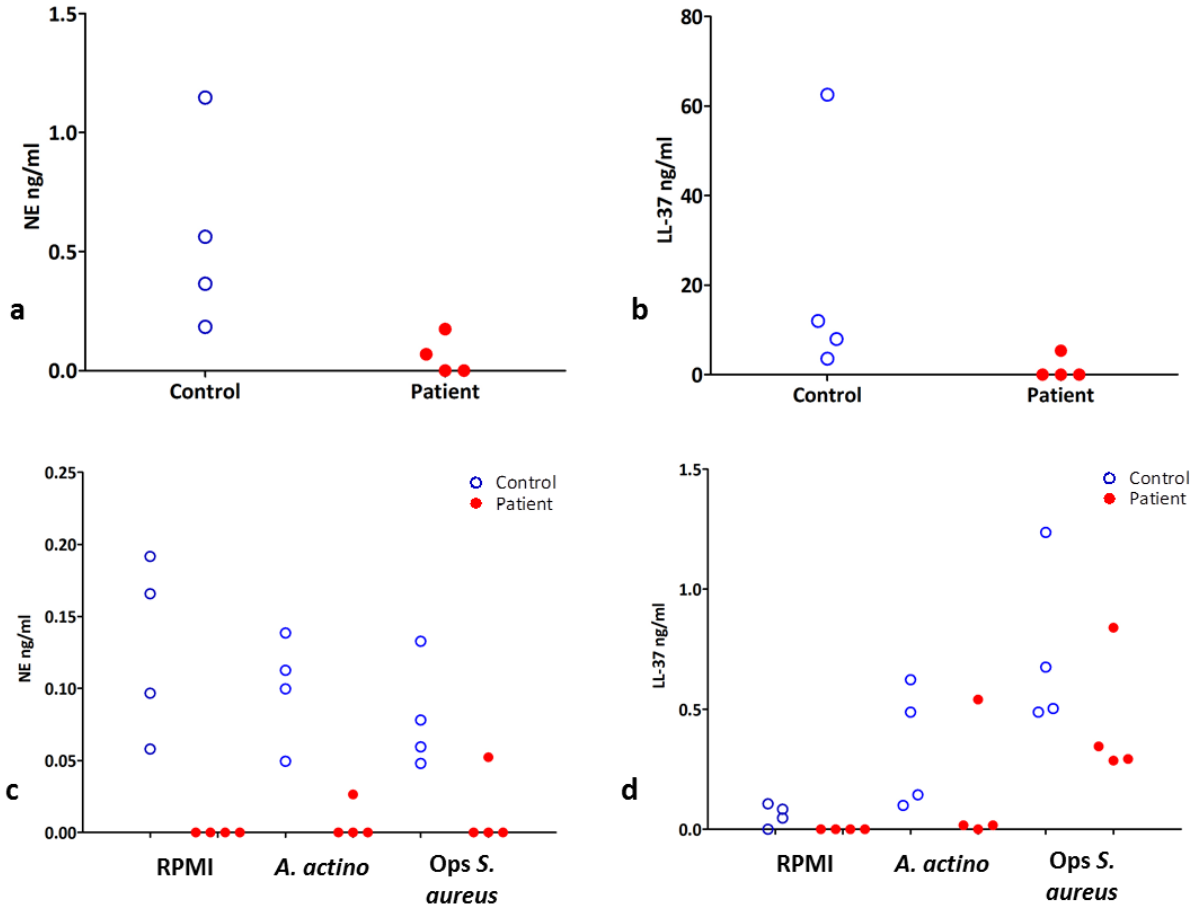

Figure 5.2 NE and LL-37 sample quantification

Neutrophils were isolated (section 2.2.2) and NE and LL-37 were quantified in plasma (section 2.3; a and b respectively) and neutorphil supernatants following an overnight culture (section 2.7.2; c and d respectively). Stimuli for cell culture included RPMI, *A. actino* or opsonised *S. aureus* (MOI 1 in 300 and 150 respectively). Due to undetectable concentrations in the patient samples no statistical analyses were performed. Blue hollow circles and filled red circles represent control and patient samples (n = 4) respectively.

5.3.2. Quantification of NETs and NET bound components

The ability of PLS patients to produces NETs was measured using a nucleic acid stain (SYTOX®) in addition to NET-associated antimicrobial peptidss (AMPs) in order to confirm the DNA measured was derived from NETs: NE, myeloperoxidase (MPO) and cathepsin G (CG). Fluorometric quantification revealed NETs were substantially decreased in patients (Figure 5.3a; $p < 0.001$), a finding confirmed by NET visualisation using fluroescence microscopy (Figure 5.3e). NET bound proteases were also substantially decreased or deficient in patients and significantly lower (where calculated) compared to controls for nearly all stimuli used (Figure 5.3b-d; $p < 0.001$). The reduced presence of NET-bound MPO further supports the lack of NET structures in these patients, who do not otherwise suffer a MPO deficiency ($p < 0.05$). NE and CG, which are both activated by CTSC, were also extremely low in PLS patients ($p < 0.05$).

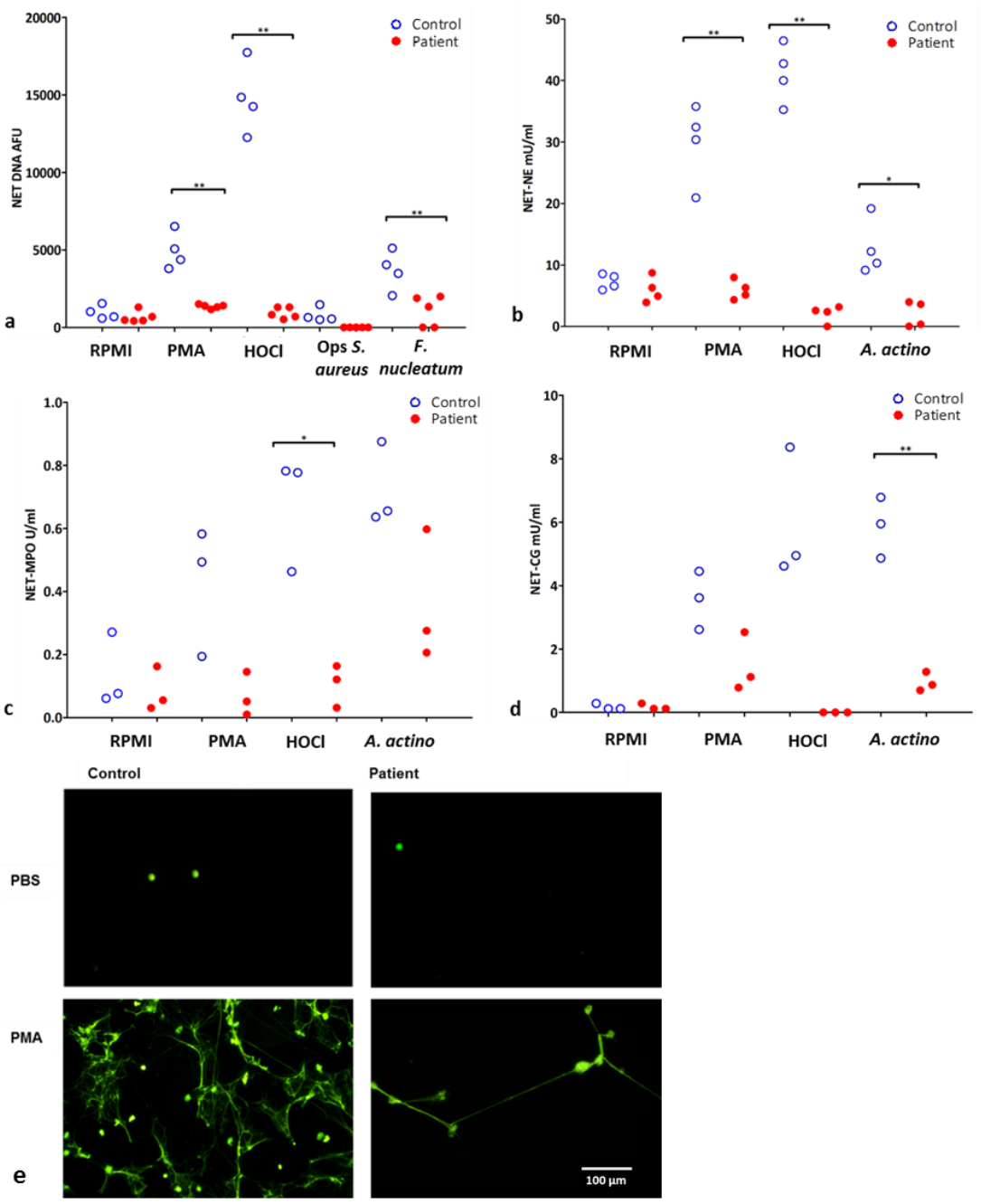

Figure 5.3 NET-DNA and NET-bound protein quantification in PLS

Neutrophils were isolated (section 2.2.2) and NETs and NET bound proteins were quantified in response to PBS (negative control), PMA (50nM), HOCl (0.75 mM) or bacteria (MOI 1 in 300) (section 632.5). Bacteria were selected for each assay on the basis of clinical relevance, in that they are implicated in PLS periodontitis (*A. actino*) and PLS-related skin abscesses (*S. aureus*). NET quantification (a) in stimulated/un-stimulated conditions (n = 5 patient n = 4 control); NET-bound elastase detection (b) after stimulation (n = 4); NET-bound MPO (c) levels (n = 3); NET-bound CG (d) (n = 3). Blue hollow circles and filled red circles represent control and patient samples respectively. Statistical test: Mann-Whitney. * = ($p < 0.05$), ** = ($p < 0.01$).Where levels could not be detected in patient samples, no statistical tests were performed. Representative NET images (e) in the absence of stimuli (PBS) and following the addition of PMA highlighting the lack of NET structures in PLS patients.

5.4. Neutrophil ROS generation and plasma protein oxidation in PLS patients

To assess the potential for differences in ROS release from PLS neutrophils relative to controls, superoxide and total and intracellular ROS were detected using the chemiluminescent reagents lucigenin, luminol and isoluminol, respectively (Figure 5.4a-c). the stimuli used activated the three different signaling pathways as previosuly described (section 1.3.1). In all conditions ROS generation was the same or higher in PLS patients compared to controls. Significance was evident in patients over controls with luminol for opsonised *S. aureus* ($p < 0.001$) and PMA ($p < 0.05$). For isoluminol and lucigenin significance was evident with PMA only ($p < 0.05$). Protein carbonylation, a ROS-induced marker of oxidative stress, was also measured by ELISA (Figure 5.4d). There was no significant difference for protein carbonylation in the plasma between patients and controls.

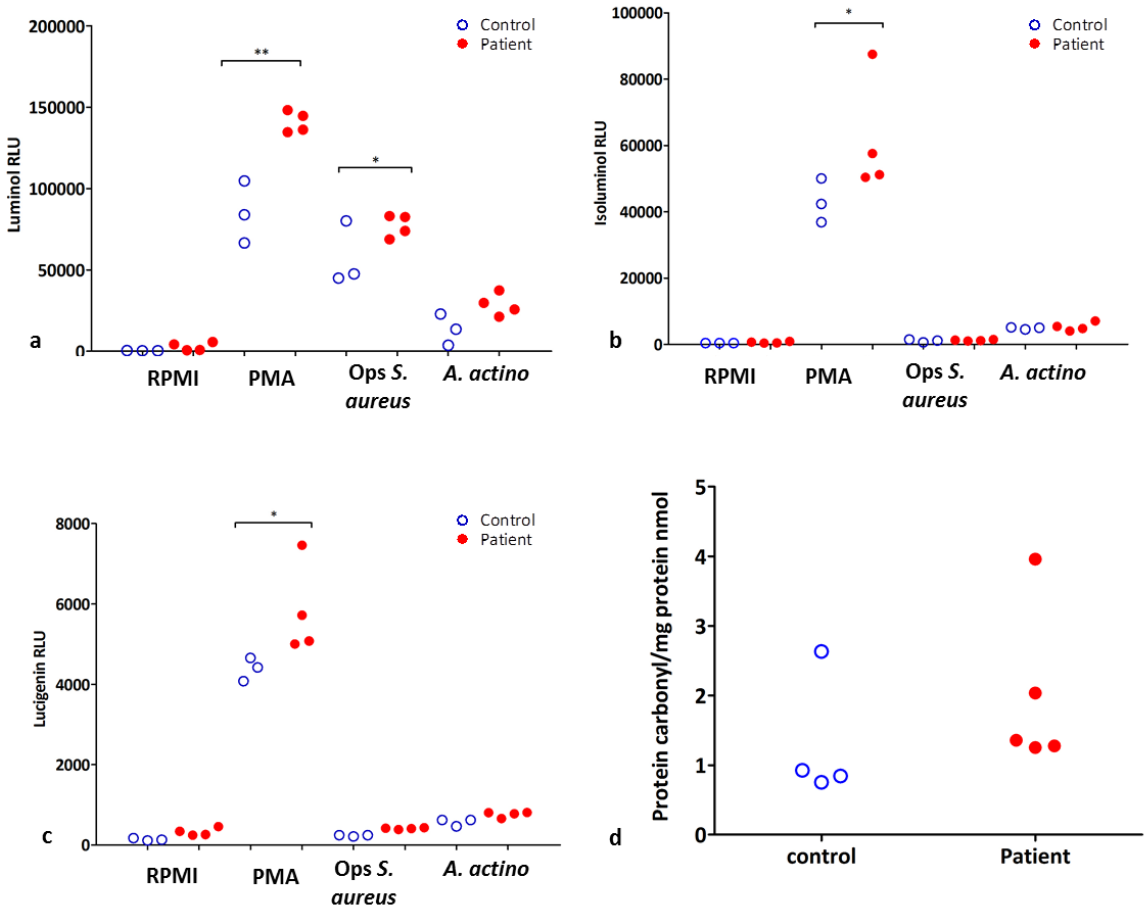

Figure 5.4 ROS and protein carbonylation in PLS

Neutrophils were isolated (section 2.2.2) and peak values for ROS generation were measured in the presence of PBS, PMA (25nM), opsonised *S. aureus* and heat killed *A. actino* (MOI 1 in 300 and 150 respectively) (section 2.4). Three different stimulation pathways were assayed: Fcγ receptor (using opsonised *S. aureus*); TLR (*F. nucleatum*); and direct receptor-independent stimulation of PKC by PMA. ROS production was meaured as total ROS (a) detected using luminol (n = 4); extracellular ROS (b) using isoluminol (n = 4); and superoxide (c) using lucigenin (n = 4). ROS release for patients was higher than controls with significance for PMA for all three chemiluminescent substrates. Plasma protein carbonylation (d), a measure of oxidative stress, was measured by anti-DNP ELISA (n = 5). Blue hollow circles and filled red circles represent control and patient samples respectively. Statistical test: ANOVA with Tukey's post-test. * = ($p < 0.05$), ** = ($p < 0.01$

5.5. Cytokine, MMP-9 and S100A8/9 quantification in PLS patients

The pro-inflammatory cytokines IL-1β, IL-6, CXCL8, MIP1α and TNFα were quantified from culture supernatants and plasma samples by Luminex assay. In addition, MMP-9 (gelatinase), the major enzyme released by neutrophils involved in the breakdown of the extracellular matrix to facilitate movement through the tissues, and the calgranulins S100A8 and A9 were quantified by ELISA.

Table 5.2 shows plasma concentrations and cell culture supernatant concentrations; Figure 5.5a-h shows neutrophil culture supernatant levels in graphical form. Where levels of the measured agents were undetectable statistical testing could not be performed, nonetheless in plasma the levels of all cytokines/MMP-9/S100A8/9 was higher in patients than controls, with significance reached for CXCL8 and MMP-9 (p=0.029). Within cultured neutrophil supernatants there was a significant increase in IL-6, CXCL8 and MIP1α (p=0.029) in the absence of stimulation indicating a hyperactive neutrophil phenotype. Following *A. actino* challenge (TLR stimulation), cytokines IL-6, CXCL8, MIP1α and TNFα were all higher in PLS patients than controls (p=0.029). In addition, S100A9 was also found to be elevated. The same results were achieved with opsonised *S. aureus* (FCγR stimulation) with the exception of IL-6.

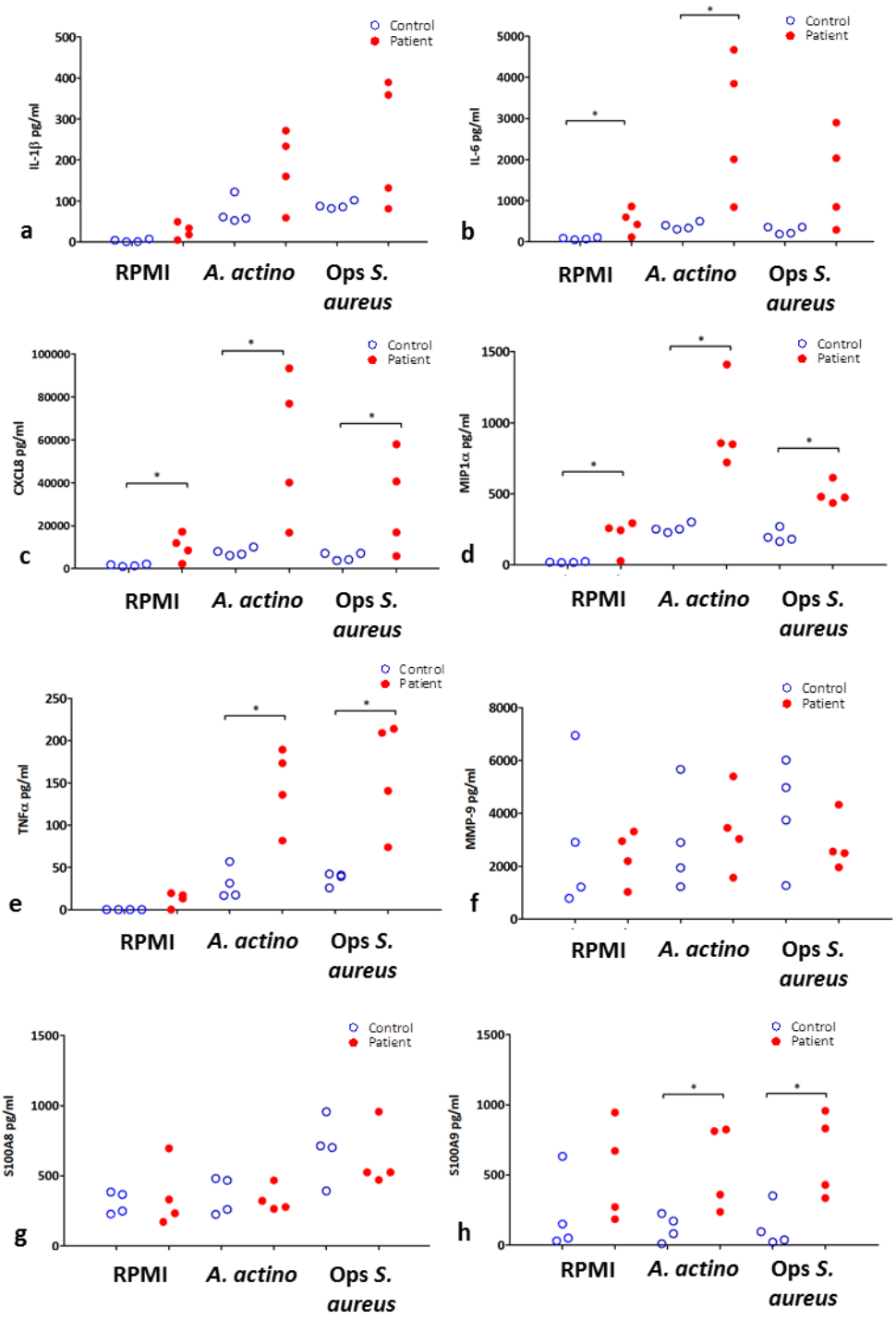

Figure 5.5 Cytokine and calgranulin quantification in PLS

Neutrophils were isolated (section 2.2.2) and cytokines IL-1β (**a**), IL-6 (**b**). CXCL8 (**c**), MIP1α (**d**), TNFα (**e**), MMP-9 (**f**), and calgranulins S100A8 (**g**) and S100A9 (**h**) release from patient and control neutrophils (n = 4 respectively) isolated and cultured for 16 hours (section 2.7) and incubated with RPMI (control), *A. actino* (TLR stimulation pathway) or opsonised *S. aureus* (FcγR stimulation pathway) (MOI of 1 in 150 and 1 in 300 respectively). Blue hollow circles and filled red circles represent control and patient samples respectively. Statistical test: Mann-Whitney. * = ($p < 0.05$).

Table 5.2 Cytokine and calgranulin quantification from cultured neutrophils in PLS

Cytokine, MMP-9 and S100A8 and -9 concentrations from isolated neutrophils cultured for 16 hours from PLS patients and controls (n = 4 respectively). Stimuli included RPMI (control), *A. actinomycetemcomitans* or opsonised *S. aureus* (MOI of 1 in 150 and 1 in 300 respectively). Green italicised text highlights results deemed significantly different at $p < 0.05$. Where levels could not be detected in patient samples, no statistical tests were performed. Statistical test: Mann-Whitney.

RPMI (Unstimulated neutrophil activity)									
Analyte	**Control (pg/ml)**				**Patient (pg/ml)**				***P* value**
	1	**2**	**3**	**4**	**2**	**3**	**4**	**5**	
IL-1β	4.38	1.34	0.65	7.58	4.8	49.37	18.15	33.9	0.057
IL-6	91.94	49.51	65.52	109.55	113.16	860.97	598.24	423.8	*0.029*
CXCL8	1838.8	990.2	1310.4	2191	2263.2	17219.4	11964.8	8476	*0.029*
MIP1α	20.72	17.99	16.82	24.12	27.64	244.58	293.55	257.74	*0.029*
TNFα	0	0	0	0	0	17.06	13.25	19.43	-
MMP-9	786.31	1210.11	2906.7	6947.75	3,311.35	2,947.85	2,192.06	1,026.27	0.886
S100A8	367.16	227.32	248.69	384.09	331.53	171.21	695.85	233.55	0.886
S100A9	150.73	30.67	50.68	632.09	671.37	271.72	944.79	185.31	0.114
***A. actinomycetemcomitans* (neutrophil reactivity)**									
Analyte	**Control (pg/ml)**				**Patient (pg/ml)**				***P* value**
	1	**2**	**3**	**4**	**2**	**3**	**4**	**5**	
IL-1β	60.98	57.45	52.77	122.47	59.03	271.97	233.73	160.1	0.114
IL-6	502.87	338.42	307.13	401.41	843.56	3847.74	4669.62	2007.99	*0.029*
CXCL8	10057.4	6768.4	6142.6	8028.2	16871.2	76954.8	93392.4	40159.8	*0.029*
MIP1α	252.06	301.12	228.88	252.31	855.99	1408.84	721.34	849.17	*0.029*
TNFα	16.71	31.35	17.39	56.85	81.78	189.43	173.33	135.79	*0.029*
MMP-9	1,224.29	1,939.96	2899.5	5,661.66	5,398.59	3,450.59	3,034.44	1,566.67	0.686
S100A8	481.18	260.27	224.64	466.93	466.93	278.09	320.84	264.73	1
S100A9	172.20	10.35	81.59	224.67	823.27	359.72	811.75	237.68	*0.029*
Opsonised *S. aureus* (neutrophil reactivity)									
Analyte	**Control (pg/ml)**				**Patient (pg/ml)**				***P* value**
	1	**2**	**3**	**4**	**2**	**3**	**4**	**5**	
IL-1β	81.99	85.88	102.26	87.63	81.05	358.62	389.46	131.65	0.343
IL-6	357.02	191.77	209.19	358.87	290.15	2033.56	2898.57	848.68	0.114
CXCL8	7140.4	3835.4	4183.8	7177.4	5803	40671.2	57971.4	16973.6	*0.029*
MIP1α	194.92	181.81	164.4	270.99	478.93	475.06	613.38	435.67	*0.029*
TNFα	39.2	42.2	40.99	25.86	73.85	209.16	213.93	140.61	*0.029*
MMP-9	1265.44	3743	6016	4979	2491	1954	2554	4328	0.496
S100A8	392.99	712.78	955.95	702.08	956.84	524.83	470.49	524.83	0.885
S100A9	20.83	37.065	95.73	350.81	956.31	428.86	831.13	336.15	*0.029*

Table 5.3 Plasma cytokine and calgranulin quantification in PLS

Cytokine, MMP-9 and S100A8 and -9 concentrations in plasma from PLS patients and controls (n = 4 respectively). Green italicised text highlights results deemed significantly different at $p < 0.05$. Where levels could not be detected in patient samples, no statistical tests were performed. Statistical test: Mann-Whitney.

Plasma									
Analyte	**Control (pg/ml)**				**Patient (pg/ml)**				***P* value**
	1	**2**	**3**	**4**	**2**	**3**	**4**	**5**	
IL-1β	0	0	0.41	0	7.06	0	1.78	0	-
IL-6	16.94	22.91	25.82	19.32	36.62	9.56	20.54	24	0.886
CXCL8	0.92	1.09	0.76	0.79	3.41	1.11	3.32	1.16	*0.029*
MIP1α	0	27.28	4.3	0.65	36.02	11.18	32.44	5.35	0.114
TNFα	0	0	0	0	47.53	0	0.57	0	-
MMP-9	24.96	11.44	37.43	6.03	449.59	135.8	554.27	282.5	*0.029*
S100A8	0	0	0	0	2674.66	494.55	1436.54	2941.09	-
S100A9	0	0	0	0	1538.19	412.51	470.74	2001.63	-

5.6. Neutrophil chemotaxis in PLS patients

Neutrophil speed, velocity and chemotactic index (CI) were measured over time in the presence of buffer (RPMI) or chemoattractant (fMLP or MIP1α). MIP1α is a target for NSPs which deactivate the chemokine. This was confirmed by preliminary chemotaxis work involving pre-incubation of CG with MIP1α prior to its use as a chemoattractant, which demonstrated that chemotaxis could not be induced (Appendix III). As NSP function is lost in PLS individuals, MIP1α was employed in the chemotaxis assays to ascertain whether neutrophils from PLS patients chemotax differently to those from healthy controls, in particular whether MIP1α chemotaxis is at all enhanced in PLS patients over controls. Speed was significantly lower in patients when exposed to MIP1α (Figure 5.6a), a trend that was consistent for both MIP1α & fMLP when velocity (Figure 5.6b) and chemotactic index (Figure 5.6c) were measured. Figure 5.7 shows the cell paths of all tracked cells per

condition, including polar plots and angle histograms, illustrating the differences in the course of the cell movements. PLS patient neutrophils showed significantly reduced speed, velocity and chemotactic accuracy compared with controls in response to MIP1α, and also a lower CI in response to fMLP.

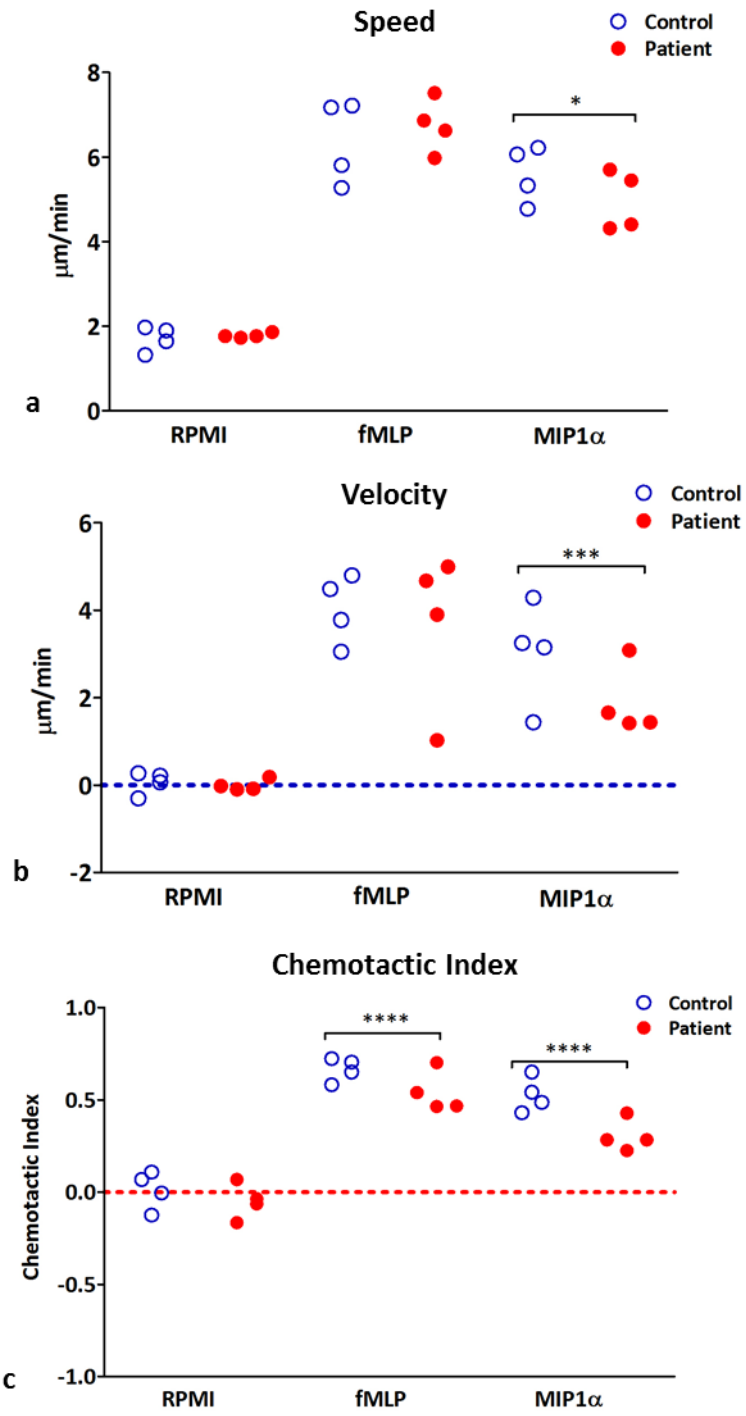

Figure 5.6 Neutrophil chemotaxis in PLS

Neutrophils were isolated (section 2.2.2) from PLS patients and controls and chemotaxis was performed (section 2.6), after which the cells were analysed (section 2.6.2) and tracked information was used to generate average speed (a), velocity (b) and CI (c) in the presence of RPMI (negative control), fMLP (10nM) and MIP1α (100ng/ml) chemoattractants. Blue hollow circles and filled red circles represent control and patient samples respectively (n = 4; 15 cells tracked per chemoattractant/RPMI). Statistical test: Mann-Whitney. * = ($p < 0.05$), *** = ($p < 0.001$), **** = ($p < 0.0001$).

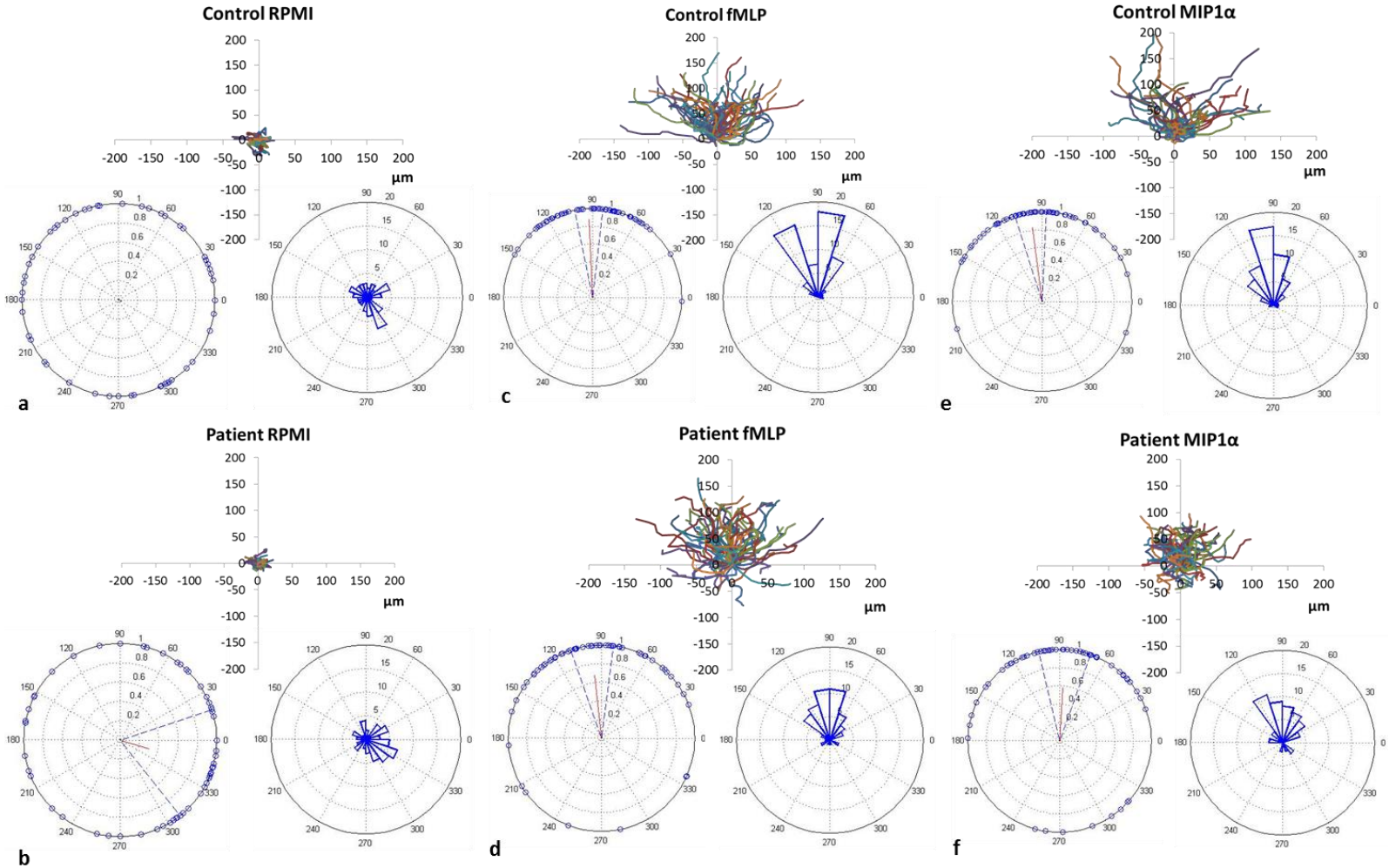

Figure 5.7 PLS neutrophil cell tracks

Cell tracks, polar plots and angle histograms overlayed for control (a, c and e) and patient (b,d and f) neutrophils were generated to give a qualitative overview of chemotaxis using RPMI (negative control), fMLP (10nM) and MIP1α (100ng/ml) chemoattractants respectively.

5.7. Discussion

The results and discussion presented here have been published from this thesis (Roberts *et al.* 2016); in addition, work demonstrating the chemotactic capabilities of LL-37 has also been published (Koro *et al.* 2016) and is detailed in section 8.6.

This chapter reports the comprehensive analysis of neutrophil function in PLS patients compared with unaffected controls and is the first to explore directional chemotaxis and cytokine release in PLS as part of the neutrophils' functional repertoire.

PLS neutrophils demonstrated negligible NET formation, as analysed by assays of NET-DNA, and an almost total absence of the NET-associated AMPs - CG, NE and MPO, despite the fact that PLS neutrophils are not MPO deficient as previously reported (Eick *et al.* 2014). Eick *et al.* seemingly demonstrated that the absence of the MPO protein, which would normally be present in PLS neutrophils, was because of a lack of NET presence rather than the lack of MPO itself. The absence of, or marked reduction in, NETs provides additional data to that recently reported in a single PLS patient (Sørensen *et al.*, 2014). NE and CG are both enzymes that are activated by CTSC, and *in vitro* studies of NSPs have demonstrated CG and NE are able to kill *A. actinomycetemcomitans* in addition to other periodotal bacteria (Bangalore, *et al.* 1990). The NSP deficiency likely compromises neutrophil antimicrobial efficacy allowing for the persistance of some pathogenic species over others in PLS. NE is known to be necessary for NETosis as demonstrated by the study of neutrophil elastase disorders such as *ELA2*-related neutropenia, where neutrophil elastase activity is deficient (Dale *et al.* 2000) and so NET formation is diminished (Papayannopoulos, *et al.* 2010). Conversely, in *HAX1*-related neutropenia elastase is functional and *HAX1*-neutropenia patients produce NETs (Happle, *et al.* 2011).

The ROS data reported here indicate an enhanced response to opsonised *S. aureus* (luminol detection only) and PMA in the PLS patients, which is consistent with a hyper-reactive

neutrophil phenotype (Matthews *et al.*, 2007a) which may contribute significantly to the oxidative stress (characterised by elevated lipid hydroperoxide levels) and compromised antioxidant levels previously reported in PLS (Battino *et al.* 2001). The increased ROS detected in PLS patient neutrophils *ex vivo* could be a major contributing factor to the host-mediated tissue damage at sites where neutrophils are the dominant immune cell, such as the periodontium. These results contribute further to previous work demonstrating decreased antioxidant defences and increased oxidative stress characterised by greater lipid hydroperoxide levels in unstimulated neutrophils from PLS patients (Battino *et al.* 2001).

Cytokine measurements demonstrated increased release of pro-inflammatory cytokines (IL-6, CXCL8 and MIP1α) from PLS neutrophils in the absence of stimulation, indicating a hyperactive phenotype. Furthermore, hyper-reactivity (to a stimulus) in terms of pro-inflammatory cytokine release and also S100A9 concentration was also evident from the supernatants of stimulated cultured neutrophils. Higher S100A8/9 concentrations have been reported in inflamed tissues and are known to be markers of neutrophil activation (Foell *et al.* 2007). S100A9 is a known target for CG (Ryckman, *et al.* 2003) to generate neutrophil immobilising factor (NIF) which has been reported to inhibit neutrophil migration and chemotaxis (Goetzi and Austen 1972). NIF acts as a negative feedback loop, limiting neutrophil influx into inflammatory regions. The absence of NIF may be another contributing factor to the lack of resolution of inflammation in PLS and the seemingly relentless periodontal tissue destruction characteristic of PLS. S100A9 can form a heterodimer with S100A8 which has been shown to be involved in the assembly of the NADPH oxidase (Kerkhoff *et al.* 2005), and thus could be one mechanism underlying higher ROS levels released by the PLS patients neutrophils in this study.

Cytokine measurement in plasma was performed to examine their presence *in vivo*; the presence of elevated cytokine/MMP-9 levels in patient plasma over controls further supports

the hypereactive PLS neutrophil phenotype, as circulating neutrophils exposed to increased concentrations of a combination of pro-inflammatory agents are likely to prime the cells within the circulation for enhanced killing activities when they reach periodontal tissues, as demonstrated with ROS release (Yao *et al.* 2015).

Neutrophil chemotaxis measurements demonstrated defects in PLS patients; a consequence of which may be to potentially increase neutrophil tissue transit times and further potentiate neutrophil-mediated tissue damage. As NSPs can de-activate MIP1α and CXCL8, the loss of NSP function in PLS may result in relentless neutrophil recruitment to periodontal tissues by such chemokines. Neutrophil speed and velocity were reduced in response to MIP1α, relative to controls, and there was a significant difference in directional chemotactic accuracy of PLS neutrophils for both MIP1α and fMLP. Previous studies have identified reduced chemotaxis in PLS, however these reports used alternative assays such as the Boyden chamber (Djawari 1978) and the Zymosan activated serum assay (Firatli *et al.* 1996), neither of which measure directional chemotaxis.

The underlying explanation for the periodontitis in PLS, in combination with the data generated in this chapter, points to two key scenarios: Firstly, continual recruitment to the periodontal tissues of neutrophils that exhibit hyper-activity/reactivity. NSPs are a very important component of antimicrobial functionality of neutrophils, and the implications of NSP deficiency has been linked to the development of periodontitis previously (Pham *et al.* 2004; de Haar *et al.* 2006). Neutrophils lacking both NE and CG are unable to undergo cytoskeletal reorganisation despite adhering to immune-complex-coated surfaces *in vitro* (Djawari *et al.* 1978), the underlying cause being a decrease in the phosphorylation of the GTPase RAC1 which is performed indirectly by CG, thus the lack of NSPs in PLS may be an underlying cause of the chemotactic defect identified in this study. Moreover, MIP1α isoforms are inactivated by NSPs (Ryu *et al.* 2005), and MIP1α has been shown to act as an

osteoclast activation factor, inducing bone resorption (Choi *et al.* 2000). The constant presence of active MIP1α and failure to generate NIF in PLS may drive a relentless recruitment and accumulation of activated neutrophils to the inflamed periodontal tissues and lead to the subsequent destruction of periodontal connective tissue and alveolar bone. Confinement of this recruitment to the periodontal tissues could be a result of the constant microbial challenge ever present in this area of the body. In addition, the deficiency of LL-37, itself a result of PR3 deficiency in PLS patients, increases the incidence of microbial infection, notably with the periodontal pathogen *A. actinomycetemcomitans* as previously reported (Eick *et al.* 2014). Furthermore, LL-37 and its carbamylated variants, which arise due to cyanate formation during the neutrophil oxidative burst, has been demonstrated to have chemoattractive properties in assays employing the Insall chamber (Koro *et al.* 2016), thus a lack of LL-37, which was not shown to be as potent as fMLP in inducing neutrophil chemotaxis, may impact on the hierarchical recruitment of neutrophils from the circulation to the site of end-point chemoattractants.

NSP dysfunction is associated with periodontal disease in other syndromes, including Chédiak Higashi Syndrome (Holt *et al.* 2006) and the allelic variant to PLS, Haim Munk Syndrome (Hart *et al.* 2000). Furthermore, neutrophils from sufferers of Specific Granule Deficiency, characterised by defects in the packaging of azurophil and specific granules (which contain NSPs and NADPH oxidase components respectively), have been shown to exhibit decreased phagocytosis, diminished ROS formation and reduced chemotaxis (Gallin *et al.* 1982).

The second scenario potentially underlying the causation of periodontal disease in PLS is compromised antimicrobial killing. PLS patients are known to suffer modest systemic infections (mostly skin abscesses), with 15-20% of patients reporting recurrent infections,

unlike patients with chronic granulomatous disease (CGD), which is characterised by the lack of a functional NADPH oxidase and the subsequent inability to produce ROS or form NETs. Interestingly CGD patients are not overtly susceptible to periodontitis (Nussbaum & Shapira 2011), suggesting that the periodontal tissue destruction seen in PLS cannot be fully explained by compromised neutrophil anti-microbial defences. PLS individuals are not systemically immunocompromised and as the results of this study show, PLS neutrophils have the capacity to respond to pathogenic stimuli, thus NSPs do not constitute the primary antimicrobial defence mechanism, and the underlying cause of periodontitis in PLS cannot be explained simply by reduced neutrophil bacterial killing. A far more likely scenario is that the periodontal tissue damage in PLS patient's results from a complex series of events arising downstream of the CTSC deficiency which depend upon the diverse range of NSP functions normally active at sites of microbial challenge.

Deficient bacterial killing as a result of impaired killing mechanisms results in persistence of pathogenic species and triggers the relentless recruitment of hyper-active/reactive neutrophils characterised by increased ROS and pro-inflammatory cytokine presence in the periodontium. Extended tissue transit times and a failure to de-activate chemokines such as MIP1α and CXCL8, likely drives the connective tissue damage and bone loss in PLS. Defects in neutrophil function have been shown in several studies of chronic periodontitis patients; peripheral neutrophils from chronic periodontitis patients exhibit hyper-reactivity with respect to ROS release (Matthews *et al.* 2007a; Ling *et al.* 2016) and pro-inflammatory cytokine production (Ling *et al.* 2015) in response to a microbial challenge, and also hyperactivity in the absence of an exogenous stimulant (Matthews *et al.*, 2007b). Chemotaxis in chronic periodontitis patients has also been found to be defective with only partial improvement after non-surgical therapy (Roberts *et al.* 2015), and oxidative stress is

also a strong feature of periodontitis. In PLS, failure to activate and release NSPs has greater far-reaching consequences than a superficial observation based purely on defective anti-microbial defences, and may thus underlie the aggressive periodontal tissue damage seen in PLS.

5.8. Chapter 5 summary

This study has characterised a range of neutrophil behaviours in PLS patients from 5 different families, representing a relatively large cohort of patients and providing new insights into the functional consequences of CTSC deficiency upon periodontal tissue destruction and tooth loss. PLS neutrophils have a substantially reduced capacity for NET production, as confirmed by the almost total absence of NET-related proteins. ROS generation was higher in PLS and directional chemotactic accuracy was compromised. NSP deficiency has previously been purported to be the cause of periodontal tissue destruction in PLS. This study adds to this association through the identification of failed key neutrophil antimicrobial activities, which likely contributes to the misdirected recruitment of hyper-responsive neutrophils into periodontal tissues, provides a plausible explanation for the severe localised periodontal inflammation and bone loss characteristic of PLS. The locality of the inflammation fits with the proposed underlying mechanisms of periodontal destruction; an area susceptible to direct and chronic bacterial challenge in which neutrophils are the dominant immune cell presence.

CHAPTER 6 RESULTS -NEUTROPHIL FUNCTION IN OBESE PATIENTS PRE- AND POST-BARIATRIC SURGERY

6.1. Introduction

Obesity is the greatest global health challenge of our time with over 500 million adults categorised as clinically obese worldwide (Swinburn *et al.* 2011). Obesity was recently characterised as a chronic inflammatory disease implicating adipocyte dysfunction and endocrine activation of adipose tissue (Capurso & Capurso 2012). The beneficial effects of weight loss are well established (Sam 2015) with a reduction in adiposity resulting in improved blood lipid levels and an increase in diet-induced thermogenesis (Werling *et al.* 2013; Faria *et al.* 2014). Bariatric surgery is an option for individuals who are morbidly obese (BMI >40kg^2) (Pataro *et al.* 2012) and have not been able to lose weight by other methods, and who suffer a medical problem related to obesity such as severe joint pain, sleep apnoea or type 2 diabetes (Balsiger *et al.* 2000).

This chapter presents results from a longitudinal assessment of neutrophil ROS and NET production, chemotaxis and cytokine release from individuals with morbid obesity prior to and following gastric band surgery, which included an initial weight loss period involving a very low calorie diet (VLCD), alongside lean gender- and age-matched healthy controls. The data generated here will add to understanding of the effects of obesity on neutrophil function and the potential improvements that may result from decreasing adiposity.

6.2. Patient background information

Section 2.1.5. describes the recruitment process for patient volunteers and healthy controls. Twenty-three patients were recruited initially however five patients (2, 3, 9, 17 and 20) chose to withdraw from the study at various stages due to personal reasons and changes to their surgery choice (patients 3 and 17 switched to gastric bypass surgery). Figure 6.1 details the temporal differences between blood collection, which occurred at three separate time points;

time point 1 (T1) in which patients were consented and embarked on a VLCD, time point 2 (T2) in which patients attended their pre-operative assessment and time point 3 (T3) which represented an approximate 3 month post-surgical appointment. At each time point patients were weighed and blood was collected. Table 6.1 describes a summary of patient demographics; a more detailed table is described in section 8.4. As expected, the majority of patients had co-morbidities – all of which are associated with obesity including sleep apnoea, hypertension, depression, hypercholesterolaemia and type 2 diabetes (NHLBI Obesity Education Initiative Expert Panel on the Identification, Evaluation 1988) and are described in table 8.4.

a

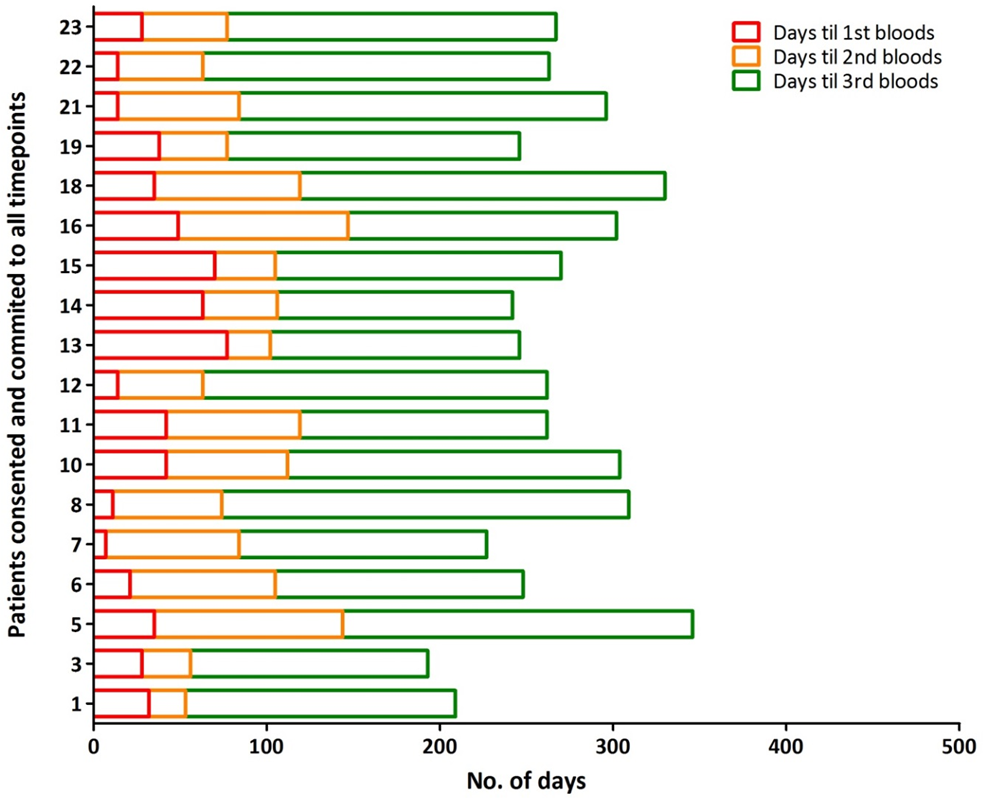

b

	Timepoint 1	Timepoint 2	Timepoint 3
No. of patients		18	
Mean no. of days	34	60	169
Standard deviation +/-	20	29	35
Range	7-77	21-109	136-235

Figure 6.1 Patient and control study flow chart

Data represented as a stacked bar chart (a) and in tabulated form (b) characterising the length of time between each blood donation (day 0 represents patient enrolment). Time point 1 represents a point before VCLD commencement, time point represents a point post-VLCD (immediately prior to surgery) and time point 3 represents a point 3 months post-surgery.

Table 6.1 Bariatric patient and control background information

	Control	Patient
Female-to-male ratio	17:1	
Mean age ±SD (range)	47 ±*9.8* (27-65)	48 ±10.5 (24-67)
No. with a single co-morbidity	n/a	4
No. with ≥2 co-morbidities	n/a	12
No. with diabetes (type 2)	n/a	7
Mean % weight loss (T1-3) ±SD (range)	n/a	14.6 ±7.1 (0.17-30.2)
No. taking lipid-lowering drugs	n/a	7

6.3. Assessment of body mass index (BMI)

Figure 6.2 details the changes in BMI, calculated by dividing weight (kg) by height (m) squared. More detailed information on patient weight loss is detailed in Appendix IV. Patient BMI reduced between the three time points, with an initial decline between T1 and T2 (representing before and after VLCD commencement) followed by a more pronounced decrease between T2 and T3 representing before and after surgery. The VLCD relied solely on patient compliance with guidance from dieticians as part of the weight loss pathway and included options such as the commercially available Cambridge Weight Plan® and Weightwatchers® as well as diets planned by the patients themselves. This ensured a calorific intake of 1,000 calories per day consuming a varied diet or by restriction to limited foods, such as milk and yoghurt only to ensure calorific deficit (Bueno *et al.* 2013). The purpose of the VLCD is to decrease the adipose tissue surrounding the liver in order to facilitate a safer surgical procedure (Lewis *et al.* 2006).

Due to challenges in recruiting lean, healthy and age-matched controls from staff within the Dental Hospital, some of the controls were within the overweight category, however it is important to note that weight gain is associated with ageing; the mean age of recruited volunteers was 47. In addition, BMI as a clinical measure of overweight/obese status has limitations when used as a sole measure of health status.

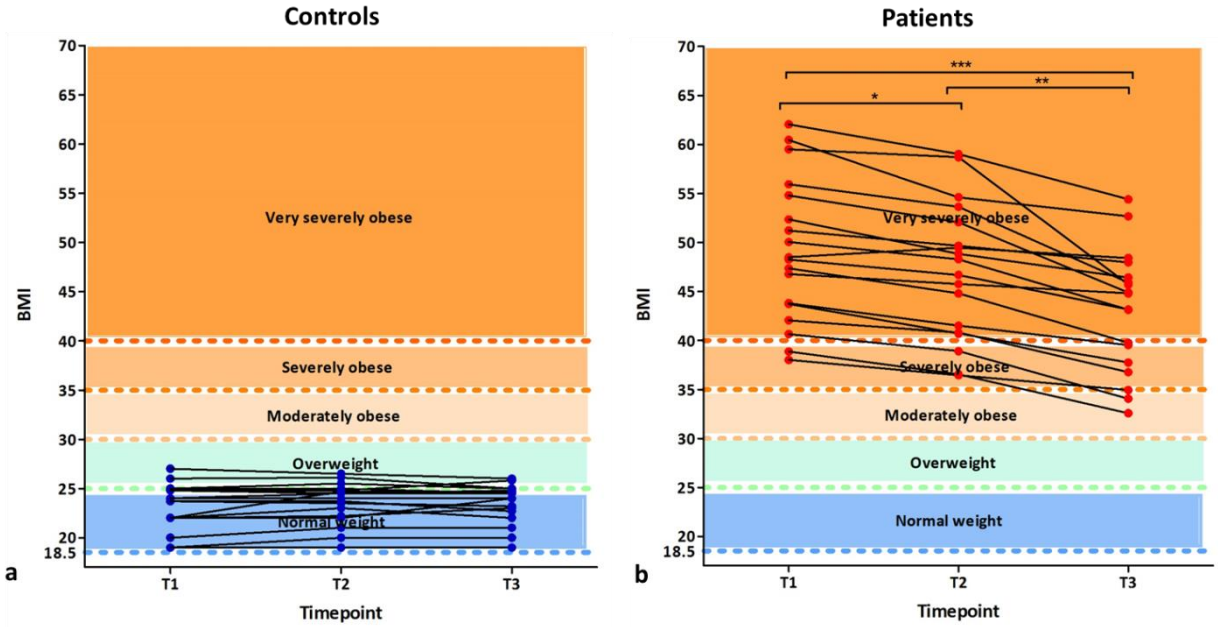

Figure 6.2 BMI changes from time points 1-3

Changes in BMI between controls (a) and patients (b) during time points 1-3. Data represented as line graphs. n = 18. Statistical test: Friedman and Dunn's post-test. * = (p < 0.05), ** = (p < 0.01), *** = (p < 0.001).

6.4. Whole blood analyses

Table 6.2 presents the statistical comparison between patients and controls for each analyte per time point. The analytes were chosen as their levels are reportedly dysregulated in obesity, and weight loss is associated with their normalisation and a reduction in associated health risks as explained in more detail in subsequent sections when comparing patients and controls separately within T1-3. When comparing patients versus controls separately, statistically significant differences were evident between patients and controls at T1 for HbA1c, high density lipoprotein (HDL) and LDL (low density liporprotein)/HDL ratio. Significance was lost for all outcomes except HDL levels by T3, which remained lower in patients versus controls.

Table 6.2 Inter-individual analysis of blood analytes

Green italicised text highlights results deemed significantly different at $p < 0.05$. Where levels could not be detected in patient samples, no statistical tests were performed. Statistical test: Wilcoxon matched-pairs.

	T1		T2		T3	
	Control	**Patient**	**Control**	**Patient**	**Control**	**Patient**
HbAc1						
Average ±SD (range)	5.4 ±1 (4.2-6.4)	7.1 ±1.4 (5.1-9.7)	5.1 ±0.45 (4.5-5.8)	6.7 ±1.1 (5.1-8.6)	5.6 ±0.77 (4.5-6.8)	5.5 ±0.9 (4.5-8.3)
***p* value**	*0.0008*		*0.0002*		0.59	
Cholesterol						
Average ±SD (range)	195 ±43 (136-264)	166 ±50 (114-336)	183 ±43 (110-257)	148 ±-47 (100-305)	183 ±36 (132-279)	162 ±43 (113-256)
***p* value**	0.055		*0.045*		0.1	
HDL						
Average ±SD (range)	75 ±15 (48-100)	54 ±13 (37-84)	68 ±18 (35-100)	48 ±14 (33-84)	72 ±16 (41-100)	58 ±17 (36-84)
***p* value**	*0.0046*		*0.0071*		*0.035*	
LDL						
Average ±SD (range)	83 ±37 (45-152)	84 ±43 (42-219)	77 ±37 (40-155)	80 ±45 (32-226)	88 ±36 (39-189)	82 ±38 (17-154)
***p* value**	0.54		0.88		0.73	
LDL/HDL						
Average ±SD (range)	1.2 ±0.6 (0.5-2.3)	1.6 ±0.8 (0.5-3.8)	1.3 ±0.8 (0.5-3.3)	1.8 ±1.2 (0.4-5.3)	1.3 ±0.7 (0.5-2.8)	1.5 ±0.7 (0.2-2.7)
***p* value**	*0.012*		*0.026*		0.51	
TG						
Average ±SD (range)	95 ±38 (50-187)	143 ±62 (63-292)	89 ±49 (50-244)	121 ±-55 (51-262)	91 ±31 (50-170)	117 ±56 (50-250)
***p* value**	*0.023*		*0.025*		0.098	

6.4.1. Measurement of glycated haemoglobin (HbA1c)

Glycated haemoglobin (HbA1c) represents the irreversible binding of glucose to the haemoglobin molecule was measured for patients and controls at the three time points (Figure 6.3). HbA1c levels reflect the level of glucose in the blood over a 3-month period (the approximate lifespan of a red blood cell) – a higher percentage reflects glycaemic status and indicates the effectiveness of diabetes management is for those already diagnosed (Kilpatrick 2008; Little *et al.* 2011). The results of this study show a decrease in patient HbA1c levels from T1 to T3 (Figure 6.3b and d) reflecting the positive effects of weight loss as previously reported (Stanford *et al.* 2012). The effect was also evident in the 7 diagnosed diabetes patients (Figure 6.3c). Control HbA1c levels showed some variation, though no significance was reached, reflecting the temporal differences in blood collection over the three time points as described in Figure 6.1; at least 6 patient/control pairs had a T1 versus T2 gap of more than 90 days and studies have shown the lifespan of red blood cells to be approximately 90 days (Cohen *et al.* 2008).

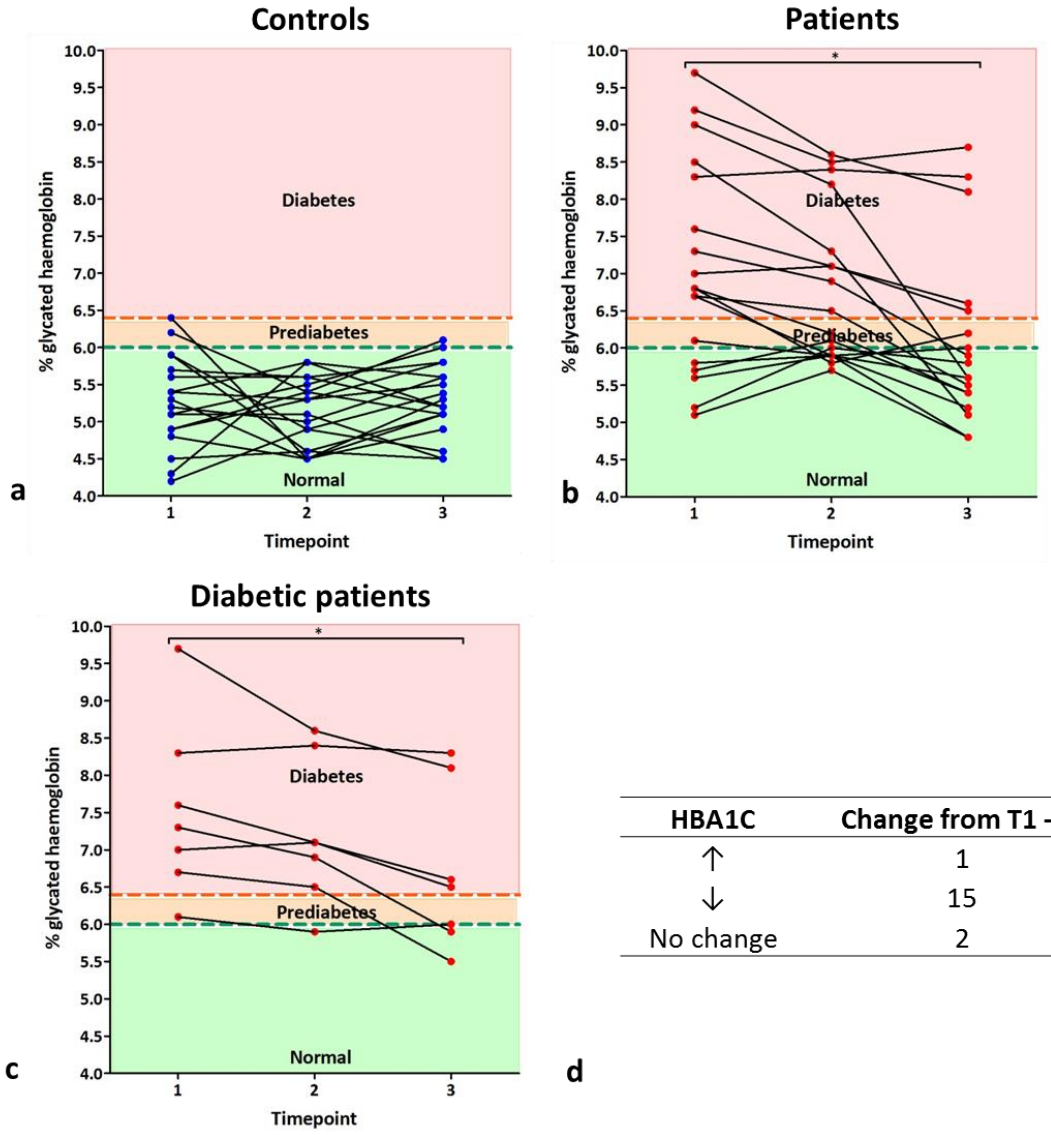

HBA1C	Change from T1 -T3
↑	1
↓	15
No change	2

Figure 6.3 Glycated haemoglobin (HbA1c) measurements in patients and controls

Controls (a) patients (b) and diabetes patients (c) HbA1c levels at each time point and in tabulated form (d). The change in HbA1c from T1 to T3 for patients also described (d). Data represented as line graphs. n = 18 for total controls and patients, n = 7 diabetes patients. Statistical test: Friedman and Dunn's test.* = ($p <$ 0.05).

6.4.2. Assessment of blood lipids

6.4.2.1. Total cholesterol

Cholesterol is a lipid-based molecule with numerous physiological functions including cell membrane structural integrity, and acting as a precursor for steroid hormones and bile acids (Hanukoglu 1992). Increased cholesterol levels are associated with an increased incidence of cardiovascular disease (Clarke *et al.* 2009). Figure 6.4a-b describes the total cholesterol levels in controls and patients respectively from T1-3. Seven patients known to be taking lipid-lowering drugs (LLD) are also shown separately (Figure 6.4c). The results show an overall reduction in lipids in patients from T1-3 (Figure 6.4d) though the magnitude was not sufficient to reach statistical significance. The dramatic reduction in cholesterol at T2 may be the effect of the VLCD which is known to modify blood lipid levels (Volek *et al.* 2005). The apparent increase in cholesterol by T3 in the majority of patients may reflect the cessation of dramatically lowered calorific intake. The administration of LLD for some of the patients may account for an independent reduction in total cholesterol. Changes in cholesterol can occur over acute time periods and are usually attributable of changes in diet and increased exercise (Lennon *et al.* 1983).

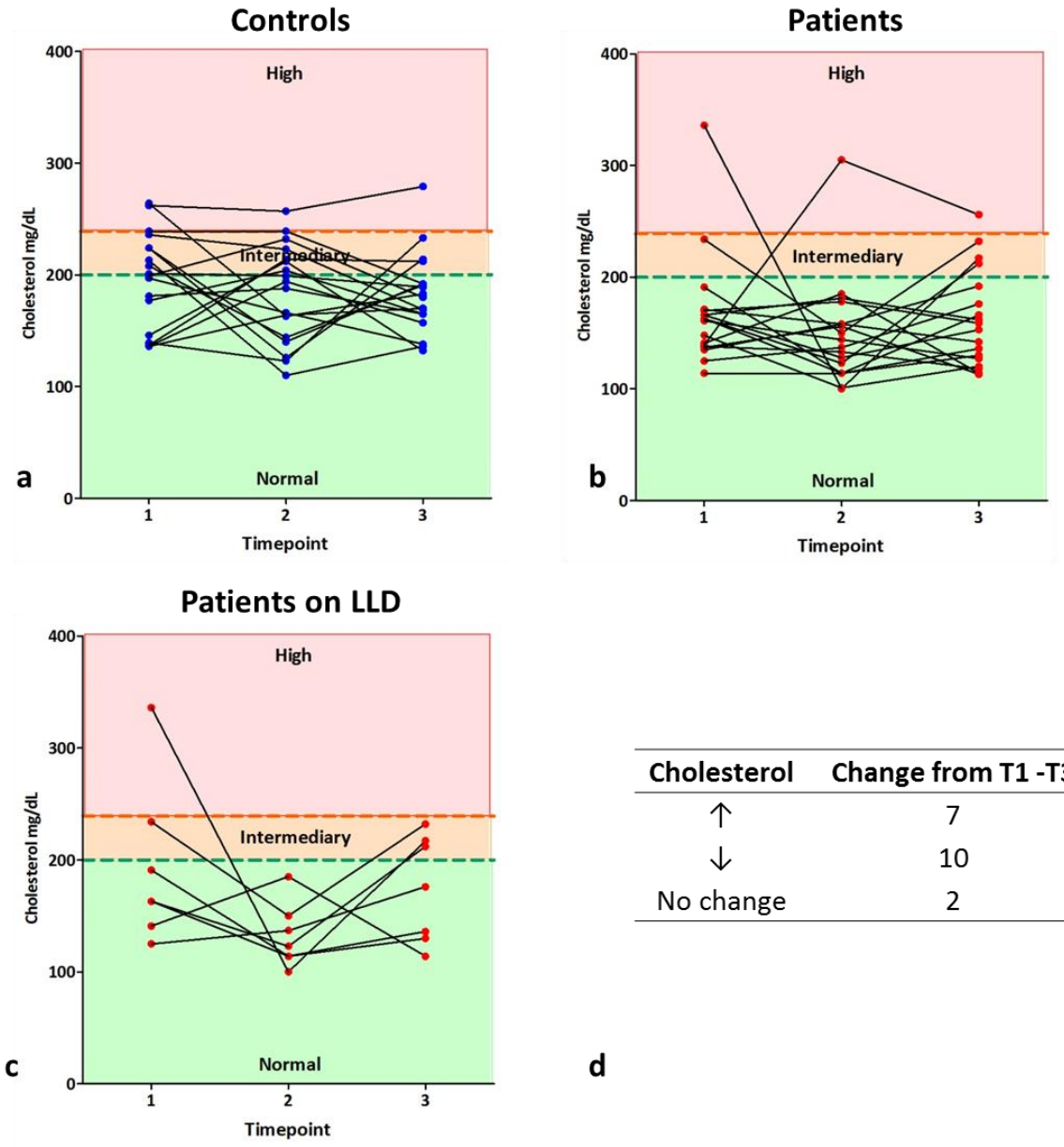

Cholesterol	Change from T1 -T3
↑	7
↓	10
No change	2

Figure 6.4 Total cholesterol measurement in patients and controls

Controls (a), patients (b) and patients known to be taking lipid lowering drugs (LLD) (c) Data represented as line graphs and in tabulated form (d). n = 18 for total patient and controls, n = 7 patients on LLD. Statistical test: Friedman and Dunn's test.

6.4.2.2. Assessment of high-density lipoproteins (HDL)

HDL is one of the major groups of lipoproteins that serve to transport lipids including cholesterol and triglycerides systemically and high levels are associated with a decreased risk in mortality (Rahilly-Tierney *et al.* 2011). HDL levels are known to be altered in obesity and sustained weight loss is associated with an increase in HDL levels (Rashid & Genest 2007). Figure 6.5a-b describes high-density lipoprotein (HDL) levels in controls and patients respectively. Patients taking LLD, which are known to increase HDL levels (Pahan 2006), are also shown separately (Figure 6.5c). The general trend is an increase in HDL across the study period (Figure 6.5d), though statistical significance was not reached.

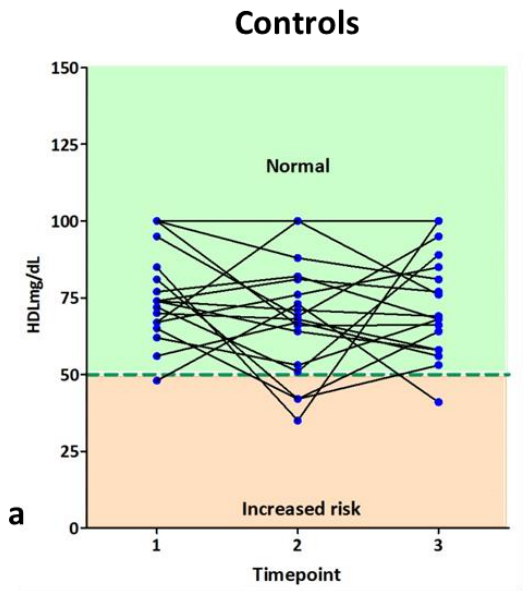

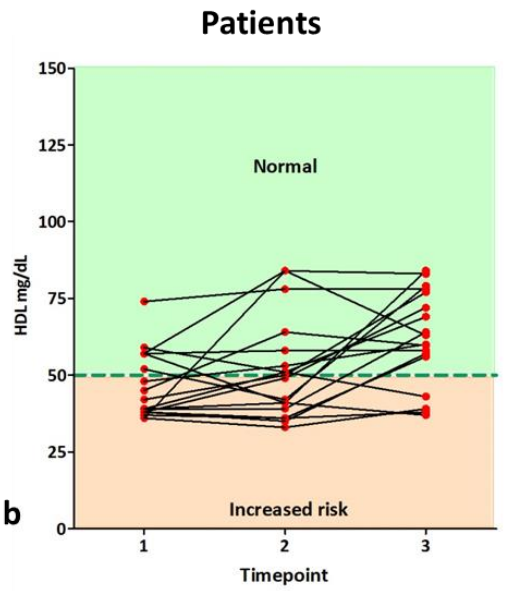

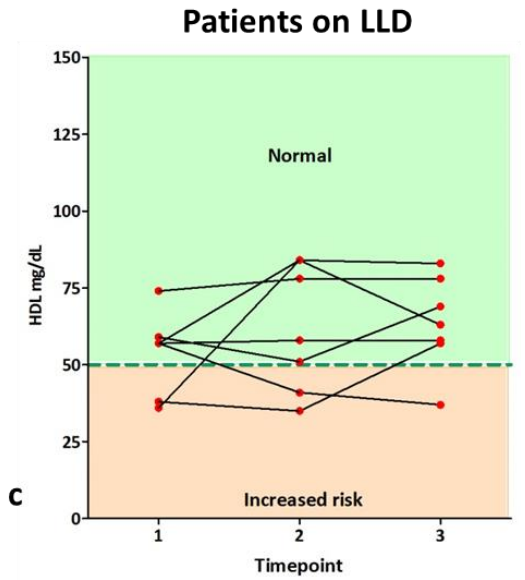

d

HDL	Change from T1 -T3
↑	14
↓	2
No change	2

Figure 6.5 High-density lipoprotein (HDL) measurement in patients and controls

Controls (a), patients (b) and patients known to be taking lipid lowering drugs (LLD) (c) Data represented as line graphs and in tabulated form (d). n = 18 for total patient and controls, n = 7 patients on LLD. Statistical test: Friedman and Dunn's test.

6.4.2.3. Assessment of low-density lipoproteins (LDL)

LDL, another major lipoprotein is also responsible for the transportation of lipids and is regarded as “bad cholesterol” due to its capacity to deposit lipid content within arterial walls (unlike HDL which can perform the reverse process) (Gordon *et al.* 1977). Figure 6.6a-b describes low-density lipoprotein (LDL) levels in control and patients respectively. Patients taking LLD, which are known to decrease LDL levels (Pahan 2006), are also shown (Figure 6.6c). The differences in LDL between T1 and T3 are mixed with nearly half increasing and decreasing respectively (Figure 6.6d). The variation in LDL levels between the time points may again reflect the dramatic changes in diet (Krauss *et al.* 2006).

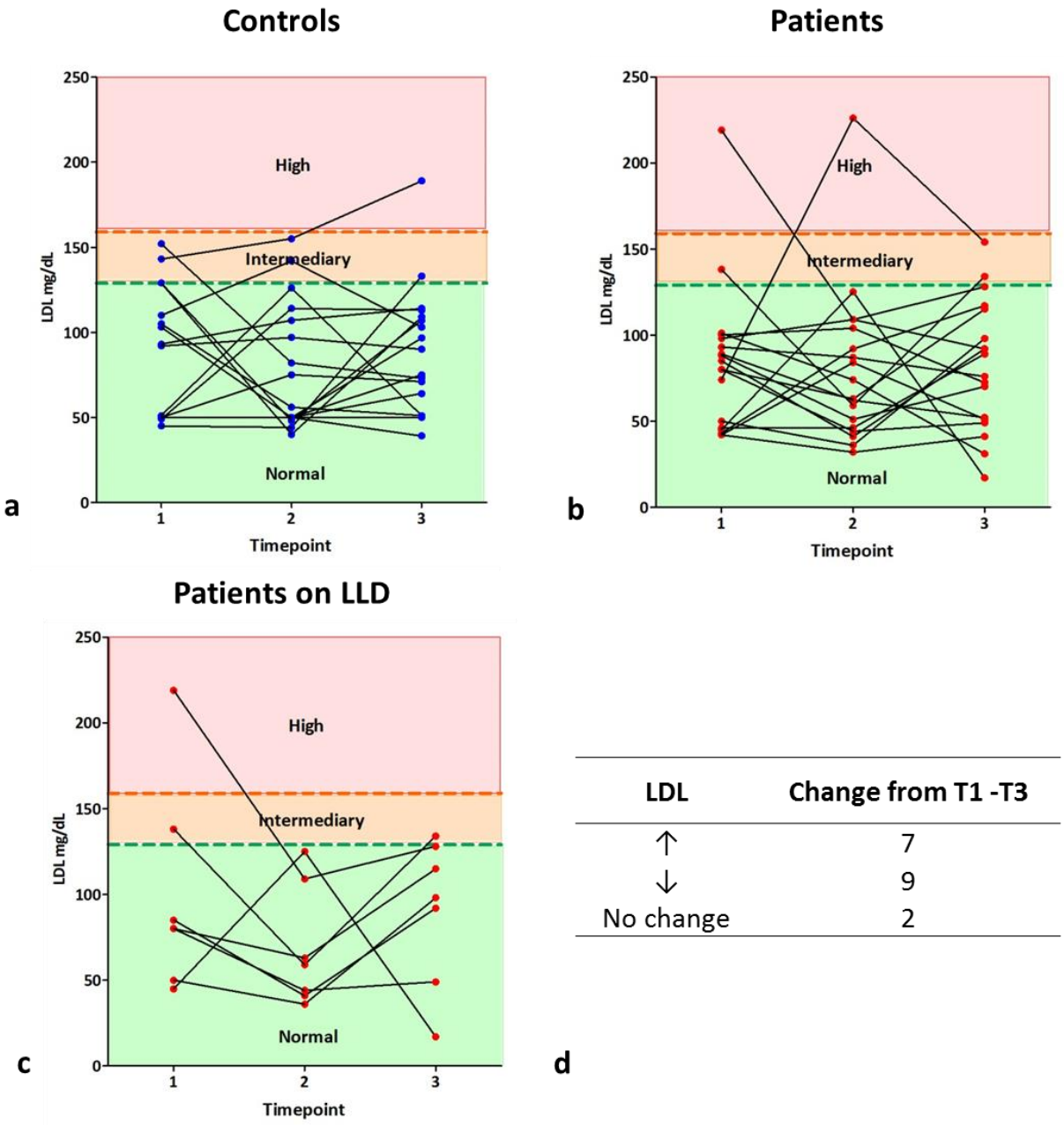

LDL	Change from T1 -T3
↑	7
↓	9
No change	2

Figure 6.6 Low-density lipoprotein (LDL) measurement in patients and controls

Controls (a), patients (b) and patients known to be taking lipid lowering drugs (LLD) (c) Data represented as line graphs and in tabulated form (d). n = 18 for total patient and controls, n = 7 patients on LLD. Statistical test: Friedman and Dunn's test.

6.4.2.4. Assessment of LDL/HDL ratio

The LDL/HDL ratio is regarded as an indicator of coronary heart disease risk and serves as a marker for potential improvements in lipid profiles (Manninen *et al.* 1992). Figure 6.7a-b describes the LDL/HDL ratio in controls and patients respectively, and patients taking LLD are also shown separately (Figure 6.7c). The patient ratios show an overall reduction but with an absence of statistical significance (Figure 6.7d), reflecting an increase in the proportion of HDL levels with weight loss (Leenen *et al.* 1993).

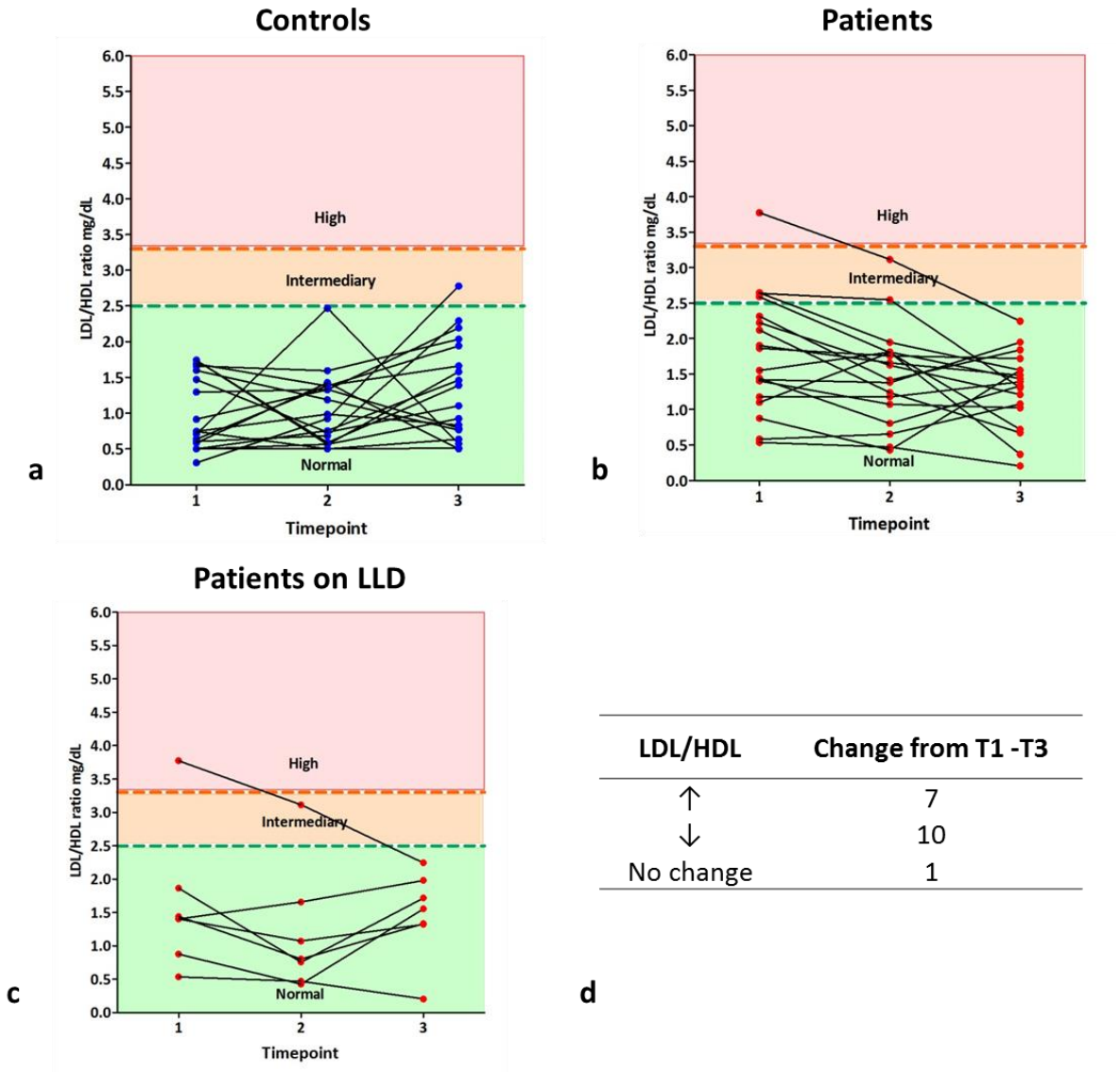

LDL/HDL	Change from T1 -T3
↑	7
↓	10
No change	1

Figure 6.7 LDL/HDL ratio measurement in patients and controls

Controls (a), patients (b) and patients known to be taking lipid lowering drugs (LLD) (c) Data represented as line graphs and in tabulated form (d). n = 18 for total patient and controls, n = 7 patients on LLD. Statistical test: Friedman and Dunn's test.

6.4.2.5. Triglycerides (TG)

Triglycerides (TG) are a type of lipid sourced from food and also produced by the liver from sugars. Typically stored within adipose tissue, TG is also a major component of LDL and high free circulating levels of TG are associated with cardiovascular disease (Austin *et al.* 1998; Sarwar *et al.* 2007). Figure 6.8a-b describes the TG levels in controls and patients respectively, and patients taking LLD are also shown separately (Figure 6.8c). Although the overall trend is a reduction in TG from T1-3 (Figure 6.8d), many of the patients show a decrease at T2 which can occur with low calorie diets (Mensink *et al.* 2016) with an increase at T3 potentially reflecting an increase in calorific intake.

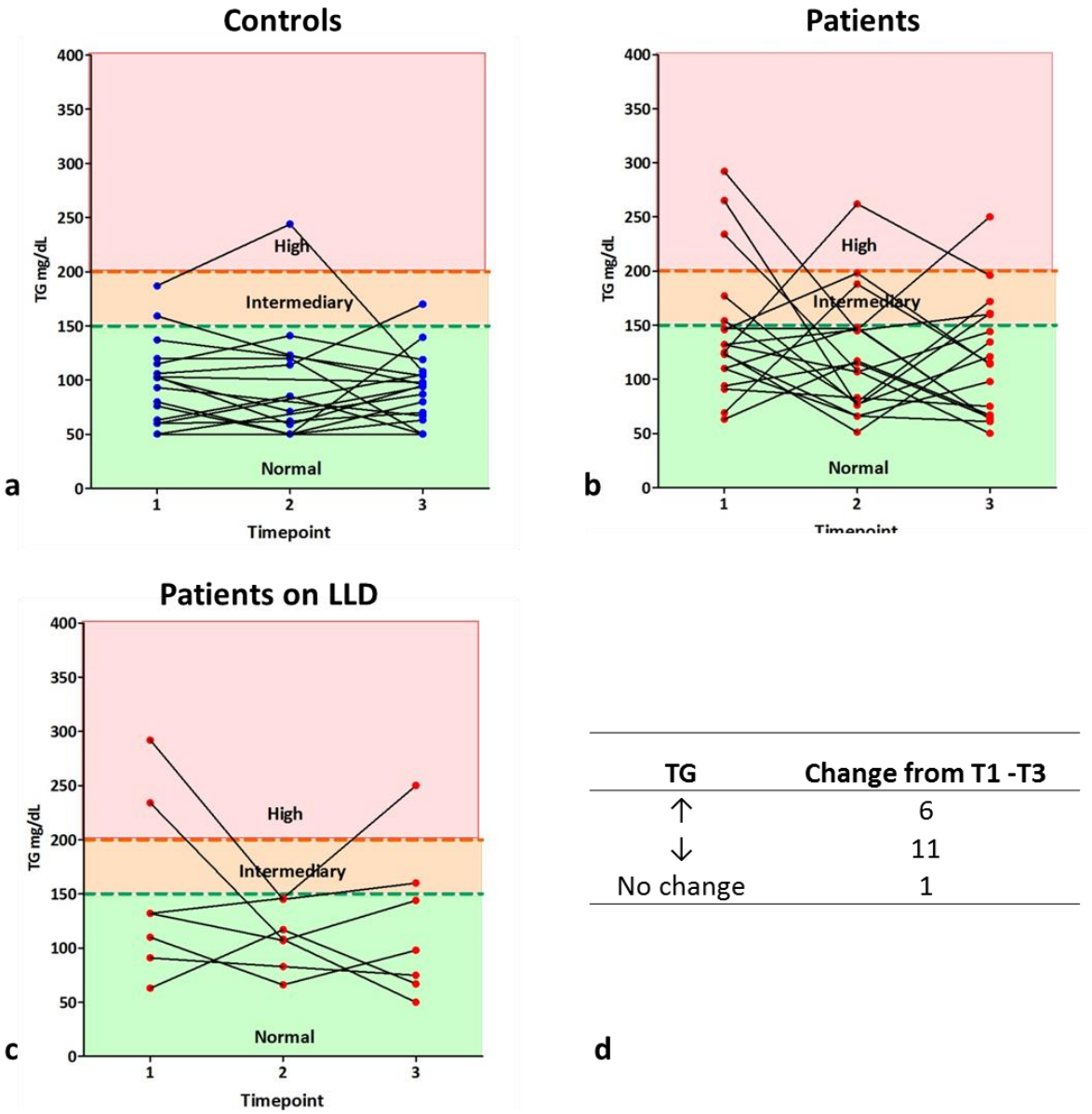

TG	Change from T1 -T3
↑	6
↓	11
No change	1

Figure 6.8 Triglyceride (TG) measurements in patients and controls

Controls (a), patients (b) and patients known to be taking lipid lowering drugs (LLD) (c) Data represented as line graphs and in tabulated form (d). n = 18 for total patient and controls, n = 7 patients on LLD. Statistical test: Friedman and Dunn's test.

6.5. Neutrophil counts

Figure 6.9 illustrates the differences in neutrophil numbers, when adjusted for collected blood volumes, between patients and controls at each time point. Neutrophil numbers in patients were higher at each time point and significantly so at T2; the lack of significance at T1 may be a result of increased variability in control numbers.

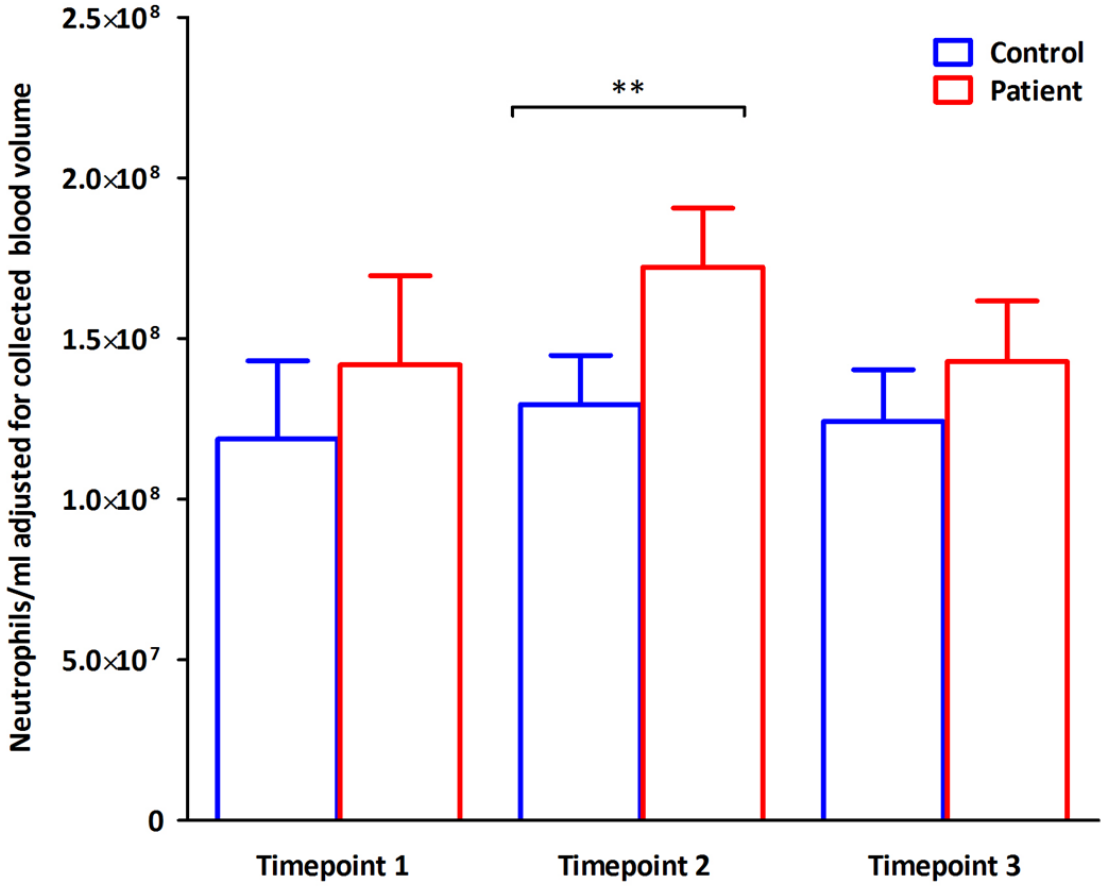

Figure 6.9 Patient and control neutrophil counts at different time points

Neutrophils were isolated (section 2.2.2) and cell counts per ml were calculated by adjusting for volume of blood collected per sample between T1-3. Data represented as a bar graph. n = 18 for total patient and controls respectively. Statistical test: Wilcoxon matched-pairs, ** = ($p < 0.01$).

6.6. Quantification of NETs in obese patients pre- and post- weight loss surgery

Figure 6.10 shows NET production by control and patient neutrophils at each time point. These results are also shown in tabulated form (Table 6.3) due to the number of stimuli and their numerical range. At T1 NET formation (Figure 6.10a) was significantly lower in patient neutrophils relative to controls for all stimuli employed ($p < 0.05$ and $p < 0.01$ for HOCl). Significance remained (although lower) at T2 (Figure 6.10b) for HOCl ($p < 0.05$) and was lost completely by T3 (Figure 6.10c). Visual representation of NET formation is shown in Figure 6.10d.

Figure 6.11 shows NET production compared within the different time points. Due to the wide day-to-day variability that has been previously reported in neutrophil assays (Udén *et al.* 1983; Roth 1993; Winkel *et al.* 1981; K. Bergström and B. Åsman 1993), it was necessary to present the data as a ratio by dividing patient values by controls per result per time point. There were significant differences in NET production by patients between T1 and T3 for PMA, HOCl and *A. viscosus* indicating that weight loss is associated with an increase in NET production (Figure 6.11a). The overall trend was an increase in NET production in all conditions (Figure 6.11b).

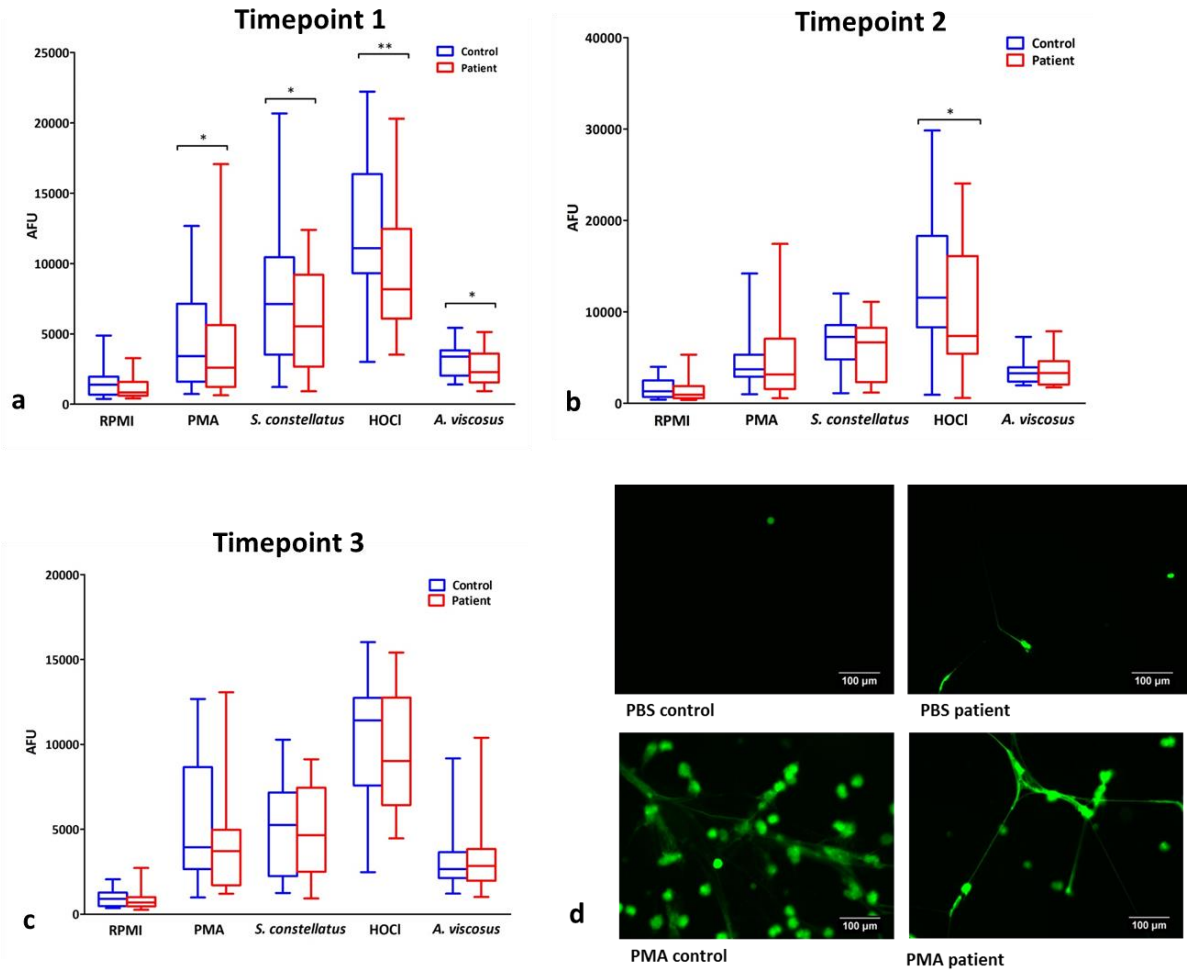

Figure 6.10 Patient and control NET release at different time points

Neutrophils were isolated (section 2.2.2) and NETs and NET bound proteins were quantified in response to PMA (50nM), *S. constellatus* (MOI 1 in 500), HOCl (0.75 mM) and *A. viscosus* (MOI 1 in 300) (section 2.5.3). Data presented as box and whisker plots (a-c); the band within the box represents the median, surrounded by the 1st and 3rd quartiles, the ends of the whiskers represent the minimum and maximum data points. n = 18 for total patient and controls respectively. Statistical test: Wilcoxon matched-pairs, * = ($p < 0.05$), ** = ($p < 0.01$).

Table 6.3 Inter-individual analysis of NET results

Green italicised text highlights results deemed significantly different at $p < 0.05$. Where levels could not be detected in patient samples, no statistical tests were performed. n = 18 for total patient and controls respectively. Statistical test: Wilcoxon matched-pairs.

	T1		T2		T3	
	Control	**Patient**	**Control**	**Patient**	**Control**	**Patient**
RPMI						
Average ±SD (range)	1560 ±1203 (378-4882)	1201 ±844 (404-3274)	1608 ±1152 (396-3984)	1374 ±3254 (999-14189)	916 ±480 (352-2060)	701 ±326 (263-1454)
***p* value**	0.34		0.23		0.14	
PMA						
Average ±SD (range)	4681 ±3426 (725-634)	3906 ±4037 (634-17064)	4680 ±3254 (999-14189)	4779 ±4608 (545-17434)	4680 ±3254 (999-14189)	4779 ±4608 (545-17435)
***p* value**	*0.032*		0.32		0.19	
S. constellatus						
Average ±SD (range)	7387 ±4726 (1233-20673)	6077 ±3451 (923-12386)	6770 ±2900 (1105-12009)	6017 ±3086 (1164-1101)	6769 ±2901 (1105-12009)	6017 ±3086 (1164-11101)
***p* value**	*0.026*		0.051		0.89	
HOCl						
Average ±SD (range)	12047 ±5249 (3009-22216)	9364 ±4420 (3519-20302)	12980 ±7115 (921-29829)	10362 ±6919 (576-24045)	9844 ±3702 (2475-16016)	9194 ±23453(4462-15406)
***p* value**	*0.008*		*0.026*		0.38	
A. viscosus						
Average ±SD (range)	3132 ±1278 (1405-5430)	2600 ±1278 (930-5133)	3460 ±1340 (1958-7258)	3698 ±1809 (1733-7869)	2983 ±1790 (1215-9173)	3183 ±2148 (1013-10390)
***p* value**	*0.032*		0.34		0.52	

a

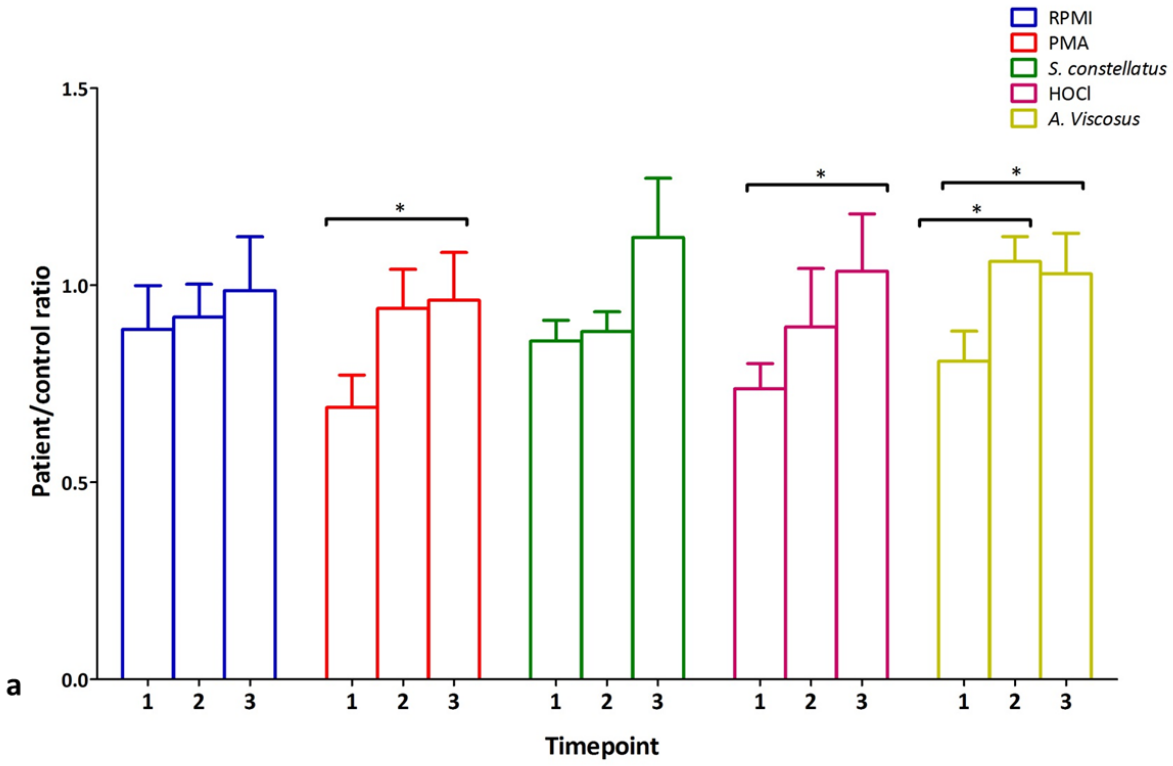

b

Change from T1 -T3	↑	↓	No change
RPMI	9	5	4
PMA	10	5	3
S. constellatus	10	6	2
HOCl	8	6	4
A. viscosus	13	4	1

Figure 6.11 Patient NET release time point comparison

Neutrophils were isolated (section 2.2.2) and NETs were quantified in response to PMA (50nM), *S. constellatus* (MOI 1 in 500), HOCl (0.75 mM) and *A. viscosus* (MOI 1 in 300) (section 2.5.3). Data presented as bar graphs of patient/control ratios (a) and in tabulated form (b) denoting the overall change in NETs between T1 and T3. n = 18 for total patient and controls respectively. Statistical test: Friedman and Dunn's post-test.

6.7. Neutrophil ROS generation in obese patients pre- and post- weight loss surgery

Figure 6.12, 6.13 and 6.14 and Tables 6.4, 6.5 and 6.6 show ROS production using the three chemiluminescent reagents luminol (total ROS), isoluminol (extracellular ROS) and lucigenin (extracellular superoxide) respectively. In addition to each stimulus alone, a priming step was also included using GM-CSF (10ng/ml). The results show patient neutrophils release significantly higher ROS in the presence of a stimulus and priming with stimulus at T1 with all three chemiluminescent reagents (Figure 6.12a, Figure 6.13a and Figure 6.14a). Over the course of the different study time points, significant differences remain for luminol and were partially lost for isoluminol and lucigenin (Figure 6.12b-c, Figure 6.13b-c, and Figure 6.14b-c). These results indicate that weight loss in the patients is accompanied by a reduction in the levels of ROS release when compared with healthy controls.

Figure 6.15a-f shows ROS production compared within the different time points for luminol, isoluminol and lucigenin respectively. The data is presented as patient/control ratios to account for day-to-day variability as was done for the NETs analysis. There were no significant differences in ROS production by patients between T1 and T3 for any of the stimuli used (Figure 6.15a,c and e), despite the overall trend indicating decreases in ROS production following stimulation and following priming with stimulation (Figure 6.15b,d and f). These results indicate that within-patient variations in ROS do not change in these patients despite weight loss.

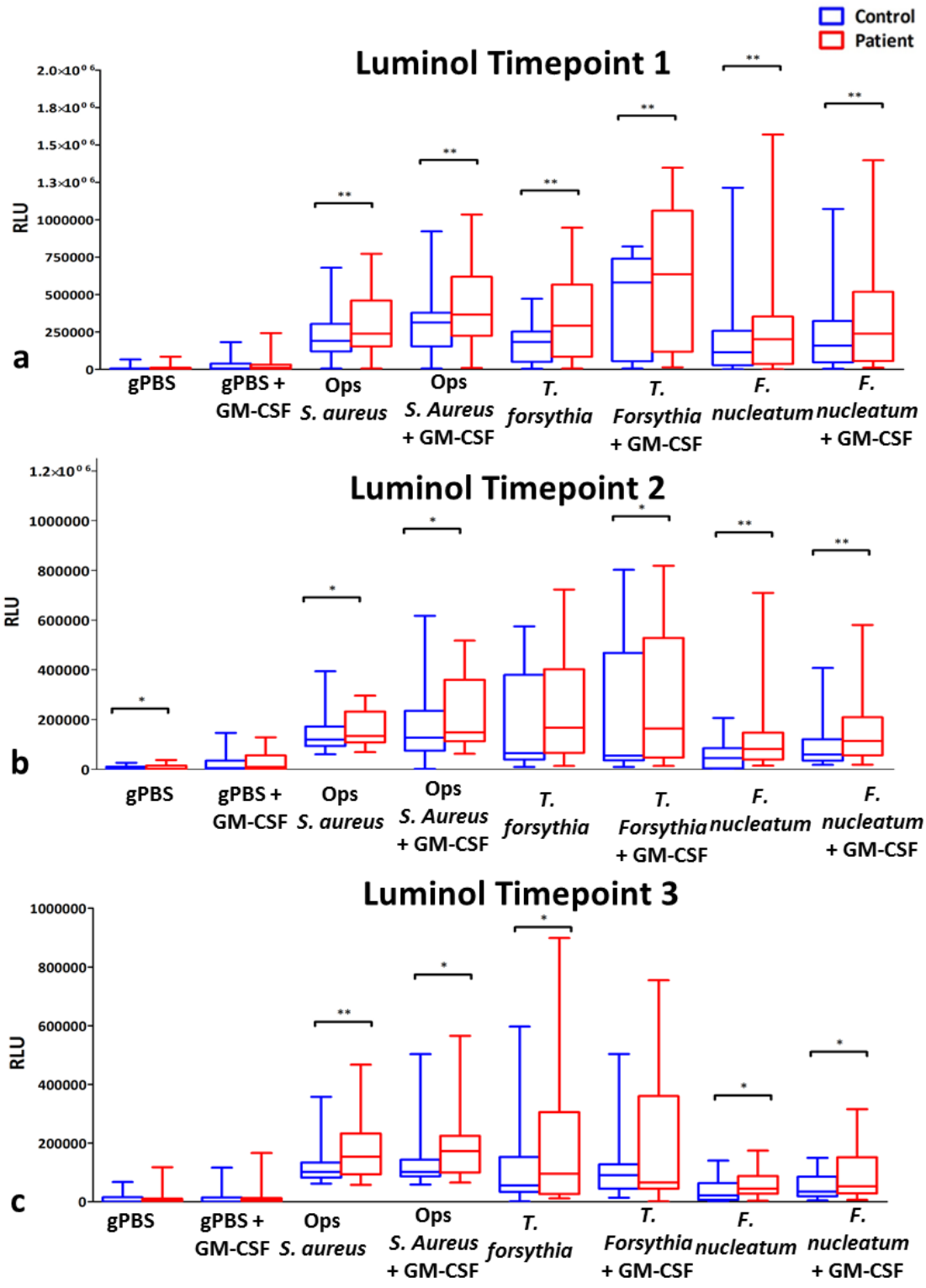

Figure 6.12 Patient and control ROS production with luminol at different time points

Neutrophils were isolated (section 2.2.2) and ROS generation was detected following priming with/without GM-CSF (10ng/ml) and stimulation using opsonised *S. aureus* (MOI 1 in 150), *T. forsythia* (MOI 1 in 300), and *F. nucleatum* (MOI 1 in 300) (section 2.4.3.2). Data presented as box and whisker plots. n = 18 for total patient and controls respectively. Statistical test: Wilcoxon matched-pairs, * = ($p < 0.05$), ** = ($p < 0.01$).

Table 6.4 Patient and control ROS inter-individual analysis with luminol

Green italicised text highlights results deemed significantly different at $p < 0.05$. Where levels could not be detected in patient samples, no statistical tests were performed. n = 18 for total patient and controls respectively. n = 18 for total patient and controls respectively. Statistical test: Wilcoxon matched-pairs.

Luminol	T1		T2		T3	
	Control	Patient	Control	Patient	Control	Patient
gPBS						
Average ±SD (range)	731 ±837 (66-3243)	696 ±780 (83-2803)	488 ±453 (91-1348)	1131 ±1432 (70-4435)	1613 ±2798 (99-10408)	1882 ±4210 (103-17167)
***p* value**	*0.03*		*0.04*		0.57	
gPBS + GM-CSF						
Average ±SD (range)	3240 ±3324 (91-11308)	3840 ±5460 (119-19771)	4762 ±6475 (107-20100)	5065 ±8286 (82-32288)	2587 ±4535 (90-16246)	2640 ±4984 (86-18850)
***p* value**	0.42		0.67		0.56	
Opsonised *S. aureus*						
Average ±SD (range)	5790 ±5376 (514-23189)	7620 ±8423 (863-37366)	3933 ±3206 (604-11045)	5048 ±4331 (925-15575)	3185 ±3479 (555-10906)	3694 ±4535 (695-19878)
***p* value**	*0.0009*		0.29		*0.03*	
Opsonised *S. aureus* + GM-CSF						
Average ±SD (range)	8483 ±7485 (687-33625)	10788 ±11420 (1081-47943)	9416 ±10320 (152-31050)	10090 ±10167 (863-36048)	4501 ±5579 (473-19709)	4220 ±4885 (666-20141)
***p* value**	*0.03*		0.46		0.26	
T. forsythia						
Average ±SD (range)	6248 ±7757 (86-32596)	9588 ±11335 (160-44300)	5121 ±5994 (181-20766)	6320 ±6031 (152-18253)	3857 ±4728 (128-16851)	4980 ±5371 (214-18615)
***p* value**	*0.03*		0.41		0.06	
***T. forsythia* + GM-CSF**						
Average ±SD (range)	11009 ±8095 (111-31013)	17039 ±14845 (329-55745)	8961 ±8318 (251-25390)	12603 ±11981 (255-35390)	5891 ±7999 (194-30877)	5684 ±5674 (255-19894)
***p* value**	*0.01*		0.14		0.91	
F. nucleatum						
Average ±SD (range)	2994 ±3828 (107-14437)	3471 ±3669 (189-12858)	1945 ±2537 (103-8245)	5299 ±9571 (168-34100)	1763 ±2872 (90-11345)	2329 ±4963 (107-20388)
***p* value**	*0.007*		*0.02*		0.78	
***F. nucleatum* + GM-CSF**						
Average ±SD (range)	5408 ±5883 (165-20458)	6671 ±7077 (284-22905)	2902 ±3303 (152-12348)	7664 ±14203 (292-48950)	4311 ±10072 (107-42794)	2919 ±5148 (103-21025)
***p* value**	0.34		*0.02*		0.32	

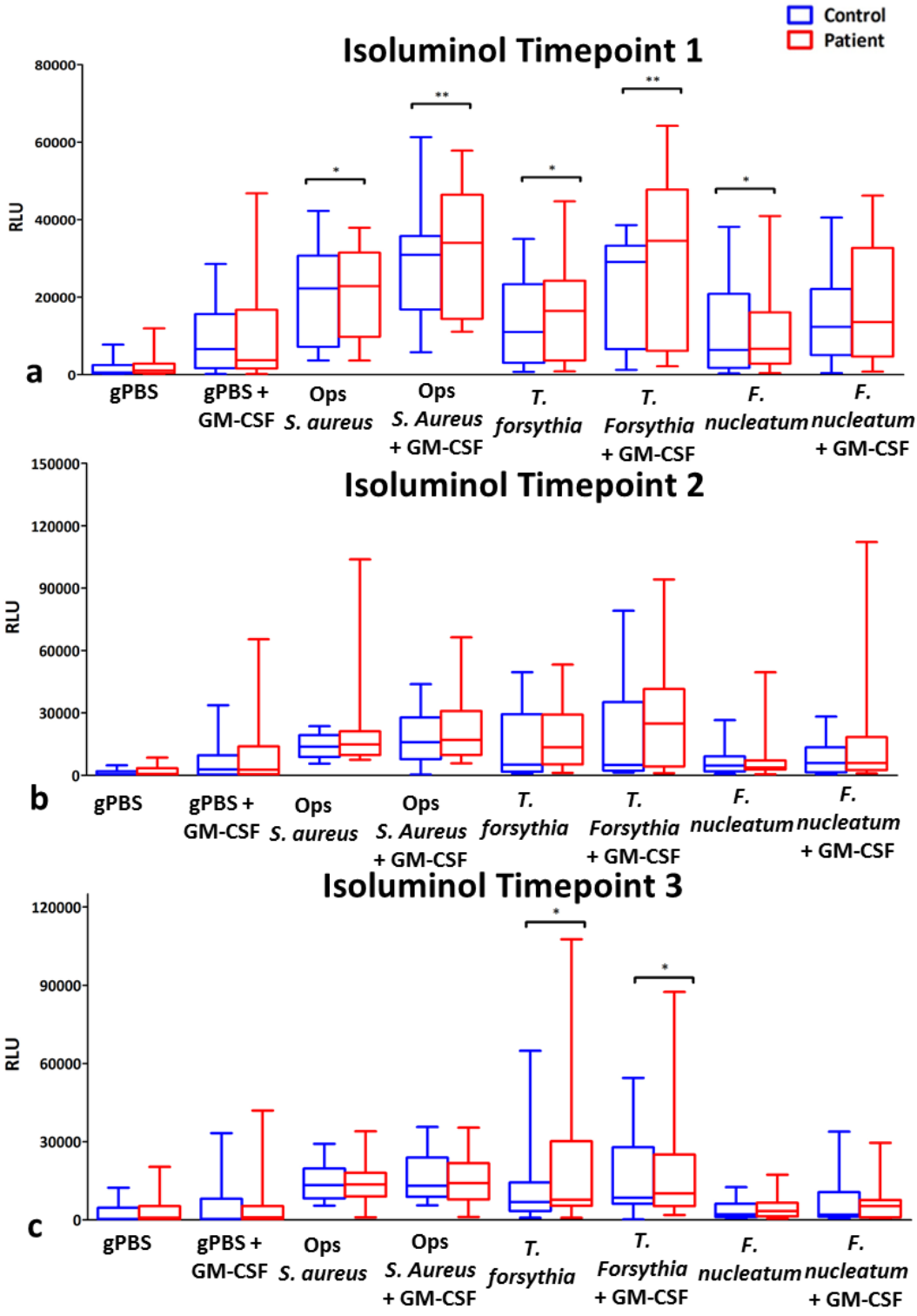

Figure 6.13 Patient and control ROS production with isoluminol at different time points

Neutrophils were isolated (section 2.2.2) and ROS generation was detected following priming with/without GM-CSF (10ng/ml) and stimulation using opsonised *S. aureus* (MOI 1 in 150), *T. forsythia* (MOI 1 in 300), and *F. nucleatum* (MOI 1 in 300) (section 2.4.3.2). Data presented as box and whisker plots. n = 18 for total patient and controls respectively. Statistical test: Wilcoxon matched-pairs, * = ($p < 0.05$), ** = ($p < 0.01$).

Table 6.5 Patient and control ROS inter-individual analysis with isoluminol

Green italicised text highlights results deemed significantly different at $p < 0.05$. Where levels could not be detected in patient samples, no statistical tests were performed. n = 18 for total patient and controls respectively. Statistical test: Wilcoxon matched-pairs.

Isoluminol	T1		T2		T3	
	Control	Patient	Control	Patient	Control	Patient
gPBS						
Average ±SD (range)	8896 ±2220 (107-7664)	2411 ±3333 (115-11924)	2206 ±3060 (140-1066)	2855 ±3274 (148-9500)	2345 ±3422 (134-12401)	3949 ±6293 (144-20358)
***p* value**	0.44		0.15		0.31	
gPBS + GM-CSF						
Average ±SD (range)	1743 ±8543 (173-28453)	11646 ±14746 (164-46753)	9933 ±15176 (222-58500)	12342 ±18005 (243-65402)	5018 ±9226 (169-33296)	4619 ±9802 (188-41995)
***p* value**	0.92		0.79		0.35	
Opsonised *S. aureus*						
Average ±SD (range)	21045 ±12498 (3686-42279)	22095 ±11696 (3633-37900)	45281 ±123358 (5635-538500)	53006 ±132676 (7456-577500)	14023 ±6513 (5512-29264)	14660 ±7963 (1045-33987)
***p* value**	0.03		0.43		0.37	
Opsonised *S. aureus* + GM-CSF						
Average ±SD (range)	28987 ±14712 (5812-61288)	33097 ±17324 (11119-57804)	64034 ±188350 (488-817000)	77534 ±231081 (5812-1001500)	15935 ±8726 (5615-35686)	16333 ±9640 (1169-35423)
***p* value**	0.002		0.19		0.26	
T. forsythia						
Average ±SD (range)	13780 ±11267 (723-35032)	17326 ±14495 (872-44707)	47461 ±138136 (839-597500)	41097 ±96418 (1139-422500)	26190 ±36335 (850-123297)	36426 ±52366 (834-183587)
***p* value**	0.02		0.29		0.03	
***T. forsythia* + GM-CSF**						
Average ±SD (range)	22539 ±13976 (1254-38596)	30153 ±21551 (2166-64205)	56396 ±157678 (1471-682500)	42122 ±72221 (1048-315000)	23743 ±26562 (186-89138)	35160 ±47673 (1965-148947)
***p* value**	0.009		0.37		0.02	
F. nucleatum						
Average ±SD (range)	11602 ±11560 (341-38152)	11736 ±12370 (440-40921)	12282 ±24402 (613-107000)	14956 ±25218 (584-99000)	3915 ±3651 (723-12546)	4518 ±4267 (506-17336)
***p* value**	0.02		0.67		0.46	
***F. nucleatum* + GM-CSF**						
Average ±SD (range)	12282 ±24403 (613-107000)	14956 ±25218 (584-99000)	15945 ±26130 (941-112150)	14956 ±25218 (584-99000)	6759 ±8872 (625-33909)	6038 ±6877 (736-29634)
***p* value**	0.02		0.79		0.89	

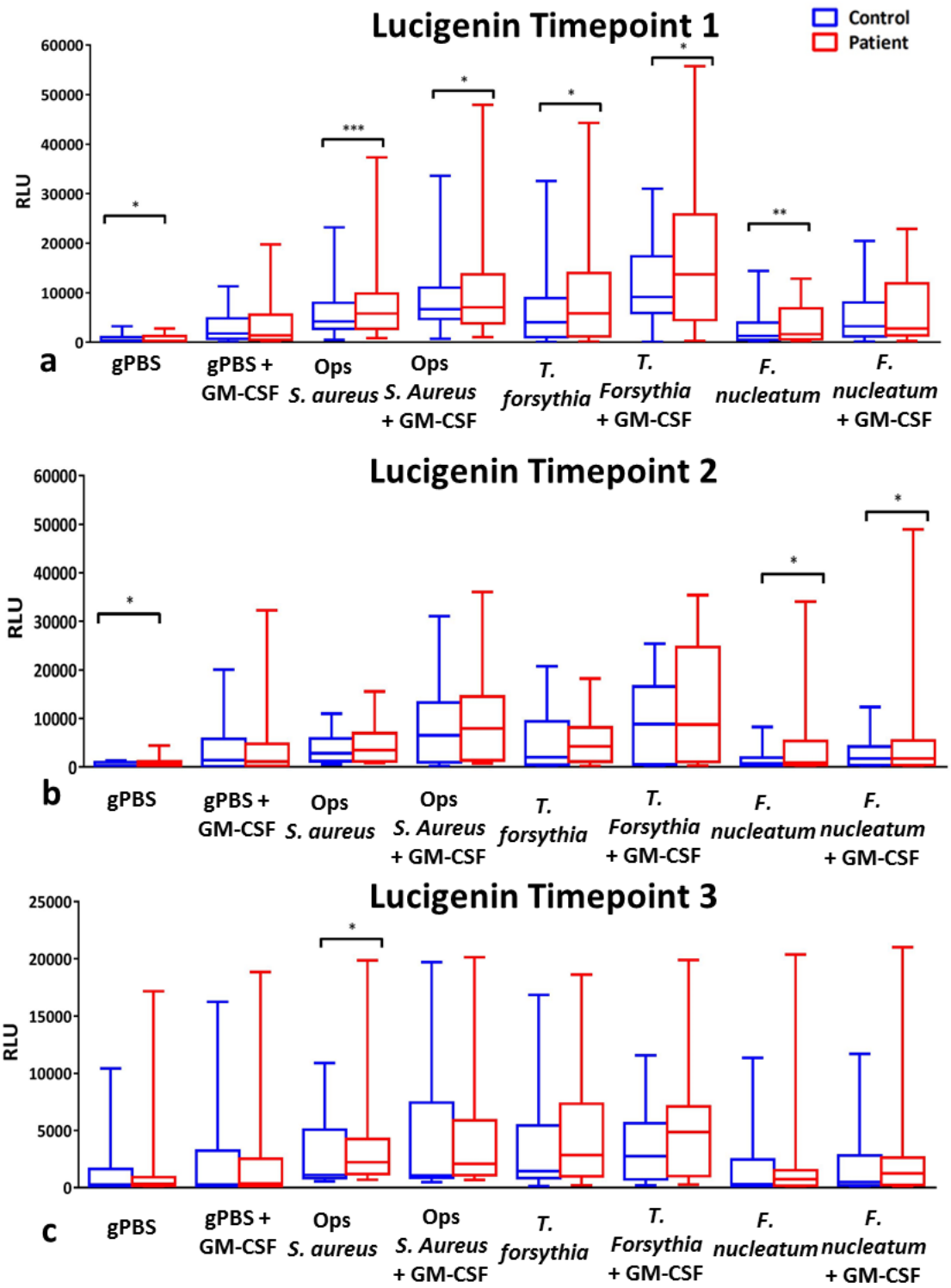

Figure 6.14 Patient and control ROS production with lucigenin at different time points

Neutrophils were isolated (section 2.2.2) and ROS generation was detected following priming with/without GM-CSF (10ng/ml) and stimulation using opsonised *S. aureus* (MOI 1 in 150), *T. forsythia* (MOI 1 in 300), and *F. nucleatum* (MOI 1 in 300) (section 2.4.3.2). Data presented as box and whisker plots. n = 18 for total patient and controls respectively. Statistical test: Wilcoxon matched-pairs, * = ($p < 0.05$), ** = ($p < 0.01$).

Table 6.6 Patient and control ROS inter-individual analysis with lucigenin

Green italicised text highlights results deemed significantly different at $p < 0.05$. Where levels could not be detected in patient samples, no statistical tests were performed. n = 18 for total patient and controls respectively. Statistical test: Wilcoxon matched-pairs.

Lucigenin	T1		T2		T3	
	Control	Patient	Control	Patient	Control	Patient
gPBS						
Average ±SD (range)	731 ±837 (66-3243)	696 ±780 (83-2803)	488 ±453 (91-1348)	1131 ±1432 (70-4435)	1613 ±2798 (99-10408)	1882 ±4210 (103-17167)
***p* value**	0.03		0.04		0.57	
gPBS + GM-CSF						
Average ±SD (range)	3240 ±3324 (91-11308)	3840 ±5460 (119-19771)	4762 ±6475 (107-20100)	5065 ±8286 (82-32288)	2587 ±4535 (90-16246)	2640 ±4984 (86-18850)
***p* value**	0.42		0.67		0.56	
Opsonised *S. aureus*						
Average ±SD (range)	5790 ±5376 (514-23189)	7620 ±8423 (863-37366)	3933 ±3206 (604-11045)	5048 ±4331 (925-15575)	3185 ±3479 (555-10906)	3694 ±4535 (695-19878)
***p* value**	0.0009		0.29		0.03	
Opsonised *S. aureus* + GM-CSF						
Average ±SD (range)	8483 ±7485 (687-33625)	10788 ±11420 (1081-47943)	9416 ±10320 (152-31050)	10090 ±10167 (863-36048)	4501 ±5579 (473-19709)	4220 ±4885 (666-20141)
***p* value**	0.03		0.46		0.26	
T. forsythia						
Average ±SD (range)	6248 ±7757 (86-32596)	9588 ±11335 (160-44300)	5121 ±5994 (181-20766)	6320 ±6031 (152-18253)	3857 ±4728 (128-16851)	4980 ±5371 (214-18615)
***p* value**	0.03		0.41		0.06	
***T. forsythia* + GM-CSF**						
Average ±SD (range)	11009 ±8095 (111-31013)	17039 ±14845 (329-55745)	8961 ±8318 (251-25390)	12603 ±11981 (255-35390)	5891 ±7999 (194-30877)	5684 ±5674 (255-19894)
***p* value**	0.01		0.14		0.91	
F. nucleatum						
Average ±SD (range)	2994 ±3828 (107-14437)	3471 ±3669 (189-12858)	1945 ±2537 (103-8245)	5299 ±9571 (168-34100)	1763 ±2872 (90-11345)	2329 ±4963 (107-20388)
***p* value**	0.007		0.02		0.78	
***F. nucleatum* + GM-CSF**						
Average ±SD (range)	5408 ±5883 (165-20458)	6671 ±7077 (284-22905)	2902 ±3303 (152-12348)	7664 ±14203 (292-48950)	4311 ±10072 (107-42794)	2919 ±5148 (103-21025)
***p* value**	0.34		0.02		0.32	

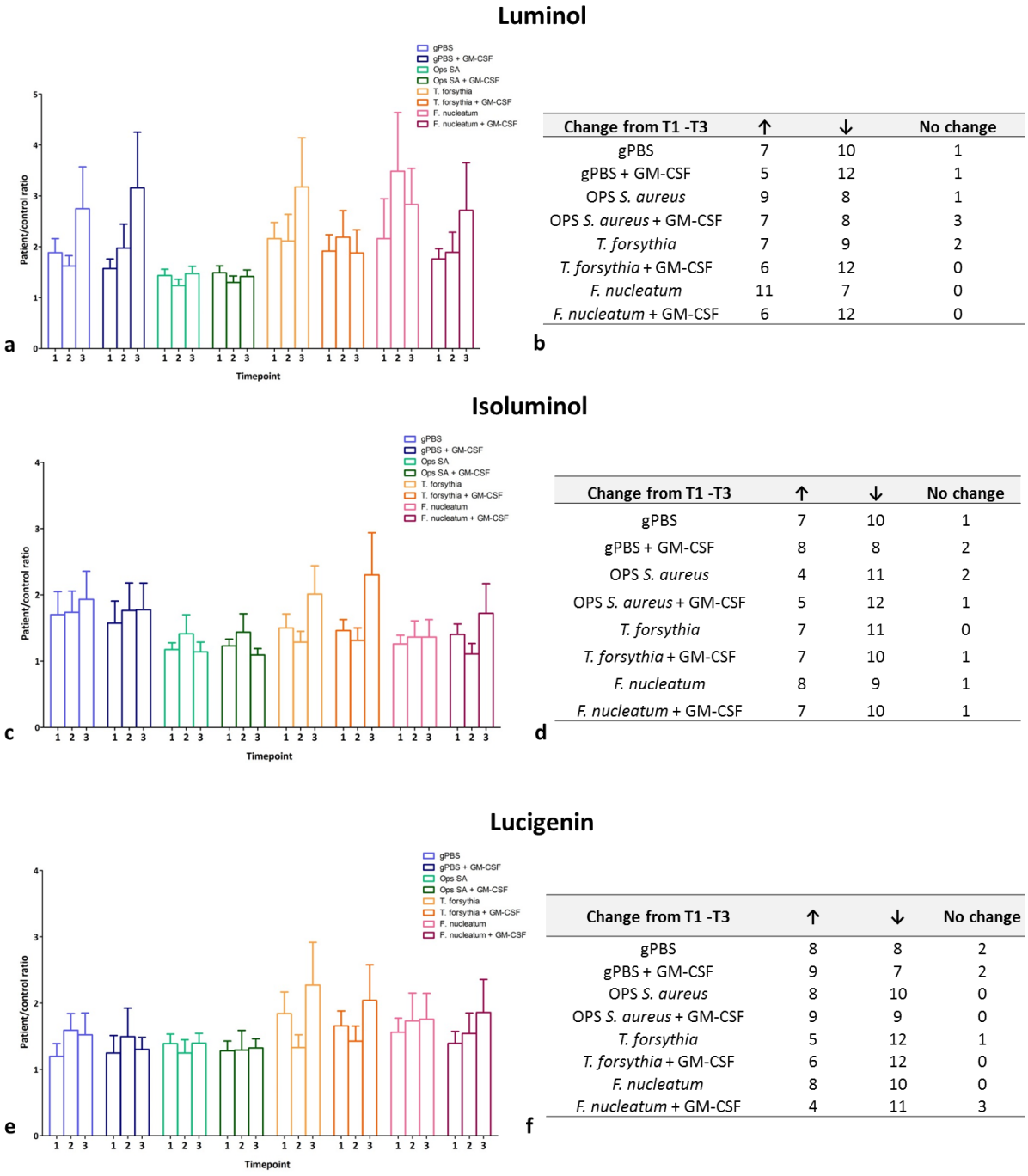

Change from T1 -T3	↑	↓	No change
gPBS	7	10	1
gPBS + GM-CSF	5	12	1
OPS *S. aureus*	9	8	1
OPS *S. aureus* + GM-CSF	7	8	3
T. forsythia	7	9	2
T. forsythia + GM-CSF	6	12	0
F. nucleatum	11	7	0
F. nucleatum + GM-CSF	6	12	0

Change from T1 -T3	↑	↓	No change
gPBS	7	10	1
gPBS + GM-CSF	8	8	2
OPS *S. aureus*	4	11	2
OPS *S. aureus* + GM-CSF	5	12	1
T. forsythia	7	11	0
T. forsythia + GM-CSF	7	10	1
F. nucleatum	8	9	1
F. nucleatum + GM-CSF	7	10	1

Change from T1 -T3	↑	↓	No change
gPBS	8	8	2
gPBS + GM-CSF	9	7	2
OPS *S. aureus*	8	10	0
OPS *S. aureus* + GM-CSF	9	9	0
T. forsythia	5	12	1
T. forsythia + GM-CSF	6	12	0
F. nucleatum	8	10	0
F. nucleatum + GM-CSF	4	11	3

Figure 6.15 Patient and control ROS production time point comparison

Neutrophils were isolated (section 2.2.2) and ROS generation was detected after with/without GM-CSF (10ng/ml) priming using opsonised *S. aureus* (MOI 1 in 150), *T. forsythia* (MOI 1 in 300), and *F. nucleatum* (MOI 1 in 300) (section 2.4.3.2). Data presented as bar graphs of patient/control ratios (a/c/e) and in tabulated form (b/d/f) denoting the overall change in ROS between T1 and T3 for luminol, isoluminol and lucigenin respectively. n = 18 for total patient and controls respectively. Statistical test: Friedman and Dunn's post-test.

6.8. Chemotaxis in obese patients pre- and post- weight loss surgery

Figure 6.16 shows the chemotaxis results from all three time points. The results are not tabulated as it was deemed unnecessary due to the lack of numerical range and because of the limited number of chemoattractants used. Figure 6.17, Figure 6.18 and Figure 6.19 show the cell paths, polar plots and angle histograms of all tracked cells per condition per time point respectively, illustrating the differences in the course of the cell movements. There were significant differences at all three time points for speed, velocity and CI, with patient neutrophil movement lower compared to controls. These results indicate that the weight loss in these patients did result in improved neutrophil chemotactic accuracy when compared with controls alone.

Figure 6.20 shows the chemotaxis results compared between the time points. The data is presented as raw values because of low numerical variability enabling statistical analyses without the need for data normalisation (as was done for the ROS and NETs analysis). There were significant differences between T1-3 with speed for both fMLP and CXCL8 chemoattractants as well as for RPMI with a trend indicating an overall increase in speed from T1-3 (Figure 6.20a). Similar findings were shown with velocity (Figure 6.20c) for fMLP and CXCL8 and only with fMLP for CI (Figure 6.20e). There were no significant differences for control values across any of the time points. These results indicate there is an increase in chemotactic accuracy between time points with weight loss when comparing patient results only (Figure 6.20b, d,and f).

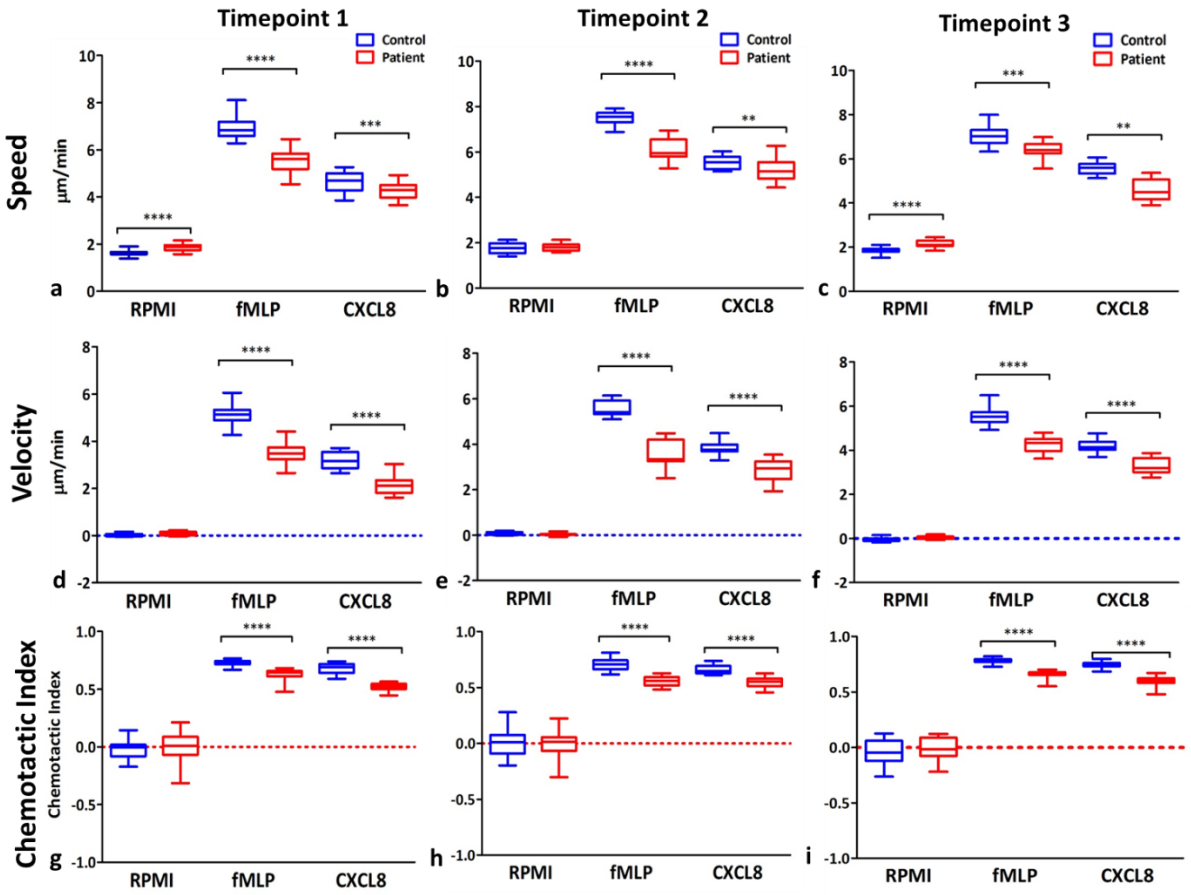

Figure 6.16 Neutrophil chemotaxis in patients and controls at different time points

Neutrophils were isolated (section 2.2.2) and chemotaxis was performed (section 2.6), after which the cells were analysed (section 2.6.2) and tracked information was used to generate average speed (a), velocity (b) and CI (c) for patient and control neutrophils in the presence of RPMI (negative control), fMLP (10nM) and CXCL8 (200ng/ml) chemoattractants. Data shown as box and whisker plots (n = 18; 15 cells tracked per chemoattractant/RPMI). Statistical test: Wilcoxon matched-pairs, * = ($p < 0.05$), *** = ($p < 0.001$), **** = ($p < 0.0001$).

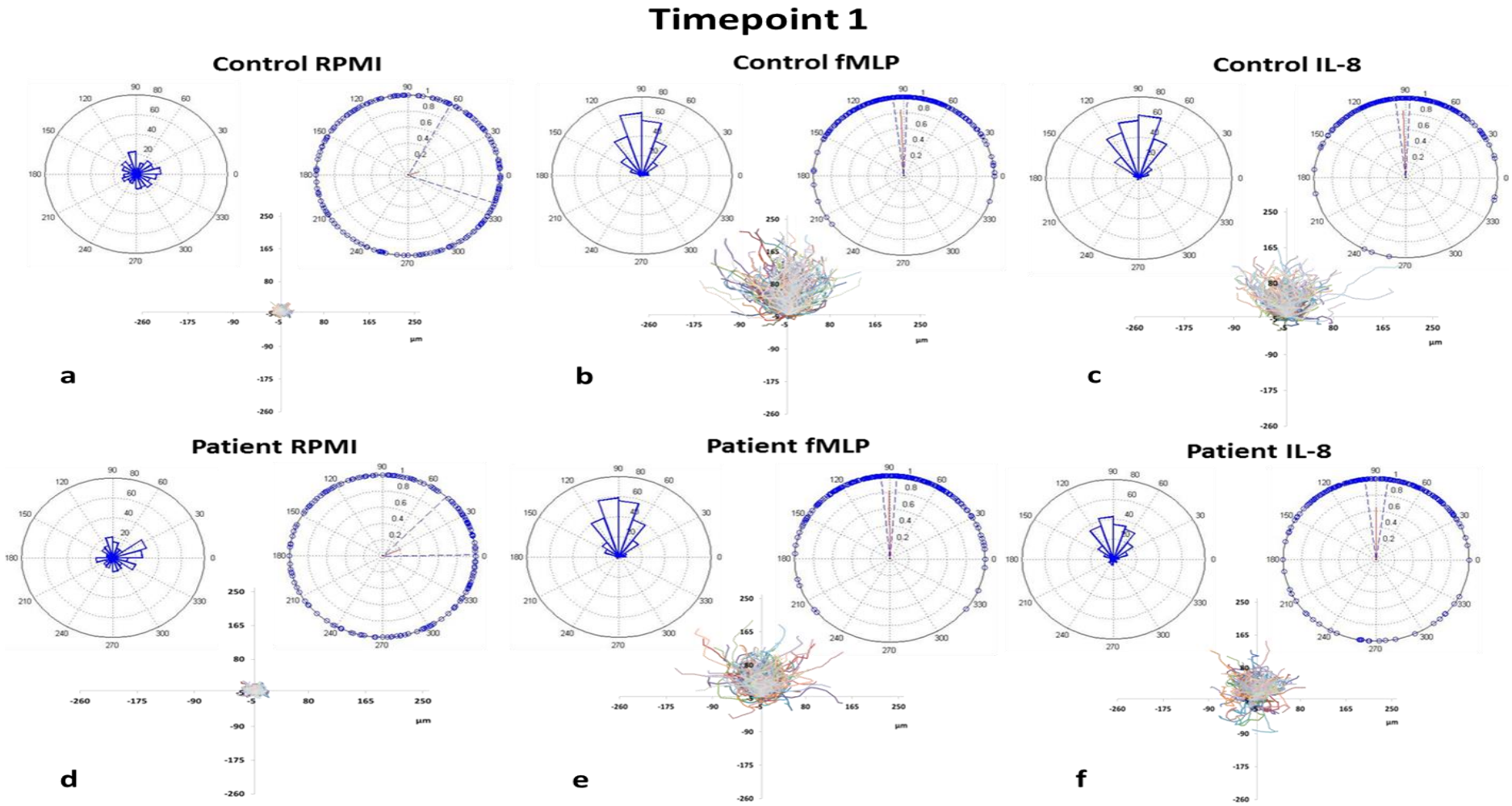

Figure 6.17 Neutrophil cell tracks Time point 1

Cell tracks, polar plots and angle histograms overlayed for control (a, b and c) and patient (d, e and f) neutrophils were generated to give a qualitative overview of chemotaxis using RPMI (negative control), fMLP (10nM) and CXCL8 (200ng/ml) chemoattractants respectively.

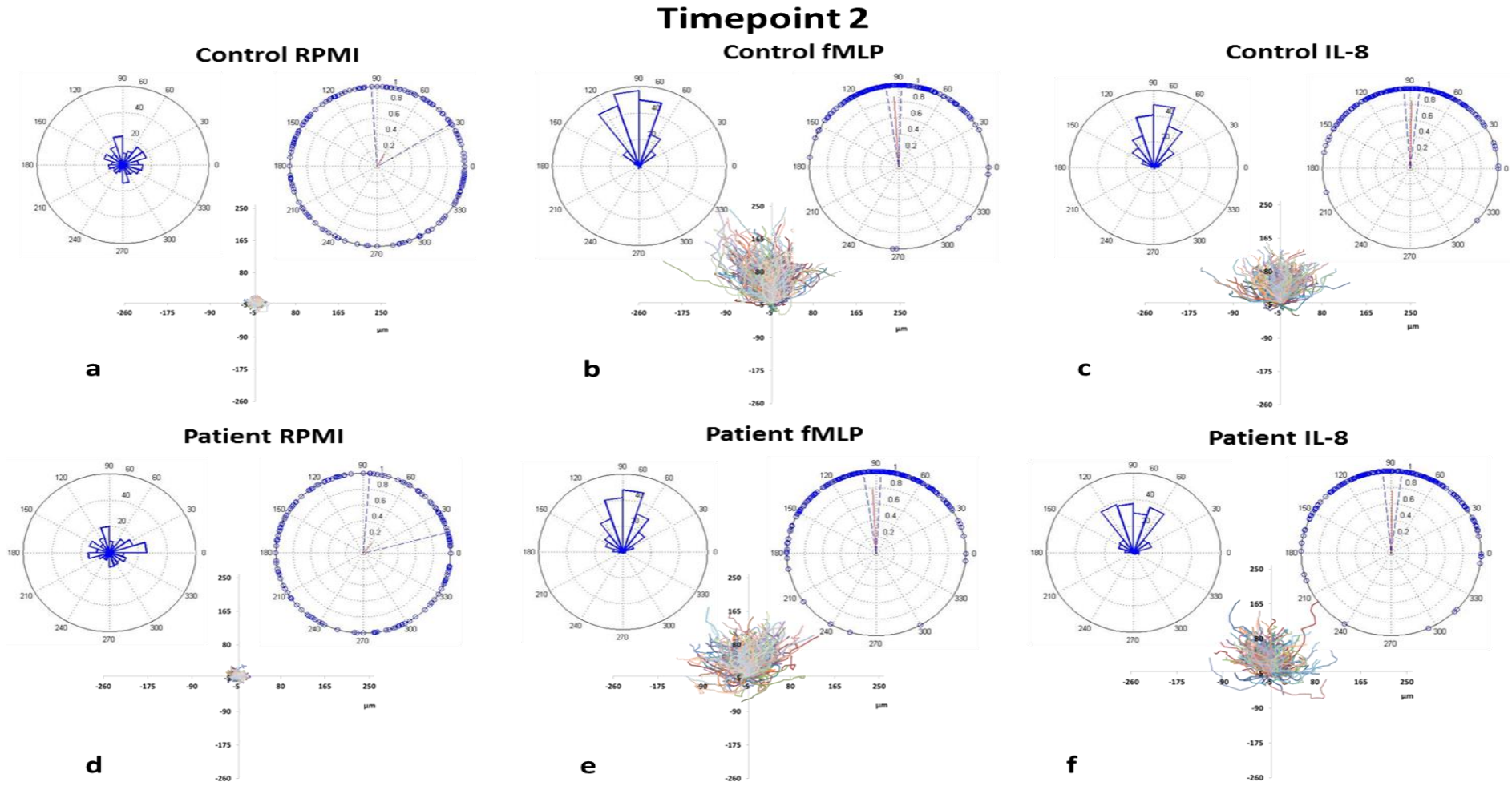

Figure 6.18 Neutrophil cell tracks Time point 2

Cell tracks, polar plots and angle histograms overlayed for control (a, b and c) and patient (d, e and f) neutrophils were generated to give a qualitative overview of chemotaxis using RPMI (negative control), fMLP (10nM) and CXCL8 (200ng/ml) chemoattractants respectively.

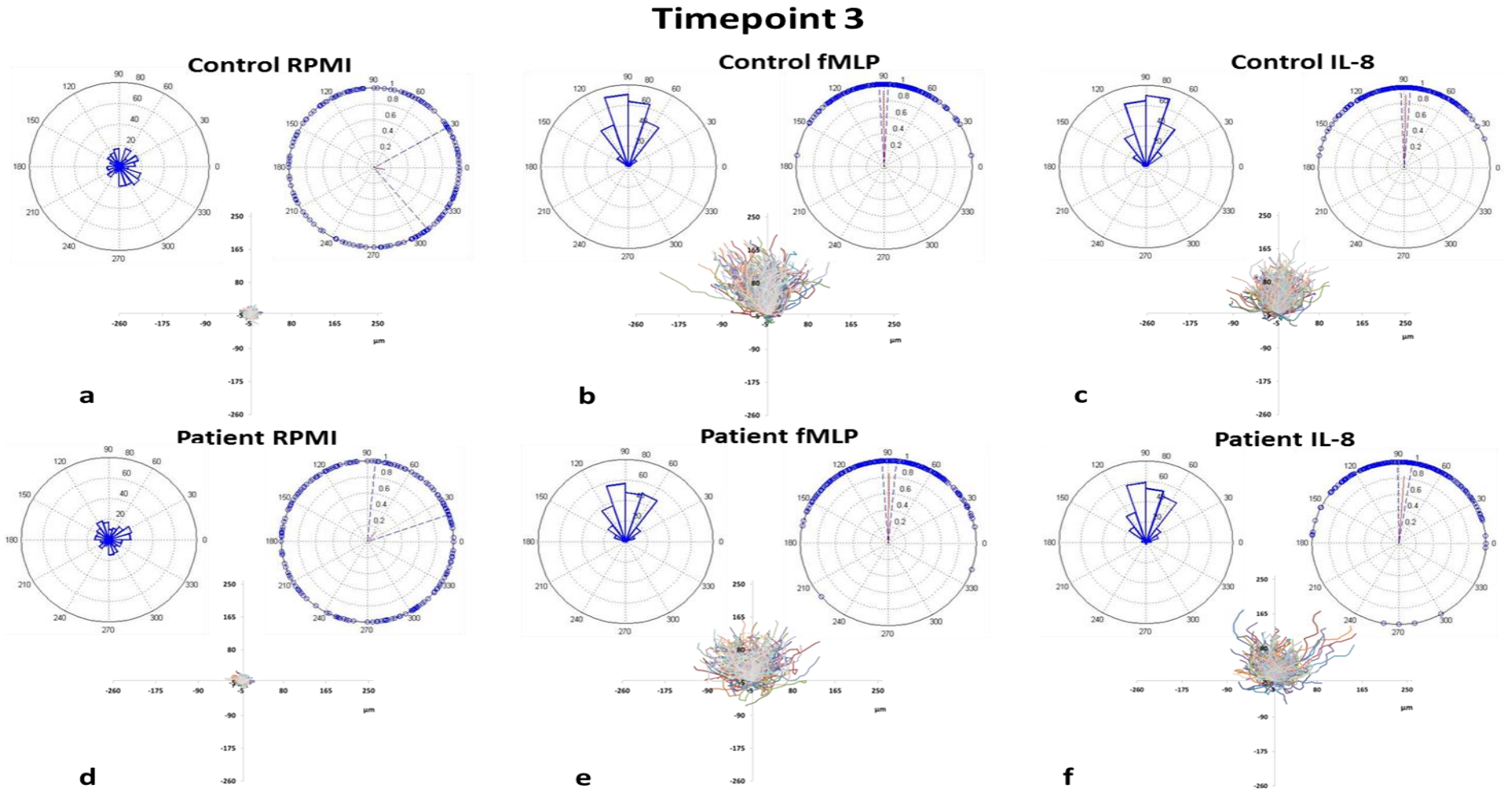

Figure 6.19 Neutrophil cell tracks Time point 3

Cell tracks, polar plots and angle histograms overlayed for control control (a, b and c) and patient (d, e and f) neutrophils were generated to give a qualitative overview of chemotaxis using RPMI (negative control), fMLP (10nM) and CXCL8 (200ng/ml) chemoattractants respectively.

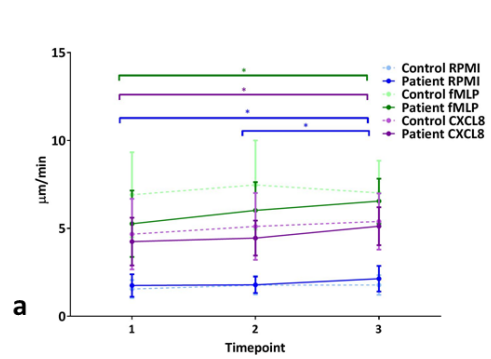

Speed

Change from T1 -T3	↑	↓	No change
RPMI	12	4	2
fMLP	13	4	1
CXCL8	14	4	0

b

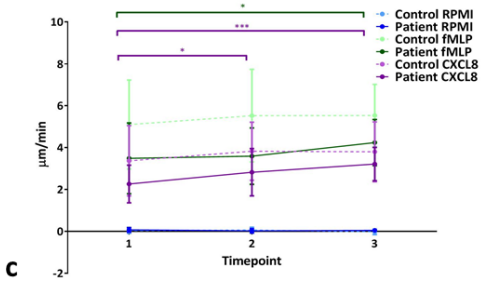

Velocity

Change from T1 -T3	↑	↓	No change
RPMI	7	8	3
fMLP	14	4	0
CXCL8	15	2	1

d

Chemotactic Index

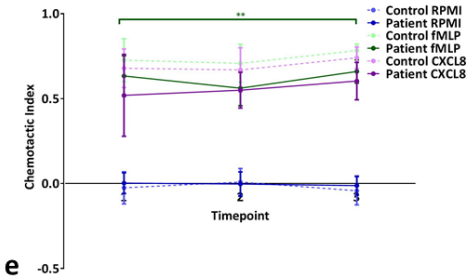

Change from T1 -T3	↑	↓	No change
RPMI	6	10	2
fMLP	7	9	2
CXCL8	12	4	2

f

Figure 6.20 Patient and control chemotaxis time point comparisons

Neutrophils were isolated (section 2.2.2) and chemotaxis was performed (section 2.6), after which the cells were analysed (section 2.6.2) and tracked information was used to generate average speed (a), velocity (c) and CI (e) for patient and control neutrophils in the presence of RPMI (negative control), fMLP (10nM) and CXCL8 (200ng/ml) chemoattractants. Data presented as line graphs of patient (solid lines) and control (dotted lines) raw data (a/c/e) and in tabulated form (b/d/f) denoting the overall change in chemotaxis between T1 and T3. n = 18 for total patient and controls respectively. Statistical test: Friedman and Dunn's post-test, * = ($p < 0.05$), ** = ($p < 0.01$), *** = ($p < 0.001$).

6.9. Cytokine release in obese patients pre- and post-bariatric surgery

Figure 6.21, Table 6.7 and Table 6.8 demonstrate the cell culture supernatant cytokine concentrations for IL-1β, IL-6, CXCL8 and TNFα in the absence/presence of relevant stimuli. The results show patient neutrophils release significantly higher cytokines in the absence/presence of stimuli at T1 compared with controls ($p < 0.05$) with some significant differences remain at T2, that are lost by T3. These results indicate that weight loss in the patients is accompanied by a reduction in the levels of pro-inflammatory cytokines released when compared to healthy controls. Figure 6.23 shows the concentrations of cytokines detected in plasma; there were no significant differences.

Figure 6.24a, b, e and f show cytokine production compared within the time points respectively. The data is presented as patient/control ratios to account for day-to-day variability as was performed for the NETs/ROS analysis. There were significant differences in IL-1β, IL-6, and TNFα release between T1-3 after exposure to LPS ($p < 0.05$). There were also significant reductions in the concentration of TNFα between T1-3 in the absence of a stimulus and after exposure to opsonised *S. aureus*. The overall trend is a decrease in cytokine production between T1 and T3 (Figure 6.24c, d, g and h) indicating that neutrophil pro-inflammatory cytokine release decreases with weight loss.

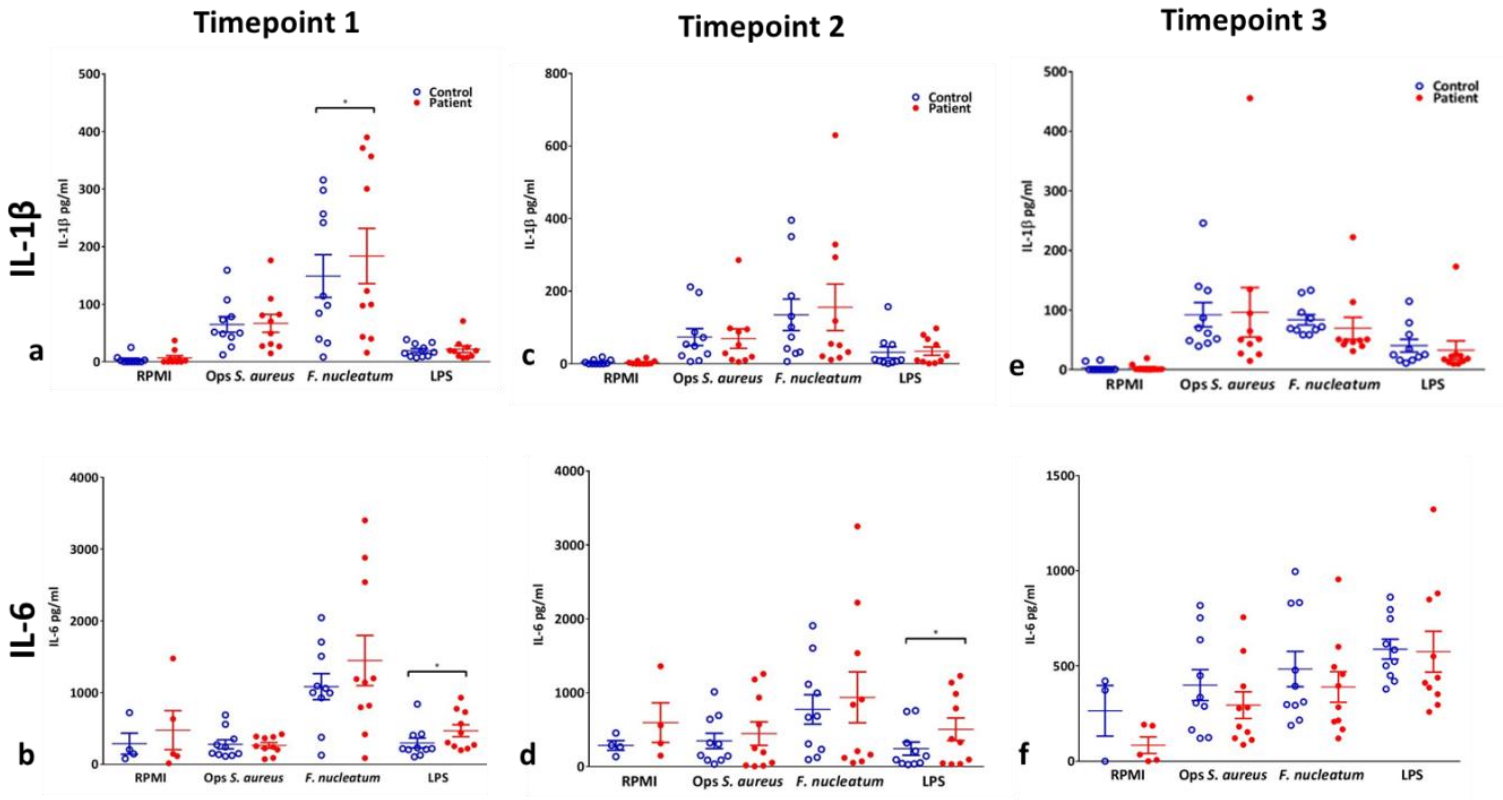

Figure 6.21 IL-1β and IL-6 quantification at different time points

Neutrophils were isolated (section 2.2.2) and cytokines IL-1β (a/c/e) and IL-6 (b/d/f) released from patient and control neutrophils per time point respectively (n = 10) following isolation and culture for 16 hours (section 2.7) and incubation with RPMI (negative control), opsonised *S. aureus* (FcγR stimulation pathway; MOI 1:150), *F. nucleatum* (TLR stimulation pathway; MOI 1 in 300) or LPS (TLR stimulation pathway). Blue hollow circles and filled red circles represent control and patient samples respectively. Statistical test: Statistical test: Wilcoxon matched-pairs, * = ($p < 0.05$), ** = ($p < 0.01$).

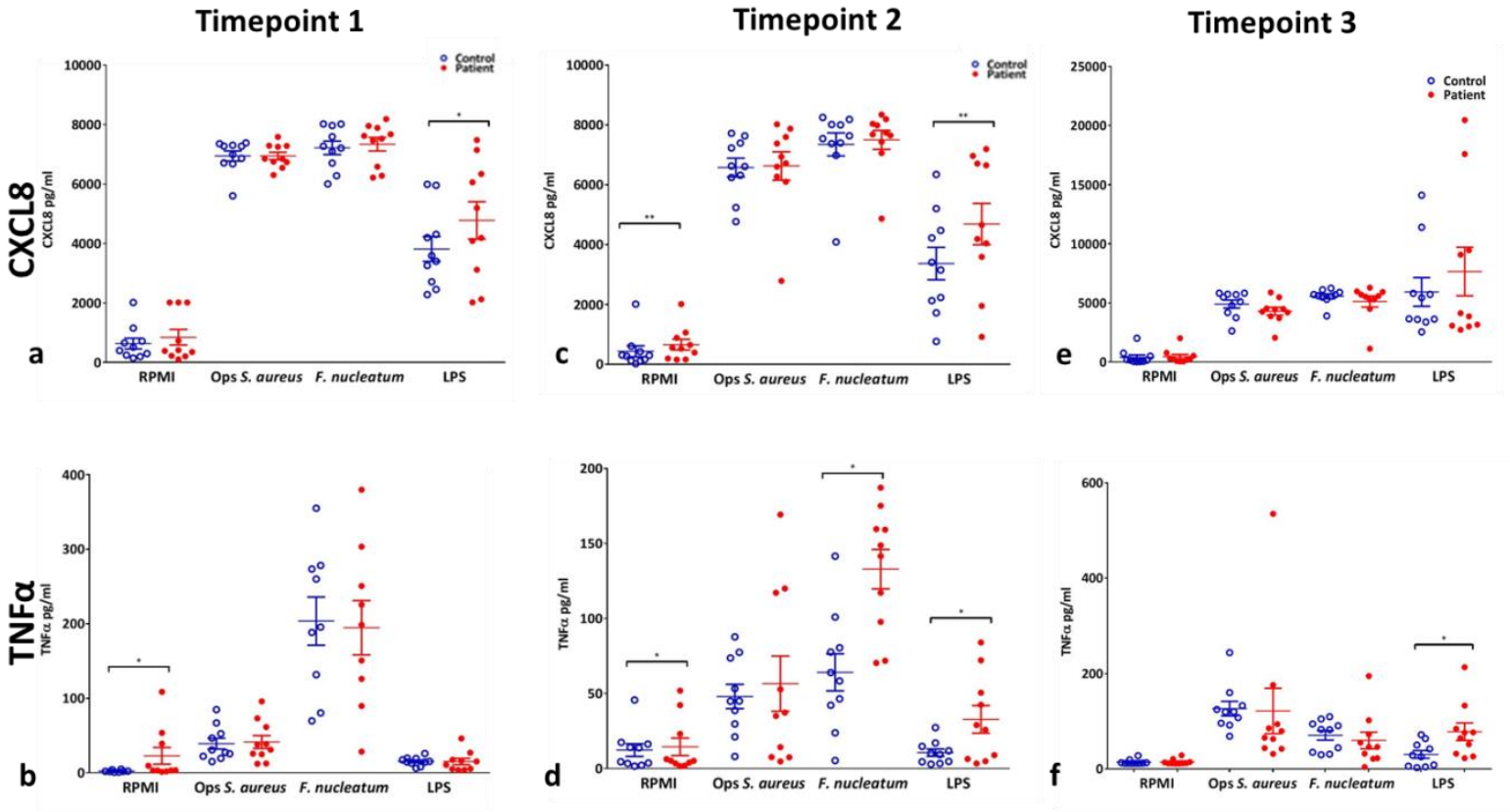

Figure 6.22 CXCL8 and TNFα quantification at different time points

Neutrophils were isolated (section 2.2.2) and cytokines CXCL8 (a/c/e) and TNFα (b/d/f) released from patient and control neutrophils per time point respectively (n = 10) following isolation and culture for 16 hours (section 2.7) and incubation with RPMI (negative control), opsonised *S. aureus* (FcγR stimulation pathway; MOI 1:150), *F. nucleatum* (TLR stimulation pathway; MOI 1 in 300) or LPS (TLR stimulation pathway). Blue hollow circles and filled red circles represent control and patient samples respectively. Statistical test: Statistical test: Wilcoxon matched-pairs, * = ($p < 0.05$), ** = ($p < 0.01$).

Table 6.7 Patient and control IL-1β (a) and IL-6 (b) release inter-individual analysis

Green italicised text highlights results deemed significantly different at $p < 0.05$. n = 10 for total patient and controls respectively. Statistical test: Wilcoxon matched-pairs.

a

IL-1β	T1		T2		T3	
	Control	Patient	Control	Patient	Control	Patient
RPMI						
Average ±SD (range)	3.76 ±7.8 (0-25)	6.9 ±12 (0-37)	4.6 ±6.7 (0-19)	3.8 ±5.6 (0-17)	3.2 ±6.4 (0.01-16)	3.2 ±6.2 (0-19.2)
***p* value**	1		1		0.24	
Ops *S. aureus*						
Average ±SD (range)	65 ±43 (12-159)	67 ±49 (15-176)	74 ±74 (6.5-212)	69 ±84 (5.3-286)	92 ±64 (39-246)	96 ±131 (15-456)
***p* value**	0.37		0.56		0.38	
F. nucleatum						
Average ±SD (range)	149 ±117 (8-315)	184 ±152 (16-390)	135 ±137 (6.6-396)	156 ±203 (11-630)	84 ±28 (59-133)	69 ±58 (31-222)
***p* value**	*0.037*		1		0.23	
LPS						
Average ±SD (range)	20 ±12 (7-39)	22 ±19 (7-71)	32 ±49 (0.92-157)	35 ±36 (0.82-98)	40 ±34 (11-115)	33 ±50(9.8-173)
p value	0.84		0.49		0.1	

b

IL-6	T1		T2		T3	
	Control	Patient	Control	Patient	Control	Patient
RPMI						
Average ±SD (range)	288 ±293 (80-721)	477 ±607 (15-1475)	438 ±580 (26-2016)	662 ±564 (160-2016)	402 ±613 (32-2016)	453 ±594 (55-2016)
***p* value**	1		*0.004*		0.25	
Ops *S. aureus*						
Average ±SD (range)	280 ±199 (114-689)	264 ±123 (72-421)	6581 ±986 (4773-7720)	6631 ±1500 (2791-8025)	4904 ±1077 (2628-5829)	4295 ±1034 (2052-5887)
***p* value**	0.77		0.49		0.23	
F. nucleatum						
Average ±SD (range)	1084 ±572 (129-2044)	1447 ±1106 (88-3401)	7350 ±1213 (4094-8254)	7501 ±998 (4870-8346)	5554 ±647 (3897-6246)	5118 ±1485 (1126-6290)
***p* value**	0.16		0.92		0.77	
LPS						
Average ±SD (range)	299 ±216 (106-841)	468 ±265 (197-930)	4690 ±2185 (821-7198)	10362 ±6919 (576-24045)	5930 ±3815 (2544-14112)	7655 ±6517 (2729-20466)
***p* value**	*0.028*		*0.006*		0.85	

Table 6.8 Patient and control CXCL8 (a) and TNFα (b) inter-individual analysis

Green italicised text highlights results deemed significantly different at $p < 0.05$. n = 10 for total patient and controls respectively. Statistical test: Wilcoxon matched-pairs.

a

CXCL8	T1		T2		T3	
	Control	Patient	Control	Patient	Control	Patient
RPMI						
Average ±SD (range)	634 ±573 (145-2016)	845 ±825 (102-2016)	230 ±171(0-455)	476 ±535 (0-1359)	265 ±231 (0-421)	84 ±97 (0-192)
***p* value**	0.65		0.75		0.5	
Ops *S. aureus*						
Average ±SD (range)	6945 ±542 (5603-7383)	6943 ±396 (6300-7582)	348 ±327 (35-1012)	447 ±503 (4-1255)	400 ±257 (121-818)	294 ±222 (87-756)
***p* value**	0.77		0.49		0.43	
F. nucleatum						
Average ±SD (range)	7216 ±716 (6004-8019)	7339 ±715 (6216-8185)	774 ±628 (97-1908)	937 ±1091 (52-3252)	484 ±293 (188-996)	390 ±253 (120-955)
***p* value**	0.56		0.84		0.63	
LPS						
Average ±SD (range)	3815 ±1318 (2281-5989)	4774 ±1283 (2019-7477)	243 ±283 (28-758)	505 ±483 (32-1227)	588 ±166 (379-862)	575 ±340 (259-1323)
***p* value**	0.04		0.049		0.56	

b

TNFα	T1		T2		T3	
	Control	Patient	Control	Patient	Control	Patient
RPMI						
Average ±SD (range)	2.5 ±1.4 (1-5)	23 ±35 (1.5-109)	12 ±13 (1.5-46)	14 ±18 (1.5-52)	14 ±5.2 (12-28)	15 ±5.7 (11-29)
***p* value**	0.034		1		0.76	
Ops *S. aureus*						
Average ±SD (range)	39 ±23 (15-85)	41 ±27 (12-96)	48 ±26 (8-88)	57 ±58 (4.7-169)	127 ±48 (69-244)	122 ±151 (32-535)
***p* value**	0.77		0.85		0.32	
F. nucleatum						
Average ±SD (range)	204 ±97 (70-355)	194 ±109 (29-380)	64 ±39 (5.3-142)	133 ±42 (70-187)	71 ±32 (30-110)	60 ±55 (4.4-195)
***p* value**	1		0.01		0.37	
LPS						
Average ±SD (range)	16 ±5.7 (6.6-26)	15.2 ±13 (4-46)	11 ±7.6 (2.9-27)	33 ±29 (3-84)	31 ±26 (3.3-72)	78 ±58 (23-214)
***p* value**	0.49		0.04		0.03	

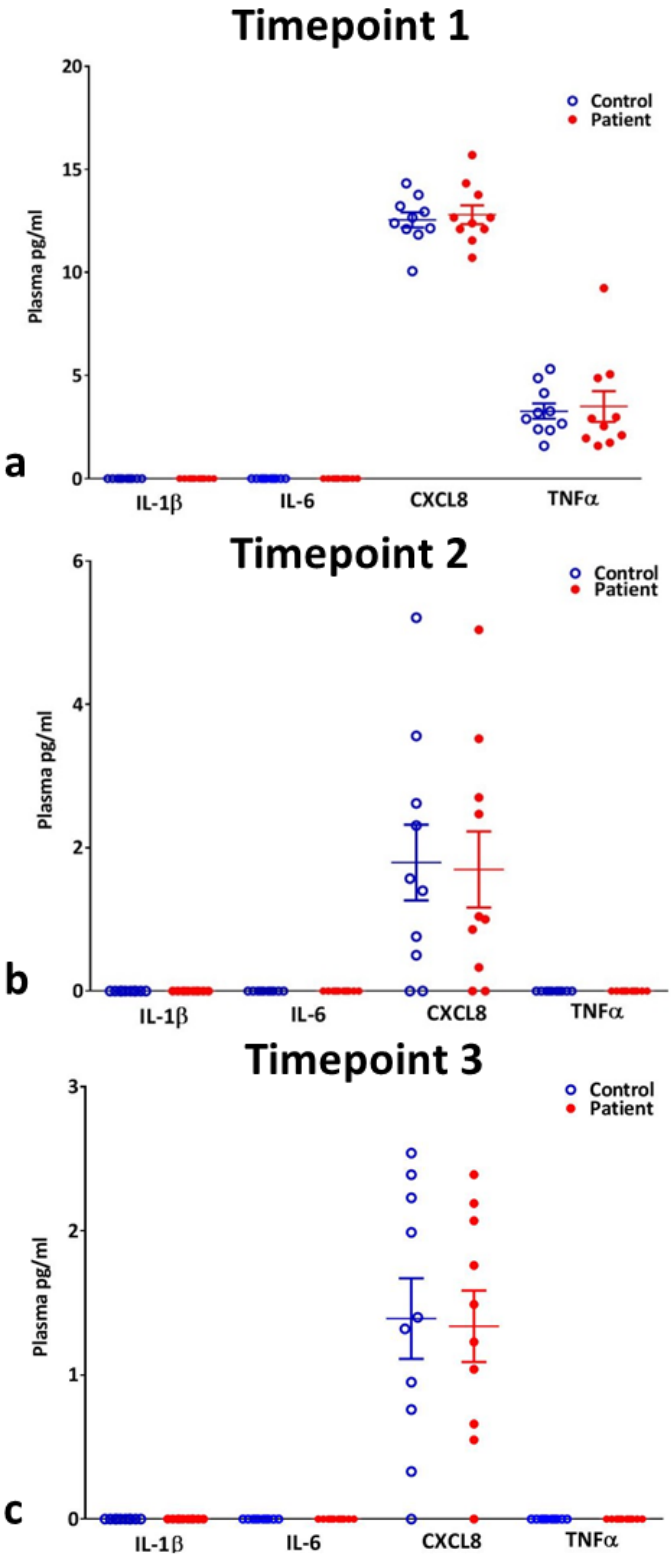

Figure 6.23 Plasma cytokine quantification in obesity all time points

Plasma was collected (section 2.3) and cytokines IL-1β, IL-6, CXCL8 and TNFα concentrations were measured in patients and controls (n = 10) per time point respectively. Levels that could not be detected were designated as 0.

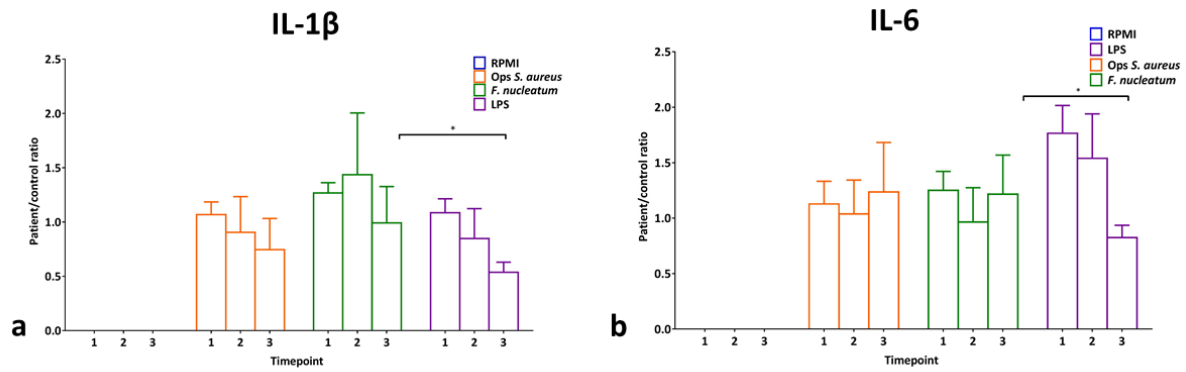

c

Change from T1 -T3	↑	↓	No change
Ops *S. aureus*	1	9	0
F. nucleatum	2	8	0
LPS	1	9	0

d

Change from T1 -T3	↑	↓	No change
Ops *S. aureus*	3	7	0
F. nucleatum	4	6	0
LPS	2	8	0

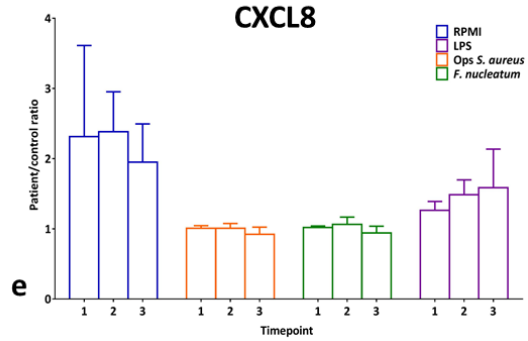

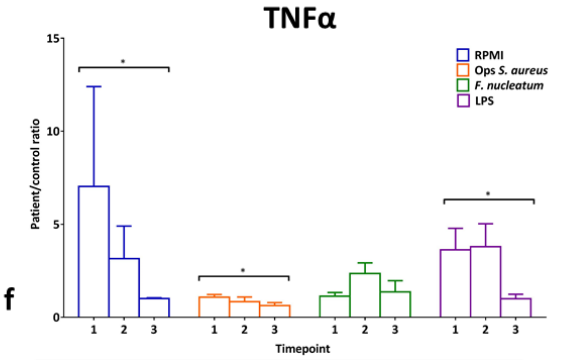

g

Change from T1 -T3	↑	↓	No change
RPMI	4	6	0
Ops *S. aureus*	3	7	0
F. nucleatum	3	6	1
LPS	3	7	0

h

Change from T1 -T3	↑	↓	No change
RPMI	2	8	0
Ops *S. aureus*	1	8	1
F. nucleatum	3	7	0
LPS	2	8	0

Figure 6.24 Patient and control cytokine release in obesity: time point comparisons

Neutrophils were isolated (section 2.2.2) and cytokines IL-1β (a), IL-6 (b). CXCL8 (e), TNFα (f), released from patient and control neutrophils (n = 10) following isolation and culture for 16 hours (2.7) and incubation with RPMI (negative control), opsonised *S. aureus* (FcγR stimulation pathway), *F. nucleatum*) (MOI of 1 in 150 and 1 in 300 respectively) or LPS (TLR stimulation pathway). Data presented as bar graphs of patient/control ratios (a/b/e/f) and in tabulated form (c/d/g/h) denoting the overall change in cytokine release between T1 and T3. Statistical test: Friedman and Dunn's post-test, * = ($p < 0.05$).

6.10. Discussion

The results presented in this chapter detail blood analyses and neutrophil assays at three different time points during the course of a VLCD and pre- and post-bariatric surgery. Of the patients recruited for the study, more than half had at least two obesity-related disorders. As expected, BMI was reduced following a VLCD and 3 months post-surgery, however despite the weight loss, which represented a significantly high percentage for some patients, many patients remained within the very severely obese category. BMI is typically the most common index used for studies involving overweight and obese individuals because of its easy calculation, however it has limitations which include an erroneous categorisation of body mass without making the distinction between adipose tissue and muscle mass per individual (Rimm *et al.* 1995). Another method of weight measurement commonly used in obesity studies is waist-to-hip ratio, which is considered a more accurate reflection of the health risks associated with excess adipose tissue in the individual (Noble 2001; Cheng *et al.* 2010), however such measurements were not taken at the time points reported here. It is also worth noting that changes in BMI as a result of calorie restriction by a VLCD do not necessarily result in a reduction in adipose tissue alone, for example, muscle mass is reported to be lost even in studies where the level of exercise is known (Dengel *et al.* 1994; Heymsfield *et al.* 2014).

HbA1c levels were significantly reduced in all patients and significance was still evident in the diabetes patients when analysed separately. The disease is associated with high HbA1c levels which can decrease with medical management in agreement with previous reports (Redmon *et al.* 2003; Redmon *et al.* 2005).

The lipids measured in this study are consistent with those used in a previous report on obesity and lipid levels (Bhatti *et al.* 2001). Blood lipid profiles infer the extent to which an

individual is at risk of suffering other obesity-related disorders, for example, coronary heart disease is positively related to LDL concentrations and inversely related to HDL concentrations (Kannel 1988). All blood lipid levels were measured with the additional analyses of patients taking LLD prior to and throughout the course of their treatment to highlight any dramatic differences in these patients which may bias overall results. Although the trend of all lipids measured showed an expected decrease (total cholesterol, LDL, LDL/HDL and triglycerides) or increase (HDL), as is expected with weight loss (Burton *et al.* 1985; Dattilo & Kris-Etherton 1992), there was a lack of significance between the time points for patients. Comparison with healthy gender-matched controls (which showed no difference intra-individually) demonstrate that positive differences had occurred with weight loss over time. Increased cholesterol synthesis is determined by body weight and is significantly associated with adiposity (Nestel *et al.* 1969). Total cholesterol results reported here showed a decrease in most patients, the underlying reason for this is thought to be a result of adipose tissue mobilisation inhibiting further cholesterol synthesis by the liver, the predominant organ involved in cholesterol synthesis (Vaswani 1983), in addition to increased cholesterol excretion in bile with weight loss (Bennion & Grundy 1975). The type of VLCD the patients self-administered throughout their treatment may have affected blood lipid levels, because even in the absence of weight loss a change in dietary habits, for example, via reduced fat intake, can change blood lipid profiles (Leenen *et al.* 1993). Conversely, some studies have reported that weight loss by diet alone is not associated with advantageous changes in blood lipid profiles (Thompson *et al.* 1979; Sörbris *et al.* 1981; Rabkin *et al.* 1981;). Overall the blood chemistry results indicate an improvement in levels with weight loss and the extent of the improvement is reflected in the fact that many patients are still very severely obese and lipid levels would therefore be expected to further improve with continued weight loss.

Several studies have focused on the effects of blood lipids on neutrophils. Neutrophils have been shown to express LDL receptors (Lara *et al.* 1997; Haverkamp *et al.* 2011) and LDL (or its oxidised form) has been reported to induce neutrophil calcium flux, oxidant release, integrin expression and chemotaxis (Lehr *et al.* 1995; van Tits *et al.* 2000; Kopprasch *et al.* 2004;). Neutrophils derived from individuals with dyslipidaemia exhibit elevated resting levels of intracellular calcium and raised levels of membrane-bound PKC, but calcium signalling in response to fMLP is decreased (which may be a possible reason for the reduced chemotaxis also reported in this chapter) (Paragh *et al.* 1999). Studies using neutrophils derived from murine models of hypercholesterolemia reported neutrophils to exhibit abnormal function in response to inflammatory stimuli including increased pro-inflammatory cytokine gene transcription (Palvinskaya *et al.* 2013) and reduced chemotaxis into the air pouch following an infection with *Klebsiella pneumoniae*; this finding was associated with decreased neutrophil chemotaxis to the CXC chemokines (Madenspacher *et al.* 2010) and fMLP (Palvinskaya *et al.* 2013).

Patient neutrophil counts were higher in patients compared with controls, a finding that has been reported in numerous studies (Fisch 1975; Nanji & Freeman 1985; Schwartz & Weiss 1991; Pratley *et al.* 1995; Nieman *et al.* 1999; Kullo *et al.* 2002; Dixon & O'Brien 2006; Herishanu *et al.* 2006; Zaldivar *et al.* 2006; Womack *et al.* 2007; Kim & Park 2008; Rensen *et al.* 2009; Al-Sufyani & Mahassni 2011; Ilavská *et al.* 2012). Weight loss is associated with a decrease in leukocyte and lymphocyte counts (Walford *et al.* 1992; Nieman *et al.* 1993); one study involving gastric band surgery reported a significant decrease in blood leukocyte counts, and in particular neutrophil counts, that correlated with BMI over a three year follow-up (Veronelli *et al.* 2004): the underlying cause was attributed to leptin, which is known to stimulate myeloid differentiation (Laharrague *et al.* 2000) and decreases after weight loss (Molina *et al.* 2003).

White blood cell counts are reported to be higher in other inflammatory disorders, such as in chronic periodontitis, in which patient numbers have been shown to be higher than in healthy gender- and age-matched controls (Al-Rasheed 2012) a characteristic that is thought to drive the inflammatory process. Furthermore, raised neutrophil counts and subsequently raised levels of MPO represent important markers of the inflammatory response and are considered predictors of cardiovascular events (Vincent & Taylor 2005). Recently it was shown in an obese mouse model that hyperlipidaemia induces neutrophilia and that neutrophils infiltrate arteries primarily during the early stages of atherosclerosis (Drechsler *et al.* 2010).

Patient NET release was significantly lower prior to weight loss compared with controls. Furthermore, during the course of the weight loss NET production increased in patients. These results are in contradiction with the literature, in which NET release is exaggerated in states of chronic inflammation, such as chronic airway disease (Wright *et al.* 2016) and vascular disorders (Kaplan & Radic 2012). A possible reason for the results reported here could be due to incubation time of the NETs assay, which was limited to two hours due to experimental time constraints. NETosis can occur via two mechanisms as previously described (section 1.6.3); suicidal NETosis occurs between 2-4 hours following stimulation and the majority of NETosis is thought to occur via this pathway rather than the shorter pathway of vital NETosis which can occur within 60 minutes (Branzk & Papayannopoulos 2013). However if this were the case a similar finding would be expected in control neutrophils. Greater patient numbers and further experimentation, such as the quantification of NET-bound proteins, needs to be performed to yield a more accurate interpretation of the effect of weight loss on NET release.

The ROS results detailed in this chapter demonstrate enhanced ROS release in patient neutrophils compared to controls pre-weight loss for all three chemiluminescent reagents used. This significance remained at both subsequent time points with total ROS release

(luminol), indicating that despite weight loss the neutrophils were still in a hyper-reactive state. Extracellular ROS release (isoluminol) and superoxide (lucigenin) were reduced compared to controls by T3, indicating a partial reduction in the hyper-active nature of neutrophils for ROS release. These results are in agreement with previous studies of neutrophil ROS production from obese individuals compared to lean controls (Brotfain *et al.* 2015) and the oxidative burst activity during phagocytosis (Nieman *et al.* 1999). Furthermore, ROS release has been reported to decrease in obese individuals after weight loss (Yaegaki *et al.* 2007). Neutrophil hyperactivity has also been demonstrated previously (Brotfain *et al.* 2015), however no statistical significance could be demonstrated in the results presented here which could be a result of small patient numbers and the effect of the time delay from blood collection to sample processing. Increased ROS production has been reported to occur within adipose tissue, leading to an elevation of systemic oxidative stress affecting other organs including the liver and aorta (Furukawa *et al.* 2004) via the effects of lipid peroxidation and direct oxidative injury (Higdon & Frei 2003; Fan & Watanabe 2003). Furthermore, high lipid and glucose levels can stimulate superoxide production via PKC-dependent activation of vascular NADPH oxidase in cultured endothelial cells (Sonta *et al.* 2004).

The redox state (GSH:GSSG ratio) of the neutrophil is known to be altered in chronic periodontitis, a chronic inflammatory condition in which systemic oxidative stress is a characteristic feature, resulting in the relocation of NADPH oxidase to the outer cell membrane (Dias *et al.* 2013a) and consequent increased extracellular superoxide release in order to ensure cell survival. The increased weight loss, which is associated with a reduction in oxidative stress, may partially restore the GSH balance, resulting in reduced superoxide release from the cell which may explain the change in extracellular superoxide release but not the overall change in total ROS release by the patient neutrophils. Patient-only

comparison of ROS release revealed no significant changes between the time points. This result may reflect the fact that many patients are still very obese and thus a systemic oxidative stress environment would be expected to remain.

Neutrophil chemotaxis revealed significant differences per time point and with patient-only analysis between the time points. There are limited studies focusing on the effects of obesity on neutrophil chemotaxis and the effects of weight loss. One study involving diet-induced obesity in mice identified defective chemotaxis following LPS-induced lung injury, a possible reason was suggested to be due to decreased surface receptor expression of the CXCR2 receptor which binds CXCL8 (Kordonowy *et al.* 2012), despite the fact that CXCL8 levels are known to be elevated in obese individuals (Trellakis *et al.* 2012). Despite this, a negative feedback loop exists between CXCL8 and CXCR1/2 receptors which could link the two independent observations (Hu *et al.* 2011). Studies of chemotactic activity from type 2 diabetes patients reported defective neutrophil functions including defective chemotaxis (Mowat & Baum 1971; Tan *et al.* 1975). Glucose can react with lipids and proteins non-enzymatically to produce advanced glycation end products (AGEs), if present at high enough levels as is expected in poorly controlled diabetes patients. The level of AGEs will increase and they have been reported to interfere with leukocyte function (Goldin *et al.* 2006). AGE presence within human neutrophils is linked to a rise in intracellular calcium and to actin polymerisation and subsequent impaired chemotaxis (Collison *et al.* 2002), suggesting that exposure to AGEs may be a possible reason for the reduced neutrophil chemotactic accuracy.

Pro-inflammatory cytokine detection from supernatants of cultured patient neutrophils revealed significantly higher levels compared to controls with several stimuli used. Significance was evident with IL-1β, IL-6, CXCL8 and TNFα at T1 in the presence of stimuli and (for TNFα only) in the absence of a stimulus. These results indicate a hyperactive and hyper-reactive neutrophil phenotype. The significance was diminished by T3 indicating a

reduction in pro-inflammatory cytokine release in patients compared to controls. No significance was measured in plasma, and only CXCL8 and TNFα could be detected. Due to time constraints and sample availability, only ten patient neutrophil supernatants were measured for cytokine levels. The pro-inflammatory cytokine results demonstrate a decrease with weight loss, however the effect is more subtle than expected which is thought to be due to the small sample size and the continued obese state of the patients.

Patient-only analysis revealed a reduction in IL-1β, IL-6 and TNFα over time with some of the stimuli, demonstrating that weight loss decreased pro-inflammatory cytokine release by patient neutrophils. These results are in agreement with reports within the literature regarding increased serum cytokine levels in obesity (Kopp *et al.* 2003; van Dielen *et al.* 2004; Tziomalos *et al.* 2010) reflecting a level of immune system activation. Systemic TNFα levels have been shown to correlate with increasing BMI (Kern *et al.* 1995). TNFα has been shown to act directly upon adipocytes and dysregulated levels have been suggested to interfere with glycaemic homeostasis and promote greater insulin resistance (Hotamisligil *et al.* 1993; Fantuzzi 2005; Cawthorn & Sethi 2008) as well as promoting endothelial dysfunction by inducing NF-κB signalling, NADPH activation and ROS production (Darvall *et al.* 2007; Gao *et al.* 2007). Circulating pro-inflammatory cytokines have been shown to prime neutrophils (Harkin *et al.* 2001; Koenderman *et al.* 2000) which would in turn account for their enhanced production when neutrophils are stimulated. Other disorders of inflammation have also reported enhanced neutrophil ROS release (Mittal *et al.*2014) in addition to enhanced pro-inflammatory cytokine production (Chollet-Martin *et al.* 1992; Nikolaus *et al.* 1998; Bordon *et al.* 2013).

It is important to note that some of the actions of pro-inflammatory cytokines on metabolism and immune responses can be paradoxical, for example, IL-6 has been shown to be abundant in obesity (Perreault *et al.* 2014) and may correlate with insulin resistance (Pradhan *et al.*

2001; Ueki *et al.* 2004) , yet studies on mice with IL-6 deficiencies have revealed that mice exhibit enhanced sensitivity to the metabolic effects of a high fat diet (Mauer *et al.* 2014). As IL-6 is generated as part of the inflammatory process involved in stimulating angiogenesis and the release of acute phase proteins (Blanchard *et al.* 2009), which generally opposes the action of insulin, IL-6 may act as a feedback regulator, attenuating catabolic and inflammatory signalling to preserve the actions of insulin. Thus IL-6 might provide an overall beneficial effect.

There are a number of limitations and confounding factors that may have contributed to the data reported in this chapter. Firstly, the small overall sample size and the need for more pronounced weight loss for greater significance in reported data. A study by Zamarron *et al.* (2015) reported continued inflammatory activation of leukocytes within adipose tissue of obese mice despite weight loss, supporting the variation in health in response to weight loss interventions. In addition, other factors such as medications, dietary and exercise habits, which may reduce weight, may not contribute to improved health and therefore immune function.

Secondly, the presence of other obesity-linked disorders, for example, several of the patients suffered from obstructive sleep apnoea (OSA), a disorder characterised by repetitive pauses of breathing caused by partial or complete collapses of upper airways during sleep (Rubinstein 1995; Salerno *et al.* 2004). OSA is associated with hypertension, strokes and coronary artery disease in addition to obesity (Shahar *et al.* 2001; Shah *et al.* 2010; Redline *et al.* 2010; Loke *et al.* 2012). The pauses in breathing are followed by a decrease in oxygen saturation leading to hypoxia which can serve as a stimulus for various peripheral blood cells, including monocytes and neutrophils (Dyugovskaya *et al.* 2002; Dyugovskaya *et al.* 2003), leading to increased burst of ROS (McCord 1985; Pilkauskaite *et al.* 2013) and endothelial dysfunction (Naruko *et al.* 2002). Furthermore, levels of TNFα and IL-6 have

been reported to be elevated in OSA (Entzian *et al.* 1996; Vgontzas *et al.* 1997) and neutrophils have been demonstrated to be a source of pro-inflammatory cytokines in OSA (Dyugovskaya *et al.* 2008). Due to limited patient background information, it was not possible to know of improvements in the OSA status of the patients or if the extent of weight loss had impacted on their condition.

Thirdly, the presence of additional inflammatory-linked disorders in the patients may confound results; a notable example is the periodontal status of the patients, which was not known in this study. Despite the strong association between obesity and periodontal disease (Dalla Vecchia *et al.* 2005; Boesing *et al.* 2009; Nilsson *et al.* 2012; Dahiya *et al.* 2012; Huttunen & Syrjänen 2013; Taylor *et al.* 2013; Suvan *et al.* 2014;) with obese females (who made up the majority of patients in this study) are reported more likely to suffer periodontal disease than obese males (Haffajee & Socransky 2009), knowledge of the periodontal status among obese individuals is limited due to patient non-compliance and the need for specialist equipment (Reilly *et al.* 2009). It would be expected that weight loss would result in improved periodontal status due to improvements in systemic inflammatory status, i.e. a reduction in the prevalence of diseases such as diabetes, a decrease in the release of pro-inflammatory cytokines as a result in a decrease in adipose tissue and a change in behavioural patterns in turn generating a healthier lifestyle (Wadden *et al.* 2001; Khader *et al.* 2009). Despite the lack of information for this chapter, periodontal status during the course of gastric band surgery in obese patients has been recently reported by Sales-Peres *et al.* (2015). Twelve months post-gastric band surgery they found no improvements in periodontal conditions despite weight reduction. One reason for this may have been related to the feeding habit changes of patients; eating more times per day in reduced quantities, thus the oral condition remained favourable to microbial biofilm support (Hague & Baechle 2008). Interestingly a recent study reported the beneficial effect of non-surgical periodontal

treatment in obese individuals; the results demonstrated GSH levels were significantly lower in obese individuals with periodontal disease than in normal weight individuals and the levels significantly increased after therapy for both periodontitis groups (Öngöz Dede *et al.* 2016). Thus improvements in disorders related to obesity but not due to weight loss may also act as potential confounders.

Interest has grown in recent years in the far-reaching effects of obesity on immune function. Recently categorised as a low-grade chronic inflammatory disorder, the effects of obesity on human health have generated new avenues to measure the effects of excess adiposity on neutrophil function. The opportunity to measure other neutrophil proteins, such as MPO and calprotectin, which are primarily secreted by neutrophils (Stríz & Trebichavský 2004; Nicholls & Hazen 2005) could provide more robust evidence for the contribution of neutrophils to the chronic inflammatory state. This, alongside more detailed background information, in particular periodontal status, for conditions in which neutrophils are the dominant cell could help develop our understanding of the underlying relationship between the two disorders. Other adipokines/cytokines could also be measured, such as IL-17α, which is increased in obesity and is released by neutrophils and adipose tissue, implicating innate immunity and adipocytes in a network which during the chronic low-grade inflammatory state of obesity may also affect acute inflammation (Pini & Fantuzzi 2010). Furthermore, IL-17α can induce other immune cells to secrete chemokines (such as CXCL8 and CXCL6) and other cytokines (IL-6 and GM-CSF) leading to an accumulation of neutrophils at inflammatory sites (Kolls & Lindén 2004).

6.11. Chapter 6 summary

This study has measured a range of neutrophil behaviours in obesity prior to and following weight loss. This data reported in this chapter supports the idea that circulating neutrophils

are involved in obesity-related inflammation. Neutrophils from obese patients exhibit excessive neutrophil activity characterised by higher ROS generation and release of cytokines, which appear to enhance the extent of local and systemic inflammation. This would be expected to affect the surrounding tissues including the blood vessels that may increase the risks of contracting associated cardiovascular disorders. Weight loss reduction was associated with improved outcomes characterised by lower ROS production and cytokine release relative to healthy controls, thus weight loss intervention resulting in a reduction in body weight associates with a decrease in pro-inflammatory activities. The absence of significant changes in patient neutrophil function over the course of the three time points could reflect experimental time constraints and challenges associated with coordinating optimal patient sample collection times.

CHAPTER 7 - CONCLUDING REMARKS

7.1. Summary of main findings

The aim of this thesis was to explore novel aspects of neutrophil function in chronic inflammatory conditions with particular emphasis on the development and use of an assay of chemotactic accuracy in concert with other assays developed by members of the research group. Specific aims were:

1. To optimise a method for the study of neutrophil chemotactic accuracy *ex vivo*
2. To assess neutrophil function in acute and chronic oral disease states
3. To assess neutrophil function in obese patients pre- and post-bariatric surgery

To study neutrophil function, neutrophils were isolated from the peripheral blood of volunteers using discontinuous Percoll gradients. The development and optimisation of an efficient re-usable chemotaxis assay (Chapter 3) enabled its employment in further studies of neutrophil function using clinical samples. As neutrophils are relatively short-lived fast-moving cells, the need for an assay that does not require lengthy cell preparation and is simple to perform were essential pre-requisites to enable measurements of neutrophil-directed movement with several different agents in a limited time period. The Insall chamber, whilst originally developed for longer-term measurements of cell movement, has been previously shown to work with neutrophils. The assay was further optimised in this thesis to decipher the optimal cell numbers to track, time course of study and chemoattractant concentrations. This work has enabled the assay to be used by others studying neutrophil movement.

Neutrophil ROS and NETs were measured in experimental 21-day gingivitis model (Chapter 4) to identify any differences before and after inducing inflammation using an acute human

model. Gingivitis precedes chronic periodontitis, however the underlying mechanisms that lead to disease progression are not fully understood; moreover not all sufferers of gingivitis will progress to periodontitis. Identifying variations in neutrophil functionality, even during a localised inflammatory event, may aid in the understanding of their role in disease progression. Neutrophils are the dominant immune cell within the periodontal tissues and excessive ROS and NET production are thought to be a major driver of periodontal tissue damage and may aid in the acquisition of nutrients by pathogenic bacterial species colonising the oral tissues. The results presented in this thesis demonstrated that at the height of acute inflammation ROS and NETs were significantly increased and that inflammation resolution reversed the excessive release of both.

Neutrophil chemotaxis was measured in a 21-day experimental gingivitis model, and for the first time, in patients with chronic periodontitis pre- and post-periodontal treatment (Chapter 4) to explore any differences between an acute inflammatory condition (experimental gingivitis) and chronic periodontal inflammation (periodontitis) on peripheral blood neutrophil behaviour. GCF collected from gingivitis volunteers and periodontitis patients was assayed for cytokine release and for its chemoattractants properties when exposed to healthy volunteer neutrophils. At the height of gingival inflammation, chemotaxis was significantly different at the height of inflammation compared with baseline. For the chronic periodontitis patients significance was evident compared to healthy-matched controls and remained following non-surgical therapy, further supporting the dysfunctional behaviour of neutrophils in chronic periodontitis that has previously been reported, notably with regard to excessive ROS generation. Not surprisingly, GCF from diseased/inflamed sites in gingivitis and chronic periodontitis significantly induced neutrophil chemotaxis, and consistent with this

was the finding of increased levels of TNFα and IL-1β detected in the GCF of inflamed experimental gingivitis and periodontitis sites.

Neutrophil function in PLS, a syndrome characterised by a severe pre-pubertal form of periodontitis, was investigated (Chapter 5). The expectation of attenuated NET production, which has been previously reported (Sorenson *et al.* 2014), was confirmed relative to healthy controls. Furthermore, specific NET analyses revealed a lack of the NET-bound NSPs NE and CG. ROS release was higher in PLS patients relative to controls which is consistent with other forms of periodontal disease. The levels of cytokines and pro-inflammatory protein production was also significantly higher in PLS patient neutrophils and in plasma, reflecting elevated local and systemic inflammation. The reduced chemotactic capabilities of PLS patients was also consistent with data from chronic periodontitis patients and points to a scenario involving increased neutrophil tissue transit times and continued neutrophil recruitment as a consequence of failed NSP activities, which are evidently intricately involved in orchestrating immune responses rather than fulfilling solely antimicrobial functions.

The effects of the low-grade chronic inflammation, which is characteristic of obese individuals was also investigated (Chapter 6). Obesity is one of the greatest global health challenges of the 21st century and interest in the link between excess adiposity and immune dysfunction has grown in recent years. The endocrine-like functions of adipose tissue and the immune cell composition of the tissue itself have attracted interest in investigating the effects of obesity upon immune cells. As neutrophils are key players of the innate and acquired immune systems, and typically reside in blood in the absence of infection, they have been postulated to be influenced by increased circulating levels of cytokines released (some

exclusively) by cells from within adipose tissue, which may prime neutrophils for a more robust/exaggerated behaviour during infection. This could explain the underlying cause for obesity as the second strongest risk factor for periodontitis as well as increased risk of obese individuals to other infectious disorders, such as pneumonia. Furthermore, obesity is linked to non-infectious diseases such as diabetes and rheumatoid arthritis making it a very complex disorder for which to accurately draw conclusions. Neutrophil function in obese individuals was measured alongside healthy controls prior to and following weight loss. The degree of weight loss was anticipated to be 10-15% by the post-surgical appointment, and some patients achieved beyond this, but several did not. As outlined, the loss of body weight does not directly correlate with a reduction in adipose tissue, however the reduction was accompanied with indicators of improved health: reduced HbA1c levels; raised HDL; and lower LDL and TG relative to healthy controls. Patient neutrophils displayed excessive ROS release, which is in accordance with other chronic inflammatory disease states, and this remained throughout the three time points in which blood was taken. Neutrophil chemotaxis was abnormal, again reflective of the systemic chronic inflammatory state, which is shared by other conditions including chronic periodontitis. Significant reductions in the chemotaxis measurements remained despite weight loss, however as stated, many of the patients remained severely obese, thus the chronic inflammatory state would be expected to reflect continued obese status. The pro-inflammatory cytokines measured were significantly higher relative to controls and significant differences become non-significant following weight loss.

7.2. Overall conclusion and recommendations for future research

The results outlined in this thesis point to various forms of dysregulated neutrophil function in chronic inflammatory disease states, which improve following appropriate treatment (periodontal treatment or weight loss). By understanding the potential contributions of

neutrophils to the progression of inflammation and in turn the extent of the effect of systemic inflammation on peripheral blood neutrophil behaviour, more effective strategies may be developed to prevent disease progression and identify effective therapies to reduce associated co-morbidities.

REFERENCES

Abadie, V. *et al*., (2005). Neutrophils rapidly migrate via lymphatics after Mycobacterium bovis BCG intradermal vaccination and shuttle live bacilli to the draining lymph nodes. *Blood*, 106(5), pp.1843–50.

Abram, C.L. & Lowell, C.A., (2009). Leukocyte adhesion deficiency syndrome: a controversy solved. *Immunology and Cell Biology*, 87(6), pp.440–2.

Adkison, A.M. *et al.*, (2002). Dipeptidyl peptidase I activates neutrophil-derived serine proteases and regulates the development of acute experimental arthritis. *Journal of Clinical Investigation*, 109(3), pp.363–71.

Adonogianaki, E. *et al*., (1994). Acute-phase proteins in gingival crevicular fluid during experimentally induced gingivitis. *Journal of Periodontal Research*, 29(3), pp.196–202.

Aguirre, V. *et al*., (2002). Phosphorylation of Ser307 in insulin receptor substrate-1 blocks interactions with the insulin receptor and inhibits insulin action. *Journal of Biological Chemistry*, 277(2), pp.1531–1537.

Albuali, W.H., (2014). Evaluation of oxidant-antioxidant status in overweight and morbidly obese Saudi children. *World Journal of Clinical Pediatrics*, 3(1), pp.6–13.

Al-Rasheed, A., (2012). Elevation of white blood cells and platelet counts in patients having chronic periodontitis. *The Saudi Dental Journal*, 24(1), pp.17–21.

Al-Sufyani, A.A. & Mahassni, S.H., (2011). Obesity and immune cells in Saudi females. *Innate immunity*, 17(5), pp.439–50.

Amar, S. *et al*., (2007). Diet-induced obesity in mice causes changes in immune responses and bone loss manifested by bacterial challenge. *Proceedings of the National Academy of Sciences of the United States of America*, 104(51), pp.20466–71.

Amar, S. & Leeman, S., (2013). Periodontal innate immune mechanisms relevant to obesity. *Molecular Oral Microbiology*, 28(5), pp.331–41.

Ames, B.N., Shigenaga, M.K. & Hagen, T.M., (1993). Oxidants, antioxidants, and the degenerative diseases of aging. *Proceedings of the National Academy of Sciences of the United States of America*, 90(17), pp.7915–22.

Ando, K. & Fujita, T., (2009). Metabolic syndrome and oxidative stress. *Free Radical Biology & Medicine*, 47(3), pp.213–8.

Andrew, N. & Insall, R.H., (2007). Chemotaxis in shallow gradients is mediated independently of PtdIns 3-kinase by biased choices between random protrusions. *Nature Cell Biology*, 9(2), pp.193–200.

Armstrong, L. *et al.*, (2009). Tumour necrosis factor-alpha processing in interstitial lung disease: a potential role for exogenous proteinase-3. *Clinical and Experimental Immunology*, 156(2), pp.336–43.

Asman, B. *et al.*, (1986). Influence of plasma components on luminol-enhanced chemiluminescence from peripheral granulocytes in juvenile periodontitis. *Journal of Clinical Periodontology*, 13(9), pp.850–5.

Austin, M.A., Hokanson, J.E. & Edwards, K.L., (1998). Hypertriglyceridemia as a Cardiovascular Risk Factor. *American Journal of Cardiology*, 81(4), p.7B–12B.

Azuma, T. *et al.*, (2011). Effects of exercise training on gingival oxidative stress in obese rats. *Archives of Oral Biology*, 56(8), pp.768–74.

Bagorda, A. & Parent, C.A., (2008). Eukaryotic chemotaxis at a glance. *Journal of Cell Science*, 121(Pt 16), pp.2621–4.

Balsiger, B.M. *et al.*, (2000). Bariatric surgery. Surgery for weight control in patients with morbid obesity. *Medical Clinics of North America*, 84(2), pp.477–89.

Bandholtz, L. *et al.*, (2006). Antimicrobial peptide LL-37 internalized by immature human dendritic cells alters their phenotype. *Scandinavian Journal of Immunology*, 63(6), pp.410–9.

Bangalore, N. *et al.*, (1990). Identification of the primary antimicrobial domains in human neutrophil cathepsin G. *Journal of Biological Chemistry*, 265(23), pp.13584–8.

Bank, U., Küpper, B. & Ansorge, S., (2000). Inactivation of interleukin-6 by neutrophil proteases at sites of inflammation. Protective effects of soluble IL-6 receptor chains. *Advances in Experimental Medicine and Biology*, 477, pp.431–7.

Baser, U. *et al.*, (2014). Is the severity of periodontitis related to gingival crevicular fluid and serum high-sensitivity C-reactive protein concentrations? *Clinical Laboratory*, 60(10), pp.1653–8.

Baser, U. *et al.*, (2015). Plasma and salivary total antioxidant capacity in healthy controls compared with aggressive and chronic periodontitis patients. Saudi Medical Journal, 36(7), pp.856–61.

Bastard, J.-P. *et al.*, (2006). Recent advances in the relationship between obesity, inflammation, and insulin resistance. *European Cytokine Network*, 17(1), pp.4–12.

Basu, S. *et al.*, (2009). Regulatory factors of basal F(2)-isoprostane formation: population, age, gender and smoking habits in humans. *Free Radical Research*, 43(1), pp.85–91.
Battino, M. *et al.*, (2001). Elevated hydroperoxide levels and antioxidant patterns in Papillon-Lefèvre syndrome. *Journal of Periodontology*, 72(12), pp.1760–6.

Battino, M. *et al.*, (1999). Oxidative injury and inflammatory periodontal diseases: the challenge of anti-oxidants to free radicals and reactive oxygen species. *Critical Reviews in Oral Biology & Medicine*, 10(4), pp.458–476.

Beauvillain, C. *et al.*, (2011). CCR7 is involved in the migration of neutrophils to lymph nodes. *Blood*, 117(4), pp.1196–204.

Belaaouaj, A., Kim, K.S. & Shapiro, S.D., (2000). Degradation of outer membrane protein A in *Escherichia coli* killing by neutrophil elastase. *Science* (New York, N.Y.), 289(5482), pp.1185–8.

Bencze, G., (1970). Relationship of systemic lupus erythematosus (SLE) to rheumatoid arthritis (RA), discoid lupus erythematosus (DLE) and Sjögren's syndrome. A clinical study. *Acta rheumatologica Scandinavica*, 16(3), pp.191–6.

Benelli, R. *et al.*, (2002). Neutrophils as a key cellular target for angiostatin: implications for regulation of angiogenesis and inflammation. *Federation of American Societies for Experimental Biology*, 16(2), pp.267–9.

Bennion, L.J. & Grundy, S.M., (1975). Effects of obesity and caloric intake on biliary lipid metabolism in man. *The Journal of Clinical Investigation*, 56(4), pp.996–1011.

Van den Berg, J.M. *et al*., (2009). Chronic granulomatous disease: the European experience. *PloS one*, 4(4), p.e5234.

Bergstrom, J. & Preber, H., (1986). The influence of cigarette smoking on the development of experimental gingivitis. *Journal of Periodontal Research*, 21(6), pp.668–676.

Berridge, M.J., Bootman, M.D. & Roderick, H.L., (2003). Calcium signalling: dynamics, homeostasis and remodelling. Nature reviews. *Molecular Cell Biology*, 4(7), pp.517–29.

Bhadbhade, S.J., Acharya, A.B. & Thakur, S., (2012). Correlation between probing pocket depth and neutrophil counts in dental plaque, saliva, and gingival crevicular fluid. *Quintessence International* (Berlin, Germany : 1985), 43(2), pp.111–7.

Bhatti, M.S., Akbri, M.Z. & Shakoor, M., (2001). Lipid profile in obesity. *Journal of Ayub Medical College*, 13(1), pp.31–3.

Bianchi, M. *et al.*, (2011). Restoration of anti-Aspergillus defense by neutrophil extracellular traps in human chronic granulomatous disease after gene therapy is calprotectin-dependent. *The Journal of Allergy and Clinical Immunology*, 127(5), pp.1243–52.e7.

Bianchi, M. *et al.*, (2009). Restoration of NET formation by gene therapy in CGD controls aspergillosis. *Blood*, 114(13), pp.2619–22.

Bianchi, M.E., (2007). DAMPs, PAMPs and alarmins: all we need to know about danger. *Journal of Leukocyte Biology*, 81(1), pp.1–5.

Biemond, P. *et al.*, (1986). Superoxide production by polymorphonuclear leucocytes in rheumatoid arthritis and osteoarthritis: in vivo inhibition by the antirheumatic drug piroxicam due to interference with the activation of the NADPH-oxidase. *Annals of the Rheumatic Diseases*, 45(3), pp.249–55.

Bienert, G.P. & Chaumont, F., (2014). Aquaporin-facilitated transmembrane diffusion of hydrogen peroxide. *Biochimica et Biophysica Acta*, 1840(5), pp.1596–604.

Biju, T. et al., (2014). Comparative evaluation of serum superoxide dismutase and glutathione levels in periodontally diseased patients: an interventional study. Indian Journal of Dental Research, 25(5), pp.613–6.

Bjorntorp, P., (1991). Metabolic Implications of Body Fat Distribution. *Diabetes Care*, 14(12), pp.1132–1143.

Blanchard, F. *et al.*, (2009). The dual role of IL-6-type cytokines on bone remodeling and bone tumors. *Cytokine & Growth Factor Reviews*, 20(1), pp.19–28.

Blüher, M. & Mantzoros, C.S., (2015). From leptin to other adipokines in health and disease: facts and expectations at the beginning of the 21st century. *Metabolism: Clinical and Experimental*, 64(1), pp.131–45.

Boesing, F. *et al*., (2009). The interface between obesity and periodontitis with emphasis on oxidative stress and inflammatory response. *Obesity Reviews*, 10(3), pp.290–7.

Bolstad, A.I., Jensen, H.B. & Bakken, V., (1996). Taxonomy, biology, and periodontal aspects of *Fusobacterium nucleatum*. *Clinical Microbiology Reviews*, 9(1), pp.55–71.

Bonecchi, R. *et al.*, (2009). Chemokines and chemokine receptors: an overview. *Frontiers in Bioscience*, 14, p.540.

Bordon, J. *et al.*, (2013). Understanding the roles of cytokines and neutrophil activity and neutrophil apoptosis in the protective versus deleterious inflammatory response in pneumonia. *International Journal of Infectious Diseases*, 17(2), pp.e76–e83.

Borish, L.C. & Steinke, J.W., (2003). 2. Cytokines and chemokines. *Journal of Allergy and Clinical Immunology*, 111(2), pp.S460–S475.

Boronat-Catalá, M., Catalá-Pizarro, M. & Bagán Sebastián, J. V, (2014). Salivary and crevicular fluid interleukins in gingivitis. *Journal of Clinical and Experimental Dentistry*, 6(2), pp.e175–9.

Borregaard, N., (2010). Neutrophils, from marrow to microbes. *Immunity*, 33(5), pp.657–70.

Borregaard, N. & Cowland, J.B., (1997). Granules of the human neutrophilic polymorphonuclear leukocyte. *Blood*, 89(10), pp.3503–21.

Bostan, M. *et al.*, (2002). Study of chemotactic activity developed by neutrophils from rheumatoid arthritis patients. *Roumanian Archives of Microbiology and Immunology*, 61(4), pp.243–58.

Bostanci, N. *et al.*, (2010). Application of label-free absolute quantitative proteomics in human gingival crevicular fluid by LC/MS E (gingival exudatome). Journal of Proteome Research, 9(5), pp.2191–9.

Boudaly, S., (2009). Activation of dendritic cells by polymorphonuclear neutrophils. *Frontiers in Bioscience*, Volume(14), p.1589.

Boyden, S., (1962). The chemotactic effect of mixtures of antibody and antigen on polymorphonuclear leucocytes. *The Journal of Experimental Medicine*, 115, pp.453–66.

Bozza, F.A. *et al.*, (2007). Cytokine profiles as markers of disease severity in sepsis: a multiplex analysis. *Critical Care* (London, England), 11(2), p.R49.

Bradley, J.R., (2007). TNF-mediated inflammatory disease. *The Journal of Pathology*, 214(2), pp.149–160.

Brahmbhatt, A.A. & Klemke, R.L., (2003). ERK and RhoA differentially regulate pseudopodia growth and retraction during chemotaxis. *The Journal of Biological Chemistry*, 278(15), pp.13016–25.

Brandes, S. *et al.*, (2015). Automated segmentation and tracking of non-rigid objects in time-lapse microscopy videos of polymorphonuclear neutrophils. *Medical Image Analysis*, 20(1), pp.34–51.

Branzk, N. & Papayannopoulos, V., (2013). Molecular mechanisms regulating NETosis in infection and disease. *Seminars in Immunopathology*, 35(4), pp.513–30.

Bratton, D.L. & Henson, P.M., (2011). Neutrophil clearance: when the party is over, clean-up begins. *Trends in Immunology*, 32(8), pp.350–7.

Bray, G.A., (2004). Medical Consequences of Obesity. *The Journal of Clinical Endocrinology & Metabolism*, 89(6), pp.2583–2589.

Brill, N., (1962). The gingival pocket fluid : Studies of its occurrence, composition, and effect., *Cph*.

Brinkmann, V. *et al*., (2004). Neutrophil extracellular traps kill bacteria. *Science* (New York, N.Y.), 303(5663), pp.1532–5.

Brotfain, E. *et al.*, (2015). Neutrophil functions in morbidly obese subjects. *Clinical and Experimental Immunology*, 181(1), pp.156–63.

Brown, A.F., (1982). Neutrophil granulocytes: adhesion and locomotion on collagen substrata and in collagen matrices. *Journal of Cell Science*, 58, pp.455–67.

Brownlee, M., (2001). Biochemistry and molecular cell biology of diabetic complications. *Nature*, 414(6865), pp.813–820.

Von Brühl, M.-L. *et al.*, (2012). Monocytes, neutrophils, and platelets cooperate to initiate and propagate venous thrombosis in mice in vivo. The Journal of Experimental Medicine, 209(4), pp.819–35.

Bruhns, P., (2012). Properties of mouse and human IgG receptors and their contribution to disease models. *Blood*, 119(24), pp.5640–9.

Bruun, J.M. *et al.*, (2004). Higher production of IL-8 in visceral vs. subcutaneous adipose tissue. Implication of nonadipose cells in adipose tissue. *American Journal of Physiology. Endocrinology and Metabolism*, 286(1), pp.E8–13.

Bruun, J.M. *et al.*, (2003). Regulation of adiponectin by adipose tissue-derived cytokines: in vivo and in vitro investigations in humans. *American Journal of Physiology-Endocrinology and Metabolism*, 285(3), pp.E527–E533.

Büchau, A.S. *et al.*, (2010). The host defense peptide cathelicidin is required for NK cell-mediated suppression of tumor growth. *Journal of Immunology* (Baltimore, Md. : 1950), 184(1), pp.369–78.

Buckley, C.D. *et al.*, (2006). Identification of a phenotypically and functionally distinct population of long-lived neutrophils in a model of reverse endothelial migration. *Journal of Leukocyte Biology*, 79(2), pp.303–11.

Buduneli, N. & Kinane, D.F., (2011). Host-derived diagnostic markers related to soft tissue destruction and bone degradation in periodontitis. *Journal of Clinical Periodontology*, 38 Suppl 1, pp.85–105.

Bueno, N.B. *et al.*, (2013). Very-low-carbohydrate ketogenic diet v. low-fat diet for long-term weight loss: a meta-analysis of randomised controlled trials. *British Journal of Nutrition*, 110(07), pp.1178–1187.

Burton, B.T. *et al.*, (19850. Health implications of obesity: an NIH Consensus Development Conference. *International Journal of Obesity*, 9(3), pp.155–70.

Buscher, K. *et al.*, (2010). The transmembrane domains of L-selectin and CD44 regulate receptor cell surface positioning and leukocyte adhesion under flow. *Journal of Biological Chemistry*, 285(18), pp.13490–13497.

Camps, M. *et al.*, (1992). Isozyme-selective stimulation of phospholipase C-beta 2 by G protein beta gamma-subunits. *Nature*, 360(6405), pp.684–6.

Cannistra, S.A. & Griffin, J.D., (1988). Regulation of the production and function of granulocytes and monocytes. *Seminars in Hematology*. p. 173.

Capurso, C. & Capurso, A., (2012). From excess adiposity to insulin resistance: the role of free fatty acids. *Vascular Pharmacology*, 57(2-4), pp.91–7.

Carlow, D.A. *et al.*, (2009). PSGL-1 function in immunity and steady state homeostasis. Immunological reviews, 230(1), pp.75–96.

Casanova, J.-L. & Abel, L., (2009). Revisiting Crohn's disease as a primary immunodeficiency of macrophages. *The Journal of Experimental Medicine*, 206(9), pp.1839–43.

Cassatella, M.A., (1999). Neutrophil-derived proteins: selling cytokines by the pound. *Advances in Immunology*, 73, pp.369–509.

Cawthorn, W.P. & Sethi, J.K., (2008). TNF-alpha and adipocyte biology. *FEBS letters*, 582(1), pp.117–31.

Cedergren, J. *et al.*, (2007). Intracellular oxidative activation in synovial fluid neutrophils from patients with rheumatoid arthritis but not from other arthritis patients. *The Journal of Rheumatology*, 34(11), pp.2162–70.

Chaffee, B.W. & Weston, S.J., (2010). Association Between Chronic Periodontal Disease and Obesity: A Systematic Review and Meta-Analysis. *Journal of Periodontology*, 81(12), pp.1708–1724.

Chapple IL, Socransky SS, Dibart S, Glenwright HD, M.J., (1996). Chemiluminescent assay of alkaline phosphatase in human gingival crevicular fluid: investigations with an experimental gingivitis model and studies on the source of the enzyme within crevicular fluid. *Journal of Clinical Periodontology*, 23, pp.587–594.

Chapple, I.L. *et al.*, (1996). Chemiluminescent assay of alkaline phosphatase in human gingival crevicular fluid: investigations with an experimental gingivitis model and studies on the source of the enzyme within crevicular fluid. *Journal of Clinical Periodontology*, 23(6), pp.587–94.

Chapple, I.L., (1996). Role of free radicals and antioxidants in the pathogenesis of the inflammatory periodontal diseases. *Clinical Molecular Pathology*, 49(5), pp.M247–55.

Chapple, I.L.C., Garner, I., Saxby, M.S., Moscrop, H., Matthews, J.B. (1999) Prediction and diagnosis of attachment loss by enhanced chemiluminescent assay of crevicular fluid alkaline phosphatase levels. *Journal of Clinical Periodontology*, 26(3), pp.190-198.

Chapple, I.L.C. *et al.*, (2002). Glutathione in gingival crevicular fluid and its relation to local antioxidant capacity in periodontal health and disease. *Molecular Pathology* : MP, 55(6), pp.367–73.

Chapple, I.L.C. & Matthews, J.B., (2007). The role of reactive oxygen and antioxidant species in periodontal tissue destruction. *Periodontology 2000*, 43(1), pp.160–232.

Chapple, I.L.C., Milward, M.R. & Dietrich, T., (2007). The prevalence of inflammatory periodontitis is negatively associated with serum antioxidant concentrations. *The Journal of Nutrition*, 137(3), pp.657–64.

Charmoy, M. *et al.*, (2010). Neutrophil-derived CCL3 is essential for the rapid recruitment of dendritic cells to the site of Leishmania major inoculation in resistant mice. *PLoS Pathogens*, 6(2), p.e1000755.

Charrière, G. *et al.*, (2003). Preadipocyte Conversion to Macrophage: evidence of plasticity. *Journal of Biological Chemistry*, 278(11), pp.9850–9855.

Chaudhari, H.L. *et al.*, (2016). Association of Interleukin-17 polymorphism (-197G/A) in chronic and localized aggressive periodontitis. *Brazilian Oral Research*, 30(1).

Chawla, A., Nguyen, K.D. & Goh, Y.P.S., (2011). Macrophage-mediated inflammation in metabolic disease. *Nature Reviews. Immunology*, 11(11), pp.738–49.

Chen, K. *et al.*, (2012). Endocytosis of soluble immune complexes leads to their clearance by FcγRIIIB but induces neutrophil extracellular traps via FcγRIIA in vivo. *Blood*, 120(22), pp.4421–31.

Cheng, C.-H. *et al.*, (2010). Waist-to-hip ratio is a better anthropometric index than body mass index for predicting the risk of type 2 diabetes in Taiwanese population. *Nutrition Research* (New York, N.Y.), 30(9), pp.585–93.

Cheng, S.S. *et al.*, (2001). Granulocyte-Macrophage Colony Stimulating Factor Up-Regulates CCR1 in Human Neutrophils. *The Journal of Immunology*, 166(2), pp.1178–1184.

Choban, P.S. *et al.*, (1995). Increased incidence of nosocomial infections in obese surgical patients. *The American Surgeon*, 61(11), pp.1001–5.

Choi, C.-H. *et al.*, (2013). Phosphorylation of actin-related protein 2 (Arp2) is required for normal development and cAMP chemotaxis in Dictyostelium. *The Journal of Biological Chemistry*, 288(4), pp.2464–74.

Choi, S.J. *et al.*, (2000). Macrophage inflammatory protein 1-alpha is a potential osteoclast stimulatory factor in multiple myeloma. *Blood*, 96(2), pp.671–5.

Chollet-Martin, S. *et al.*, (1992). Subpopulation of hyperresponsive polymorphonuclear neutrophils in patients with adult respiratory distress syndrome. Role of cytokine production. *The American Review of Respiratory Disease*, 146(4), pp.990–6.

Chun, H.-Y. *et al.*, (2007). Cytokine IL-6 and IL-10 as biomarkers in systemic lupus erythematosus. *Journal of Clinical Immunology*, 27(5), pp.461–6.

Cicchetti, G., Allen, P.G. & Glogauer, M., (2002). Chemotactic Signaling Pathways in Neutrophils: From Receptor To Actin Assembly. *Critical Reviews in Oral Biology & Medicine*, 13(3), pp.220–228.

Cinti, S. *et al.*, (2005). Adipocyte death defines macrophage localization and function in adipose tissue of obese mice and humans. *Journal of Lipid Research*, 46(11), pp.2347–2355.

Claesson, R. *et al.*, (2002). Release and activation of matrix metalloproteinase 8 from human neutrophils triggered by the leukotoxin of Actinobacillus actinomycetemcomitans. *Journal of Periodontal Research* 37(5), pp.353–9.

Clapham, D.E., (2007). Calcium signaling. *Cell*, 131(6), pp.1047–58.

Clark, S.R. *et al.*, (2007). Platelet TLR4 activates neutrophil extracellular traps to ensnare bacteria in septic blood. *Nature Medicine*, 13(4), pp.463–9.

Clarke, R. *et al.*, (2009). Life expectancy in relation to cardiovascular risk factors: 38 year follow-up of 19,000 men in the Whitehall study. BMJ (Clinical research ed.), 339, p.b3513.

Cloutier, A. *et al.*, (2007). Differential involvement of NF-kappaB and MAP kinase pathways in the generation of inflammatory cytokines by human neutrophils. *Journal of Leukocyte Biology*, 81(2), pp.567–77.

Cloutier, A. *et al*., (2009). Inflammatory cytokine production by human neutrophils involves C/EBP transcription factors. Journal of Immunology (Baltimore, Md. : 1950), 182(1), pp.563–71.

Cochran, D.L., (2008). Inflammation and bone loss in periodontal disease. *Journal of Periodontology*, 79(8 Suppl), pp.1569–76.

Coeshott, C. *et al.*, (1999). Converting enzyme-independent release of tumor necrosis factor alpha and IL-1beta from a stimulated human monocytic cell line in the presence of activated neutrophils or purified proteinase 3. *Proceedings of the National Academy of Sciences of the United States of America*, 96(11), pp.6261–6.

Cohen, R.M. *et al.*, (2008). Red cell life span heterogeneity in hematologically normal people is sufficient to alter HbA1c. *Blood*, 112(10), pp.4284–91.

Colgan, S.P. *et al.*, (1993). Lipoxin A4 modulates transmigration of human neutrophils across intestinal epithelial monolayers. *The Journal of Clinical Investigation*, 92(1), pp.75–82.

Collison, K.S. *et al.*, (2002). RAGE-mediated neutrophil dysfunction is evoked by advanced glycation end products (AGEs). *Journal of Leukocyte Biology*, 71(3), pp.433–44.

Condliffe, A.M., Kitchen, E. & Chilvers, E.R., (1998). Neutrophil priming: pathophysiological consequences and underlying mechanisms. *Clinical Science*, 94(5), pp.461–472.

Cooper, P.R., Palmer, L.J. & Chapple, I.L.C., (2013). Neutrophil extracellular traps as a new paradigm in innate immunity: friend or foe? *Periodontology 2000*, 63(1), pp.165–97.

Cordelières, F.P. *et al.*, (2013). Automated cell tracking and analysis in phase-contrast videos (iTrack4U): development of Java software based on combined mean-shift processes. *PloS One*, 8(11), p.e81266.

Cotter, T.G., Spears, P. & Henson, P.M., (1981). A monoclonal antibody inhibiting human neutrophil chemotaxis and degranulation. *Journal of Immunology* (Baltimore, Md. : 1950), 127(4), pp.1355–60.

Curnutte, J.T., (1993). Chronic granulomatous disease: the solving of a clinical riddle at the molecular level. *Clinical Immunology and Immunopathology*, 67(3 Pt 2), pp.S2–15.

Cursiefen, C. *et al.*, (2004). VEGF-A stimulates lymphangiogenesis and hemangiogenesis in inflammatory neovascularization via macrophage recruitment. *The Journal of Clinical Investigation*, 113(7), pp.1040–50.

D'Aiuto, F. *et al.*, (2010). Oxidative stress, systemic inflammation, and severe periodontitis. Journal of dental research, 89(11), pp.1241–6.

Dahiya, P., Kamal, R. & Gupta, R., (2012). Obesity, periodontal and general health: Relationship and management. Indian journal of endocrinology and metabolism, 16(1), pp.88–93.

Dahlgren, C. & Karlsson, A., (1999). Respiratory burst in human neutrophils. *Journal of Immunological Methods*, 232(1-2), pp.3–14.

Dale, D.C. *et al.*, (2000). Mutations in the gene encoding neutrophil elastase in congenital and cyclic neutropenia. *Blood*, 96(7), pp.2317–22.

Dalla Vecchia, C.F. *et al.*, (2005). Overweight and obesity as risk indicators for periodontitis in adults. *Journal of Periodontology*, 76(10), pp.1721–8.

Dalli, J. *et al*., (2008). Annexin 1 mediates the rapid anti-inflammatory effects of neutrophil-derived microparticles. *Blood*, 112(6), pp.2512–9.

Daniel, M. *et al.*, (1993). Defective chemotaxis and calcium response in localized juvenile periodontitis neutrophils. *Journal of Periodontology*, 64(7), pp.617–21.

Darbousset, R. *et al.*, (2012). Tissue factor-positive neutrophils bind to injured endothelial wall and initiate thrombus formation. *Blood*, 120(10), pp.2133–43.

Darvall, K.A.L. *et al.*, (2007). Obesity and thrombosis. European Journal of Vascular and Endovascular Surgery. 33(2), pp.223–33.

Dattilo, A.M. & Kris-Etherton, P.M., (1992). Effects of weight reduction on blood lipids and lipoproteins: a meta-analysis. *The American Journal of Clinical Nutrition*, 56(2), pp.320–8.

Dean, R.T. *et al*., (1997). Biochemistry and pathology of radical-mediated protein oxidation. *The Biochemical Journal*, 324 (1), pp.1–18.

Dean, S.N., Bishop, B.M. & van Hoek, M.L., (2011). Susceptibility of Pseudomonas aeruginosa Biofilm to Alpha-Helical Peptides: D-enantiomer of LL-37. *Frontiers in Microbiology*, 2, p.128.

Debeir, O. *et al.*, (2008). Models of cancer cell migration and cellular imaging and analysis. , *Transworld Research Network*. pp.123–156.

DeFronzo, R.A. & Ferrannini, E., (1991). Insulin resistance. A multifaceted syndrome responsible for NIDDM, obesity, hypertension, dyslipidemia, and atherosclerotic cardiovascular disease. *Diabetes Care*, 14(3), pp.173–94.

Dengel, D.R. *et al.*, (1994). Effects of weight loss by diet alone or combined with aerobic exercise on body composition in older obese men. *Metabolism: Clinical and Experimental*, 43(7), pp.867–71.

Dewhirst, F.E. *et al.*, (2010). The human oral microbiome. *Journal of Bacteriology*, 192(19), pp.5002–17.

Dhanrajani, P.J., (2009). Papillon-Lefèvre syndrome: clinical presentation and a brief review. *Oral surgery, oral medicine, oral pathology, oral radiology, and endodontics*, 108(1), pp.e1–7.

Dias, I.H.K. *et al.,* (2011). Activation of the neutrophil respiratory burst by plasma from periodontitis patients is mediated by pro-inflammatory cytokines. *Journal of Clinical Periodontology*, 38(1), pp.1–7.

Dias, I.H.K. *et al.,* (2013). Sulforaphane restores cellular glutathione levels and reduces chronic periodontitis neutrophil hyperactivity in vitro. *PloS One*, 8(6), p.e66407.

Dickinson, B.C. & Chang, C.J., (2011). Chemistry and biology of reactive oxygen species in signaling or stress responses. *Nature Chemical Biology*, 7(8), pp.504–11.

Van Dielen, F.M.H. *et al.*, (2004). Macrophage inhibitory factor, plasminogen activator inhibitor-1, other acute phase proteins, and inflammatory mediators normalize as a result of weight loss in morbidly obese subjects treated with gastric restrictive surgery. *The Journal of Clinical Endocrinology and Metabolism*, 89(8), pp.4062–8.

Dietrich, T. *et al*., (2013). The epidemiological evidence behind the association between periodontitis and incident atherosclerotic cardiovascular disease. *Journal of Periodontology*, 84(4 Suppl), pp.S70–84.

Dinarello, C.A., (2009). Immunological and inflammatory functions of the interleukin-1 family. *Annual Review of Immunology*, 27, pp.519–50.

Dixon, J.B. & O'Brien, P.E., (2006). Obesity and the white blood cell count: changes with sustained weight loss. *Obesity Surgery*, 16(3), pp.251–7.

Djawari, D., (1978). Deficient Phagocytic Function in Papillon-Lefèvre Syndrome. *Dermatology*, 156(3), pp.189–192.

Dobrovolskaia, M.A. *et al.*, (2003). Induction of in vitro reprogramming by Toll-like receptor (TLR)2 and TLR4 agonists in murine macrophages: effects of TLR "homotolerance" versus "heterotolerance" on NF-kappa B signaling pathway components. *Journal of Immunology* 170(1), pp.508–19.

Dong, C., Skalak, R. & Sung, K.L., (1991). Cytoplasmic rheology of passive neutrophils. *Biorheology*, 28(6), pp.557–67.

Drechsler, M. *et al.,* (2010). Hyperlipidemia-triggered neutrophilia promotes early atherosclerosis. *Circulation,* 122(18), pp.1837–45.

Dröge, W., (2002). Free radicals in the physiological control of cell function. *Physiological Reviews*, 82(1), pp.47–95.

Van Dyke, T.E. *et al.,* (1987). Association of an abnormality of neutrophil chemotaxis in human periodontal disease with a cell surface protein. *Infection and Immunity*, 55(9), pp.2262–7.

Van Dyke, T.E. *et al.*, (1986). Neutrophil function in localized juvenile periodontitis. Phagocytosis, superoxide production and specific granule release. *Journal of Periodontology*, 57(11), pp.703–8.

Van Dyke, T.E. *et al.*, (1981). Reduced chemotactic peptide binding in juvenile periodontitis: A model for neutrophil function. *Biochemical and Biophysical Research Communications*, 100(3), pp.1278–1284.

Dyugovskaya, L. *et al.*, (2008). Delayed neutrophil apoptosis in patients with sleep apnea. *American Journal of Respiratory and Critical Care Medicine*, 177(5), pp.544–54.

Dyugovskaya, L., Lavie, P. & Lavie, L., (2002). Increased adhesion molecules expression and production of reactive oxygen species in leukocytes of sleep apnea patients. *American Journal of Respiratory and Critical Care Medicine*, 165(7), pp.934–9.

Dyugovskaya, L., Lavie, P. & Lavie, L., (2003). Phenotypic and functional characterization of blood gammadelta T cells in sleep apnea. *American Journal of Respiratory and Critical Care Medicine*,168(2), pp.242–9.

Eash, K.J. *et al.*, (2009). CXCR4 is a key regulator of neutrophil release from the bone marrow under basal and stress granulopoiesis conditions. *Blood*, 113(19), pp.4711–9.

Eckel, R.H., Grundy, S.M. & Zimmet, P.Z., (2005). The metabolic syndrome. *Lancet*, 365(9468), pp.1415–28.

Eder, K. *et al.*, (2009). The major inflammatory mediator interleukin-6 and obesity. *Inflammation Research*, 58(11), pp.727–736.

Edgeworth, J. *et al.*, (1991). Identification of p8,14 as a highly abundant heterodimeric calcium binding protein complex of myeloid cells. *The Journal of Biological Chemistry*, 266(12), pp.7706–13.

Edwards, S.W., (2005). Biochemistry and Physiology of the Neutrophil, *Cambridge University Press*.

Ehrlich, P., (1880). Methodologische beiträge zur physiologie und pathologie der verschiedenen formen der leukocyten. *Zeitschrift Klinische Medizinische*.

Eick, S. *et al.*, 2014. Lack of cathelicidin processing in Papillon-Lefèvre syndrome patients reveals essential role of LL-37 in periodontal homeostasis. *Orphanet Journal of Rare Diseases*, 9(1), p.148.

Ekman, A.-K. & Cardell, L.O., (2010). The expression and function of Nod-like receptors in neutrophils. *Immunology*, 130(1), pp.55–63.

Ekuni, D. *et al.*, (2008). Relationship between body mass index and periodontitis in young Japanese adults. *Journal of Periodontal Research*, 43(4), pp.417–421.

El-Benna, J., Dang, P.M.-C. & Gougerot-Pocidalo, M.-A., (2008). Priming of the neutrophil NADPH oxidase activation: role of p47phox phosphorylation and NOX2 mobilization to the plasma membrane. *Seminars in Immunopathology*, 30(3), pp.279–89.

Elgazar-Carmon, V. *et al.*, (2008). Neutrophils transiently infiltrate intra-abdominal fat early in the course of high-fat feeding. *Journal of Lipid Research*, 49(9), pp.1894–903.

Entzian, P. *et al.*, (1996). Obstructive sleep apnea syndrome and circadian rhythms of hormones and cytokines. *American Journal of Respiratory and Critical Care Medicine*, 153(3), pp.1080–6.

Erridge, C., Bennett-Guerrero, E. & Poxton, I.R., (2002). Structure and function of lipopolysaccharides. *Microbes and Infection*, 4(8), pp.837–851.

Esche, C., Stellato, C. & Beck, L.A., (2005). Chemokines: key players in innate and adaptive immunity. *The Journal of Investigative Dermatology*, 125(4), pp.615–28.

Esposito, K. *et al.*, (2003). Cytokine milieu tends toward inflammation in type 2 diabetes. *Diabetes Care*, 26(5), p.1647.

Evans, T.J. *et al.*, (1996). Cytokine-treated human neutrophils contain inducible nitric oxide synthase that produces nitration of ingested bacteria. *Proceedings of the National Academy of Sciences*, 93(18), pp.9553–8.

Falagas, M.E. *et al.*, (2009). Effect of body mass index on the outcome of infections: a systematic review. *Obesity Reviews*, 10(3), pp.280–9.

Falagas, M.E. & Kompoti, M., (2006). Obesity and infection. *The Lancet. Infectious diseases*, 6(7), pp.438–46.

Fan, J. & Watanabe, T., (2003). Inflammatory reactions in the pathogenesis of atherosclerosis. Journal of Atherosclerosis and Thrombosis, 10(2), pp.63–71.

Fantuzzi, G., (2005). Adipose tissue, adipokines, and inflammation. *The Journal of Allergy and Clinical Immunology*, 115(5), pp.911–9; quiz 920.

Faria, S.L. *et al.*, (2014). Diet-induced thermogenesis and respiratory quotient after Roux-en-Y gastric bypass surgery: a prospective study. *Surgery for Obesity and Related Diseases*, 10(1), pp.138–43.

Farooqi, S. & O'Rahilly, S., (2006). Genetics of obesity in humans. *Endocrine Reviews*, 27(7), pp.710–18.

Fasshauer, M. *et al.*, (2003). Adiponectin gene expression and secretion is inhibited by interleukin-6 in 3T3-L1 adipocytes. *Biochemical and Biophysical Research Communications*, 301(4), pp.1045–1050.

Faurschou, M. & Borregaard, N., (2003). Neutrophil granules and secretory vesicles in inflammation. *Microbes and Infection*, 5(14), pp.1317–27.

Feldmann, M., (2008). Many cytokines are very useful therapeutic targets in disease. *The Journal of Clinical Investigation*, 118(11), pp.3533–6.

Feng, D. *et al*., (1998). Neutrophils emigrate from venules by a transendothelial cell pathway in response to FMLP. *The Journal of Experimental Medicine*, 187(6), pp.903–15.

Firatli, E., Tüzün, B. & Efeoğlu, A., (1996). Papillon-Lefèvre syndrome. Analysis of neutrophil chemotaxis. *Journal of Periodontology*, 67(6), pp.617–20.

Fisch, I.R., (1975). Smoking, Oral Contraceptives, and Obesity. *Journal of the American Medical Association*, 234(5), p.500.

Foell, D. *et al*., (2007). S100 proteins expressed in phagocytes: a novel group of damage-associated molecular pattern molecules. *Journal of Leukocyte Biology*, 81(1), pp.28–37.

Forsman, H. *et al.*, (2013). Reactivation of desensitized formyl peptide receptors by platelet activating factor: a novel receptor cross talk mechanism regulating neutrophil superoxide anion production. *PloS one*, 8(3), p.e60169.

Foxman, E.F., Campbell, J.J. & Butcher, E.C., (1997). Multistep navigation and the combinatorial control of leukocyte chemotaxis. *Journal of Cell Biology*, 139(5), pp.1349–60.

Foxman, E.F., Kunkel, E.J. & Butcher, E.C., (1999). Integrating conflicting chemotactic signals. The role of memory in leukocyte navigation. *Journal of Cell Biology*, 147(3), pp.577–88.

Frellick, M., (2013). AMA declares obesity is a disease. *AMA 2013 Annual Meeting*.

Friedl, P., Borgmann, S. & Bröcker, E.B., (2001). Amoeboid leukocyte crawling through extracellular matrix: lessons from the Dictyostelium paradigm of cell movement. *Journal of Leukocyte Biology*, 70(4), pp.491–509.

Fu, Y. *et al.*, (2002). Fc gamma receptor genes as risk markers for localized aggressive periodontitis in African-Americans. *Journal of Periodontology*, 73(5), pp.517–23.

Fuchs, T.A. *et al.*, (2007). Novel cell death program leads to neutrophil extracellular traps. *Science Signalling*, 176(2), p.231.

Fujita, T. *et al.*, (2005). CD38 expression in neutrophils from patients with localized aggressive periodontitis. *Journal of Periodontology*, 76(11), pp.1960–5.

Furukawa, S. *et al.*, (2004). Increased oxidative stress in obesity and its impact on metabolic syndrome. *Journal of Clinical Investigation*, 114(12), pp.1752–61.

Furze, R.C. & Rankin, S.M., (2008). Neutrophil mobilization and clearance in the bone marrow. *Immunology*, 125(3), pp.281–8.

Futosi, K., Fodor, S. & Mócsai, A., (2013). Neutrophil cell surface receptors and their intracellular signal transduction pathways. *International Immunopharmacology*, 17(3), pp.638–50.

Gaffen, S.L., (2008). An overview of IL-17 function and signaling. *Cytokine*, 43(3), pp.402–7.

Galli, S.J., Borregaard, N. & Wynn, T.A., (2011). Phenotypic and functional plasticity of cells of innate immunity: macrophages, mast cells and neutrophils. *Nature Immunology*, 12(11), pp.1035–44.

Gallin, J.I. *et al.*, (1982). Human neutrophil-specific granule deficiency: a model to assess the role of neutrophil-specific granules in the evolution of the inflammatory response. *Blood*, 59(6), pp.1317–29.

Gambardella, L. & Vermeren, S., (2013). Molecular players in neutrophil chemotaxis--focus on PI3K and small GTPases. *Journal of Leukocyte Biology*, 94(4), pp.603–12.

Gamonal, J. *et al.*, (2001). Characterization of cellular infiltrate, detection of chemokine receptor CCR5 and interleukin-8 and RANTES chemokines in adult periodontitis. *Journal of Periodontal Research*, 36(3), pp.194–203.

Gao, X. *et al.*, (2007). Tumor necrosis factor-alpha induces endothelial dysfunction in Lepr(db) mice. *Circulation*, 115(2), pp.245–54.

Garwicz, D. *et al*., (2005). Biosynthetic profiles of neutrophil serine proteases in a human bone marrow-derived cellular myeloid differentiation model. *Haematologica*, 90(1), pp.38–44.

Gasson, J.C., (1991). Molecular physiology of granulocyte-macrophage colony-stimulating factor. *Blood*, 77(6), pp.1131–45.

Geering, B. & Simon, H.-U., (2011). Peculiarities of cell death mechanisms in neutrophils. *Cell Death and Differentiation*, 18(9), pp.1457–69.

Gemmell, E., Marshall, R.I. & Seymour, G.J., (1997). Cytokines and prostaglandins in immune homeostasis and tissue destruction in periodontal disease. *Periodontology 2000*, 14, pp.112–43.

Di Gennaro, A. & Haeggström, J.Z., (2012). The leukotrienes: immune-modulating lipid mediators of disease. *Advances in Immunology*, 116, pp.51–92.

Gerhardt, C.C. *et al*., (2001). Chemokines control fat accumulation and leptin secretion by cultured human adipocytes. *Molecular and Cellular Endocrinology*, 175(1-2), pp.81–92.

Gesta, S., Tseng, Y.H. & Kahn, C.R., (2007). Developmental origin of fat: tracking obesity to its source. *Cell*, 131(2), pp.242–256.

Giannopoulou, C., Cappuyns, I. & Mombelli, A., (2003). Effect of smoking on gingival crevicular fluid cytokine profile during experimental gingivitis. *Journal of Clinical Periodontology*, 30(11), pp.996–1002.

Gierschik, P., Sidiropoulos, D. & Jakobs, K., (1989). Two distinct Gi-proteins mediate formyl peptide receptor signal transduction in human leukemia (HL-60) cells. *Journal of Biological Chemistry*, 264(36), pp.21470–21473.

Goetzi EJ, A.K., (1972). A neutrophil-immobilizing factor derived from human leukocytes : I. Generation and partial characterization. *Journal of Experimental Medicine*, 136(6), pp.1564–1580.

Goldin, A. *et al.,* (2006). Advanced glycation end products: sparking the development of diabetic vascular injury. *Circulation*, 114(6), pp.597–605.

Gonzáles, J.R. *et al.,* (2001). Concentration of interleukin-1beta and neutrophil elastase activity in gingival crevicular fluid during experimental gingivitis. *Journal of Clinical Periodontology*, 28(6), pp.544–9.

Gordon, T. *et al.,* (1977). High density lipoprotein as a protective factor against coronary heart disease. *The American Journal of Medicine*, 62(5), pp.707–714.

Grabcanovic-Musija, F. *et al.,* (2015). Neutrophil extracellular trap (NET) formation characterises stable and exacerbated COPD and correlates with airflow limitation. *Respiratory Research*, 16, p.59.

Grant, M.M., Brock, G.R., *et al.,* (2010). Crevicular fluid glutathione levels in periodontitis and the effect of non-surgical therapy. *Journal of Clinical Periodontology*, 37(1), pp.17–23.

Grant, M.M., Creese, A.J., *et al.,* (2010). Proteomic Analysis of a Noninvasive Human Model of Acute Inflammation and Its Resolution : The Twenty-one Day Gingivitis Model research articles. *Journal of Proteome Research*, 9, pp.4732–4744.

Graves, D.T. & Cochran, D., (2003). The contribution of interleukin-1 and tumor necrosis factor to periodontal tissue destruction. *Journal of Periodontology*, 74(3), pp.391–401.

Greenberg, S. *et al.,* (1996). Clustered syk tyrosine kinase domains trigger phagocytosis. *Proceedings of the National Academy of Sciences*, 93(3), pp.1103–7.

Grenda, D.S. *et al.,* (2007). Mutations of the ELA2 gene found in patients with severe congenital neutropenia induce the unfolded protein response and cellular apoptosis. *Blood*, 110(13), pp.4179–87.

Grimbaldeston, M.A. *et al.,* (2003). S100A8 induction in keratinocytes by ultraviolet A irradiation is dependent on reactive oxygen intermediates. *The Journal of Investigative Dermatology*, 121(5), pp.1168–74.

Grossi, S.G.1., Zambon, J.J., Ho, A.W., Koch, G., Dunford, R.G., Machtei, E.E., Norderyd, O.M., Genco, R.J. (1994). Assessment of risk for periodontal disease. I. Risk indicators for attachment loss. *Journal of Periodontology*, 65(3), pp.260-7.

Van Guilder, G.P. *et al.,* (2006). Influence of metabolic syndrome on biomarkers of oxidative stress and inflammation in obese adults. *Obesity*, 14(12), pp.2127–31.

Gupta, A.K. *et al.*, (2010). Activated endothelial cells induce neutrophil extracellular traps and are susceptible to NETosis-mediated cell death. *FEBS letters*, 584(14), pp.3193–7.

Gupta, A.K. *et al.*, (2005). Induction of neutrophil extracellular DNA lattices by placental microparticles and IL-8 and their presence in preeclampsia. *Human Immunology*, 66(11), pp.1146–54.

Gustafsson, a, Asman, B. & Bergström, K., (1997). Priming response to inflammatory mediators in hyperreactive peripheral neutrophils from adult periodontitis. *Oral Diseases*, 3(3), pp.167–71.

Gustafsson, A. & Åsman, B., (1996). Increased release of free oxygen radicals from peripheral neutrophils in adult periodontitis after Feγ-receptor stimulation. *Journal of Clinical Periodontology*, 23(1), pp.38–44.

Gutteridge, J.M.C. *et al.*, (1981). Inhibition of lipid peroxidation by the iron-binding protein lactoferrin. *Biochemical Journal*, 199(1), pp.259–261.

De Haar, S.F. *et al.*, (2004). Loss-of-function mutations in cathepsin C in two families with Papillon-Lefèvre syndrome are associated with deficiency of serine proteinases in PMNs. *Human Mutation*, 23(5), p.524.

De Haar, S.F. *et al.*, (2006). Role of polymorphonuclear leukocyte-derived serine proteinases in defense against Actinobacillus actinomycetemcomitans. *Infection and Immunity*, 74(9), pp.5284–91.

Van Haastert, P.J.M. & Devreotes, P.N., (2004). Chemotaxis: signalling the way forward. *Nature Reviews. Molecular Cell Biology*, 5(8), pp.626–34.

Haffajee, A.D. *et al.*, (1998). Subgingival microbiota in healthy, well-maintained elder and periodontitis subjects. *Journal of Clinical Periodontology*, 25(5), pp.346–353.

Haffajee, A.D. & Socransky, S.S., (2009). Relation of body mass index, periodontitis and *Tannerella forsythia*. *Journal of Clinical Periodontology*, 36(2), pp.89–99.

Häger, M., Cowland, J.B. & Borregaard, N., (2010). Neutrophil granules in health and disease. *Journal of Internal Medicine*, 268(1), pp.25–34.

Hague, A.L. & Baechle, M., (2008). Advanced caries in a patient with a history of bariatric surgery. *Journal of Dental Hygiene*, 82(2), p.22.

Hakkim, A. *et al.*, (2010). Impairment of neutrophil extracellular trap degradation is associated with lupus nephritis. *Proceedings of the National Academy of Sciences*, 107(21), pp.9813–8.

Hallett, M.B. & Lloyds, D., (1995). Neutrophil priming: the cellular signals that say "amber"but not "green." *Immunology Today*, 16(6), pp.264–268.
Halliwell, B. & Cross, C.E., (1994). Oxygen-derived species: their relation to human disease and environmental stress. *Environmental Health Perspectives*, 102 Suppl , pp.5–12.

Han, J.C., Lawlor, D.A. & Kimm, S.Y.S., (2010). Childhood obesity. *Lancet*, 375(9727), pp.1737–48.

Hanna, S. & Etzioni, A., (2012). Leukocyte adhesion deficiencies. *Annals of the New York Academy of Sciences*, 1250, pp.50–5.

Hanukoglu, I., (1992). Steroidogenic enzymes: Structure, function, and role in regulation of steroid hormone biosynthesis. *The Journal of Steroid Biochemistry and Molecular Biology*, 43(8), pp.779–804.

Happle, C., Germeshausen, M., Zeidler, Karl Welte, K., and Skokowa, J., (2011.) Neutrophil Extracellular Traps (NETs) in Patients with Congenital Neutropenia. *53rd American Society of Haematology Annual meeting.*

Harkin, D.W. *et al.*, (2001). Circulating neutrophil priming and systemic inflammation in limb ischaemia-reperfusion injury. International Angiology, 20(1), pp.78–89.

Harrison, C.A. *et al.*, (1999). Oxidation regulates the inflammatory properties of the murine S100 protein S100A8. *The Journal of Biological Chemistry*, 274(13), pp.8561–9.

Harrison, J.E. & Schultz, J., (1976). Studies on the chlorinating activity of myeloperoxidase. *Journal of Biological Chemistry*, 251(5), pp.1371–4.

Hart, T.C. *et al.*, (2000). Haim-Munk syndrome and Papillon-Lefèvre syndrome are allelic mutations in cathepsin C. *Journal of Medical Genetics*, 37(2), pp.88–94.

Hart, T.C. *et al.*, (1999). Mutations of the cathepsin C gene are responsible for Papillon-Lefèvre syndrome. *Journal of Medical Genetics*, 36(12), pp.881–7.

Hart, T.C. & Shapira, L., (1994). Papillon-Lefèvre syndrome. *Periodontology 2000*, 6(1), pp.88–100.

Harvath, L. *et al.*, (1987). Inhibition of human neutrophil chemotaxis by the protein kinase inhibitor, 1-(5-isoquinolinesulfonyl) piperazine. *Journal of Immunology*, 139(9), pp.3055–61.

Hatanaka, E. *et al.*, (2006). Neutrophils and monocytes as potentially important sources of proinflammatory cytokines in diabetes. *Clinical and Experimental Immunology*, 146(3), pp.443–7.

Haverkamp, J.M. *et al.*, (2011). *In vivo* suppressive function of myeloid-derived suppressor cells is limited to the inflammatory site. *European Journal of Immunology*, 41(3), pp.749–59.

Heasman, P.A. *et al.*, (1993). Flurbiprofen in the prevention and treatment of experimental gingivitis. *Journal of Clinical Periodontology*, 20(10), pp.732–8.

Heit, B. *et al.*, (2002). An intracellular signaling hierarchy determines direction of migration in opposing chemotactic gradients. *The Journal of Cell Biology*, 159(1), pp.91–102.

Heit, B., Liu, L., *et al.*, (2008). PI3K accelerates, but is not required for, neutrophil chemotaxis to fMLP. *Journal of Cell Science*, 121(Pt 2), pp.205–14.

Heit, B., Robbins, S.M., *et al.*, (2008). PTEN functions to "prioritize" chemotactic cues and prevent "distraction" in migrating neutrophils. *Nature Immunology*, 9(7), pp.743–52.

Herishanu, Y. *et al.*, (2006). Leukocytosis in obese individuals: possible link in patients with unexplained persistent neutrophilia. *European Journal of Haematology*, 76(6), pp.516–20.

Herlaar, E. & Brown, Z., (1999). p38 MAPK signalling cascades in inflammatory disease. *Molecular Medicine Today*, 5(10), pp.439–447.

Herlihy, S.E., Pilling, D., *et al.*, (2013). Dipeptidyl peptidase IV is a human and murine neutrophil chemorepellent. *Journal of Immunology*, 190(12), pp.6468–77.

Herlihy, S.E., Tang, Y. & Gomer, R.H., (2013). A *Dictyostelium* secreted factor requires a PTEN-like phosphatase to slow proliferation and induce chemorepulsion. *PloS One*, 8(3), p.e59365.

Herring, M.E. & Shah, S.K., (2006). Periodontal Disease and Control of Diabetes Mellitus. J *American Osteopath Association*, 106(7), pp.416–421.

Hessian, P., Edgeworth, J. & Hogg, N., (1993). MRP-8 and MRP-14, two abundant Ca(2+)-binding proteins of neutrophils and monocytes. *Journal of Leukocyte Biology*, 53(2), pp.197–204.

Heymsfield, S.B. *et al.*, (2014). Weight loss composition is one-fourth fat-free mass: a critical review and critique of this widely cited rule. *Obesity Reviews*, 15(4), pp.310–21.

Higdon, J. V & Frei, B., (2003). Obesity and oxidative stress: a direct link to CVD? *Arteriosclerosis, Thrombosis, and Vascular Biology*, 23(3), pp.365–7.

Hill, H.R. *et al.*, (1974). Defect in neutrophil granulocyte chemotaxis in Job's syndrome of recurrent "cold" staphylococcal abscesses. *Lancet*, 2(7881), pp.617–9.

Hirschfeld, J. *et al.*, (2015). Neutrophil extracellular trap formation in supragingival biofilms. *International Journal of Medical Microbiology*, 305(4-5), pp.453–63.

Hold, G.L. & El-Omar, M.E., (2008). Genetic aspects of inflammation and cancer. *Biochemical Journal*, 410(2), pp.225–235.

Holt, O.J., Gallo, F. & Griffiths, G.M., (2006). Regulating secretory lysosomes. *Journal of Biochemistry*, 140(1), pp.7–12.

Hopkins, N.K., Schaub, R.G. & Gorman, R.R., (1984). Acetyl glyceryl ether phosphorylcholine (PAF-acether) and leukotriene B4-mediated neutrophil chemotaxis through an intact endothelial cell monolayer. *Biochimica et biophysica acta*, 805(1), pp.30–6.

Horuk, R., (1996). Chemoattractant Ligands and Their Receptors, *CRC Press*.

Hotamisligil, G.S., (2006). Inflammation and metabolic disorders. *Nature*, 444(7121), pp.860–7.

Hotamisligil, G.S., Shargill, N.S. & Spiegelman, B.M., (1993). Adipose expression of tumor necrosis factor-alpha: direct role in obesity-linked insulin resistance. *Science* (New York, N.Y.), 259(5091), pp.87–91.

Houghton, A.M. *et al.,* (2010). Neutrophil elastase-mediated degradation of IRS-1 accelerates lung tumor growth. *Nature Medicine*, 16(2), pp.219–23.

Hu, N. *et al*., (2009). Coexpression of CD177 and membrane proteinase 3 on neutrophils in antineutrophil cytoplasmic autoantibody-associated systemic vasculitis: anti-proteinase 3-mediated neutrophil activation is independent of the role of CD177-expressing neutrophils. *Arthritis and Rheumatism*, 60(5), pp.1548–57.

Hu, N. *et al.,* (2011). Decreased CXCR1 and CXCR2 expression on neutrophils in anti-neutrophil cytoplasmic autoantibody-associated vasculitides potentially increases neutrophil adhesion and impairs migration. *Arthritis Research & Therapy*, 13(6), p.R201.

Huber, A.R. *et al.*, (1991). Regulation of transendothelial neutrophil migration by endogenous interleukin-8. *Science*, 254(5028), p.99.

Hume, D.A. *et al*., (2002). The mononuclear phagocyte system revisited. *Journal of Leukocyte Biology*, 72(4), pp.621–627.

Huttunen, R. & Syrjänen, J., (2013). Obesity and the risk and outcome of infection. *International Journal of Obesity*, 37(3), pp.333–40.

Ichikawa, S. *et al.,* (2012). MyD88 associated ROS generation is crucial for Lactobacillus induced IL-12 production in macrophage. *PloS One*, 7(4), p.e35880.

Iizawa, O., Akamatsu, H. & Niwa, Y. (1995) Neutrophil chemotaxis, phagocytosis, and generation of reaction oxygen species show a hierarchy of responsiveness to increasing concentrations of N-formyl-Met-Leu-Phe. *Biological Signals*, 4(1), pp.14–8.

Ilavská, S. *et al.,* (2012). Association between the human immune response and body mass index. *Human Immunology*, 73(5), pp.480–5.

Inoue, T. & Meyer, T., (2008). Synthetic activation of endogenous PI3K and Rac identifies an AND-gate switch for cell polarization and migration. *PloS One*, 3(8), p.e3068.

Insall, R.H., (2010). Understanding eukaryotic chemotaxis: a pseudopod-centred view. *Nature Reviews Molecular Cell Biology*, 11(6), pp.453–457.

Introne, W.J. *et al.,* (2015). Chediak-Higashi Syndrome. *GeneReviews.*

Ionita, M.G. *et al.,* (2010). High neutrophil numbers in human carotid atherosclerotic plaques are associated with characteristics of rupture-prone lesions. *Arteriosclerosis, Thrombosis, and Vascular Biology*, 30(9), pp.1842–8.

Irimia, D., (2010). Microfluidic technologies for temporal perturbations of chemotaxis. *Annual Review of Biomedical Engineering*, 12, pp.259–84.

Jenne, C.N. *et al.*, (2013). Neutrophils recruited to sites of infection protect from virus challenge by releasing neutrophil extracellular traps. *Cell Host & Microbe*, 13(2), pp.169–80.

Jönsson, S. *et al.*, (2011). Increased levels of leukocyte-derived MMP-9 in patients with stable angina pectoris. *PloS One*, 6(4), p.e19340.

K. Bergström and B. Åsman, (1993). Luminol enhanced Fc-receptor dependent chemiluminescence from peripheral PMN cells. A methodological study. *Scandinavian Journal of Clinical & Laboratory Investigation*, 53, pp.171–177.

Kannel, W.B., (1988). Contributions of the Framingham Study to the conquest of coronary artery disease. *The American Journal of Cardiology*, 62(16), pp.1109–12.

Kannel, W.B., (1979). Diabetes and Cardiovascular Disease. *Journal of the American Medical Association*, 241(19), p.2035.

Kaplan, M.J. & Radic, M., (2012). Neutrophil extracellular traps: double-edged swords of innate immunity. *Journal of Immunology*, 189(6), pp.2689–95.

Karjalainen, S. *et al.*, (2009). Long-term physical inactivity and oral health in Finnish adults with intellectual disability. Acta Odontologica Scandinavica, 60(1), pp.50–55.

Karlsson, A., Nixon, J. & McPhail, L., (2000). Phorbol myristate acetate induces neutrophil NADPH-oxidase activity by two separate signal transduction pathways: dependent or independent of phosphatidylinositol 3-kinase. *Journal of Leukocyte Biology*, 67(3), pp.396–404.

Kaul, H., Cui, Z. & Ventikos, Y., (2013). A multi-paradigm modeling framework to simulate dynamic reciprocity in a bioreactor. *PloS One*, 8(3), p.e59671.

Kaye, K.S. *et al*., (2011). Predictors of nosocomial bloodstream infections in older adults. *American Geriatrics Society*, 59(4), pp.622–7.

Kennedy, A.D. *et al.*, (2007). Dectin-1 promotes fungicidal activity of human neutrophils. *European Journal of Immunology*, 37(2), pp.467–78.

Kent, L.W. *et al*., (1998). Effect of lipopolysaccharide and inflammatory cytokines on interleukin-6 production by healthy human gingival fibroblasts. *Infection and Immunity*, 66(2), pp.608–14.

Kerkhoff, C. *et al.*, (2005). The arachidonic acid-binding protein S100A8/A9 promotes NADPH oxidase activation by interaction with p67phox and Rac-2. *Federation of American Societies for Experimental Biology*, 19(3), pp.467–9.

Kern, P.A. *et al.*, (1995). The expression of tumor necrosis factor in human adipose tissue. Regulation by obesity, weight loss, and relationship to lipoprotein lipase. *The Journal of Clinical Investigation*, 95(5), pp.2111–9.

Keshari, R.S. *et al.*, (2013). Reactive oxygen species-induced activation of ERK and p38 MAPK mediates PMA-induced NETs release from human neutrophils. *Journal of Cellular Biochemistry*, 114(3), pp.532–40.

Kessel, C., Holzinger, D. & Foell, D., (2013). Phagocyte-derived S100 proteins in autoinflammation: putative role in pathogenesis and usefulness as biomarkers. *Clinical Immunology*, 147(3), pp.229–41.

Kessenbrock, K. *et al.*, (2009). Netting neutrophils in autoimmune small-vessel vasculitis. *Nature Medicine*, 15(6), pp.623–5.

Khader, Y.S. *et al.*, (2009). The association between periodontal disease and obesity among adults in Jordan. *Journal of Clinical Periodontology*, 36(1), pp.18–24.

Khan, A.I. *et al.*,(1994) Lipopolysaccharide: a p38 MAPK-dependent disrupter of neutrophil chemotaxis. *Microcirculation*, 12(5), pp.421–32.

Khanna-Gupta, A. *et al.*, (2007). Growth factor independence-1 (Gfi-1) plays a role in mediating specific granule deficiency (SGD) in a patient lacking a gene-inactivating mutation in the C/EBPepsilon gene. *Blood*, 109(10), pp.4181–90.

Khovidhunkit, W. *et al.*, (2004). Effects of infection and inflammation on lipid and lipoprotein metabolism: mechanisms and consequences to the host. *The Journal of Lipid Research*, 45(7), pp.1169–1196.

Kikkert, R. *et al.*, (2007). Activation of toll-like receptors 2 and 4 by gram-negative periodontal bacteria. *Oral Microbiology and Immunology*, 22(3), pp.145–51.

Kilpatrick, E.S., (2008). Haemoglobin A1c in the diagnosis and monitoring of diabetes mellitus. Journal of clinical pathology, 61(9), pp.977–82.

Kim, B.J. *et al.*, (2009). The effect of calcipotriol on the expression of human beta defensin-2 and LL-37 in cultured human keratinocytes. *Clinical & Developmental Immunology*, p.645898.

Kim, D. & Haynes, C.L., (2012). Neutrophil chemotaxis within a competing gradient of chemoattractants. *Analytical Chemistry*, 84(14), pp.6070–8.

Kim, D. & Haynes, C.L., (2013). The role of p38 MAPK in neutrophil functions: single cell chemotaxis and surface marker expression. *The Analyst*, 138(22), pp.6826–33.

Kim, F. *et al.*, (2007). Toll-like receptor-4 mediates vascular inflammation and insulin resistance in diet-induced obesity. *Circulation Research*, 100(11), pp.1589–96.

Kim, J.A. & Park, H.S., (2008). White blood cell count and abdominal fat distribution in female obese adolescents. *Metabolism: Clinical and Experimental*, 57(10), pp.1375–9.

Kim, J.-Y. *et al.*, (2007). Obesity-associated improvements in metabolic profile through expansion of adipose tissue. *The Journal of Clinical Investigation*, 117(9), pp.2621–37.

Kimura, M. *et al.*, (1998). T lymphopenia in obese diabetic (dbdb) mice is non-selective and thymus independent. *Life Sciences*, 62(14), pp.1243–1250.

Kinane, D.F. *et al*., (1991). Immunocytochemical characterization of cellular infiltrate, related endothelial changes and determination of GCF acute-phase proteins during human experimental gingivitis. *Journal of Periodontal Research*, 26(3 Pt 2), pp.286–8.

Klebanoff, S.J., (2005). Myeloperoxidase: friend and foe. *Journal of Leukocyte Biology*, 77(5), pp.598–625.

Klos, A. *et al.*, (2013). International Union of Pharmacology. LXXXVII. Complement Peptide C5a, C4a, and C3a Receptors. *Pharmacological Reviews*, 65(1), pp.500–543.

Klöting, N. & Blüher, M., (2014). Adipocyte dysfunction, inflammation and metabolic syndrome. *Reviews in Endocrine & Metabolic Disorders*, 15(4), pp.277–87.

Kobayashi, S.D. *et al.*, (2005) Neutrophils in the innate immune response. *Archivum Immunologiae et Therapiae Experimentalis*, 53(6), pp.505–17.

Koenderman, L. *et al.*, (2000). Monitoring of neutrophil priming in whole blood by antibodies isolated from a synthetic phage antibody library. *Journal of Leukocyte Biology*, 68(1), pp.58–64.

Kohidai, L. *et al*., (2003). Characterization of chemotactic ability of peptides containing N-formyl-methionyl residues in Tetrahymena fMLP as a targeting ligand. *Cell Biology International*, 27(8), pp.695–700.

Kolls, J.K. & Lindén, A., (2004). Interleukin-17 family members and inflammation. *Immunity*, 21(4), pp.467–76.

Konuganti, K. *et al.*, (2012). A comparative evaluation of whole blood total antioxidant capacity using a novel nitroblue tetrazolium reduction test in patients with periodontitis and healthy subjects: A randomized, controlled trial. *Journal of Indian Society of Periodontology*, 16(4), pp.620–2.

Kopelman, P., (2007). Health risks associated with overweight and obesity. *Obesity Reviews*, 8 Suppl 1, pp.13–7.

Kopp, H.P. *et al.*, (2003). Impact of weight loss on inflammatory proteins and their association with the insulin resistance syndrome in morbidly obese patients. *Arteriosclerosis, Thrombosis, and Vascular Biology*, 23(6), pp.1042–7.

Kopprasch, S. *et al*., (2004). The pivotal role of scavenger receptor CD36 and phagocyte-derived oxidants in oxidized low density lipoprotein-induced adhesion to endothelial cells. *International Journal of Biochemistry and Cell Biology*, 36(3), pp.460–471.

Kordonowy, L.L. *et al.*, (2012). Obesity is associated with neutrophil dysfunction and attenuation of murine acute lung injury. *American Journal of Respiratory Cell and Molecular Biology*, 47(1), pp.120–7.

Korkmaz, B. *et al*., (2010). Neutrophil elastase, proteinase 3, and cathepsin G as therapeutic targets in human diseases. *Pharmacological Reviews*, 62(4), pp.726–59.

Koro, C. *et al.*, (2016). Carbamylated LL-37 as a modulator of the immune response. *Innate Immunity*, 22(3), pp.218–29.

Kowashi, Y., Jaccard, F. & Cimasoni, G., (1980). Sulcular polymorphonuclear leucocytes and gingival exudate during experimental gingivitis in man. *Journal of Periodontal Research*, 15(2), pp.151–8.

Krauss, R.M. *et al.*, (2006). Separate effects of reduced carbohydrate intake and weight loss on atherogenic dyslipidemia. *American Journal of Clinical Nutrition*, 83(5), pp.1025–1031.

Kuiper, J.W.P. *et al.*, (2011). Rac regulates PtdInsP_3 signaling and the chemotactic compass through a redox-mediated feedback loop. *Blood*, 118(23), pp.6164–71.

Kullo, I.J., Hensrud, D.D. & Allison, T.G., (2002). Comparison of numbers of circulating blood monocytes in men grouped by body mass index. *American Journal of Cardiology*, 89(12), pp.1441–3.

Kumanyika, S. *et al*., (2002). Public Health Approaches to the Prevention of Obesity (PHAPO) Working Group of the International Obesity Task Force (IOTF). Obesity prevention: the case for action. *Journal of Obesity and Related Metabolic Disorders*, 26, pp.425–436.

Kumar, R.S. & Prakash, S., (2012). Impaired neutrophil and monocyte chemotaxis in chronic and aggressive periodontitis and effects of periodontal therapy. *Indian Journal of Dental Research*, 23(1), pp.69–74.

Kurihara, H. *et al.*, (1993). Calcium-dependent protein kinase C activity of neutrophils in localized juvenile periodontitis. *Infection and Immunity*., 61(8), pp.3137–3142.

Lago, F. *et al.*, (2007). Adipokines as emerging mediators of immune response and inflammation. *Nature Clinical Practice Rheumatology*, 3(12), pp.716–724.

Laharrague, P. *et al.*, (2000). High concentration of leptin stimulates myeloid differentiation from human bone marrow CD34+ progenitors: potential involvement in leukocytosis of obese subjects. *International Journal of Obesity*, 24(9), pp.1212–1216.

Lambeth, J.D., (1988). Activation of the respiratory burst oxidase in neutrophils: On the role of membrane-derived second messengers, Ca++, and protein kinase C. *Journal of Bioenergetics and Biomembranes*, 20(6), pp.709–733.

Lamster, I.B., Oshrain, R.L. & Gordon, J.M., (1986). Enzyme activity in human gingival crevicular fluid: considerations in data reporting based on analysis of individual crevicular sites. *Journal of Clinical Periodontology*, 13(8), pp.799–804.

Lande, R. *et al.*, (2007). Plasmacytoid dendritic cells sense self-DNA coupled with antimicrobial peptide. *Nature*, 449(7162), pp.564–9.

Lara, L.L. *et al.*, (1997). Low density lipoprotein receptor expression and function in human polymorphonuclear leucocytes. *Clinical and Experimental Immunology*, 107(1), pp.205–12.

Laroux, F.S. *et al.*, (2005). Cutting edge: MyD88 controls phagocyte NADPH oxidase function and killing of gram-negative bacteria. *Journal of Immunology*, (175(9), pp.5596–600.

Leavell, K., Peterson, M. & Gross, T., (1997). Human neutrophil elastase abolishes interleukin-8 chemotactic activity. *Journal of Leukocyte. Biology*., 61(3), pp.361–366.

Lee, A., Whyte, M.K. & Haslett, C., (1993). Inhibition of apoptosis and prolongation of neutrophil functional longevity by inflammatory mediators. *Journal of Leukocyte Biology*, 54(4), pp.283–8.

Leenen, R. *et al.*, (1993). Relative effects of weight loss and dietary fat modification on serum lipid levels in the dietary treatment of obesity. *Journal of Lipid Research*, 34(12), pp.2183–91.

Lehman, J.A. *et al.*, (2001). MAP kinase upregulation after hematopoietic differentiation: role of chemotaxis. *Cell Physiology*, 280(1), pp.C183–91.

Lehr, H.A. *et al.*, (1995). *In vitro* effects of oxidized low density lipoprotein on CD11b/CD18 and L-selectin presentation on neutrophils and monocytes with relevance for the *in vivo* situation. *American Journal of Pathology*, 146(1), pp.218–27.

Lehr, S., Hartwig, S. & Sell, H., (2012). Adipokines: a treasure trove for the discovery of biomarkers for metabolic disorders. *Proteomics. Clinical Applications*, 6(1-2), pp.91–101.

Lehrke, M. *et al.*, (2004). An inflammatory cascade leading to hyperresistinemia in humans. *PLoS Medicine*, 1(2), p.e45.

Leik, C.E. & Walsh, S.W., (2004). Neutrophils infiltrate resistance-sized vessels of subcutaneous fat in women with preeclampsia. *Hypertension*, 44(1), pp.72–7.

Lemieux, I. *et al.*, (2001). Elevated C-reactive protein: another component of the atherothrombotic profile of abdominal obesity. *Arteriosclerosis, Thrombosis, and Vascular Biology*, 21(6), pp.961–7.

Lennon, D.L. *et al.*, (1983). Total cholesterol and HDL-cholesterol changes during acute, moderate-intensity exercise in men and women. *Metabolism: Clinical and Experimental*, 32(3), pp.244–9.

Levine, H. & Rappel, W.-J., (2013). The physics of eukaryotic chemotaxis. *Physics Today*, 66(2), p.24.

Lewis, M.C. *et al.*, (2006). Change in liver size and fat content after treatment with Optifast very low calorie diet. *Obesity Surgery*, 16(6), pp.697–701.

Li Jeon, N. *et al.*, (2002). Neutrophil chemotaxis in linear and complex gradients of interleukin-8 formed in a microfabricated device. *Nature Biotechnology*, 20(8), pp.826–30.

Li, X. *et al.*, (2011). The β-glucan receptor Dectin-1 activates the integrin Mac-1 in neutrophils via Vav protein signaling to promote Candida albicans clearance. *Cell Host & Microbe*, 10(6), pp.603–15.

Li, Z.-Y., Wang, P. & Miao, C.-Y., (2011). Adipokines in inflammation, insulin resistance and cardiovascular disease. *Clinical and Experimental Pharmacology & Physiology*, 38(12), pp.888–96.

Lin, F. *et al.*, (2004). Effective neutrophil chemotaxis is strongly influenced by mean IL-8 concentration. *Biochemical and Biophysical Research Communications*, 319(2), pp.576–81.

Ling, M.R., *2015.* Neutrophil function in chronic periodontitis. *Univeristy of Birmingham*.

Ling, M.R., Chapple, I.L. & Matthews, J.B., (2015). Peripheral blood neutrophil cytokine hyper-reactivity in chronic periodontitis. *Innate Immunity*, 21(7), pp.714–725.

Ling, M.R., Chapple, I.L.C. & Matthews, J.B., (2016). Neutrophil superoxide release and plasma C-reactive protein levels pre- and post-periodontal therapy. *Journal of Clinical Periodontology*. 43(8):652-8.

Listgarten, M.A., (1986). Pathogenesis of periodontitis. *Journal of Clinical Periodontology*, 13(5), pp.418–425.

Little, R.R., Rohlfing, C.L. & Sacks, D.B., (2011). Status of hemoglobin A1c measurement and goals for improvement: from chaos to order for improving diabetes care. *Clinical Chemistry*, 57(2), pp.205–14.

Liu, P.T. *et al.*, (2006). Toll-like receptor triggering of a vitamin D-mediated human antimicrobial response. *Science*, 311(5768), pp.1770–3.

Liu, W. *et al.*, (2012). Olfactomedin 4 inhibits cathepsin C-mediated protease activities, thereby modulating neutrophil killing of *Staphylococcus aureus* and *Escherichia coli* in mice. *Journal of Immunology*, 189(5), pp.2460–7.

Liu, Z. *et al.*, (2000). The Serpin α1-Proteinase Inhibitor Is a Critical Substrate for Gelatinase B/MMP-9 In Vivo. *Cell*, 102(5), pp.647–655.

Lobene, R.R., Soparkar, P.M. & Newman, M.B., (1982) Use of dental floss. Effect on plaque and gingivitis. *Clinical Preventive Dentistry*, 4(1), pp.5–8.

Locksley, R.M., Killeen, N. & Lenardo, M.J., (2001). The TNF and TNF receptor superfamilies: integrating mammalian biology. *Cell*, 104(4), p.487.

Löe H, Theilade E, J.S., (1965). Experimental ginigvitis in man. *Journal of Periodontal Research*, 36, pp.177–87.

Löe, H. *et al*., (1967). Experimental gingivitis in man. *Journal of Periodontal Research*, 2(4), pp.282–289.

Loffreda, S. *et al.*, (1998). Leptin regulates proinflammatory immune responses. *The FASEB Journal*, 12(1), pp.57–65.

Loke, Y.K. *et al.*, (2012). Association of obstructive sleep apnea with risk of serious cardiovascular events: a systematic review and meta-analysis. *Circulation. Cardiovascular Quality and Outcomes*, 5(5), pp.720–8.

Louie, J.K. *et al.*, (2011). A novel risk factor for a novel virus: obesity and 2009 pandemic influenza A (H1N1). *Clinical Infectious Diseases*, 52(3), pp.301–12.

Lumeng, C.N., Bodzin, J.L. & Saltiel, A.R., (2007). Obesity induces a phenotypic switch in adipose tissue macrophage polarization. *The Journal of Clinical Investigation*, 117(1), pp.175–84.

Lundqvist, H. *et al.*, (1996). Phorbol myristate acetate-induced NADPH oxidase activity in human neutrophils: only half the story has been told. *Journal of Leukocyte Biology*, 59(2), pp.270–279.

Lusitani, D., Malawista, S.E. & Montgomery, R.R., (2003). Calprotectin, an abundant cytosolic protein from human polymorphonuclear leukocytes, inhibits the growth of Borrelia burgdorferi. *Infection and Immunity*, 71(8), pp.4711–6.

Madenspacher, J.H. *et al.*, (2010). Dyslipidemia Induces Opposing Effects on Intrapulmonary and Extrapulmonary Host Defense through Divergent TLR Response Phenotypes. *The Journal of Immunology*, 185(3), pp.1660–1669.

Magidson, V. & Khodjakov, A., (2013). Circumventing photodamage in live-cell microscopy. *Methods in Cell Biology*, 114, pp.545–60.

Manninen, V. *et al.*, (1992). Joint effects of serum triglyceride and LDL cholesterol and HDL cholesterol concentrations on coronary heart disease risk in the Helsinki Heart Study. Implications for treatment. *Circulation*, 85(1), pp.37–45.

Mantovani, A. *et al.*, (2011). Neutrophils in the activation and regulation of innate and adaptive immunity. *Nature Reviews. Immunology*, 11(8), pp.519–31.

Mantzoros, C.S. *et al.*, (2011). Leptin in human physiology and pathophysiology. American journal of physiology. *Endocrinology and Metabolism*, 301(4), pp.E567–84.

Marchesi, V.T. & Florey, H.W., (1960). Electron micrographic observations on the emigration of leucocytes. *Quarterly Journal of Experimental Physiology and Cognate Medical Sciences*, 45(4), pp.343–348.

Mathias, J.R. *et al.*, (2006). Resolution of inflammation by retrograde chemotaxis of neutrophils in transgenic zebrafish. *Journal of Leukocyte Biology*, 80(6), pp.1281–8.

Matsuda, M. *et al.*, (1996). Glomerular expression of macrophage colony-stimulating factor and granulocyte-macrophage colony-stimulating factor in patients with various forms of glomerulonephritis. *Laboratory Investigation*, 75(3), pp.403–12.

Matsuzawa-Nagata, N. *et al.*, (2008). Increased oxidative stress precedes the onset of high-fat diet-induced insulin resistance and obesity. *Metabolism: Clinical and Experimental*, 57(8), pp.1071–7.

Matthews, J.B., Wright, H.J., Roberts, A., Cooper, P.R., *et al*., (2007a). Hyperactivity and reactivity of peripheral blood neutrophils in chronic periodontitis. *Clinical and Experimental Immunology*, 147(2), pp.255–64.

Matthews, J.B., Wright, H.J., Roberts, A., Ling-Mountford, N., *et al.*, (2007b). Neutrophil hyper-responsiveness in periodontitis. *Journal of Dental Research*, 86(8), pp.718–22.

Mauch, L. *et al.*, (2007). Chronic granulomatous disease (CGD) and complete myeloperoxidase deficiency both yield strongly reduced dihydrorhodamine 123 test signals but can be easily discerned in routine testing for CGD. *Clinical Chemistry*, 53(5), pp.890–6.

Mauer, J. *et al.*, (2014). Signaling by IL-6 promotes alternative activation of macrophages to limit endotoxemia and obesity-associated resistance to insulin. *Nature Immunology*, 15(5), pp.423–30.

McCord, J.M., (1985). Oxygen-derived free radicals in postischemic tissue injury. *New England Journal of Medicine*, 312(3), pp.159–63.

McDonald, B. *et al.*, (2012). Intravascular neutrophil extracellular traps capture bacteria from the bloodstream during sepsis. *Cell Host & Microbe*, 12(3), pp.324–33.

McDonald, P.P., Bald, A. & Cassatella, M.A., (1997). Activation of the NF-kappaB pathway by inflammatory stimuli in human neutrophils. *Blood*, 89(9), pp.3421–33.

McGuire, M.J., Lipsky, P.E. & Thiele, D.L., (1993). Generation of active myeloid and lymphoid granule serine proteases requires processing by the granule thiol protease dipeptidyl peptidase I. *The Journal of Biological Chemistry*, 268(4), pp.2458–67.

Mensink, M. *et al.*, (2016). Effect of Caloric Restriction and Dietary Composition on Liver Triglyceride Content in Subjects with Abdominal Obesity: the Wageningen Belly Fat Study. *FASEB Journal*, 30(1), p.291.4.

Merchant, A.T. *et al.*, (2003). Increased physical activity decreases periodontitis risk in men. *European Journal of Epidemiology*, 18(9), pp.891–8.

Metzler, K.D. *et al.*, (2011). Myeloperoxidase is required for neutrophil extracellular trap formation: implications for innate immunity. *Blood*, 117(3), pp.953–9.

Michalowicz, B.S. *et al.*, (1991). Periodontal findings in adult twins. *Journal of Periodontology*, 62(5), pp.293–9.

Miesel, R., Murphy, M.P. & Kröger, H., (1996). Enhanced mitochondrial radical production in patients which rheumatoid arthritis correlates with elevated levels of tumor necrosis factor alpha in plasma. *Free Radical Research*, 25(2), pp.161–9.

Mittal, M. *et al.*, (2014). Reactive oxygen species in inflammation and tissue injury. *Antioxidants & Redox Signaling*, 20(7), pp.1126–67.

Molica, F. *et al.*, (2015). Adipokines at the crossroad between obesity and cardiovascular disease. *Thrombosis and Haemostasis*, 113(3), pp.553–66.

Molina, A. *et al.*, (2003). Insulin resistance, leptin and TNF-alpha system in morbidly obese women after gastric bypass. *Obesity Surgery*, 13(4), pp.615–21.

Montreekachon, P. *et al.*, (2011). Involvement of P2X(7) purinergic receptor and MEK1/2 in interleukin-8 up-regulation by LL-37 in human gingival fibroblasts. *Journal of Periodontal Research*, 46(3), pp.327–37.

Morel, F., Doussiere, J. & Vignais, P. V, (1991). The superoxide-generating oxidase of phagocytic cells. Physiological, molecular and pathological aspects. *European Journal of Biochemistry* 201(3), pp.523–46.
Mosser, D.M. & Edwards, J.P., (2008). Exploring the full spectrum of macrophage activation. *Nature Reviews. Immunology*, 8(12), pp.958–69.

Mowat, A.G. & Baum, J., (1971). Chemotaxis of polymorphonuclear leukocytes from patients with rheumatoid arthritis. *The Journal of Clinical Investigation*, 50(12), pp.2541–9.

Mraz, M. & Haluzik, M., (2014). The role of adipose tissue immune cells in obesity and low-grade inflammation. *The Journal of Endocrinology*, 222(3), pp.R113–27.

Muinonen-Martin, A.J. *et al.*, (2010). An improved chamber for direct visualisation of chemotaxis. PloS One, 5(12), p.e15309.

Muinonen-Martin, A.J. *et al.*, (2013). Measuring chemotaxis using direct visualization microscope chambers. *Methods in Molecular Biology*, 1046, pp.307–21.

Nagasawa, T. *et al.*, (2007). Roles of receptor activator of nuclear factor-kappaB ligand (RANKL) and osteoprotegerin in periodontal health and disease. *Periodontology 2000*, 43, pp.65–84.

Nakano, A. *et al.*, (2001). Papillon-Lefèvre syndrome: mutations and polymorphisms in the cathepsin C gene. *The Journal of Investigative Dermatology*, 116(2), pp.339–43.

Nanji, A.A. & Freeman, J.B., (1985). Relationship between body weight and total leukocyte count in morbid obesity. *American Journal of Clinical Pathology*, 84(3), pp.346–7.

Di Nardo, A., Vitiello, A. & Gallo, R.L., (2003). Cutting Edge: Mast Cell Antimicrobial Activity Is Mediated by Expression of Cathelicidin Antimicrobial Peptide. *Journal of Immunology*, 170(5), pp.2274–2278.

Naruko, T. *et al.*, (2002). Neutrophil infiltration of culprit lesions in acute coronary syndromes. *Circulation*, 106(23), pp.2894–900.

Nathan, C., (2002). Points of control in inflammation. *Nature*, 420(6917), pp.846–52.

Nelson, R.D., Quie, P.G. & Simmons, R.L., (1975). Chemotaxis under agarose: a new and simple method for measuring chemotaxis and spontaneous migration of human polymorphonuclear leukocytes and monocytes. *Journal of Immunology*, 115(6), pp.1650–6.

Nestel, P.J., Whyte, H.M. & Goodman, D.S., (1969). Distribution and turnover of cholesterol in humans. *Journal of Clinical Investigation*, 48(6), pp.982–91.

Neumann, A. *et al.*, (2014). The antimicrobial peptide LL-37 facilitates the formation of neutrophil extracellular traps. *The Biochemical Journal*, 464(1), pp.3–11.

NHLBI Obesity Education Initiative Expert Panel on the identification, evaluation, and treatment. of obesity in adults. (US), (1988). *National Heart, Lung, and Blood Institute*.

Nibali, L. *et al.*, (2008). Association between interleukin-6 promoter haplotypes and aggressive periodontitis. *Journal of Clinical Periodontology*, 35(3), pp.193–8.

Nibali, L. *et al.*, (2013). Clinical review: Association between metabolic syndrome and periodontitis: a systematic review and meta-analysis. *The Journal of Clinical Endocrinology and Metabolism*, 98(3), pp.913–20.

Nibbs, R.J.B. & Graham, G.J., (2013). Immune regulation by atypical chemokine receptors. *Nature Reviews Immunology*, 13(11), pp.815–829.

Nicholls, S.J. & Hazen, S.L., (2005). Myeloperoxidase and cardiovascular disease. Arteriosclerosis, *Thrombosis, and Vascular Biology*, 25(6), pp.1102–11.

Nick, J.A. *et al.*, (1997). Common and distinct intracellular signaling pathways in human neutrophils utilized by platelet activating factor and FMLP. *The Journal of Clinical Investigation*, 99(5), pp.975–86.

Nieman, D.C. *et al.*, (1999). Influence of obesity on immune function. *Journal of the American Dietetic Association*, 99(3), pp.294–9.

Nieman, D.C. *et al.*, (1993). Physical activity and immune function in elderly women. *Medicine and Science in Sports and Exercise*, 25(7), pp.823–31.

Niethammer, P. *et al.*, (2009). A tissue-scale gradient of hydrogen peroxide mediates rapid wound detection in zebrafish. *Nature*, 459(7249), pp.996–9.

Nijhuis, J. *et al.*, (2009). Neutrophil Activation in Morbid Obesity, Chronic Activation of Acute Inflammation. *Obesity*, 17(11), pp.2014–2018.

Nijnik, A. & Hancock, R.E.W., (2009). The roles of cathelicidin LL-37 in immune defences and novel clinical applications. *Current Opinion in Hematology*, 16(1), pp.41–7.

Nikolaus, S. *et al.*, (1998). Increased secretion of pro-inflammatory cytokines by circulating polymorphonuclear neutrophils and regulation by interleukin 10 during intestinal inflammation. *Gut*, 42(4), pp.470–6.

Nilsson, C. *et al.*, (2012). Laboratory animals as surrogate models of human obesity. *Acta Pharmacologica Sinica*, 33(2), pp.173–181.

Nishizuka, Y., (1986). Studies and perspectives of protein kinase C. *Science*, 233(4761), pp.305–312.

Noble, R.E., (2001). Waist-to-hip ratio versus BMI as predictors of cardiac risk in obese adult women. *Western Journal of Medicine*, 174(4), pp.240–1.

Noguera, A. *et al*., (2001). Enhanced neutrophil response in chronic obstructive pulmonary disease. *Thorax*, 56(6), pp.432–437.

Nordenfelt, P. & Tapper, H., (2011). Phagosome dynamics during phagocytosis by neutrophils. *Journal of Leukocyte Biology*, 90(2), pp.271–84.

Nussbaum, G. & Shapira, L., (2011). How has neutrophil research improved our understanding of periodontal pathogenesis? *Journal of Clinical Periodontology*, 38 Suppl 1, pp.49–59.

O'Rourke, R.W., (2009). Inflammation in obesity-related diseases. *Surgery*, 145(3), pp.255–9.

O'Shea, J.J. & Murray, P.J., (2008). Cytokine signaling modules in inflammatory responses. *Immunity*, 28(4), pp.477–87.

Odink, K. *et al.*, (1987). Two calcium-binding proteins in infiltrate macrophages of rheumatoid arthritis. *Nature*, 330(6143), pp.80–2.

Offenbacher, S. *et al.*, (2010). Changes in gingival crevicular fluid inflammatory mediator levels during the induction and resolution of experimental gingivitis in humans. *Journal of Clinical Periodontology*, 37(4), pp.324–33.

Oh, H. *et al*., (2015). Effects of initial periodontal therapy on interleukin-1β level in gingival crevicular fluid and clinical periodontal parameters. *Journal of Oral Science*, 57(2), pp.67–71.

Ohashi, K. *et al.*, (2010). Adiponectin promotes macrophage polarization toward an anti-inflammatory phenotype. *Journal of Biological Chemistry*, 285(9), pp.6153–6160.

Öngöz Dede, F. *et al.*, (2016). Glutathione levels in plasma, saliva and gingival crevicular fluid after periodontal therapy in obese and normal weight individuals. *Journal of Periodontal Research*.

Otero, M. *et al.*, (2006). Towards a pro-inflammatory and immunomodulatory emerging role of leptin. *Rheumatology*, 45(8), pp.944–950.

Ottonello, L. *et al*., (2005). CCL3 (MIP-1alpha) induces in vitro migration of GM-CSF-primed human neutrophils via CCR5-dependent activation of ERK 1/2. *Cellular Signalling*, 17(3), pp.355–63.

Ouchi, N. *et al*., (2011). Adipokines in inflammation and metabolic disease. *Nature Reviews* Immunology, 11(2), pp.85–97.

Ouchi, N. *et al.*, (2000). Adiponectin, an adipocyte-derived plasma protein, inhibits endothelial NF-kappaB signaling through a cAMP-dependent pathway. *Circulation*, 102(11), pp.1296–301.

Owen, C.A. & Campbell, E.J., (1999). The cell biology of leukocyte-mediated proteolysis. *Journal of Leukocyte Biology*, 65(2), pp.137–50.

Padrines, M. *et al*., (1994). Interleukin-8 processing by neutrophil elastase, cathepsin G and proteinase-3. *FEBS letters*, 352(2), pp.231–5.

Page, R.C. & Schroeder, H.E., (1976). Pathogenesis of inflammatory periodontal disease. A summary of current work. *Laboratory Investigation*, 34(3), pp.235–49.

Pahan, K., (2006). Lipid-lowering drugs. *Cellular and Molecular Life Sciences*, 63(10), pp.1165–78.

Palmer, R.M. *et al.*, (2005). Mechanisms of action of environmental factors--tobacco smoking. Journal of Clinical Periodontology, 32 Suppl 6, pp.180–95.

Palmer, L.J. *et al*., (2012). Hypochlorous acid regulates neutrophil extracellular trap release in humans. *Clinical and Experimental Immunology*, 167(2), pp.261–8.

Palmer, L.J. *et al.*, (2015). Influence of complement on neutrophil extracellular trap release induced by bacteria. *Journal of Periodontal Research*.

Palvinskaya, T. *et al.*, (2013). Effects of acute and chronic low density lipoprotein exposure on neutrophil function. *Pulmonary Pharmacology & Therapeutics*, 26(4), pp.405–11.

Pannala, R. *et al.*, (2009). New-onset diabetes: a potential clue to the early diagnosis of pancreatic cancer. *The Lancet. Oncology*, 10(1), pp.88–95.

Papayannopoulos, V. *et al.*, (2010). Neutrophil elastase and myeloperoxidase regulate the formation of neutrophil extracellular traps. The Journal of Cell Biology, 191(3), pp.677–91.

Papayannopoulos, V. & Zychlinsky, A., (2009). NETs: a new strategy for using old weapons. *Trends in Immunology*, 30(11), pp.513–21.

Papillon MM & Lefèvre P., (1924). Deux cas de keratodermie palmaire et plantaire symmetrique familiale (maladie de Meleda) chez le frere et la soeur: coexistense dans les duex cas d'alterations dentaires gravis. *Bull Soc Fr Dermatol Syphilis*, 31, pp.81–87.

Paragh, G. *et al.*, (1999). Altered signal pathway in granulocytes from patients with hypercholesterolemia. *Journal of Lipid Research*, 40(9), pp.1728–33.

Parker, L.C. *et al*., (2005). The expression and roles of Toll-like receptors in the biology of the human neutrophil. *Journal of Leukocyte Biology*, 77(6), pp.886–92.

Pataro, A.L. *et al*., (2012). Influence of obesity and bariatric surgery on the periodontal condition. *Journal of Periodontology*, 83(3), pp.257–66.

Patel, L. *et al.*, (2003). Resistin is expressed in human macrophages and directly regulated by PPAR gamma activators. *Biochemical and Biophysical Research Communications*, 300(2), pp.472–6.

Pengelly, C.D.R. & Morris, J., (2009). Body mass index and weight distribution. *Scottish Medical Journal*, 54(3), pp.17–21.

Perera, N.C. *et al*., (2012). NSP4, an elastase-related protease in human neutrophils with arginine specificity. *Proceedings of the National Academy of Sciences*, 109(16), pp.6229–34.

Perlstein, M.I. & Bissada, N.F., (1977). Influence of obesity and hypertension on the severity of periodontitis in rats. *Oral Surgery, Oral Medicine, and Oral Pathology*, 43(5), pp.707–19.

Perreault, M. *et al.*, (2014). A distinct fatty acid profile underlies the reduced inflammatory state of metabolically healthy obese individuals. *PloS One*, 9(2), p.e88539.

Pertoft, H. *et al*., (1978). Density gradients prepared from colloidal silica particles coated by polyvinylpyrrolidone (Percoll). *Analytical Biochemistry*, 88(1), pp.271–282.

Pfosser, A. *et al.*, (2010). NF kappaB activation in embryonic endothelial progenitor cells enhances neovascularization via PSGL-1 mediated recruitment: novel role for LL37. *Stem Cells*, 28(2), pp.376–85.

Pham, C.T. & Ley, T.J., (1999). Dipeptidyl peptidase I is required for the processing and activation of granzymes A and B in vivo. *Proceedings of the National Academy of Sciences*, 96(15), pp.8627–32.

Pham, C.T.N., (2006). Neutrophil serine proteases: specific regulators of inflammation. *Nature Reviews. Immunology*, 6(7), pp.541–50.

Pham, C.T.N. et al., (2004). Papillon-Lefèvre Syndrome: Correlating the Molecular, Cellular, and Clinical Consequences of Cathepsin C/Dipeptidyl Peptidase I Deficiency in Humans. *Journal of Immunology*, 173(12), pp.7277–7281.

Phillips, J.E. & Gomer, R.H., (2012). A secreted protein is an endogenous chemorepellant in Dictyostelium discoideum. *Proceedings of the National Academy of Sciences*, 109(27), pp.10990–5.

Phillipson, M. & Kubes, P., (2011). The neutrophil in vascular inflammation. *Nature Medicine*, 17(11), pp.1381–90.

Pihlstrom, B.L., Michalowicz, B.S. & Johnson, N.W., (2005). Periodontal diseases. *Lancet*, 366(9499), pp.1809–20.

Pilcher, B.K. *et al.*, (1997). The activity of collagenase-1 is required for keratinocyte migration on a type I collagen matrix. *Journal of Cell Biology*, 137(6), pp.1445–57.

Pilkauskaite, G., Miliauskas, S. & Sakalauskas, R., (2013). Reactive oxygen species production in peripheral blood neutrophils of obstructive sleep apnea patients. *Scientific World Journal*, p.421763.

Pillay, J. *et al.*, (2010). In vivo labeling with 2H2O reveals a human neutrophil lifespan of 5.4 days. *Blood*, 116(4), pp.625–7.

Pilsczek, F.H. *et al*., (2010). A novel mechanism of rapid nuclear neutrophil extracellular trap formation in response to *Staphylococcus aureus*. *Journal of Immunology*, 185(12), pp.7413–25.

Pini, M. & Fantuzzi, G., (2010). Enhanced production of IL-17A during zymosan-induced peritonitis in obese mice. *Journal of Leukocyte Biology*, 87(1), pp.51–8.

Pischon, N. *et al.*, (2008). Association among rheumatoid arthritis, oral hygiene, and periodontitis. *Journal of Periodontology*, 79(6), pp.979–86.

Pluskota, E. *et al.*, (2008). Expression, activation, and function of integrin alphaMbeta2 (Mac-1) on neutrophil-derived microparticles. *Blood*, 112(6), pp.2327–35.

Pradhan, A.D. *et al*., (2001). C-reactive protein, interleukin 6, and risk of developing type 2 diabetes mellitus. *Journal of the American Medical Association*, 286(3), pp.327–34.

Pratley, R.E., Wilson, C. & Bogardus, C., (1995). Relation of the white blood cell count to obesity and insulin resistance: effect of race and gender. *Obesity Research*, 3(6), pp.563–71.

Preshaw, P.M. *et al.*, (2012). Periodontitis and diabetes: a two-way relationship. *Diabetologia*, 55(1), pp.21–31.

Pugin, J. *et al.*, (1999). Human neutrophils secrete gelatinase B in vitro and in vivo in response to endotoxin and proinflammatory mediators. *American Journal of Respiratory Cell and Molecular Biology*, 20(3), pp.458–64.

Rabkin, S.W., Boyko, E. & Streja, D.A., (1981). Relationship of weight loss and cigarette smoking to changes in high-density lipoprotein cholesterol. *American Journal of Clinical Nutrition*, 34(9), pp.1764–8.

Rahilly-Tierney, C.R. *et al.*, (2011). Relation between high-density lipoprotein cholesterol and survival to age 85 years in men (from the VA normative aging study*). American Journal of Cardiology*, 107(8), pp.1173–7.

Rahman, I., Skwarska, E. & MacNee, W., (1997). Attenuation of oxidant/antioxidant imbalance during treatment of exacerbations of chronic obstructive pulmonary disease. *Thorax*, 52(6), pp.565–8.

Rashid, S. & Genest, J., (2007). Effect of obesity on high-density lipoprotein metabolism. *Obesity*, 15(12), pp.2875–88.

Rausch, M.E. *et al.*, (2008). Obesity in C57BL/6J mice is characterized by adipose tissue hypoxia and cytotoxic T-cell infiltration. International Journal of Obesity (2005), 32(3), pp.451–63.

Redinger, R.N., (2009). Fat storage and the biology of energy expenditure. *Translational Research*, 154(2), pp.52–60.

Redline, S. *et al.*, (2010). Obstructive sleep apnea-hypopnea and incident stroke: the sleep heart health study. *American Journal of Respiratory and Critical Care Medicine*, 182(2), pp.269–77.

Redmon, J.B. *et al.*, (2003). One-year outcome of a combination of weight loss therapies for subjects with type 2 diabetes: a randomized trial. *Diabetes Care*, 26(9), pp.2505–11.

Redmon, J.B. *et al.*, (2005). Two-year outcome of a combination of weight loss therapies for type 2 diabetes. *Diabetes Care*, 28(6), pp.1311–5.

Reeves, E.P. *et al.*, (2002). Killing activity of neutrophils is mediated through activation of proteases by K+ flux. *Nature*, 416(6878), pp.291–7.

Reilly, D., Boyle, C.A. & Craig, D.C., (2009). Obesity and dentistry: a growing problem. *British Dental Journal*, 207(4), pp.171–5.

Reilly, S.M. & Saltiel, A.R., (2014). Countering inflammatory signals in obesity. *Nature Immunology*, 15(5), pp.410–1.

Rensen, S.S. *et al.*, (2009). Increased hepatic myeloperoxidase activity in obese subjects with nonalcoholic steatohepatitis. *The American Journal of Pathology*, 175(4), pp.1473–82.

Requena, J.R. *et al.*, (2001). Glutamic and aminoadipic semialdehydes are the main carbonyl products of metal-catalyzed oxidation of proteins. *Proceedings of the National Academy of Sciences*, 98(1), pp.69–74.

Richardson, L.C. & Pollack, L.A., (2005). Therapy insight: Influence of type 2 diabetes on the development, treatment and outcomes of cancer. *Nature Clinical Practice. Oncology*, 2(1), pp.48–53.

Rimm, E.B. *et al.*, (1995). Body size and fat distribution as predictors of coronary heart disease among middle-aged and older US men. *American Journal of Epidemiology*, 141(12), pp.1117–27.

Robache-Gallea, S. *et al.*, (1995). In Vitro Processing of Human Tumor Necrosis Factor- . *Journal of Biological Chemistry*, 270(40), pp.23688–23692.

Roberts, H. *et al.*, (2016). Characterization of neutrophil function in Papillon-Lefèvre syndrome. *Journal of Leukocyte Biology*.

Roberts, H.M. *et al.*, (2015). Impaired neutrophil directional chemotactic accuracy in chronic periodontitis patients. *Journal of Clinical Periodontology*, 42(1), pp.1–11.

Robinson, J.M., (2008). Reactive oxygen species in phagocytic leukocytes. *Histochemistry and Cell Biology*, 130(2), pp.281–97.

Rollins, B.J., (1997). Chemokines. *Blood*, 90(3), pp.909–28.

Roth, J.A., (1993). Evaluation of the influence of potential toxins on neutrophil function. *Toxicologic Pathology*, 21(2), pp.141–6.

Rouault, C. *et al.*, (2013). Roles of chemokine ligand-2 (CXCL2) and neutrophils in influencing endothelial cell function and inflammation of human adipose tissue. *Endocrinology*, 154(3), pp.1069–79.

Rubinstein, I., (1995). Nasal inflammation in patients with obstructive sleep apnea. *The Laryngoscope*, 105(2), pp.175–7.

Ryckman, C., Vandal, K., *et al.*, (2003). Proinflammatory activities of S100: proteins S100A8, S100A9, and S100A8/A9 induce neutrophil chemotaxis and adhesion. *Journal of Immunology*, 170(6), pp.3233–42.

Ryckman, C., McColl, S.R., *et al.*, (2003). Role of S100A8 and S100A9 in neutrophil recruitment in response to monosodium urate monohydrate crystals in the air-pouch model of acute gouty arthritis. *Arthritis and Rheumatism*, 48(8), pp.2310–20.

Ryu, O.H. *et al.*, (2005). Proteolysis of macrophage inflammatory protein-1alpha isoforms LD78beta and LD78alpha by neutrophil-derived serine proteases. *Journal of Biological Chemistry*, 280(17), pp.17415–21.

Saberi, M. *et al.*, (2009). Hematopoietic cell-specific deletion of toll-like receptor 4 ameliorates hepatic and adipose tissue insulin resistance in high-fat-fed mice. *Cell Metabolism*, 10(5), pp.419–29.

Sadik, C.D., Kim, N.D. & Luster, A.D., (2011). Neutrophils cascading their way to inflammation. *Trends in Immunology*, 32(10), pp.452–460.

Saito, H. *et al.*, (2005). Effect of antithrombin III on neutrophil deformability. Journal of leukocyte biology, 78(3), pp.777–84.

Saito, T. *et al.*, (2001). Relationship between Upper Body Obesity and Periodontitis. *Journal of Dental Research*, 80(7), pp.1631–1636.

Sakai, J. *et al.*, (2012). Reactive oxygen species-induced actin glutathionylation controls actin dynamics in neutrophils. *Immunity*, 37(6), pp.1037–49.

Salerno, F.G. *et al.*, (2004). Airway inflammation in patients affected by obstructive sleep apnea syndrome. *Respiratory Medicine*, 98(1), pp.25–8.

Sales-Peres, S.H. de C. *et al.*, (2015). Periodontal status and pathogenic bacteria after gastric bypass: a cohort study. Journal of Clinical Periodontology, 42(6), pp.530–6.

Sam, S., (2015). Adiposity and metabolic dysfunction in polycystic ovary syndrome. *Hormone Molecular Biology and Clinical Investigation*, 21(2), pp.107–16.

Sandborg, R.R. & Smolen, J.E., (1988). Early biochemical events in leukocyte activation. *Laboratory Investigation*, 59(3), pp.300–20.

Sandgren, S. *et al.*, (2004). The human antimicrobial peptide LL-37 transfers extracellular DNA plasmid to the nuclear compartment of mammalian cells via lipid rafts and proteoglycan-dependent endocytosis. *Journal of Biological Chemistry*, 279(17), pp.17951–6.

Sanikop, S., Patil, S. & Agrawal, P., (2012). Gingival crevicular fluid alkaline phosphatase as a potential diagnostic marker of periodontal disease. *Journal of Indian Society of Periodontology*, 16(4), pp.513–8.

Sapey, E. *et al.*, (2011). Behavioral and structural differences in migrating peripheral neutrophils from patients with chronic obstructive pulmonary disease. *American Journal of Respiratory and Critical Care Medicine*, 183(9), pp.1176–86.

Sapey, E. *et al.*, (2014). Phosphoinositide 3-kinase inhibition restores neutrophil accuracy in the elderly: toward targeted treatments for immunosenescence. *Blood*, 123(2), pp.239–48.

Sarwar, N. *et al*., (2007). Triglycerides and the risk of coronary heart disease: 10,158 incident cases among 262,525 participants in 29 Western prospective studies. *Circulation*, 115(4), pp.450–8.

Scapini, P. *et al.*, (2000). The neutrophil as a cellular source of chemokines. *Immunological Reviews*, 177(1), pp.195–203.

Scapini, P., Bazzoni, F. & Cassatella, M.A., (2008). Regulation of B-cell-activating factor (BAFF)/B lymphocyte stimulator (BLyS) expression in human neutrophils. *Immunology Letters*, 116(1), pp.1–6.

Schönbeck, U., Mach, F. & Libby, P., (1998). Generation of biologically active IL-1 beta by matrix metalloproteinases: a novel caspase-1-independent pathway of IL-1 beta processing. *Journal of immunology*, 161(7), pp.3340–6.

Schwartz, J. & Weiss, S.T., (1991). Host and Environmental Factors Influencing the Peripheral Blood Leukocyte Count. *American Journal of Epidemiology*., 134(12), pp.1402–1409.

Schymeinsky, J., Mócsai, A. & Walzog, B., (2007). Neutrophil activation via β2 integrins (CD11/CD18): Molecular mechanisms and clinical implications. *Thrombosis and Haemostasis*, 98(2), pp.262–273.

Scott, D.A. & Krauss, J., (2012). Neutrophils in periodontal inflammation. *Frontiers of Oral Biology*, 15, pp.56–83.

Semins, M.J. *et al.*, (2012). The impact of obesity on urinary tract infection risk. *Urology*, 79(2), pp.266–9.

Sergejeva, S. & Lindén, A., (2009). Impact of IL-17 on cells of the monocyte lineage in health and disease. *Endocrine, Metabolic & Immune Disorders Drug Targets*, 9(2), pp.178–86.

Sethi, J.K. & Vidal-Puig, A.J., (2007). Thematic review series: adipocyte biology. Adipose tissue function and plasticity orchestrate nutritional adaptation. *Journal of Lipid Research*, 48(6), pp.1253–62.

Shah, T.J., Leik, C.E. & Walsh, S.W., (2010). Neutrophil infiltration and systemic vascular inflammation in obese women. *Reproductive Sciences*, 17(2), pp.116–24.

Shahar, E. *et al.*, (2001). Sleep-disordered breathing and cardiovascular disease: cross-sectional results of the Sleep Heart Health Study. *American Journal of Respiratory and Critical Care Medicine*, 163(1), pp.19–25.

Sheppard, F.R. *et al*., (2005). Structural organization of the neutrophil NADPH oxidase: phosphorylation and translocation during priming and activation. *Journal of Leukocyte Biology*, 78(5), pp.1025–42.

Shi, H. *et al*., (2006). TLR4 links innate immunity and fatty acid-induced insulin resistance. *The Journal of Clinical Investigation*, 116(11), pp.3015–25.

Shin, J., Ji, S. & Choi, Y., (2008). Ability of oral bacteria to induce tissue-destructive molecules from human neutrophils. *Oral Diseases*, 14(4), pp.327–34.

Showell, H.J., (1976). The structure-activity relations of synthetic peptides as chemotactic factors and inducers of lysosomal secretion for neutrophils. *Journal of Experimental Medicine*, 143(5), pp.1154–1169.

Signat, B. *et al.*, (2011). *Fusobacterium nucleatum* in periodontal health and disease. *Current Issues in Molecular Biology*, 13, pp.25–36.

Skurk, T. *et al.*, (2007). Relationship between adipocyte size and adipokine expression and secretion. *Journal of Clinical Endocrinology & Metabolism*, 92(3), pp.1023–1033.

Smith, A., (1994). Neutrophils, host defense, and inflammation: a double-edged sword. *Journal of Leukocyte Biology*, 56, pp.672–686.

Smith, P.K. *et al.*, (1985). Measurement of protein using bicinchoninic acid. *Analytical Biochemistry*, 150(1), pp.76–85.

Socransky, S.S. & Haffajee, A.D., (2005). Periodontal microbial ecology. *Periodontology 2000*, 38, pp.135–87.

Sonta, T. *et al.*, (2004). Evidence for contribution of vascular NAD(P)H oxidase to increased oxidative stress in animal models of diabetes and obesity. *Free Radical Biology & Medicine*, 37(1), pp.115–23.

Sood, R. *et al.*, (2008). Binding of LL-37 to model biomembranes: insight into target vs host cell recognition. *Biochimica et Biophysica Acta*, 1778(4), pp.983–96.

Sörbris, R., Petersson, B.G. & Nilsson-Ehle, P., (1981). Effects of weight reduction on plasma lipoproteins and adipose tissue metabolism in obese subjects. *European Journal of Clinical Investigation*, 11(6), pp.491–8.

Sørensen, O.E. *et al.*, (2001). Human cathelicidin, hCAP-18, is processed to the antimicrobial peptide LL-37 by extracellular cleavage with proteinase 3. *Blood*, 97(12), pp.3951–9.

Sørensen, O.E. *et al.*, (2014). Papillon-Lefèvre syndrome patient reveals species-dependent requirements for neutrophil defenses. *Journal of Clinical Investigation*, 124(124(10)), pp.4539–4548.

Sossin, W.S., Fisher, J.M. & Scheller, R.H., (1990). Sorting within the regulated secretory pathway occurs in the trans-Golgi network. *The Journal of Cell Biology*, 110(1), pp.1–12.

Sperandio, M., Gleissner, C.A. & Ley, K., (2009). Glycosylation in immune cell trafficking. *Immunological Reviews*, 230(1), pp.97–113.

Stanford, J. *et al.*, (2012). The effect of weight loss on fasting blood sugars and hemoglobin A1c in overweight and obese diabetics and non-diabetics. *Journal of Diabetes Mellitus*, 02(01), pp.126–130.

Stark, M.A. *et al.*, (2005). Phagocytosis of apoptotic neutrophils regulates granulopoiesis via IL-23 and IL-17. *Immunity*, 22(3), pp.285–94.

Steegmaier, M. *et al.*, (1997). The E-selectin-ligand ESL-1 is located in the Golgi as well as on microvilli on the cell surface. *Journal of Cell Science*, 110(6), pp.687–694.

Van den Steen, P.E. *et al.*, (2003). Gelatinase B/MMP-9 and neutrophil collagenase/MMP-8 process the chemokines human GCP-2/CXCL6, ENA-78/CXCL5 and mouse GCP-2/LIX and modulate their physiological activities. *European Journal of Biochemistry*, 270(18), pp.3739–3749.

Van den Steen, P.E. *et al.*, (2000). Neutrophil gelatinase B potentiates interleukin-8 tenfold by aminoterminal processing, whereas it degrades CTAP-III, PF-4, and GRO-alpha and leaves RANTES and MCP-2 intact. *Blood*, 96(8), pp.2673–81.

Stoyanov, B. *et al.*, (1995). Cloning and characterization of a G protein-activated human phosphoinositide-3 kinase. *Science*, 269(5224), pp.690–693.

Stríz, I. & Trebichavský, I., (2004). Calprotectin - a pleiotropic molecule in acute and chronic inflammation. *Physiological Research / Academia Scientiarum Bohemoslovaca*, 53(3), pp.245–53.

Subrahmanyam, M. V & Sangeetha, M., (2003). Gingival crevicular fluid a marker of the periodontal disease activity. *Indian Journal of Clinical Biochemistry*, 18(1), pp.5–7.

Sun, L. & Ye, R.D., (2012). Role of G protein-coupled receptors in inflammation. *Acta Pharmacologica Sinica*, 33(3), pp.342–50.

Suvan, J. *et al.*, (2011). Association between overweight/obesity and periodontitis in adults. A systematic review. *Obesity Reviews*, 12(5), pp.e381–404.

Suvan, J. *et al.*, (2014). Body mass index as a predictive factor of periodontal therapy outcomes. *Journal of Dental Research*, 93(1), pp.49–54.

Suvan, J.E. *et al.*, (2015). Association between overweight/obesity and increased risk of periodontitis. *Journal of Clinical Periodontology*.

Swinburn, B.A. *et al.*, (2011). The global obesity pandemic: shaped by global drivers and local environments. *Lancet*, 378(9793), pp.804–14.

T.E. Van Dyke, M. Warbington, M. Gardner, and S.O., (1990). Surface Protein Markers Indicators of Defective Chemotaxis in LJP. *Journal of Periodontology*, 61(3), pp.180–184.

Talukdar, S. *et al.*, (2012). Neutrophils mediate insulin resistance in mice fed a high-fat diet through secreted elastase. *Nature Medicine*, 18(9), pp.1407–12.

Tan, J.S. *et al.*, (1975). Neutrophil dysfunction in diabetes mellitus. *The Journal of Laboratory and Clinical Medicine*, 85(1), pp.26–33.

Tani-Ishii, N. *et al.*, (1999). Autocrine regulation of osteoclast formation and bone resorption by IL-1 alpha and TNF alpha. *Journal of Dental Research*, 78(10), pp.1617–23.

Taylor, J.J., Preshaw, P.M. & Lalla, E., (2013). A review of the evidence for pathogenic mechanisms that may link periodontitis and diabetes. *Journal of Clinical Periodontology*, 40 Suppl 1, pp.S113–34.

Tecchio, C., Micheletti, A. & Cassatella, M.A., (2014). Neutrophil-Derived Cytokines: Facts Beyond Expression. *Frontiers in Immunology*, 5.

Telle-Hansen, V.H. *et al.*, (2013). Altered expression of genes involved in lipid metabolism in obese subjects with unfavourable phenotype. *Genes & Nutrition*, 8(4), pp.425–34.

Test, S.T. & Weiss, S.J., (1986). The generation of utilization of chlorinated oxidants by human neutrophils. *Advances in Free Radical Biology & Medicine*, 2(1), pp.91–116.

Theilgaard-Mönch, K. *et al.*, (2005). The transcriptional program of terminal granulocytic differentiation. *Blood*, 105(4), pp.1785–1796.

Thelen, M., Dewald, B. & Baggiolini, M., (1993). Neutrophil signal transduction and activation of the respiratory burst. *Physiological Reviews*, 73(4), pp.797–821.

Thompson, P.D. *et al.*, (1979). Unexpected decrease in plasma high density lipoprotein cholesterol with weight loss. *The American Journal of Clinical Nutrition*, 32(10), pp.2016–21.

van Tits, L.J. *et al.*, (2000). Oxidized low-density lipoprotein induces calcium influx in polymorphonuclear leukocytes. *Free Radical Biology & Medicine*, 29(8), pp.747–55.

Toetsch, S. *et al.*, (2009). The evolution of chemotaxis assays from static models to physiologically relevant platforms. *Integrative Biology*., 1(2), pp.170–181.

Toker, A. & Cantley, L.C., (1997). Signalling through the lipid products of phosphoinositide-3-OH kinase. *Nature*, 387(6634), pp.673–6.

Tomofuji, T. *et al.*, (2009). Effects of improvement in periodontal inflammation by toothbrushing on serum lipopolysaccharide concentration and liver injury in rats. *Acta Odontologica Scandinavica*, 67(4), pp.200–5.

Tonetti, M.S. & Claffey, N., (2005). Advances in the progression of periodontitis and proposal of definitions of a periodontitis case and disease progression for use in risk factor research. Group C consensus report of the 5th European Workshop in Periodontology. *Journal of Clinical Periodontology*, 32 Suppl 6, pp.210–3.

Toomes, C. *et al.*, (1999). Loss-of-function mutations in the cathepsin C gene result in periodontal disease and palmoplantar keratosis. *Nature Genetics*, 23(4), pp.421–4.

Trellakis, S. *et al.*, (2012). Low adiponectin, high levels of apoptosis and increased peripheral blood neutrophil activity in healthy obese subjects. *Obesity Facts*, 5(3), pp.305–18.

Trinchieri, G. & Sher, A., (2007). Cooperation of Toll-like receptor signals in innate immune defence. *Nature Reviews. Immunology*, 7(3), pp.179–90.

Tsai, C.C. *et al.*, (2005). Lipid peroxidation: a possible role in the induction and progression of chronic periodontitis. *Journal of Periodontal Research*, 40(5), pp.378–84.

Tziomalos, K., Dimitroula, H.V., Katsiki, N., Savopoulos, C. and Hatzitolios, A.I., (2010). Effects of Lifestyle Measures, Antiobesity Agents, and Bariatric Surgery on Serological Markers of Inflammation in Obese Patients. *Mediators of Inflammation*, 2010.

Uchida, K. & Stadtman, E.R., (1993). Covalent attachment of 4-hydroxynonenal to glyceraldehyde-3-phosphate dehydrogenase. A possible involvement of intra- and intermolecular cross-linking reaction. *The Journal of Biological Chemistry*, 268(9), pp.6388–93.

Udén, A.M. *et al.*, (1983). Neutrophil functions and clinical performance after total fasting in patients with rheumatoid arthritis. *Annals of the Rheumatic Diseases*, 42(1), pp.45–51.

Ueki, K. *et al.*, (2004). Central role of suppressors of cytokine signaling proteins in hepatic steatosis, insulin resistance, and the metabolic syndrome in the mouse. *Proceedings of the National Academy of Sciences of the United States of America*, 101(28), pp.10422–7.

Urban, C.F. *et al.*, (2006). Neutrophil extracellular traps capture and kill Candida albicans yeast and hyphal forms. *Cellular Microbiology*, 8(4), pp.668–76.

Urban, C.F. *et al.*, (2009). Neutrophil extracellular traps contain calprotectin, a cytosolic protein complex involved in host defense against Candida albicans. *PLoS pathogens*, 5(10), p.e1000639.

Vandal, K. *et al.*, (2003). Blockade of S100A8 and S100A9 Suppresses Neutrophil Migration in Response to Lipopolysaccharide. *The Journal of Immunology*, 171(5), pp.2602–2609.

Vandamme, D. *et al.*, (2012). A comprehensive summary of LL-37, the factotum human cathelicidin peptide. *Cellular Immunology*, 280(1), pp.22–35.

Vaswani, A.N., (1983). Effect of weight reduction on circulating lipids: an integration of possible mechanisms. *Journal of the American College of Nutrition*, 2(2), pp.123–132.

Vázquez, L.A. *et al.*, (2005). Effects of changes in body weight and insulin resistance on inflammation and endothelial function in morbid obesity after bariatric surgery. *Journal of Clinical Endocrinology and Metabolism*, 90(1), pp.316–22.

Veronelli, A. *et al.*, (2004). White blood cells in obesity and diabetes: effects of weight loss and normalization of glucose metabolism. *Diabetes Care*, 27(10), pp.2501–2.

Verploegen, S. *et al.*, (2002). Role of Ca2+/calmodulin regulated signaling pathways in chemoattractant induced neutrophil effector functions. *European Journal of Biochemistry*, 269(18), pp.4625–4634.

Vgontzas, A.N. *et al.*, (1997). Elevation of plasma cytokines in disorders of excessive daytime sleepiness: role of sleep disturbance and obesity. *Journal of Clinical Endocrinology and Metabolism*, 82(5), pp.1313–6.

Vincent, H.K. & Taylor, A.G., (2005). Biomarkers and potential mechanisms of obesity-induced oxidant stress in humans. *International Journal of Obesity*, 30(3), pp.400–418.

Vissers, M.C. & Winterbourn, C.C., (1991). Oxidative damage to fibronectin. I. The effects of the neutrophil myeloperoxidase system and HOCl. *Archives of Biochemistry and Biophysics*, 285(1), pp.53–9.

Vogl, T. *et al.*, (2007). Mrp8 and Mrp14 are endogenous activators of Toll-like receptor 4, promoting lethal, endotoxin-induced shock. *Nature Medicine*, 13(9), pp.1042–9.

Volek, J.S., Sharman, M.J. & Forsythe, C.E., (2005). Modification of Lipoproteins by Very Low-Carbohydrate Diets. *Journal of Nutrition*, 135(6), pp.1339–1342.

Wadden, T.A. *et al.*, (2001). Psychosocial aspects of obesity and obesity surgery. *Surgical clinics of North America*, 81(5), pp.1001–24.

Waddington, R.J., Moseley, R. & Embery, G., (2000). Reactive oxygen species: a potential role in the pathogenesis of periodontal diseases. *Oral Diseases*, 6(3), pp.138–51.

Wakai, K. *et al.*, (1999). Associations of medical status and physical fitness with periodontal disease. *Journal of Clinical Periodontology*, 26(10), pp.664–672.

Wakelin, S.J. *et al.*, (2006). "Dirty little secrets"--endotoxin contamination of recombinant proteins. *Immunology Letters*, 106(1), pp.1–7.

Walford, R.L., Harris, S.B. & Gunion, M.W., (1992). The calorically restricted low-fat nutrient-dense diet in Biosphere 2 significantly lowers blood glucose, total leukocyte count, cholesterol, and blood pressure in humans. *Proceedings of the National Academy of Sciences,* 89(23), pp.11533–11537.

Wang, Y. *et al.,* (2004). Human PAD4 regulates histone arginine methylation levels via demethylimination. *Science,* 306(5694), pp.279–83.

Wang, Y. *et al.,* (2009). Histone hypercitrullination mediates chromatin decondensation and neutrophil extracellular trap formation. *Journal of Cell Biology*, 184(2), pp.205–13.

Ware, C.F., (2008). Targeting lymphocyte activation through the lymphotoxin and LIGHT pathways. *Immunological Reviews*, 223, pp.186–201.

Weinrauch, Y. *et al*., (2002). Neutrophil elastase targets virulence factors of enterobacteria. *Nature,* 417(6884), pp.91–4.

Welin, A. *et al.,* (2013). The human neutrophil subsets defined by the presence or absence of OLFM4 both transmigrate into tissue in vivo and give rise to distinct NETs in vitro. *PloS one,* 8(7), p.e69575.

Wellen, K.E. & Hotamisligil, G.S., (2005). Inflammation, stress, and diabetes. *Journal of Clinical Investigation*, 115(5), pp.1111–1119.

Wells, A., (2000). Tumor invasion: role of growth factor-induced cell motility. *Advances in Cancer Research*, 78, pp.31–101.

Werling, M. *et al.,* (2013). Increased postprandial energy expenditure may explain superior long term weight loss after Roux-en-Y gastric bypass compared to vertical banded gastroplasty. *PloS One*, 8(4), p.e60280.

Wheeler, M.A. *et al.,* (1997). Bacterial infection induces nitric oxide synthase in human neutrophils. *Journal of Clinical Investigation*, 99(1), pp.110–6.

White, P., (2015). The role of neutrophil extracellular traps in the pathogenesis of periodontal diseases. *University of Birmingham*.

Whitehead, J.P. *et al.,* (2005). Adiponectin–a key adipokine in the metabolic syndrome. *Diabetes, Obesity and Metabolism*, 8(3), pp.264–280.

WHO, (2013). *Obesity and overweight. Factsheet No.311.,*

Wilkie-Grantham, R.P. *et al.,* (2015). Myeloperoxidase-dependent lipid peroxidation promotes the oxidative modification of cytosolic proteins in phagocytic neutrophils. *Journal of biological Chemistry*, 290(15), pp.9896–905.

Williams, M.R. *et al.,* (2011). Emerging mechanisms of neutrophil recruitment across endothelium. *Trends in Immunology,* 32(10), pp.461–9.

Wilson, M., Bronson, P. & Hamilton, R., (1995). Immunoglobulin G2 antibodies promote neutrophil killing of Actinobacillus actinomycetemcomitans. *Infection and Immunity*., 63(3), pp.1070–1075.

Winkel, P. *et al.,* (1981). Within-day physiologic variation of leukocyte types in healthy subjects as assayed by two automated leukocyte differential analyzers. *American Journal of Clinical Pathology*, 75(5), pp.693–700.

Winterbourn, C.C., (1985). Comparative reactivities of various biological compounds with myeloperoxidase-hydrogen peroxide-chloride, and similarity of the oxidant to hypochlorite. *Biochimica et Biophysica Acta*, 840(2), pp.204–10.

Wiseman, H. & Halliwell, B., (1996). Damage to DNA by reactive oxygen and nitrogen species: role in inflammatory disease and progression to cancer. *Biochemical Journal*, 313, pp.17–29.

Witko-Sarsat, V. *et al.,* (2000). Neutrophils: Molecules, Functions and Pathophysiological Aspects. *Laboratory Investigation*, 80(5), pp.617–653.

Wolf, I. *et al.,* (2005). Diabetes mellitus and breast cancer. *The Lancet. Oncology*, 6(2), pp.103–11.

Womack, J. *et al.,* (2007). Obesity and immune cell counts in women. *Metabolism: Clinical and Experimental*, 56(7), pp.998–1004.

Wong, J.H., Ng, T.B., *et al.,* (2011). Antifungal action of human cathelicidin fragment (LL13-37) on Candida albicans. *Peptides*, 32(10), pp.1996–2002.

Wong, J.H., Legowska, A., *et al.,* (2011). Effects of cathelicidin and its fragments on three key enzymes of HIV-1. *Peptides*, 32(6), pp.1117–22.

Woodfin, A. *et al.,* (2011). The junctional adhesion molecule JAM-C regulates polarized transendothelial migration of neutrophils *in vivo*. *Nature Immunology*, 12(8), pp.761–9.

Worthen, G.S. *et al.,* (1994). FMLP activates Ras and Raf in human neutrophils. Potential role in activation of MAP kinase. *Journal of Clinical Investigation*, 94(2), pp.815–23.

Wright, H.J. *et al.,* (2008). Periodontitis associates with a type 1 IFN signature in peripheral blood neutrophils. *Journal of Immunology*, 181(8), pp.5775–84.

Wright, H.J., Chapple, I.L.C. & Matthews, J.B., (2003). Levels of TGFbeta1 in gingival crevicular fluid during a 21-day experimental model of gingivitis. *Oral Diseases*, 9(2), pp.88–94.

Wright, T.K. *et al.,* (2016). Neutrophil extracellular traps are associated with inflammation in chronic airway disease. *Respirology*, 21(3), pp.467–75.

Wulster-Radcliffe, M.C. *et al.,* (2004). Adiponectin differentially regulates cytokines in porcine macrophages. *Biochemical and Biophysical Research Communications*, 316(3), pp.924–929.

Xu, W.D. *et al.,* (1989). Cytokines in chronic inflammatory arthritis. II. Granulocyte-macrophage colony-stimulating factor in rheumatoid synovial effusions. *Journal of Clinical Investigation*, 83(3), pp.876–82.

Yaegaki, M. *et al.,* (2007). Change in the capability of reactive oxygen species production by neutrophils following weight reduction in female judoists. *British Journal of Sports Medicine,* 41(5), pp.322–7.

Yang, D. *et al.,* (2009). Alarmins link neutrophils and dendritic cells. *Trends in Immunology*, 30(11), pp.531–7.

De Yang *et al.,* (2000). LL-37, the neutrophil granule- and epithelial cell-derived cathelicidin, utilizes formyl peptide receptor-like 1 (FPRL1) as a receptor to chemoattract human peripheral blood neutrophils, monocytes, and T cells. *Journal of Experimental Medicine,* 192(7), pp.1069–74.

Yao, Y. *et al.,* (2015). Neutrophil priming occurs in a sequential manner and can be visualized in living animals by monitoring IL-1β promoter activation. *Journal of Immunology*, 194(3), pp.1211–24.

Yipp, B.G. & Kubes, P., (2013). NETosis: how vital is it? *Blood,* 122(16), pp.2784–94.

Ylöstalo, P. *et al.,* (2008). Association between body weight and periodontal infection. *Journal of Clinical Periodontology*, 35(4), pp.297–304.

Yoshikawa, T. *et al.,* (2007). Impaired neutrophil chemotaxis in chronic obstructive pulmonary disease. *American Journal of Respiratory and Critical Care Medicine*, 175(5), pp.473–9.

Yu, B.P., (1994). Cellular defenses against damage from reactive oxygen species. *Physiological Reviews*, 74(1), pp.139–62.

Yu, H. *et al.,* (2011). Risk factors for severe illness with 2009 pandemic influenza A (H1N1) virus infection in China. *Clinical Infectious Diseases*, 52(4), pp.457–65.

Zaldivar, F. *et al.,* (2006). Body fat and circulating leukocytes in children. *International Journal of Obesity* (2005), 30(6), pp.906–11.

Zamarron, B. *et al*., (2015). Impact of weight loss on obese adipose tissue immune cell function (CAM1P.154). *Journal of Immunology,* 194(1 Supplement), pp.48.11–48.11.

Zarkesh-Esfahani, H. *et al*., (2004). Leptin indirectly activates human neutrophils via induction of TNF-alpha. *Journal of Immunology*, 172(3), pp.1809–14.

Zeidler, C. *et al.,* (2009). Clinical implications of ELA2-, HAX1-, and G-CSF-receptor (CSF3R) mutations in severe congenital neutropenia. *British Journal of Haematology*, 144(4), pp.459–67.

Zelkha, S.A., Freilich, R.W. & Amar, S., (2010). Periodontal innate immune mechanisms relevant to atherosclerosis and obesity. *Periodontology 2000*, 54(1), pp.207–21.

Zengel, P. *et al*., (2011). μ-Slide Chemotaxis: a new chamber for long-term chemotaxis studies. *BMC Cell Biology*, 12, p.21.

Zeyda, M. & Stulnig, T.M., (2007). Adipose tissue macrophages. *Immunology Letters*, 112(2), p.61.

Zhang, S. *et al.*, (1999). Differential effects of leukotactin-1 and macrophage inflammatory protein-1 alpha on neutrophils mediated by CCR1. *Journal of Immunology*, 162(8), pp.4938–42.

Zhang, Z. *et al.*, (2009). Evidence that cathelicidin peptide LL-37 may act as a functional ligand for CXCR2 on human neutrophils. *European Journal of Immunology*, 39(11), pp.3181–94.

Zhang, T. *et al.*, (2010). Aggregatibacter actinomycetemcomitans accelerates atherosclerosis with an increase in atherogenic factors in spontaneously hyperlipidemic mice. *FEMS Immunology and Medical Microbiology*, 59(2), pp.143–51.

Zhou, Q., Leeman, S.E. & Amar, S., (2009). Signaling mechanisms involved in altered function of macrophages from diet-induced obese mice affect immune responses. *Proceedings of the National Academy of Sciences of the United States of America*, 106(26), pp.10740–5.

Zhu, M. & Nikolajczyk, B.S., (2014). Immune cells link obesity-associated type 2 diabetes and periodontitis. *Journal of Dental Research*, 93(4), pp.346–52.

Zicha, D., Dunn, G.A. & Brown, A.F., (1991). A new direct-viewing chemotaxis chamber. *Journal of Cell Science*, 99 (Pt 4), pp.769–75.

Zigmond, S.H., (1977). Ability of polymorphonuclear leukocytes to orient in gradients of chemotactic factors. *Journal of Cell Biology*, 75(2 Pt 1), pp.606–16.

Zimmermann, G.S. *et al.*, (2013). Local and Circulating Levels of Adipocytokines in Obese and Normal Weight Individuals With Chronic Periodontitis. *Journal of Periodontology*, 84(5), pp.624–633.

Zlotnik, A. & Yoshie, O., (2000). Chemokines: a new classification system and their role in immunity. *Immunity*, 12(2), pp.121–7.

CHAPTER 8 - APPENDICES

8.1. Appendix I: 2-dimensional (2-D) μ-slide chemotaxis chamber

Cell migration assays based on microfluidic devices are becoming increasingly popular. The μ-slide (IBIDI, 80111) chemotaxis chamber is a 2-D microfluidic chamber that allows for long-term analysis of chemotaxing cells and for the observation of human leukocyte movement (Zengel *et al.* 2011). The device features two chambers connected by an internal channel to which cells are added via channel ports and allowed to adhere (Figure 8.1a). A gradient is then created by adding chemoattractant agents to either or both of the two chambers via the reservoir ports and migration of the cells is observed by video microscopy (Figure 8.1b).

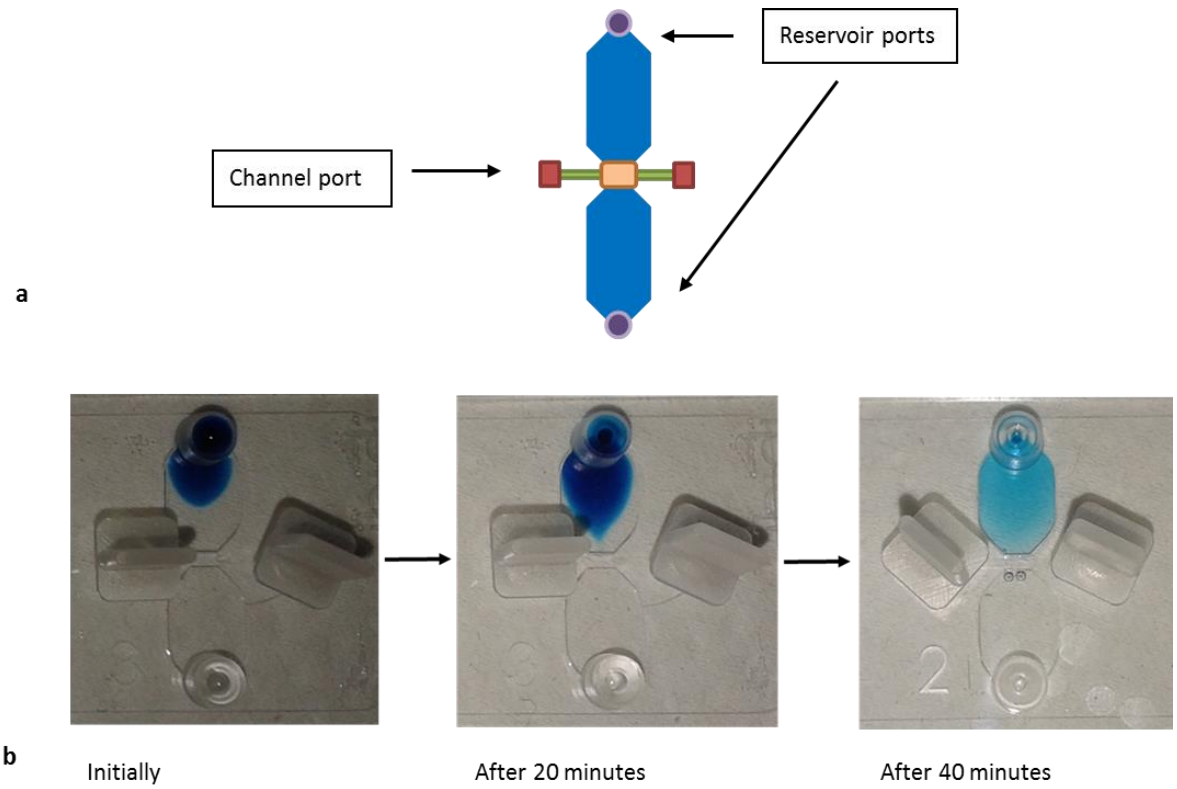

Figure 8.1 The µ-slide chamber

Diagrammatic representation of the chamber (a). Visualisation of the addition of chemoattractant showing gradient formation (b).

8.1.1. µ-slide chemotaxis method

The chamber was prepared by coating the internal channel with collagen IV (10µl, 100µg/ml in 0.05M HCl; Sigma, C5544). The chamber ports were all sealed with provided caps and incubated for 24 hours at room temperature. Post-incubation the collagen was aspirated out and the chamber was left to dry for an hour at room temperature. Cells (6µl, 5 x 10^6/ml) were introduced and the chamber was re-sealed and incubated at room temperature for 30 minutes. RPMI (negative control; 40µl), was added to both of the reservoirs. fMLP (10nM; 18µl) was added to one of the channel ports and the liquid was aspirated from the other side to allow diffusion through the reservoir (Figure I shows this; fMLP was dyed blue for visual purposes). Video microscopy was performed 40 minutes after addition of fMLP using the same parameters as the Insall chamber (ref. section in methods).

8.1.2. µ-slide chemotaxis analysis

The Manual tracking plugin (Fiji) was used to track cells using the µ-slide chamber. Ten cells were tracked in total and data was processed further using the Chemotaxis and Migration Tool (IBIDI website) which generates visual diagrams as well as qualitative measures.

8.1.3. Results

Figure 8.2a shows tracked cells and 8.2b shows the cell tracks with the same point of origin with the chemoattractant above, the centre of mass (blue cross) indicates the orientation of the cells is in an upwards fashion towards the source of the chemoattractant. Qualitative measurements included average speed, accumulated speed, Euclidean distance (distance in a particular direction) and the forward mass index (FMI) as shown in Figure 8.2c. These provide similar information to the analysis of chemotaxis using the Insall Chamber. An

additional statistical test provided by the Chemotaxis and Migration Tool and MATLAB (for use with the Insall chamber) is the Rayleigh test, a statistical test of the uniformity of a circular distribution of points, in which $p < 0.05$ accepts a heterogeneous spread of cells (I.e. cells lie more to one side of the circle than the other). In the example described here, $p = 0.0035$, however use of this test with RPMI (negative control) can yield similar p values which can give a misleading result. The Rayleigh test strongly depends on the number of cells analysed and so was not selected as an additional tool for chemotaxis analysis using the Insall chamber.

a

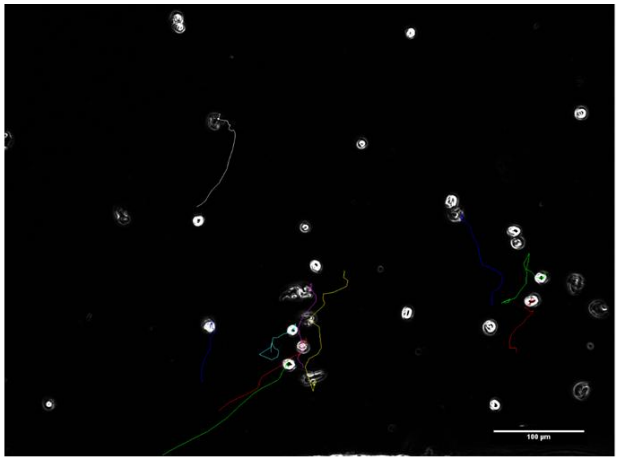

b

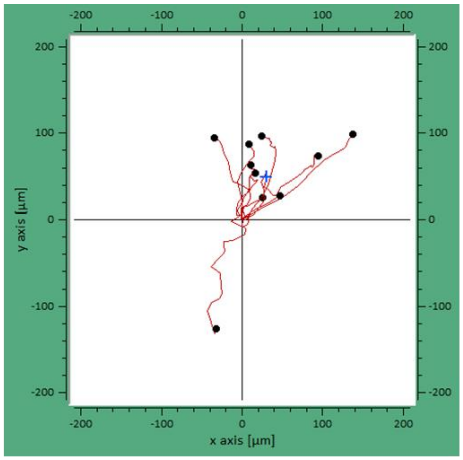

c

Track Number	Accumulated distance [µm]	Average speed (µm/min)	Euclidean distance [µm]	FMI
1	72.9	3.6	64.8	0.9
2	171.4	8.6	168.4	0.6
3	130.2	6.5	119.8	0.6
4	104.1	5.2	36.3	0.3
5	101.3	5.1	87.9	0.9
6	184.6	9.2	129.1	-0.7
7	125.7	6.3	99.6	0.8
8	120.4	6.0	100.9	0.8
9	129.9	6.5	54.1	0.2
10	81.1	4.1	56.1	0.7

Figure 8.2 Results generated from µ-slide chemotaxis assay

Neutrophils were isolated (section 2.2.2) and chemotaxis was performed (section 2.6), after which the cells were analysed using the Chemotaxis and Migration Tool. Cells were tracked using Fiji (a). Images of the cells can be generated with the same point of origin (b). Qualitative data of cell movements can also be calculated (c). (FMI = Forward Mass Index).

8.1.4. Conclusion

The µ-slide is another chemotaxis chamber appropriate for the study of leukocyte chemotaxis. The level of qualitative information that can be gathered using this chamber and its associated software is comparable to the Insall chamber; however difficulties were encountered with its use making it unsuitable for using with clinical samples. One such drawback was the long time required to establish the chemoattractant gradient, despite the improved linearity of the gradient once formed. The time-consuming application of the chamber, used for a short window of viewing (20 minutes) makes it a less attractive option. Furthermore, the chamber can only be used once whereas the Insall chamber requires only washing with distilled water and drying with lint wipes (Kimtech), making it a more cost-effective choice.

8.2. Appendix II: Periodontitis study additional information

8.2.1. Clinical attachment loss (CAL)

Clinical attachment loss (CAL) was calculated prior to treatment by summation of periodontal pocket depth and gingival recession measurements. The mean CAL and percentage sites with 1-2, 3-4 and >4mm CAL are shown in Table 8.1, which corresponds to mild, moderate and severe disease, respectively. Of the 20 patients initially recruited, one withdrew (patient 13) and another had a low cell count and could therefore not be used for measuring neutrophil chemotaxis (patient 19). Twelve patients (67%) presented with generalised moderate and localised severe chronic periodontitis, 3 patients (17%) presented with generalised mild and localised severe chronic periodontitis, and a further 3 patients also presented with generalised severe chronic periodontitis.

8.2.2. Periodontal pocket depth (PPD)

The number of periodontal probing depth (PPD) sites measuring over 4mm was significantly higher in patients, compared with healthy controls (unpaired t-test $p < 0.0001$, n = 18 pairs). Following treatment the difference was less compared with controls (unpaired t-test $p < 0.001$, n =18 pairs). The number of sites exceeding 4mm PPD in the patients significantly differed pre- versus post-treatment ($p = 0.0023$, n = 18 pairs), demonstrating the effect of non-surgical therapy in reducing pocket depths (unpaired t-test $p = 0.0023$, n = 18 pairs) in patients (Table 8.2).

8.2.3. Bleeding on probing (BOP)

The percentage of sites that displayed bleeding on probing (BOP) pre-treatment was significantly higher in patients before treatment compared with healthy controls (unpaired t-test $p < 0.0001$, n = 18 pairs). Following treatment the difference between patients and controls reduced but remained significant (unpaired t-test $p = 0.0478$, n = 18 pairs). The percentage of sites that bled upon probing in periodontitis patients was reduced when compared with pre-treatment measurements (unpaired t-test $p < 0.0001$, n = 18 pairs) (Table 8.3).

Table 8.1 Clinical attachment loss (CAL) measurements in periodontitis patients and healthy controls

Measurements from patients pre-treatment (n = 18). Data is presented as percentage sites with 1-2, 3-4 and >4mm clinical attachment loss (mean ± SD and range).

Patient no.	**Clinical attachment loss**				**Classification of chronic periodontitis**
	Mean ± SD (mm)	% sites 1-2mm	% sites 3-4mm	% sites >4mm	
1	4.4±3.2	39.1	21.8	39.1	Generalised severe
2	2.4±1.9	66.7	26.3	7	Generalised moderate, localised severe
3	3.7±2.1	36.5	35.3	28.2	Generalised moderate, localised severe
4	3.5±1.8	35.9	41	23.1	Generalised moderate, localised severe
5	2.8±1.6	59	24.4	16.6	Generalised moderate, localised severe
6	3.7±2.1	37	31.2	31.8	Generalised severe
7	3.4±2.4	55.6	21.6	22.8	Generalised moderate, localised severe
8	2.4±0.9	67.9	28.6	3.5	Generalised moderate, localised severe
9	3.4±1.6	36.9	45.8	16.3	Generalised moderate, localised severe
10	2.8±1.3	44.4	48.3	7.2	Generalised moderate, localised severe
11	2.2±1.8	85.7	5.4	8.9	Generalised mild, localised severe
12	2.9±2.6	66.1	13.3	20.6	Generalised moderate, localised severe
14	3.3±2.0	46.4	34.5	19	Generalised moderate, localised severe
15	3.9±1.6	20.1	50.3	29.6	Generalised moderate, localised severe
16	3.2±2.2	55.7	25.9	18.4	Generalised moderate, localised severe
17	5.9±3.3	25.6	11.9	62.5	Generalised severe
18	2.2±1.5	78	16.7	5.3	Generalised mild, localised severe
20	1.9±1.4	79	15.6	5.4	Generalised mild, localised severe
Mean	**3.4**	**48.7**	**28.2**	**23**	
SD	**1.1**	**21.1**	**12.4**	**16.8**	

Table 8.2 Probing pocket depth (PPD) measurements in periodontitis patients and healthy controls

Measurements from patients pre-treatment and post-treatment, compared with healthy matched controls (n = 18). Data is presented as probing pocket depths (mean ± SD and range) and the number of sites >4mm.

Patient no.	**Probing pocket depths**								
	Patient pre-treatment			**Patient post-treatment**			**Healthy control**		
	Mean ± SD (mm)	Range (mm)	No. sites >4mm	Mean ± SD (mm)	Range (mm)	No. sites >4mm	Mean ± SD (mm)	Range (mm)	No. sites >4mm
1	3.5±2.8	1-12	45	2.7±1.4	1-9	24	2.1±0.9	1-5	1
2	2.2±1.5	1-12	7	2.2±0.9	1-7	8	2.1±0.9	1-5	1
3	3.4±2.0	1-9	36	2.7±1.3	1-7	15	1.8±0.7	1-4	0
4	3.4±1.7	1-9	33	1.6±0.7	0-4	0	2.0±0.8	1-5	3
5	2.6±1.5	1-7	22	2.0±0.8	0-5	2	1.2±0.4	1-2	0
6	3.4±2.1	1-8	45	2.5±1.0	1-7	7	1.5±0.6	1-3	0
7	2.9±1.9	1-12	28	2.2±1.4	1-10	9	1.7±0.6	1-4	0
8	2.3±0.9	1-7	5	1.4±0.8	0-5	1	2.2±0.9	1-5	4
9	3.4±1.6	1-8	29	2.4±1.1	1-6	7	1.3±0.5	1-3	0
10	2.6±1.2	1-7	10	1.8±0.9	1-4	0	1.4±0.6	1-3	0
11	2.1±1.8	1-9	14	1.5±1.1	0-9	2	1.1±0.4	1-3	0
12	2.8±2.4	0-12	35	2.5±2.1	1-10	23	1.1±0.4	1-3	0
14	2.9±1.7	0-8	25	1.8±1.2	0-6	5	1.8±0.9	1-5	1
15	2.8±1.4	1-7	23	2.4±1.5	1-8	16	1.3±0.5	1-3	0
16	3.2±2.2	1-9	32	2.0±1.3	0-9	9	1.1±0.3	1-3	0
17	4.8±2.7	1-12	91	3.5±2.2	1-10	52	1.4±0.5	1-3	0
18	2.1±1.5	0-11	8	1.5±0.9	0-7	1	1.7±0.7	1-4	0
20	1.5±1.0	1-7	5	1.5±0.8	1-7	1	1.3±0.6	1-4	0
Mean	**2.9**			**2.2**			**1.6**		
SD	**0.66**			**0.5**			**0.4**		

Table 8.3 Bleeding on probing (BOP) in periodontitis patients

Percentage of sites that bled from the pocket base after periodontal probing in periodontitis patients pre- and post-treatment and healthy controls (n = 18). Data is presented as percentage sites with bleeding on periodontal probing.

	% BOP		
Patient no.	**Patient pre-treatment**	**Patient post-treatment**	**Control**
1	37	23	39
2	16	14	17
3	87	33	0
4	51	8	0
5	26	5	0
6	47	12	0
7	44	11	16
8	42	18	20
9	72	15	0
10	63	13	1
11	21	10	0
12	53	22	0
14	70	14	20
15	23	20	2
16	21	5	0
17	63	35	9
18	33	5	16
20	17	3	8
Mean	**43.7**	**14.8**	**8.2**
±SD	**21.3**	**9.1**	**11.0**

8.3. Appendix III: Chemotaxis with cathepsin G

Cathepsin G (CG) is known to cleave MIP1α chemoattractant (Ryu *et al.* 2005). This was confirmed by pre-incubating MIP1α with a concentration of cathepsin G known to be effective against bacterial lysis (25μg/ml; (Edwards 2005). Figure 8.3 shows the speed, velocity and chemotactic index (CI) using cathepsin G. RPMI and fMLP (10nm) were used as negative and positive controls to provide a reference for the other conditions, which included MIPα (100ng/ml) with/without GM-CSF (20pg/ml) priming and pre-incubation of the MIP1α with CG (25μg/ml) with/without GM-CSF priming.

The results demonstrated that exposure of MIP1α to CG results in attenuated chemotaxis. MIPα with/ GM-CSF priming showed significantly greater speed, velocity and a CI above that of MIPα in the absence of priming and in all conditions in which CG was incubated with MIPα prior to use in the assay.

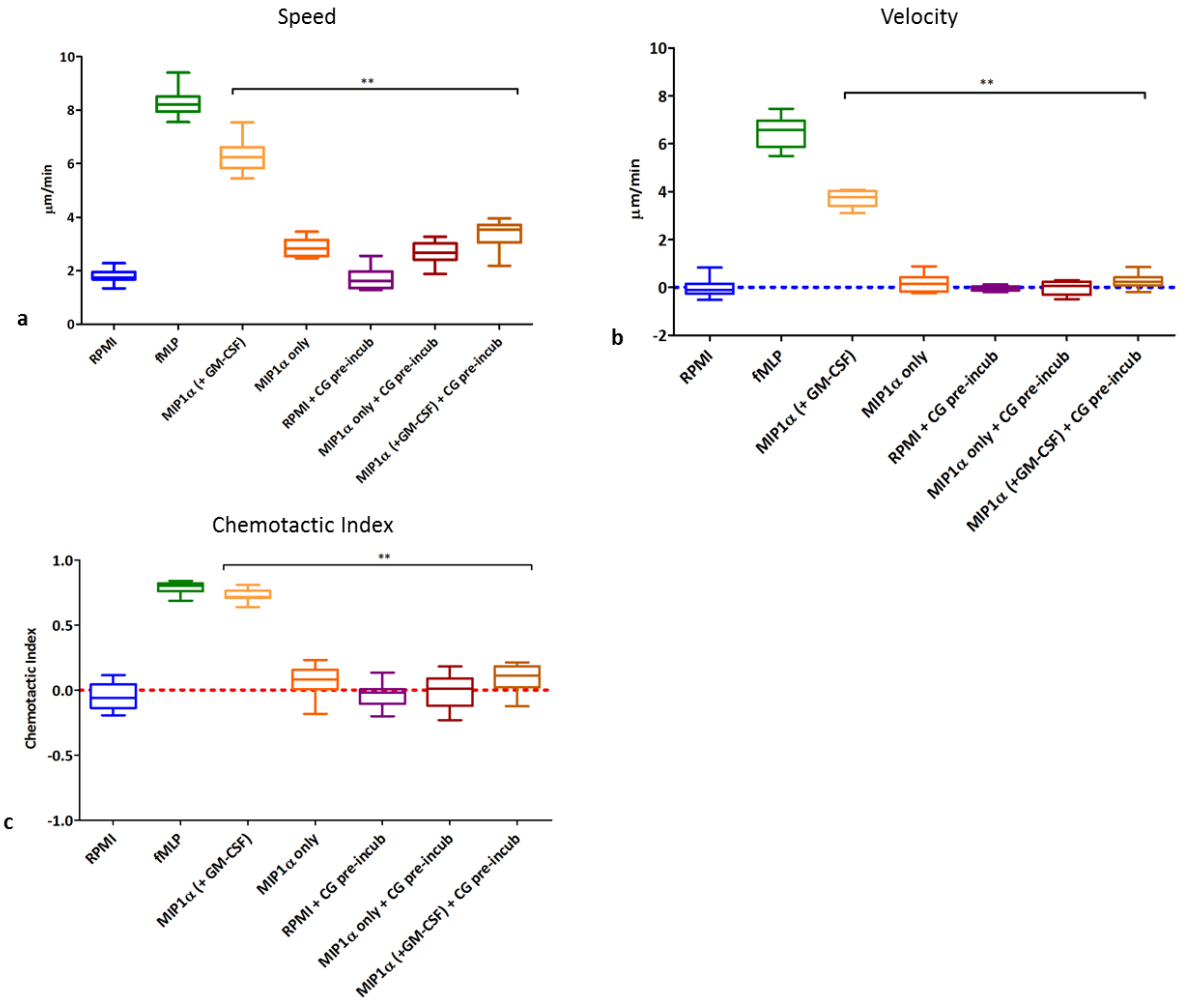

Figure 8.3 Chemotaxis with cathepsin G

Neutrophils were isolated (section 2.2.2) and chemotaxis was performed (section 2.6), after which the cells were analysed (section 2.6.2) and tracked information was used to generate speed (a), velocity (b) and CI (c) using MIP1α (100ng/ml) pre-incubated with/without CG (25µg/ml) and with/without GM-CSF priming (20pg/ml). (n = 10 different blood donors; 15 cells tracked per chemoattractant/RPMI). Statistical test: One Way ANOVA and Tukey's multiple comparisons test. * = ($p < 0.05$), *** = ($p < 0.001$).

8.3.1. Conclusion

These results show the importance of CG, and therefore NSPs, in regulating immune responses. The inactivation of chemokines such as MIP1α by NSPs released from neutrophils would serve to limit the further recruitment of neutrophils to the site of infection, as would occur during an infection in the oral tissues. These results outline an important role of NSP activity in the resolution of the immune response, supporting their loss of function as a major contributing factor to the development of periodontal disease in PLS.

8.4. Appendix IV: Obesity study additional information

Table 8.4 Bariatric patients and controls background information

Patient no.	Patient age	Control age	Gender	Patient co-morbidities
1	56	54	Male	Depression, hypertension, oedema
3	40	40	Female	osteoarthritis and sleep apnoea
5	58	56	Female	sleep apnoea, type 2 diabetes, dyslipidaemia
6	54	37	Female	Hypertension, Hyperlipidaemia, Osteoarthritis
7	38	39	Female	Sleep apnoea
8	43	38	Female	N/A
10	40	40	Female	Depression, osteoarthritis
11	42	48	Female	Diabetes (type 2), hypothyroidism, asthma, eczema,
12	50	52	Female	Diabetes (type 2), hypertension, osteoarthritis
13	58	56	Female	Sleep apnoea
14	41	41	Female	N/A
15	41	43	Female	Diabetes (type 2)
16	57	55	Female	Diabetes (type 2), hypertension
18	67	65	Female	Hypertension, sleep apnoea, depression, arthritis
19	45	43	Female	Sleep apnoea
21	61	61	Female	Diabetes (type 2), hypercholesterolaemia, hypertension, depression
22	24	27	Female	Arthritis, hypertension, 2 x knee replacements
23	51	51	Female	Osteoarthritis, Diabetes (type 2)
Mean ± SD (range)	48 ±10.5 (24-67)	47 ±*9.8* (27-65)		

Table 8.5 Patient weight loss

Patient No.	T1 Weight (kg)	T2 Weight (kg)	T3 Weight (kg)	Total weight loss (kg)	% Total weight loss between T1-3
1	150	141.9	126	24	19.0
3	162	159.8	124.4	37.6	30.2
5	101	98	88.3	12.7	14.4
6	148	143.5	138.6	9.4	6.8
7	134	125	118.8	15.2	12.8
8	106	101.6	97.4	8.6	8.8
10	115	117.3	114.8	0.2	0.2
11	151	143.6	132.4	18.6	14.0
12	132	129.1	126.4	5.6	4.4
13	149	134.6	129.8	19.2	14.8
14	112	107.2	93.8	18.2	19.4
15	122	118	109.1	12.9	11.8
16	147.4	140	120.7	26.7	22.1
18	119.2	113	107.6	11.6	10.8
19	120.2	116	103.6	16.6	16.0
21	145	139	119	26	21.8
22	101	94	87.2	13.8	15.8
23	117	110	98	19	19.4
Mean ± SD (range)	129.5 ±*19.3* (101-162)	123.9 ±*18.5* (94-109)	113.1 ±*15.7* (87-138)	16.4 ±*8.6* (0.2-37.6)	**14.6 ±*7.1* (0.17-30.2)**

8.5. Conference abstracts

- Helen Roberts*, Phillipa White, Irundika Dias, Sarah McKaig, Ratna Veeramachaneni, Nalin Thakker, Melissa Grant and Iain Chapple. "Characterisation of neutrophil dysfunction in Papillon-Lefévre Syndrome". Oral presentations at the British Society of Periodontology conference, Oxford 2016 and at the International Association of Dental Research Seoul, South Korea 2016.
- Helen Roberts*, Melissa Grant, Phillipa White & Iain Chapple. "An Assessment of neutrophil function in children with Papillon-Lefévre Syndrome". Oral presentation at the British Society for Oral and Dental Research conference in Cardiff September 14th-16th 2015.
- Helen Roberts*, Melissa Grant, Phillipa White & Iain Chapple. "An Assessment of neutrophil function in children with Papillon-Lefévre Syndrome". Poster presentation at the European Congress of Immunology in Vienna September 6-9th 2015.
- Helen Roberts*, Melissa Grant, Rishi Singhal, Paul Super & Iain Chapple. "Effect of obesity on innate immune function". Poster presentation at the International Association for Dental Research conference in Boston 2015.
- Helen Roberts* Phillipa White, Melissa Grant and Iain Chapple. "Neutrophil directional chemotaxis in children with Papillon-Lefévre Syndrome". Leukocyte Migration Conference 2015
- Helen Roberts*, Melissa Grant, Rishi Singhal, Paul Super & Iain Chapple. "Effect of obesity on neutrophil function". Poster presentation at Biochemical Society Meeting: Metabolic drivers of Immunity in Birmingham 2015
- Helen Roberts*, Martin Ling, Melissa Grant, Robert Insall and Iain Chapple. "Neutrophil chemotactic accuracy in periodontitis patients pre- and post-treatment" Poster presentation at the International Association for Dental Research conference in Cape Town 2014.
- Helen Roberts*, Martin Ling, Melissa Grant and Iain Chapple. "Neutrophils from periodontitis patients exhibit defective chemotaxis" presentation at the British Society for Oral and Dental Research conference in Bath September 2013.
- Helen Roberts*, Melissa Grant, Janet Lord, Jeremy Tomlinson & Iain Chapple "Effect of adipokine priming upon neutrophil reactive oxygen species (ROS) & extracellular trap release in response to stimulation by periodontal bacteria". Poster presentation at the Society for Free Radical Research in London 2012.

8.6. Awards, funding and other

- MRC-funded PhD
- Winner of the Sir Wilfred Fish Research Prize at the British Society of Periodontology conference, Oxford 2016.
- University of Birmingham Research Travel Grant 2015. Successful written grant proposal.

- BSODR Travel Bursary Award September 2015. Successful written grant proposal.
- University of Birmingham Research Showcase 2013. Oral presentation, 2nd prize.

8.7. Publications

Roberts, H., Ling, M., Insall, R., Kalna, G., Spengler, J., Grant, M., Chapple I. (2015) Impaired neutrophil directional chemotactic accuracy in chronic periodontitis patients. *Journal of Clinical Periodontology*. 42 (1) 1-11.

Roberts, H., White, P., Dia., I., McKaig S., Veeramachaneni, R., Thakker, N., Grant, M., Chapple, I. (2016) Characterization of neutrophil function in Papillon-Lefèvre Syndrome. *Journal of Leukocyte Biology* 100 (2) 433-444.

Koro C, Hellvard A, Delaleu N, Binder V, Scavenius C, Bergum B, Główczyk I, Roberts HM, Chapple IL, Grant MM, Rapala-Kozik M, Klaga K, Enghild JJ, Potempa J, Mydel P. (2016) Carbamylated LL-37 as a modulator of the immune response. *Innate Immunity*. 22(3) 218-29.

Muzila M., Rumpunen, K., Wright, H., Roberts, H., Grant, M., Nybom H., Sehic, J., Ekholm, A., Widén, C. (2016). Alteration of Neutrophil Reactive Oxygen Species Production by Extracts of Devil's Claw (Harpagophytum). *Oxidative Medicine and Cellular Longevity*. Volume 2016, Article ID 3841803, 9 pages.

IN PRESS: Hirschfeld, J., Roberts, H., Chapple, I., Parcina, M., Jepsen, S., Johansson, A., Claesson, R. (2016) Effects of Aggregatibacter actinomycetemcomitans leukotoxin. *Journal of Oral Microbiology*.

IN PRESS: White, P., Sakellari, D., Roberts, H., Risafi, I., Ling, M., Cooper, P., Milward, M., Chapple, I. (2016). Peripheral Blood Neutrophil Extracellular Trap Production and Degradation in Chronic Periodontitis. *Journal of Clinical Periodontology*.

J Clin Periodontol 2015; 42: 1–11 doi: 10.1111/jcpe.12326

Journal of Clinical Periodontology

Impaired neutrophil directional chemotactic accuracy in chronic periodontitis patients

Helen M. Roberts, Martin R. Ling, Robert Insall, Gabriela Kalna, Julia Spengler, Melissa M. Grant* and Iain L.C. Chapple*

Periodontal Research Group and MRC Centre for Immune Regulation, University of Birmingham, Birmingham, UK

*These authors contributed equally to this manuscript.

Roberts HM, Ling MR, Insall R, Kalna G, Spengler J, Grant MM, Chapple ILC. Impaired neutrophil directional chemotactic accuracy in chronic periodontitis patients. Journal of Clinical Periodontology 2015; 42: 1–11. doi: 10.1111/jcpe.12326.

Abstract

Aim: To investigate the chemotactic accuracy of peripheral blood neutrophils from patients with chronic periodontitis compared with matched healthy controls, before and after non-surgical periodontal therapy.

Material & Methods: Neutrophils were isolated from patients and controls (n = 18) by density centrifugation. Using the Insall chamber and video microscopy, neutrophils were analysed for directional chemotaxis towards *N*-formyl-methionyl-leucyl-phenylalanine [fMLP (10 nM), or CXCL8 (200 ng/ml)]. Circular statistics were utilized for the analysis of cell movement.

Results: Prior to treatment, neutrophils from patients with chronic periodontitis had significantly reduced speed, velocity and chemotactic accuracy compared to healthy controls for both chemoattractants. Following periodontal treatment, patient neutrophils continued to display reduced speed in response to both chemoattractants. However, velocity and accuracy were normalized for the weak chemoattractant CXCL8 while they remained significantly reduced for fMLP.

Conclusions: Chronic periodontitis is associated with reduced neutrophil chemotaxis, and this is only partially restored by successful treatment. Dysfunctional neutrophil chemotaxis may predispose patients with periodontitis to their disease by increasing tissue transit times, thus exacerbating neutrophil-mediated collateral host tissue damage.

Key words: chemoattractant; chemotaxis; neutrophil; periodontitis; treatment

Accepted for publication 27 October 2014

Chronic periodontitis is a disease that is initiated by the emergence of a pathogenic biofilm and characterized by non-resolving inflammation which leads to host-mediated tissue damage and bone loss around the teeth (Grossi et al. 1994). Chronic periodontitis can itself be a risk factor for other inflammatory diseases including type 2 diabetes (Chapple et al. 2013), rheumatoid arthritis (RA) (de Pablo et al. 2009) and cardiovascular diseases (Dietrich et al. 2013). The disease is characterized by a strong neutrophil tissue infiltrate (Van Dyke 2009) and tissue damage progresses as a result of abnormal host inflammatory-immune processes, eventually resulting in bone resorption and a receding gingival epithelial attachment (Graves & Cochran 2003).

The oral tissues are constantly exposed to foreign and potentially harmful microorganisms, and in order to combat potential infections in this vulnerable area, immune surveillance involves leucocyte infiltration into the tissues from the blood stream in response to endogenous and exogenous chemoattractants (Gamonal et al. 2001). Immune cells, including neutrophils, are recruited to the site of infection by chemokines such as CXCL8 (Interleukin-8) and CCL3 (macrophage inhibitory

Conflict of interest and source of funding statement

The authors declare that they have no conflict of interests arising from this work. This work was supported by the Birmingham and the Black Country Comprehensive Local Research Network (NIHR UKCRN Study ID 10318) and by the Medical Research Council.

© 2014 The Authors Journal of Clinical Periodontology Published by John Wiley & Sons Ltd
This is an open access article under the terms of the Creative Commons Attribution License, which permits use, distribution and reproduction in any medium, provided the original work is properly cited.

protein-1alpha-MIP1α) and other inflammatory stimuli including the bacteria-derived *N*-formyl-methionyl-leucyl-phenylalanine (fMLP). The ability of neutrophils to efficiently reach the site of inflammation is crucial in order to eliminate potentially pathogenic agents, whilst minimizing collateral host tissue damage. Pathogen-associated molecular patterns (PAMPs), damage-associated molecular patterns (DAMPs) and other molecules with chemoattractive properties, which include complement proteins such as C5a, and eicosanoids (leukotriene B4) and platelet activating factor (PAF), have different potencies, forming a chemical hierarchy that serves to recruit neutrophils to the source of inflammation. Those that elicit the strongest migration are molecules that emerge from the inflammation/infection source, including bacterial products such as fMLP.

Chemotaxis, the directional movement of cells in response to chemical gradients, is a highly conserved process occurring in a diverse number of organisms; in particular, there are strong similarities between cell movement in the unicellular *Dictyostelium discoideum* and neutrophils, both of which are able to navigate along shallow chemoattractant gradients (Van Haastert & Devreotes 2004). In the case of neutrophils, chemotaxis allows the cell to reach the infected/colonized area, in order to effect phagocytosis and subsequent destruction of the microorganisms by reactive oxygen species (ROS) and proteolytic enzymes, within the safe confines of the phagolysosome (Cooper et al. 2013). A number of interacting processes must occur for effective, coordinated cell movement, including recognition of the chemoattractant, internal signalling to reach the cells motility centre and gradient detection to influence movement in a persistent direction (Kolaczkowska & Kubes 2013). Chemoattractant binding induces polymerization of F-actin, the formation of new pseudopods at the leading edge and retraction at the posterior edge of the cell (Andrew & Insall 2007). In the absence of chemoattractants, these protrusions occur randomly at all edges of the cell. However, when a chemoattractant is detected, the protrusions are directed towards the source of the chemoattractant, determining the direction of migration (Andrew & Insall 2007).

To recognize the chemoattractant signal, neutrophils employ a number of receptors that are members of the transmembrane G-protein-coupled receptor (GPCR) family, activation of which triggers various signalling cascades that enable movement in a direction-specific manner. Both exogenous agents, such as bacteria-derived products, and endogenous factors, such as chemokines, activate respective GPCRs resulting in internalization, chemokine degradation and receptor recycling back to the cell membrane (Samanta et al. 1990). Downstream signalling (Fig. 1) results in the activation of the cytoskeleton in order for the cell to move. Receptor–ligand binding of chemoattractants results in the activation of phosphatidylinositol 3′-kinases (PI3Ks), protein kinases C (PKCs), tyrosine kinases, mitogen-activated protein kinases (MAPKs) and GTP binding proteins (Worthen et al. 1994). GPCR stimulation also induces intracellular calcium release via the inositol triphosphate and ryanodine receptors, which has been shown to be important for cellular chemotaxis (Berridge et al. 2003). Another receptor, activating intracellular calcium stores in neutrophils, stimulated by fMLP is the CD38 membrane glycoprotein (Partida-Sanchez et al. 2001). Intracellular calcium is released via the ryanodine receptor as a result of CD38 binding (Kurihara et al. 1993), and PI3K catalyses the formation of phosphatidylinositol 3,4,5-triphosphate (PIP_3)

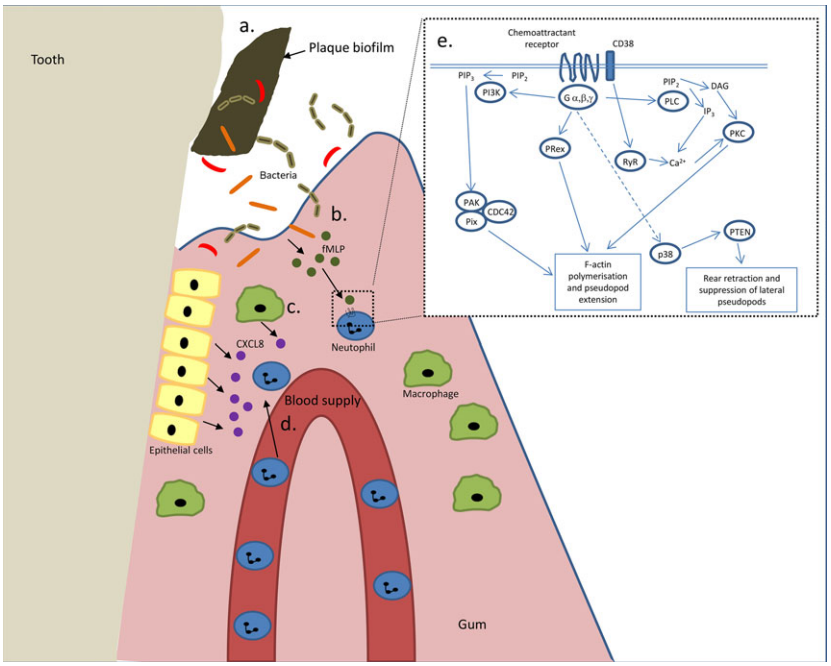

Fig. 1. Neutrophil recruitment to inflamed periodontal tissues. (a) The plaque biofilm is formed of diverse species of bacteria. (b) During infection, bacteria and their products penetrate the tissues surrounding the tooth and bacterial degradation products, such as fMLP, are released. fMLP is a potent chemoattractant. (c) After exposure to bacteria, resident macrophages and epithelial cells secrete CXCL8, another potent chemoattractant. (d) CXCL8 and fMLP attract circulating neutrophils, which leave the blood supply and enter the tissues to combat bacterial invasion. (e) Schematic representation of signalling events downstream of chemoattractant–receptor ligation. Upon binding to GPCR G-proteins dissociate and activate various proteins eventually resulting in movement of the cell via actin polymerization. Abbreviations: fMLP, formyl-methionyl-leucyl-phenylalanine; CXCL8, interleukin-8; PIP3, phosphatidylinositol 3,4,5-triphosphate; PIP2, phosphatidylinositol 4,5-biphosphate; PI3K, Phosphatidylinositol 3-kinase; PAK, p21-activated kinase; Prex, phosphatidylinositol-3,4,5-trisphosphate-dependent Rac exchange factor; RyR, ryanodine receptor located on intracellular calcium stores (e.g. endoplasmic reticulum); PLC, phospholipase C; PKC, protein kinase C; PTEN, phosphatase and tensin homologue.

© 2014 The Authors Journal of Clinical Periodontology Published by John Wiley & Sons Ltd

from phosphatidylinositol 4,5-biphosphate (PIP_2). PIP_3 acts as a second messenger controlling cell adhesion and cytoskeletal reorganization (Toker & Cantley 1997). In a cell, responding to a chemoattractant PIP_3 is found at the leading edge of the cell (Bagorda & Parent 2008). Downstream of receptor signalling the MAPK signalling pathway is also activated (Tsai et al. 2013). At the lagging end of the cell, retraction of the cell membrane is mediated by the phosphatase and tensin homologue (PTEN).

In addition to being a powerful microbicidal weapon employed by neutrophils, reactive oxygen species (ROS) produced by NADPH oxidases are also generated by chemoattractant stimulation and have been shown to play a role in signal transduction of cell movement (Dickinson & Chang 2011). Sakai et al. 2012 demonstrated that ROS produced by NADPH oxidase activity could regulate pseudopod formation and chemotactic migration in neutrophils via actin glutathionylation and polymerization. They also showed that inhibition of NADPH oxidase-dependent ROS formation within healthy neutrophils led to diminished chemotaxis efficiency when exposed to a chemoattractive gradient. Hydrogen peroxide, a membrane-permeable ROS, was able to direct cell movement in a gradient-driven manner (Niethammer et al. 2009), a finding supported by another study in which ROS were found to deactivate PTEN resulting in the build-up of PIP_3 at the leading edge of the migrating cell, necessary for chemotaxis (Kuiper et al. 2011).

Defective neutrophil chemotaxis features in several diseases including actin dysfunction syndrome, Chediak–Higashi syndrome, Crohn's disease and localized aggressive periodontitis (LAP) (Lakshman & Finn 2001). Although some studies have been published on neutrophil migratory behaviour in periodontitis (Clark et al. 1977, Van Dyke et al. 1980, Daniel et al. 1993), very few have been dedicated to the study of chronic periodontitis. In LAP, previously known as localized juvenile periodontitis (LJP) (Kantarci et al. 2003), a significant number (65–75%) of LAP sufferers have been shown to exhibit defective neutrophil chemotaxis (Lavine et al. 1979, Van Dyke et al. 1980, 1987, Page et al. 1985). Chemotaxis studies using Boyden chambers have reported impairment of neutrophil movement in chronic periodontitis relative to control subjects (Kumar & Prakash 2012). However, there is no information on visualization of chemotaxis in patients with chronic periodontitis; this measures the cell migration path in more detail, recording the direction, speed, velocity and morphology of the cells undergoing chemotaxis (Sackmann et al. 2014).

We have previously shown that peripheral blood neutrophils isolated from patients with chronic periodontitis display both a hyperactive phenotype (i.e. excess ROS production when unstimulated) and a hyperreactive phenotype (i.e. excess ROS production upon stimulation) relative to age- and gender-matched controls (Matthews et al. 2007a,b). Here, in order to expand on these findings and to evaluate neutrophil chemotaxis, we characterize the chemotactic response of peripheral neutrophils from patients with chronic periodontitis, compared with age- and gender-matched controls, prior to and following non-surgical periodontal therapy using advanced time-lapse microscopy techniques developed to study neutrophil movement in shallow chemoattractant gradients.

Materials and Methods

Study populations

Thirty-six volunteers were enrolled into this intervention study, including 18 with chronic mild–moderate periodontitis (eight females; 10 males; age mean ± standard deviation 46 ± 7 years) and 18 gender- and age-matched periodontally healthy controls (46 ± 8 years). All volunteers were never smokers and otherwise in good general health, as confirmed by a detailed medical history questionnaire. Chronic periodontitis was defined as the presence of at least two non-adjacent sites per quadrant with probing pocket depths >4 mm, which bled on probing and which demonstrated radiographic bone loss ≥30% of the root length (non-first molar or incisor sites) (Matthews et al. 2007a). Control patients had no evidence of attachment loss, no probing pocket depths >4 mm and whole-mouth bleeding scores <10%. Inclusion criteria were the complete absence of vitamin supplements, no use of anti-inflammatory or antibiotic medication in the previous 3 months, no pregnancy, mouthwash use or special dietary needs (Brock et al. 2004). All volunteers provided written informed consent, and ethical approval for the study was obtained from the West Midlands Research Ethics Committee (number 10/H1208/48). After enrolment, all volunteers were re-appointed for collection of baseline blood samples and clinical measures. Patients received oral hygiene instruction and conventional non-surgical therapy, in the form of scaling and root surface debridement (RSD), performed under local anaesthesia on a quadrant-by-quadrant basis within a maximum of 4 weeks. Patients were recalled 3-months post-therapy to provide a repeat blood sample and clinical measures. A 3-month recall was chosen to allow for initial healing and to reduce the risk of re-infection/disease re-activation (Chapple et al. 2007a,b). Neutrophil isolation and chemotaxis data were obtained for volunteers following treatment along with their matched healthy controls. Clinical data for the patients with periodontitis pre- and post-treatment and for the healthy volunteers is shown in Table 1.

Collection of blood and preparation of neutrophils

Venous blood was collected from the ante-cubital fossa into VacutainerTM lithium heparin (17 IU/ml) tubes, and neutrophils were isolated using Percoll density gradients (GE Healthcare) as previously described (Matthews et al. 2007a). Briefly, two discontinuous gradients, 1.079 and 1.098, were used for neutrophil isolation with concomitant erythrocyte lysis (0.83% NH_4Cl containing 1% $KHCO_3$, 0.04% EDTA and 0.25% BSA). Isolated cells were re-suspended in PBS supplemented with glucose (1 mM) and cations (1 mM $MgCl_2$, 1.5 mM $CaCl_2$) at 1×10^6 cells/ml. Cell viability, typically >98%, was determined by dye exclusion (trypan blue). Cell purity was determined by cytospin and

© 2014 The Authors Journal of Clinical Periodontology Published by John Wiley & Sons Ltd

Table 1. Age, probing pocket depths, number of sites >4 mm, percentage sites with bleeding on probing, and gingival and plaque indices of patient and healthy control volunteers

	Patients with chronic periodontitis		Healthy controls (n = 18)
	Pre-treatment (n = 18)	Post-treatment (n = 16)	
Probing pocket depths (mean ± SD)	3.0 ± 0.9 ($p < 0.001$)*	2.2 ± 0.6 ($p < 0.001$)#	1.6 ± 0.4
Probing pocket depths >4 mm (median; range)	26.5 (5–91) ($p < 0.001$)*	7.5 (0–52) ($p < 0.01$)#	0 (0–4)
% bleeding on probing (median; range)	41.5 (16–87) ($p < 0.001$)*	14 (3–35) ($p < 0.001$)#	1.5 (0–39)
Gingival index (median; range)	2 (1–3) ($p < 0.001$)*	1 (0–1) ($p < 0.01$)#	1 (0–1)
Plaque index (median; range)	2 (1–3) ($p < 0.01$)*	1 (0–2) ($p < 0.01$)#	1 (0–2)

*p values in parenthesis are comparisons with controls.
#p values in parenthesis are comparisons with chronic periodontitis before treatment.

fluorescence-activated cell sorting (FACS) using CD15 and CD66 neutrophil surface markers.

Chemotaxis protocol

The Insall chamber was used to visualize chemotaxis (Muinonen-Martin et al. 2010). For each sample, isolated neutrophils (400 µl in RPMI, final density 1 × 10^6/ml) were added to acid washed (0.2 M HCl), dried and blocked (7.5%, BSA 400 µl, Sigma) coverslips (22 mm, VWR International), which were then incubated at room temperature (approximately 23°C) for 30 min. to allow the cells to adhere. The coverslip was then inverted and placed at the top of the chemotaxis chamber ensuring that the chemoattractant loading bays were exposed (Fig. 2). The desired chemoattractant (80 µl, fMLP (10 nM) or CXCL8 (used at 200 ng/ml after assessing a range of concentrations) or control (RPMI media) was injected into the chemoattractant channels. Cell movement was analysed using a Zeiss Primovert microscope (Carl Zeiss Imaging, Thornwood, NY, USA) and Images captured every 30 s for up to 40 frames per condition using a Q Imaging Retiga 2000R camera (Qimaging, Surry, Canada).

Image analysis

The images generated by video microscopy were processed using Q pro-imaging software (Surrey, Canada) and analysed further using ImageJ 1.45SR software (National Institutes of Health, Bethesda, USA). The manual tracking plug-in (MtrackJ) was employed, and for each set of images, 15 cells were chosen at random and tracked through the frames. The numerical data generated was used to calculate cell speed, cell velocity and chemotactic index (CI) per experiment. The numerical data generated were then used to calculate cell migration, which was defined as follows:

1 Cell speed: the average speed of a cell in any direction over the time course.
2 Cell velocity: the average speed of a cell in its most prominent direction over the time course.
3 Chemotactic Index: this is a measure of the directional accuracy of chemotaxis. It is calculated as a change in the angle of a cell along the Y axis according to the cosine plot (Andrew & Insall 2007).

Statistical analysis

XY coordinates of the cells were generated using the Manual tracking Plugin and ImageJ software (Rasband, W.S., ImageJ, U. S. National Institutes of Health, Bethesda, MD, USA) and these were further analysed with the circular statistics (CircStat) toolbox from MATLAB (Mathworks, Natick, MA, USA) software to ascertain the significance of the cells' movement over the time course. The CircStat toolbox provides statistics for directional data, including the mean direction, known as the resultant vector, the length of which indicates the strength of the direction taken by the cells. Results are represented as circular diagrams. Two representations are shown (Figs 3 and 4): (1) resultant vector plots showing the distribution of the final angle of all cells in the experiment with a vector line showing the mean angle and vector length, illustrating the strength of the movement; and (2) rose plots showing the proportion of cells in each

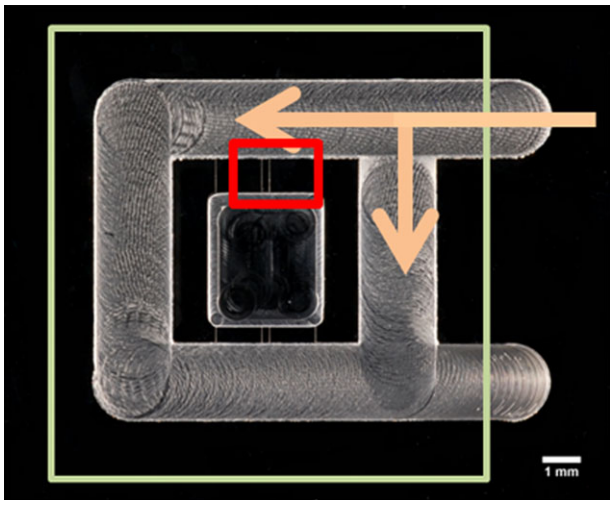

Fig. 2. Photograph of the Insall chamber. Large square illustrates position of the coverslip with adhered neutrophils. Arrows show the application of the chemoattractant. Small red rectangle shows the area visualized by video microscopy.

© 2014 The Authors Journal of Clinical Periodontology Published by John Wiley & Sons Ltd

of 18 segments around the circle, the larger the bar the greater proportion of cells that moved in that direction. Data were further summarized in box and whisker plots, and statistical analysis of these was performed by Wilcoxon test using Prism 5.0 software (GraphPad, San Diego, California USA). Volunteer age was compared by paired *t*-test and probing pocket depths by repeated measures ANOVA followed by Tukey–Kramer multiple comparisons test. The number of probing pocket depths >4 mm, percentage bleeding on probing, and gingival and plaque indices were compared using Friedman test followed by Dunn's multiple comparisons test.

Results

Clinical findings for patients and their matched controls, pre- and post-treatment, are shown in Table 1. Figures 3 and 4 depict summaries of all the data collected pre- or post treatment, respectively. Each dataset comprises three graphs: the top image is a "spider plot" of individual cell movement tracks towards the "12.00 o'clock" position; the lower left image is a rose plot that clusters groups of cells according to their direction of movement; and the lower right image is a vector plot that indicates the strength and angle of movement. It is clear to see the difference in the strength of the two chemoattractants CXCL8 and fMLP, with fMLP producing the strongest response evidenced by longer cell tracks in the spider diagrams. The control-treated cells (RPMI), as anticipated, show very little movement and no obvious directionality of movement.

Statistical analyses of these data (Figs 5 and 6) demonstrate that before treatment, neutrophils from patients with periodontitis have significantly lower speed, velocity and directional accuracy (chemotactic index and resultant vector length) than neutrophils from healthy controls for both chemoattractants, CXCL8 and fMLP. Following treatment, they still display significantly reduced speed, velocity and accuracy than neutrophils from healthy

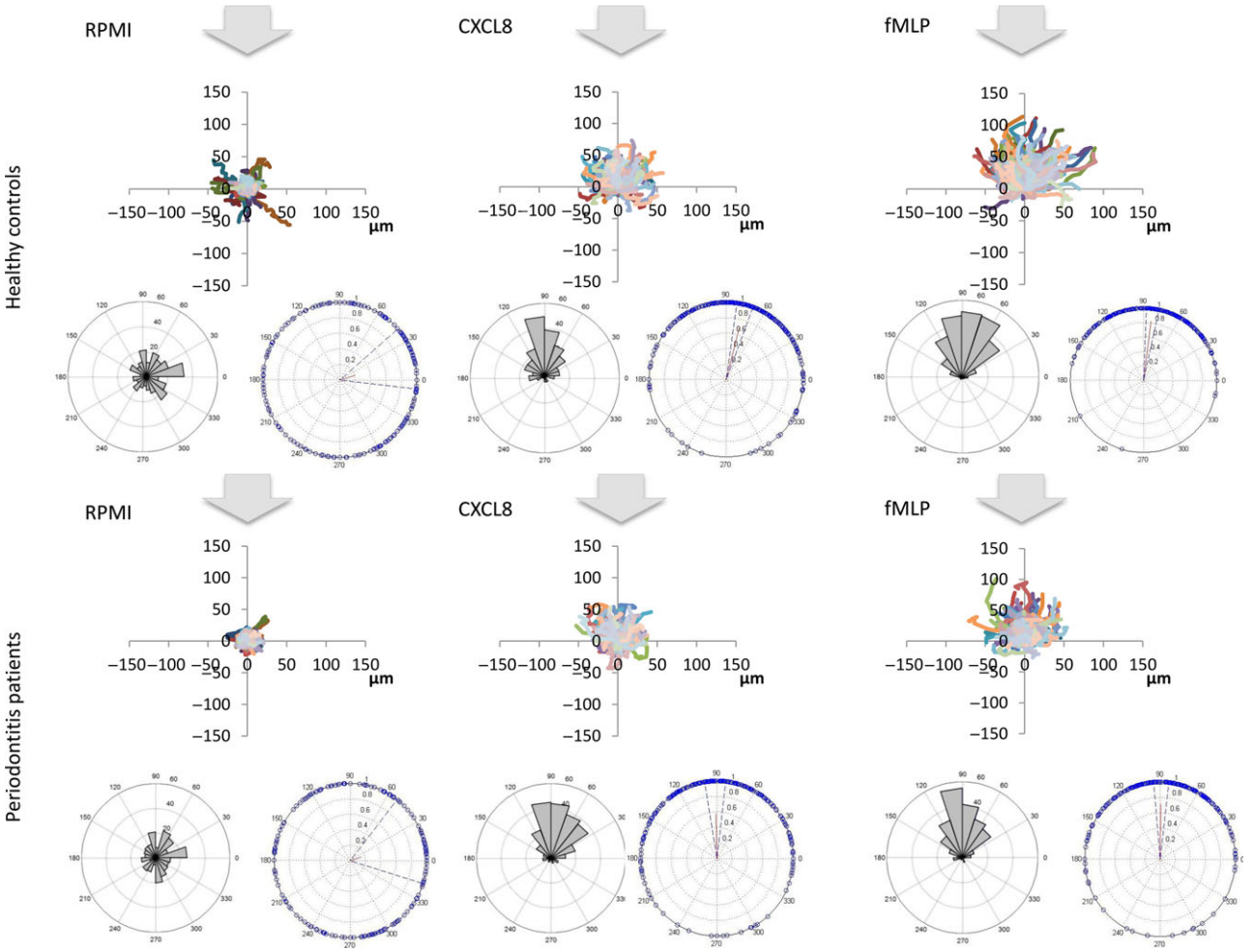

Fig. 3. Summary of Pre-treatment results: arrows denote the origin of the chemoattractant, cells should be attracted towards the arrow; spider diagrams show movement of all cells (um) from place of origin; left hand side vector plots show the proportion of cells in each segment and the angle of the segment towards the arrow; right hand side rose plots show the strength of movement and its directionality for the whole cohort of cells, the small red line shows the vector and the bounding dashed lines show the variation within the data. All diagrams are represented at the same scale to aid comparison.

© 2014 The Authors Journal of Clinical Periodontology Published by John Wiley & Sons Ltd

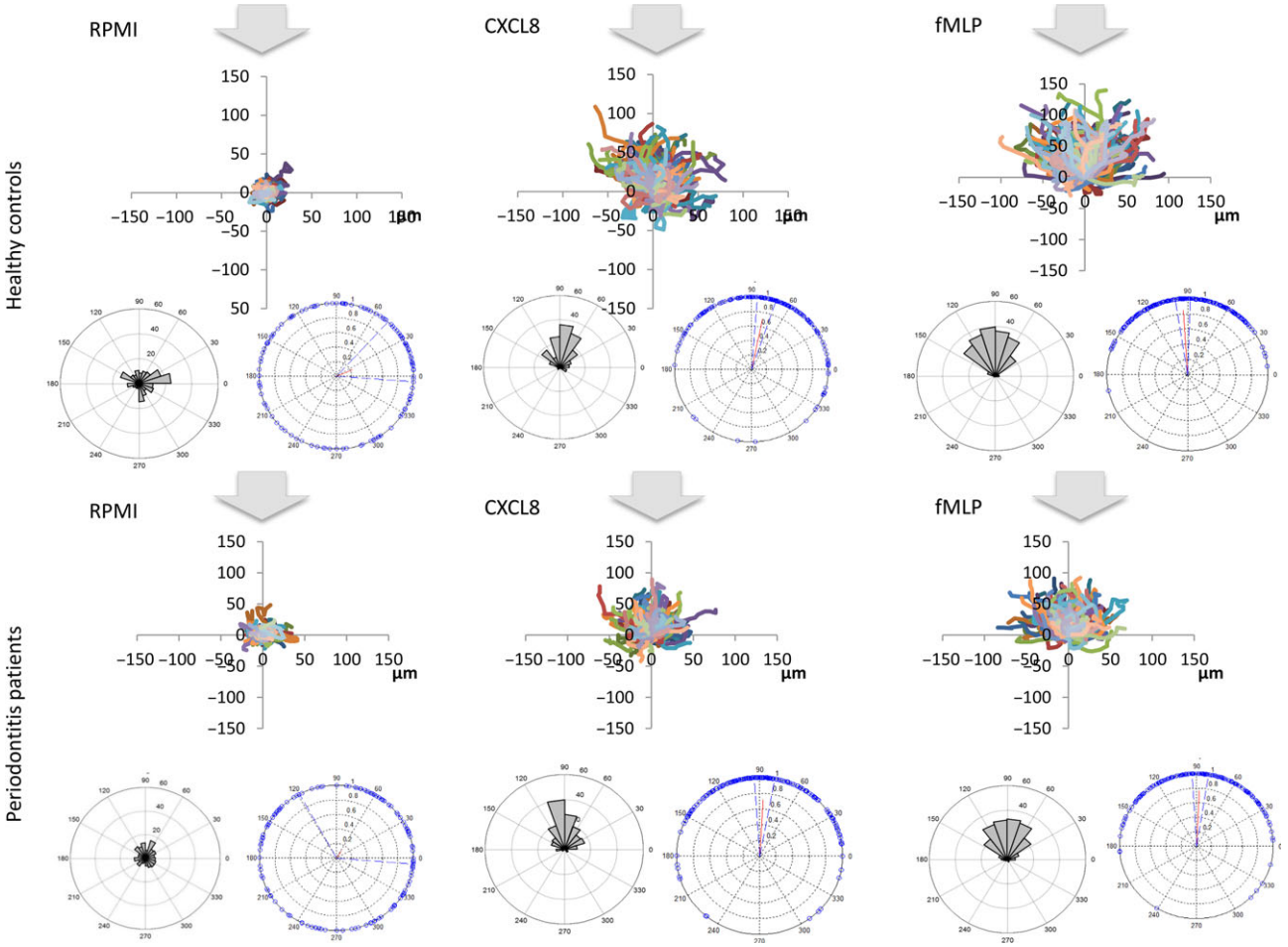

Fig. 4. Summary of post-treatment results. The diagrams illustrate three plots per condition, as described in Fig. 3.

control volunteers for fMLP; however, with the exception of speed, the neutrophils from patients with periodontitis were not significantly different in their response to CXCL8 following therapy, in comparison to neutrophils from healthy volunteers. Patient and control pre- and post-treatment results were analysed separately because of the high inter-individual variation that arises when neutrophils are analysed on different days. Therefore, patient and control cells were analysed synchronously at both baseline and then again simultaneously following therapy, but no attempt was made to compare patients' cells pre- and post-treatment (or controls).

Discussion

This study has demonstrated for the first time that neutrophils from patients with chronic periodontitis exhibit reduced chemotactic accuracy compared to gender- and age-matched controls. Patient neutrophils were less responsive to the widely used chemoattractants fMLP and CXCL8 with regard to chemokinesis and chemotaxis when compared to respective controls.

Direct visualization chambers, including the Zigmond, Dunn and the Insall chambers (the latter was used in this study) allow cells to be observed migrating using time-lapse video microscopy in real time (Wells 2000). Bridge chambers provide a visualization platform for observing the behaviour of cells between two wells. These chambers provide gradients for the cells to accelerate towards rather than exposure to absolute concentrations alone. The majority of studies examining the defects in neutrophil chemotaxis over the last 30 years used the Boyden chamber (and its derivatives) to study chemotaxis (Clark et al. 1977, Van Dyke et al. 1980, 1987, Offenbacher et al. 1987, Daniel et al. 1993, Yagi et al. 2009). Other studies (Henry et al. 1984) employed the checkerboard assay described by Zigmond & Hirsch (1973). The use of the Insall chamber has recently expanded (Phillips & Gomer 2012, Choi et al. 2013, Herlihy et al. 2013a,b, Kaul et al. 2013) and opened up new research questions, which informed the present study. Here, we report on speed, velocity and chemotactic accuracy. Chemotactic accuracy has been expressed as both chemotactic index (Sapey et al. 2011) and as resultant vector analysis (Andrew & Insall 2007); however, here, we have demonstrated that these two factors are interchangeable (Fig. S1, Bland-Altman analysis).

Although there are few studies examining chemotaxis in chronic periodontitis (Kumar & Prakash

© 2014 The Authors Journal of Clinical Periodontology Published by John Wiley & Sons Ltd

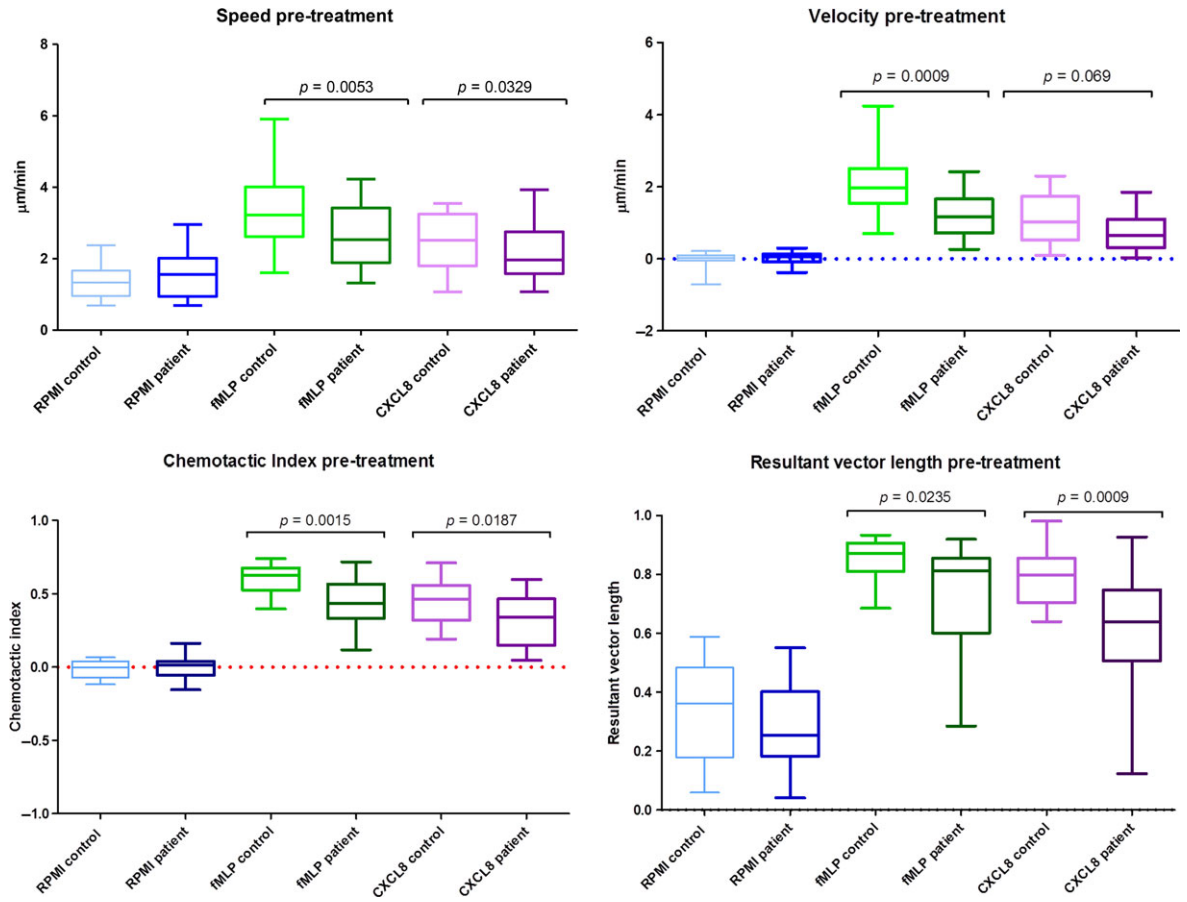

Fig. 5. Analysis of pre-treatment results: extracted values for each individual's speed, velocity, chemotactic index and resultant vector length were analysed for statistical difference (Wilcoxon test). The midline of each box represents median, bounding box the 25th and 75th percentiles and the whiskers the extremities of the data sets.

2012), there is a wealth of data concerning chemotaxis in patients with localized aggressive periodontitis (LAP). It is important to note that LAP is distinctly different from chronic periodontitis as it occurs in otherwise systemically healthy adolescents; the bacteria that colonize the oral tissues in these individuals are different in composition to chronic periodontitis; and there is a strong genetic pre-disposition to the disease (Fu et al. 2002, Nibali et al. 2008). Defective LAP neutrophils, however, offer an attractive platform to better understand and characterize defects in the ability of neutrophils to chemotax and the mechanism of neutrophil movement in response to stimuli presented as chemical gradients. LAP is the best-characterized periodontal disease showing impaired neutrophil function. Whether there is cross-correlation between neutrophil abnormalities in patients with chronic periodontitis and patients with LAP remains to be elucidated.

We have previously reported that peripheral blood neutrophils from patients with chronic periodontitis are both hyperactive and hyperreactive with respect to ROS generation (Matthews et al. 2007a,b) and that potential stimulants of these responses within plasma include GM-CSF, CXCL8 and interferon-α (IFN-α) (Dias et al. 2011). IFN-α is also capable of priming neutrophils within the circulation of patients with periodontitis and demonstrates elevated plasma levels, consistent with reported IFN-α responsive gene expression profile in neutrophils from patients with periodontitis (Wright et al. 2008). However, an element of ROS hyperactivity in periodontitis neutrophils appears to be constitutive (an innate property), and this may be due to an altered intracellular redox state in neutrophils from patients with periodontitis (Dias et al. 2013). Additionally, *Porphyromonas gingivalis*-derived gingipains can cleave CXCL8, potentially impacting upon ROS production and chemotaxis (Dias et al. 2008). This may be one plausible explanation why, in the present study, we observed a normalization of patient neutrophil responses to CXCL8 following successful treatment, but not for fMLP. Of the various neutrophil chemoattractants reported in the literature, a number of the host-derived chemoattractants demonstrated a similar pattern of activity to IL-8. We found similar results to IL-8 for GM-CSF and macrophage inhibitory protein 1alpha (MIP1α) (data not shown) whose receptors are all G-protein-coupled receptor linked. The enhanced ROS generation we have reported previously and the defective chemotactic accuracy observed in this study of patients with chronic periodontitis have also been shown in individuals with other inflammatory-driven

© 2014 The Authors Journal of Clinical Periodontology Published by John Wiley & Sons Ltd

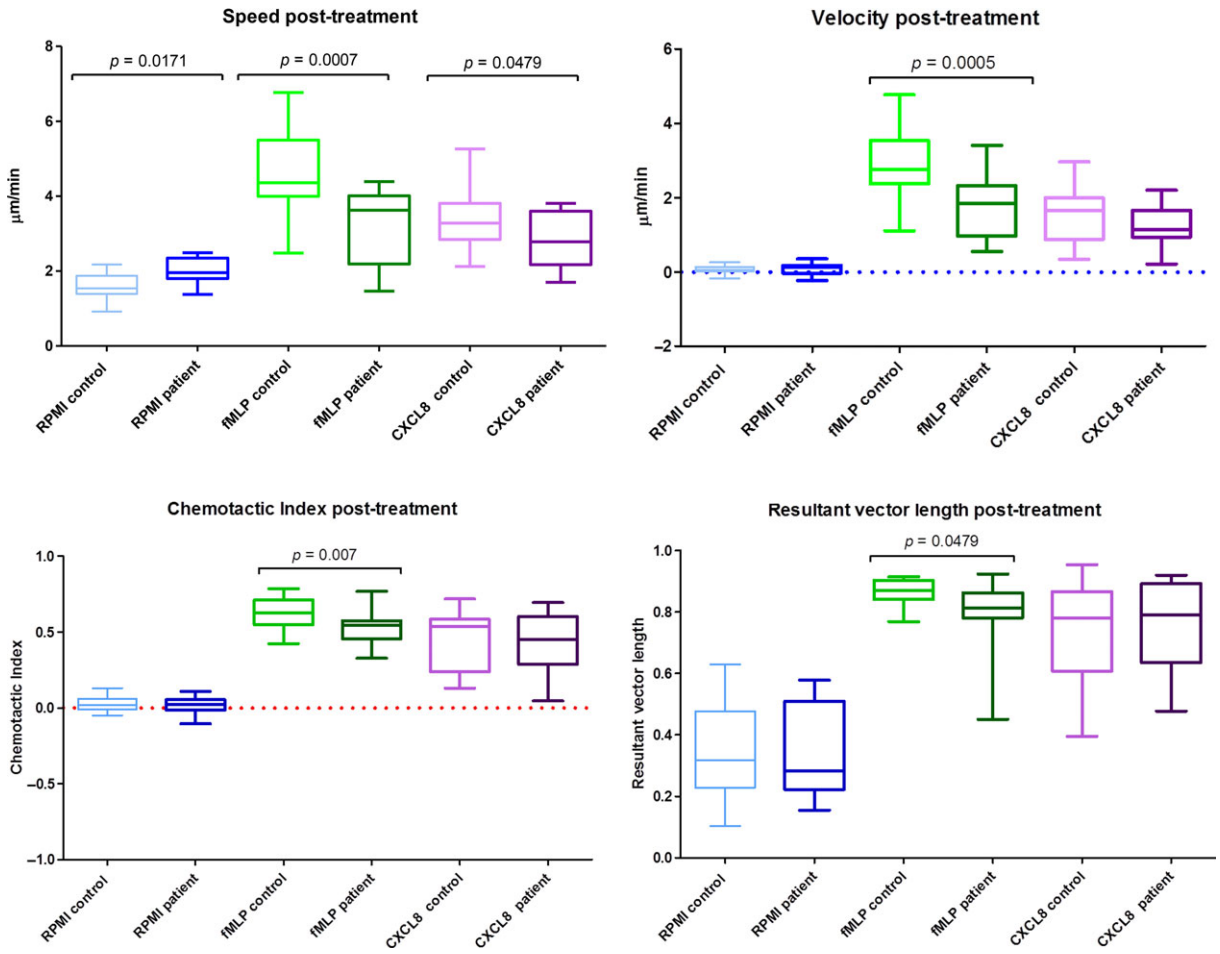

Fig. 6. Analysis of post-treatment results: as described in Fig. 5.

diseases, such as rheumatoid arthritis (RA) (Biemond et al. 1986, Miesel et al. 1996, Bostan et al. 2002, Cedergren et al. 2007) and chronic obstructive pulmonary disease (COPD) (Rahman et al. 1997, Yoshikawa et al. 2007; Sapey at al. 2011).

Information on the mechanisms underlying altered neutrophil chemotaxis in LAP neutrophils may help in understanding aberrant chemotaxis in chronic periodontitis neutrophils. Several studies have reported a diminished capacity of labelled fMLP to bind to neutrophils in individuals with LAP, indicating a reduction in the number of peptide binding sites on the surface of LAP neutrophils, though the receptors themselves appear to be functional (Van Dyke et al. 1981, 1986). This would explain the diminished responsiveness of these neutrophils to a chemoattractive gradient. Defective LAP neutrophils also express lower levels of the surface glycoprotein gp110 (ADRM1 or hRpn13) (Van Dyke et al. 1987, 1990); the significance of this receptor was demonstrated by use of the monoclonal antibody to GP110 called NCD-1, which diminished chemotaxis in healthy neutrophils when exposed to fMLP (Cotter et al. 1981). LAP-defective neutrophils also have a reduced expression of CD38, another receptor for the chemoattractant fMLP (Fujita et al. 2005).

Chemoattractant–receptor binding results in the activation of numerous signalling pathways, including PI3K, which in turn mediates the activity of phosphoinositide dependent kinase 1 (PDK1), which has been shown to be an essential regulator of neutrophil chemotaxis (Fig. 1). A study by Yagi et al. (2009) demonstrated that neutrophils from LAP patients had reduced PDK-1 expression and activity. Proteomic analysis of defective LAP neutrophils revealed upregulation of four proteins, of which the actin binding protein caldesmon was considered the most significant and it was suggested that an increase in expression of this protein within the cell may suppress motility by stabilizing actin filaments (Mizuno et al. 2011). Other findings in defective neutrophils include reduced influx of extracellular calcium, lower calcium-dependent PKC activity in unstimulated defective LAP neutrophils, accumulation of diacylglycerol (DAG) and reduced DAG kinase activity in defective LAP neutrophils compared to healthy matched controls (Agarwal et al. 1989, Tyagi et al. 1992, Kurihara et al. 1993). DAG is an activator of PKC, functioning as a second messenger in a variety of cell functions including superoxide production and chemotaxis (Nishizuka 1986, Harvath et al.

© 2014 The Authors Journal of Clinical Periodontology Published by John Wiley & Sons Ltd

1987, Lambeth 1988). Elevated DAG levels in abnormal LAP neutrophils support these neutrophils being kept in a primed state for activation. The actin polymerization and depolymerization in LAP individuals was found to be normal, supporting studies that show defects in the chemotaxis signalling cascade (Champagne et al. 1998). There is limited data in the literature on chemotaxis in neutrophils derived from patients with CP and all the above factors need to be analysed in patients with chronic periodontitis, such that we can further understand the altered processes in neutrophil chemotaxis in this disease. Indeed, it is interesting to speculate that such neutrophil deficiencies may represent a common mechanistic link between the different clinical definitions of periodontitis (e.g. LAP and CP).

Neutrophils are one of the key cells involved in protecting the host from bacterial challenge. Disruption to neutrophil functions such as chemotaxis may pre-dispose the individual to further infection and inflammation, exacerbating disease pathogenesis. Impaired neutrophil function impacts strongly on the ability of an individual to cope with microbial challenge as in periodontitis. Reduced neutrophil chemotactic accuracy and velocity may affect the transit time of neutrophils that have exited the circulation to reach the site of infection, potentially allowing bacteria to establish themselves in the periodontal tissues with greater potency. Collateral tissue damage may also arise as a result of prolonged tissue transit times secondary to defective chemotaxis, thus contributing to the chronic inflammatory burden.

In conclusion, we have demonstrated for the first time that neutrophils from patients with chronic periodontitis have reduced speed, velocity and chemotactic accuracy. Anti-infective treatment partially restores velocity and speed of neutrophil movement towards CXCL8 to control levels following periodontal therapy, but not for fMLP. Coupled with our previous knowledge that neutrophils from patients with periodontitis are both hyperactive and hyperreactive with respect to extracellular ROS production, which may drive increased tissue destruction, these findings may help to understand the potential role of dysfunctional neutrophils in the pathogenesis of periodontitis.

Acknowledgements

The authors are very grateful to Dr. John B Matthews for proof reading this manuscript and his constructive comments.

References

Agarwal, S., Reynolds, M. A., Duckett, L. D. & Suzuki, J. B. (1989) Altered free cytosolic calcium changes and neutrophil chemotaxis in patients with juvenile periodontitis. *Journal of Periodontal Research* **24**, 149–154.

Andrew, N. & Insall, R. H. (2007) Chemotaxis in shallow gradients is mediated independently of PtdIns 3-kinase by biased choices between random protrusions. *Nature Cell Biology* **9**, 193–200.

Bagorda, A. & Parent, C. A. (2008) Eukaryotic chemotaxis at a glance. *Journal of Cell Science* **121**, 2621–2624.

Berridge, M. J., Bootman, M. D. & Roderick, H. L. (2003) Calcium signalling: dynamics, homeostasis and remodelling. *Nature Reviews Molecular Cell Biology* **4**, 517–529.

Biemond, P., Swaak, A. J., Penders, J. M., Beindorff, C. M. & Koster, J. F. (1986) Superoxide production by polymorphonuclear leucocytes in rheumatoid arthritis and osteoarthritis: in vivo inhibition by the antirheumatic drug piroxicam due to interference with the activation of the NADPH-oxidase. *Annals of the Rheumatic Diseases* **45**, 249–255.

Bostan, M., Constantin, M. C., Nicolau, A., Hirt, M., Galatiuc, C., Matei, I., Braşoveanu, L. I. & Iordăchescu, D. (2002) Study of chemotactic activity developed by neutrophils from rheumatoid arthritis patients. *Roumanian Archives of Microbiology and Immunology* **61**, 243–258.

Brock, G. R., Butterworth, C. J., Matthews, J. B. & Chapple, I. L. (2004) Local and systemic total antioxidant capacity in periodontitis and health. *Journal of Clinical Periodontology* **31**, 515–521.

Cedergren, J., Forslund, T., Sundqvist, T. & Skogh, T. (2007) Intracellular oxidative activation in synovial fluid neutrophils from patients with rheumatoid arthritis but not from other arthritis patients. *Journal of Rheumatology* **34**, 2162–2170.

Champagne, C. M., Vaikuntam, J., Warbington, M. L., Rose, L., Daniel, M. A. & Van Dyke, T. E. (1998) Cytoskeletal actin reorganization in neutrophils from patients with localized juvenile periodontitis. *Journal of Periodontology* **69**, 209–218.

Chapple, I. L., Brock, G. R., Milward, M. R., Ling, N. & Matthews, J. B. (2007a) Compromised GCF total antioxidant capacity in periodontitis: cause or effect? *Journal of Clinical Periodontology* **34**, 103–110.

Chapple, I. L., Genco, R. & Working group 2 of joint, E. F. P. A. A. P. w. (2013) Diabetes and periodontal diseases: consensus report of the Joint EFP/AAP Workshop on Periodontitis and Systemic Diseases. *Journal of Clinical Periodontology* **40** (Suppl. 14), S106–S112.

Chapple, I. L., Milward, M. R. & Dietrich, T. (2007b) The prevalence of inflammatory periodontitis is negatively associated with serum antioxidant concentrations. *Journal of Nutrition* **137**, 657–664.

Choi, C. H., Thomason, P. A., Zaki, M., Insall, R. H. & Barber, D. L. (2013) Phosphorylation of actin-related protein 2 (Arp2) is required for normal development and cAMP chemotaxis in Dictyostelium. *Journal of Biological Chemistry* **288**, 2464–2474.

Clark, R. A., Page, R. C. & Wilde, G. (1977) Defective neutrophil chemotaxis in juvenile periodontitis. *Infection and Immunity* **18**, 694–700.

Cooper, P. R., Palmer, L. J. & Chapple, I. L. (2013) Neutrophil extracellular traps as a new paradigm in innate immunity: friend or foe?. *Periodontology 2000* **63**, 165–197.

Cotter, T. G., Spears, P. & Henson, P. M. (1981) A monoclonal antibody inhibiting human neutrophil chemotaxis and degranulation. *Journal of Immunology* **127**, 1355–1360.

Daniel, M. A., McDonald, G., Offenbacher, S. & Van Dyke, T. E. (1993) Defective chemotaxis and calcium response in localized juvenile periodontitis neutrophils. *Journal of Periodontology* **64**, 617–621.

Dias, I. H., Chapple, I. L., Milward, M., Grant, M. M., Hill, E., Brown, J. & Griffiths, H. R. (2013) Sulforaphane restores cellular glutathione levels and reduces chronic periodontitis neutrophil hyperactivity in vitro. *PLoS ONE* **8**, e66407.

Dias, I. H., Marshall, L., Lambert, P. A., Chapple, I. L., Matthews, J. B. & Griffiths, H. R. (2008) Gingipains from Porphyromonas gingivalis increase the chemotactic and respiratory burst-priming properties of the 77-amino-acid interleukin-8 variant. *Infection and Immunity* **76**, 317–323.

Dias, I. H., Matthews, J. B., Chapple, I. L., Wright, H. J., Dunston, C. R. & Griffiths, H. R. (2011) Activation of the neutrophil respiratory burst by plasma from periodontitis patients is mediated by pro-inflammatory cytokines. *Journal of Clinical Periodontology* **38**, 1–7.

Dickinson, B. C. & Chang, C. J. (2011) Chemistry and biology of reactive oxygen species in signaling or stress responses. *Nature Chemical Biology* **7**, 504–511.

Dietrich, T., Sharma, P., Walter, C., Weston, P. & Beck, J. (2013) The epidemiological evidence behind the association between periodontitis and incident atherosclerotic cardiovascular disease. *Journal of Periodontology* **84**, S70–S84.

Fu, Y., Korostoff, J. M., Fine, D. H. & Wilson, M. E. (2002) Fc gamma receptor genes as risk markers for localized aggressive periodontitis in African-Americans. *Journal of Periodontology* **73**, 517–523.

Fujita, T., Kantarci, A., Warbington, M. L., Zawawi, K. H., Hasturk, H., Kurihara, H. & Van Dyke, T. E. (2005) CD38 expression in neutrophils from patients with localized aggressive periodontitis. *Journal of Periodontology* **76**, 1960–1965.

Gamonal, J., Acevedo, A., Bascones, A., Jorge, O. & Silva, A. (2001) Characterization of cellular infiltrate, detection of chemokine receptor CCR5 and interleukin-8 and RANTES chemokines in adult periodontitis. *Journal of Periodontal Research* **36**, 194–203.

Graves, D. T. & Cochran, D. (2003) The contribution of interleukin-1 and tumor necrosis factor to periodontal tissue destruction. *Journal of Periodontology* **74**, 391–401.

© 2014 The Authors Journal of Clinical Periodontology Published by John Wiley & Sons Ltd

Grossi, S. G., Zambon, J. J., Ho, A. W., Koch, G., Dunford, R. G., Machtei, E. E., Norderyd, O. M. & Genco, R. J. (1994) Assessment of risk for periodontal disease. I. Risk indicators for attachment loss. *Journal of Periodontology* **65**, 260–267.

Harvath, L., McCall, C. E., Bass, D. A. & McPhail, L. C. (1987) Inhibition of human neutrophil chemotaxis by the protein kinase inhibitor, 1-(5-isoquinolinesulfonyl) piperazine. *Journal of Immunology* **139**, 3055–3061.

Henry, C. A., Thaweboon, B. & Sirisinha, S. (1984) Neutrophil chemotaxis and periodontal health relationships of young adult people in Thailand. *Archives of Oral Biology* **29**, 617–622.

Herlihy, S. E., Pilling, D., Maharjan, A. S. & Gomer, R. H. (2013a) Dipeptidyl peptidase IV is a human and murine neutrophil chemorepellent. *Journal of Immunology* **190**, 6468–6477.

Herlihy, S. E., Tang, Y. & Gomer, R. H. (2013b) A Dictyostelium secreted factor requires a PTEN-like phosphatase to slow proliferation and induce chemorepulsion. *PLoS ONE* **8**, e59365.

Kantarci, A., Oyaizu, K. & Van Dyke, T. E. (2003) Neutrophil-mediated tissue injury in periodontal disease pathogenesis: findings from localized aggressive periodontitis. *Journal of Periodontology* **74**, 66–75.

Kaul, H., Cui, Z. & Ventikos, Y. (2013) A multiparadigm modeling framework to simulate dynamic reciprocity in a bioreactor. *PLoS ONE* **8**, e59671.

Kolaczkowska, E. & Kubes, P. (2013) Neutrophil recruitment and function in health and inflammation. *Nature Reviews Immunology* **13**, 159–175.

Kuiper, J. W., Sun, C., Magalhaes, M. A. & Glogauer, M. (2011) Rac regulates PtdInsP(3) signaling and the chemotactic compass through a redox-mediated feedback loop. *Blood* **118**, 6164–6171.

Kumar, R. S. & Prakash, S. (2012) Impaired neutrophil and monocyte chemotaxis in chronic and aggressive periodontitis and effects of periodontal therapy. *Indian Journal of Dental Research* **23**, 69–74.

Kurihara, H., Murayama, Y., Warbington, M. L., Champagne, C. M. & Van Dyke, T. E. (1993) Calcium-dependent protein kinase C activity of neutrophils in localized juvenile periodontitis. *Infection and Immunity* **61**, 3137–3142.

Lakshman, R. & Finn, A. (2001) Neutrophil disorders and their management. *Journal of Clinical Pathology* **54**, 7–19.

Lambeth, J. D. (1988) Activation of the respiratory burst oxidase in neutrophils: on the role of membrane-derived second messengers, Ca++, and protein kinase C. *Journal of Bioenergetics and Biomembranes* **20**, 709–733.

Lavine, W. S., Maderazo, E. G., Stolman, J., Ward, P. A., Cogen, R. B., Greenblatt, I. & Robertson, P. B. (1979) Impaired neutrophil chemotaxis in patients with juvenile and rapidly progressing periodontitis. *Journal of Periodontal Research* **14**, 10–19.

Matthews, J. B., Wright, H. J., Roberts, A., Cooper, P. R. & Chapple, I. L. (2007a) Hyperactivity and reactivity of peripheral blood neutrophils in chronic periodontitis. *Clinical and Experimental Immunology* **147**, 255–264.

Matthews, J. B., Wright, H. J., Roberts, A., Ling-Mountford, N., Cooper, P. R. & Chapple, I. L. (2007b) Neutrophil hyper-responsiveness in periodontitis. *Journal of Dental Research* **86**, 718–722.

Miesel, R., Murphy, M. P. & Kröger, H. (1996) Enhanced mitochondrial radical production in patients with rheumatoid arthritis correlates with elevated levels of tumor necrosis factor alpha in plasma. *Free Radical Research* **25**, 161–169.

Mizuno, N., Niitani, M., Shiba, H., Iwata, T., Hayashi, I., Kawaguchi, H. & Kurihara, H. (2011) Proteome analysis of proteins related to aggressive periodontitis combined with neutrophil chemotaxis dysfunction. *Journal of Clinical Periodontology* **38**, 310–317.

Muinonen-Martin, A. J., Veltman, D. M., Kalna, G. & Insall, R. H. (2010) An improved chamber for direct visualisation of chemotaxis. *PLoS ONE* **5**, e15309.

Nibali, L., Griffiths, G. S., Donos, N., Parkar, M., D'Aiuto, F., Tonetti, M. S. & Brett, P. M. (2008) Association between interleukin-6 promoter haplotypes and aggressive periodontitis. *Journal of Clinical Periodontology* **35**, 193–198.

Niethammer, P., Grabher, C., Look, A. T. & Mitchison, T. J. (2009) A tissue-scale gradient of hydrogen peroxide mediates rapid wound detection in zebrafish. *Nature* **459**, 996–999.

Nishizuka, Y. (1986) Studies and perspectives of protein kinase C. *Science* **233**, 305–312.

Offenbacher, S., Scott, S. S., Odle, B. M., Wilson-Burrows, C. & Van Dyke, T. E. (1987) Depressed leukotriene B4 chemotactic response of neutrophils from localized juvenile periodontitis patients. *Journal of Periodontology* **58**, 602–606.

de Pablo, P., Chapple, I. L., Buckley, C. D. & Dietrich, T. (2009) Periodontitis in systemic rheumatic diseases. *Nature Reviews Rheumatology* **5**, 218–224.

Page, R. C., Sims, T. J., Geissler, F., Altman, L. C. & Baab, D. A. (1985) Defective neutrophil and monocyte motility in patients with early onset periodontitis. *Infection and Immunity* **47**, 169–175.

Partida-Sanchez, S., Cockayne, D. A., Monard, S., Jacobson, E. L., Oppenheimer, N., Garvy, B., Kusser, K., Goodrich, S., Howard, M., Harmsen, A., Randall, T. D. & Lund, F. E. (2001) Cyclic ADP-ribose production by CD38 regulates intracellular calcium release, extracellular calcium influx and chemotaxis in neutrophils and is required for bacterial clearance in vivo. *Nature Medicine* **7**, 1209–1216.

Phillips, J. E. & Gomer, R. H. (2012) A secreted protein is an endogenous chemorepellant in *Dictyostelium discoideum*. *Proceedings of the National Academy of Sciences of the United States of America* **109**, 10990–10995.

Rahman, I., Skwarska, E. & MacNee, W. (1997) Attenuation of oxidant/antopxidant imbalance during treatment of exacerbations of cheonic obstructive pulmonary disease. *Throrax* **52**, 565–568.

Sackmann, E. K., Fulton, A. L. & Beebe, D. J. (2014) The present and future role of microfluidics in biomedical research. *Nature* **507**, 181–189.

Samanta, A. K., Oppenheim, J. J. & Matsushima, K. (1990) Interleukin 8 (monocyte-derived neutrophil chemotactic factor) dynamically regulates its own receptor expression on human neutrophils. *Journal of Biological Chemistry* **265**, 183–189.

Sapey, E., Stockley, J. A., Greenwood, H., Ahmad, A., Bayley, D., Lord, J. M., Insall, R. H. & Stockley, R. A. (2011) Behavioral and structural differences in migrating peripheral neutrophils from patients with chronic obstructive pulmonary disease. *American Journal of Respiratory and Critical Care Medicine* **183**, 1176–1186.

Toker, A. & Cantley, L. C. (1997) Signalling through the lipid products of phosphoinositide-3-OH kinase. *Nature* **387**, 673–676.

Tsai, Y. R., Wang, Y. J., Lee, M. R., Hsu, M. F. & Wang, J. P. (2013) p38 Mitogen-activated protein kinase and extracellular signal-regulated kinase signaling pathways are not essential regulators of formyl peptide-stimulated p47(phox) activation in neutrophils. *European Journal of Pharmacology* **701**, 96–105.

Tyagi, S. R., Uhlinger, D. J., Lambeth, J. D., Champagne, C. & Van Dyke, T. E. (1992) Altered diacylglycerol level and metabolism in neutrophils from patients with localized juvenile periodontitis. *Infection and Immunity* **60**, 2481–2487.

Van Dyke, T. E. (2009) The etiology and pathogenesis of periodontitis revisited. *Journal of Applied Oral Science* **17**, 0–0.

Van Dyke, T. E., Horoszewicz, H. U., Cianciola, L. J. & Genco, R. J. (1980) Neutrophil chemotaxis dysfunction in human periodontitis. *Infection and Immunity* **27**, 124–132.

Van Dyke, T. E., Levine, M. J., Tabak, L. A. & Genco, R. J. (1981) Reduced chemotactic peptide binding in juvenile periodontitis: a model for neutrophil function. *Biochemical and Biophysical Research Communications* **100**, 1278–1284.

Van Dyke, T. E., Warbington, M., Gardner, M. & Offenbacher, S. (1990) Neutrophil surface protein markers as indicators of defective chemotaxis in LJP. *Journal of Periodontology* **61**, 180–184.

Van Dyke, T. E., Wilson-Burrows, C., Offenbacher, S. & Henson, P. (1987) Association of an abnormality of neutrophil chemotaxis in human periodontal disease with a cell surface protein. *Infection and Immunity* **55**, 2262–2267.

Van Dyke, T. E., Zinney, W., Winkel, K., Taufiq, A., Offenbacher, S. & Arnold, R. R. (1986) Neutrophil function in localized juvenile periodontitis. Phagocytosis, superoxide production and specific granule release. *Journal of Periodontology* **57**, 703–708.

Van Haastert, P. J. & Devreotes, P. N. (2004) Chemotaxis: signalling the way forward. *Nature Reviews Molecular Cell Biology* **5**, 626–634.

Wells, A. (2000) Tumor invasion: role of growth factor-induced cell motility. *Advances in Cancer Research* **78**, 31–101.

Worthen, G. S., Avdi, N., Buhl, A. M., Suzuki, N. & Johnson, G. L. (1994) FMLP activates Ras and Raf in human neutrophils. Potential role in activation of MAP kinase. *Journal of Clinical Investigation* **94**, 815–823.

Wright, H. J., Matthews, J. B., Chapple, I. L., Ling-Mountford, N. & Cooper, P. R. (2008) Periodontitis associates with a type 1 IFN signature in peripheral blood neutrophils. *Journal of Immunology* **181**, 5775–5784.

Yagi, M., Kantarci, A., Iwata, T., Omori, K., Ayilavarapu, S., Ito, K., Hasturk, H. & Van Dyke, T. E. (2009) PDK1 regulates chemotaxis in human neutrophils. *Journal of Dental Research* **88**, 1119–1124.

Yoshikawa, T., Dent, G., Ward, J., Angco, G., Nong, G., Nomura, N., Hirata, K. & Djukanovic, R. (2007) Impaired neutrophil chemotaxis in chronic obstructive pulmonary disease. *American*

© 2014 The Authors Journal of Clinical Periodontology Published by John Wiley & Sons Ltd

Journal of Respiratory and Critical Care Medicine **175**, 473–479.
Zigmond, S. H. & Hirsch, J. G. (1973) Leukocyte locomotion and chemotaxis. New methods for evaluation, and demonstration of a cell-derived chemotactic factor. *Journal of Experimental Medicine* **137**, 387–410.

Address:
Iain L.C. Chapple
School of Dentistry, University of Birmingham
St Chads Queensway
Birmingham B4 6NN
UK
E-mail: i.l.c.chapple@bham.ac.uk

Clinical Relevance

Scientific rationale for the study: Neutrophils are the predominant cell in the periodontal tissues. They are essential for clearance of bacteria but can also elicit host damage by inaccurately targeted responses. Movement of neutrophils to the epithelial surface requires degradation of tissue. Inaccurate movement can exacerbate tissue destruction.
Principal findings: Neutrophils from patients with chronic periodontitis display aberrant neutrophil movement that is only partially restored to healthy levels upon treatment.
Practical implications: Understanding sustained atypical neutrophil behaviour in periodontitis may help in the development of new therapeutic approaches.

© 2014 The Authors Journal of Clinical Periodontology Published by John Wiley & Sons Ltd

Hindawi Publishing Corporation
Oxidative Medicine and Cellular Longevity
Volume 2016, Article ID 3841803, 9 pages
http://dx.doi.org/10.1155/2016/3841803

Research Article

Alteration of Neutrophil Reactive Oxygen Species Production by Extracts of Devil's Claw (*Harpagophytum*)

Mbaki Muzila,[1,2] Kimmo Rumpunen,[1] Helen Wright,[3] Helen Roberts,[3] Melissa Grant,[3] Hilde Nybom,[1] Jasna Sehic,[1] Anders Ekholm,[1] and Cecilia Widén[4]

[1]*Department of Plant Breeding, Swedish University of Agricultural Sciences, Balsgård, Fjälkestadsvägen 459, 291 94 Kristianstad, Sweden*
[2]*Biological Sciences, University of Botswana, Private Bag UB 00704, Gaborone, Botswana*
[3]*School of Dentistry and MRC Centre for Immune Regulation, University of Birmingham, Saint Chads Queensway, Birmingham B4 7ET, UK*
[4]*School of Health and Society, University of Kristianstad, 291 88 Kristianstad, Sweden*

Correspondence should be addressed to Cecilia Widén; cecilia.widen@hkr.se

Received 11 February 2016; Accepted 29 May 2016

Academic Editor: Giuseppe Cirillo

Copyright © 2016 Mbaki Muzila et al. This is an open access article distributed under the Creative Commons Attribution License, which permits unrestricted use, distribution, and reproduction in any medium, provided the original work is properly cited.

Harpagophytum, Devil's Claw, is a genus of tuberiferous xerophytic plants native to southern Africa. Some of the taxa are appreciated for their medicinal effects and have been traditionally used to relieve symptoms of inflammation. The objectives of this pilot study were to investigate the antioxidant capacity and the content of total phenols, verbascoside, isoverbascoside, and selected iridoids, as well as to investigate the capacity of various *Harpagophytum* taxa in suppressing respiratory burst in terms of reactive oxygen species produced by human neutrophils challenged with phorbol myristate acetate (PMA), opsonised *Staphylococcus aureus,* and *Fusobacterium nucleatum*. *Harpagophytum* plants were classified into different taxa according to morphology, and DNA analysis was used to confirm the classification. A putative new variety of *H. procumbens* showed the highest degree of antioxidative capacity. Using PMA, three *Harpagophytum* taxa showed anti-inflammatory effects with regard to the PBS control. A putative hybrid between *H. procumbens* and *H. zeyheri* in contrast showed proinflammatory effect on the response of neutrophils to *F. nucleatum* in comparison with treatment with vehicle control. *Harpagophytum* taxa were biochemically very variable and the response in suppressing respiratory burst differed. Further studies with larger number of subjects are needed to corroborate anti-inflammatory effects of different taxa of *Harpagophytum*.

1. Introduction

Many diseases have an inflammatory pathogenesis and a large number of plant species have for centuries been utilized for their anti-inflammatory and healing effects. The medicinal tuberiferous xerophyte Devil's Claw (*Harpagophytum*) belongs to the family Pedaliaceae and is native to southern Africa [1]. This genus includes two species: *Harpagophytum procumbens* and *H. zeyheri*. There are also a few known subspecies of both species, as well as novel and hybrid taxa with less clear identity. Extracts made from the tubers of *H. procumbens* are known to relieve symptoms of inflammation and pain [2, 3] but there has been some argument about whether medicinal properties of *H. zeyheri* are sufficient for the acceptance of this species for use in anti-inflammatory preparations [4–6]. The pharmacological actions of Devil's Claw root tubers have been attributed to the presence of iridoid glycosides and verbascoside [4, 7, 8]. Studies have demonstrated anti-inflammatory properties such as inhibition of COX-2, inhibition of NF-kB activation, and downregulation of iNOS [9–11]. However, the effects of Devil's Claw have also been associated with the presence of other compounds such as flavonoids [11].

Neutrophil-mediated oxidant injury is a feature of many inflammatory diseases [12, 13]. The initial response to infection is often mediated by neutrophils because of their rapid chemotactic response towards bacteria [14]. Neutrophils inhibit infection activity by ingestion of microorganisms,

synthesis of reactive oxygen species (ROS), and release of cytokines. Neutrophils are important in both the innate and the acquired immune responses and microorganisms are recognized through receptor-mediated mechanisms, for example, by the antibody-antigen complex mediated Fc receptor (FcR) and bacterial product mediated Toll-like receptors (TLR) [15, 16]. These receptors represent specific, adaptive immune responses and nonspecific, innate immune responses, respectively, and activate intracellular signal transduction such as protein kinase C, MAPK cascades, and the NADPH-oxidase enzyme complex [17]. The NADPH-oxidase enzyme complex produces ROS at the expense of NADPH. In resting cells from healthy donors little ROS is produced, limiting potential bystander damage to adjacent tissues. Upon stimulation ROS are produced in the local environment where they react rapidly with proximal molecules. In chronic inflammatory disease, such as severe gum disease (periodontitis), both resting and stimulated neutrophils are hyperactive [18]. Therapeutic strategies are continuously sought to decrease these characteristics and prevent excessive collateral tissue damage in infectious situations without preventing the primary infection fighting capacity. Neutrophils may therefore be used as a model to explore mechanisms and possible therapeutic modulation of inflammation.

The specific objective of this paper was (1) to identify and to select genetically diverse *Harpagophytum* plant material that adequately represents the pharmacological capability of the genus and (2) to determine the potential of root tuber ethanol extracts of various taxa to suppress the production of ROS in human neutrophils. We also investigated the antioxidant capacity and the content of ascorbate, verbascoside, isoverbascoside, major iridoids, and total phenols in the extracts.

2. Materials and Methods

2.1. DNA Studies and Plant Material Selection. Seed capsules (for taxonomic and DNA-based species determination) and secondary root tubers (for analysis of chemical content and *in vitro* studies) of 24 *Harpagophytum* accessions were sampled in Botswana (Table 1, Figure 1).

To select genetically diverse samples and to corroborate the taxonomical classification based on morphological characters DNA analyses were performed. One seed capsule was collected from each of the *Harpagophytum* accessions; seeds were germinated and one seedling per accession was used for extraction of DNA. DNA was extracted with the E.Z.N.A.™ SP DNA mini kit (Omega Bio-Tek, Norcross, GA, USA). DNA quality was determined in 2% agarose gel. The DNA samples were analyzed with 2 inter-simple sequence repeat (ISSR) and 6 random amplified polymorphic DNA (RAPD) primers, using previously described methodology [19]. RAPD and ISSR bands were scored as present or absent, and a total of 107 polymorphic DNA bands were obtained. Based on the DNA studies 6 accessions representing 5 taxa were selected for use in the subsequent neutrophil and biochemical study: *H. procumbens* ssp. *transvaalense* (Accession 17; O1APT), a putative new variety of *H. procumbens* ssp. *transvaalense* (Accession 3; K1APN), *H. zeyheri* ssp. *zeyheri* (Accession 24; T1AZZ), and *H. zeyheri* ssp. *sublobatum* (Accession 14; MP3AZS) and two samples with unclear taxonomic identity but most likely interspecific hybrids between *H. procumbens* and *H. zeyheri* (Accession 16; O1APH and Accession 11; MP1APH) according to morphological characters of the tuber-bearing plants [20].

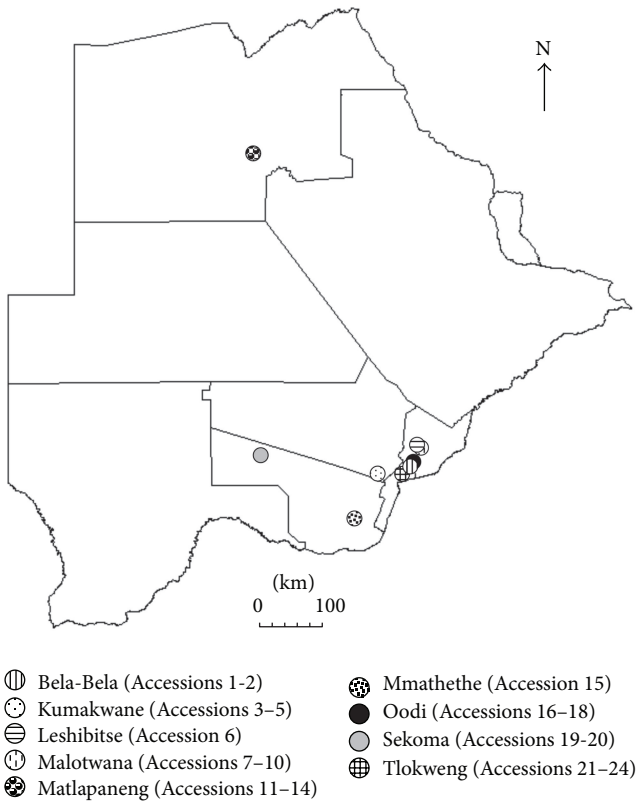

Figure 1: Sampling sites in Botswana for accessions used in the DNA marker, biochemical and neutrophil studies.

2.2. Root Sample Preparation. Samples of the root tubers were obtained by sectioning the specimen into halves, and the peel and pulp were separated, weighed, and freeze-dried at the Department of Plant Breeding, Balsgård, Swedish University of Agricultural Sciences. Vacuum was applied at <0.2 mbar and the condenser temperature was set at −70°C during the freeze-drying process. The initial temperature of the sample tray was −5°C, and after 16 h a temperature gradient was applied from −35°C to 10°C. The temperature was then maintained at 10°C until the extracts were completely dry. The dry extracts were ground to a fine powder in a laboratory mill (Yellow line, A10, IKA-Werke, Staufen, Germany).

2.3. Extract Preparation. Extracts were made fresh before each experiment by adding 1 mL of 50% ethanol containing 0.05 M H_3PO_4 to 250 μg (for *in vitro* studies) or 50 mg (for biochemical studies) of finely ground *Harpagophytum* tuber powder. The extracts were kept in an ultrasonic bath for 15 min before centrifugation at 16000 g for 10 min and the

Table 1: Accessions of *Harpagophytum* subjected to DNA analysis.

Accession	Taxon	Location
(1) B1AZZ	*H. zeyheri* ssp. *zeyheri*	Bela-Bela (24°30.7′S, 26°2.27′E) introgression zone
(2) B1APH	Putative hybrid (between *H. procumbens* and *H. zeyheri*)	Bela-Bela (24°30.7′S, 26°2.27′E) introgression zone
(3) K1APN*	Putative new variety of *H. procumbens* ssp. *transvaalense*	Kumakwane (24°37.9′S, 25°41.1′E) introgression zone
(4) K1APH	Putative hybrid (between *H. procumbens* and *H. zeyheri*)	Kumakwane (24°37.9′S, 25°41.1′E) introgression zone
(5) K1AZZ	*H. zeyheri* ssp. *zeyheri*	Kumakwane (24°37.9′S, 25°41.1′E) introgression zone
(6) L1APT	*H. procumbens* ssp. *transvaalense*	Leshibitse (24°16.9′S, 26°9.41′E) introgression zone
(7) ML1APN	Putative new variety of *H. procumbens* ssp. *transvaalense*	Malotwana (24°17.5′S, 26°09.27′E) introgression zone
(8) ML1BPN	Putative new variety of *H. procumbens* ssp. *transvaalense*	Malotwana (24°17.5′S, 26°09.27′E) introgression zone
(9) ML2APN	Putative new variety of *H. procumbens* ssp. *transvaalense*	Malotwana (24°17.5′S, 26°09.27′E) introgression zone
(10) ML3APN	Putative new variety of *H. procumbens* ssp. *transvaalense*	Malotwana (24°17.5′S, 26°09.27′E) introgression zone
(11) MP1APH*	Putative hybrid (between *H. procumbens* and *H. zeyheri*)	Matlapaneng (19°55.4′S, 23°32.9′E) *H. zeyheri* ssp. *sublobatum* allopatric zone
(12) MP1AZS	*H. zeyheri* ssp. *sublobatum*	Matlapaneng (19°55.4′S, 23°32.9′E) *H. zeyheri* ssp. *sublobatum* allopatric zone
(13) MP2AZS	*H. zeyheri* ssp. *sublobatum*	Matlapaneng (19°55.4′S, 23°32.9′E) *H. zeyheri* ssp. *sublobatum* allopatric zone
(14) MP3AZS*	*H. zeyheri* ssp. *sublobatum*	Matlapaneng (19°55.4′S, 23°32.9′E) *H. zeyheri* ssp. *sublobatum* allopatric zone
(15) MT1APT	*H. procumbens* ssp. *transvaalense*	Mmathethe *H. procumbens* ssp. *transvaalense* allopatric zone
(16) O1APH*	Putative hybrid (between *H. procumbens* and *H. zeyheri*)	Oodi (24°28.1′S, 26°2.83′E) introgression zone
(17) O1APT*	*H. procumbens* ssp. *transvaalense*	Oodi (24°28.1′S, 26°2.83′E) introgression zone
(18) O2APT	*H. procumbens* ssp. *transvaalense*	Oodi (24°28.1′S, 26°2.83′E) introgression zone
(19) S1APP	*H. procumbens* ssp. *procumbens*	Sekoma (24°24.8′S, 23°47.8′E) *H. procumbens* ssp. *procumbens* allopatric zone
(20) S2APP	*H. procumbens* ssp. *procumbens*	Sekoma (24°24.8′S, 23°47.8′E) *H. procumbens* ssp. *procumbens* allopatric zone
(21) T1APT	*H. procumbens* ssp. *transvaalense*	Tlokweng (24°37.8′S, 25°59.1′E) introgression zone
(22) T1BPT	*H. procumbens* ssp. *transvaalense*	Tlokweng (24°37.8′S, 25°59.1′E) introgression zone
(23) T2APT	*H. procumbens* ssp. *transvaalense*	Tlokweng (24°37.8′S, 25°59.1′E) introgression zone
(24) T1AZZ*	*H. zeyheri* ssp. *zeyheri*	Tlokweng (24°37.8′S, 25°59.1′E) introgression zone

*Accessions used in the neutrophil and biochemical study.

supernatant was collected. This resulted in a 100% stock with a concentration of 250 μg/mL. This stock was then diluted (v/v) with phosphate-buffered saline (PBS) to produce final concentrations of 50%, 10%, and 5%.

2.4. Determination of Total Phenolics. To measure the total phenolic content according to the Folin-Ciocalteu method [21] the sample was mixed with Folin-Ciocalteu reagent (Merck, Darmstadt, Germany), H_2O, and 15% Na_2CO_3 and the absorbance measured at 765 nm after 1 h incubation at room temperature. Gallic acid was used as a standard and the total content of phenols was expressed as mg gallic acid equivalents (GAE) per g dry weight (dw). For comparison, total phenolic content was analyzed also in commercially obtained, external standards of 8-O-p-coumaroyl-harpagide, harpagoside, and verbascoside.

2.5. Determination of Ferric Reducing Ability of Plasma. The ferric reducing ability of plasma (FRAP) of the extracts was measured according to the method developed by Benzie and Strain [22] but modified to fit a 96-well format [23]. The different extracts were diluted 20–100-fold. Ten μL of these extracts was incubated at 37°C and then mixed with 260 μL of ferric-TPTZ reagent (prepared by mixing 300 mM acetate

buffer, pH 3.6; 10 mM of 2,4,6-tripyridyl-s-triazine in 40 mM HCl; and 20 mM $FeCl_3$ in the ratio of 4 : 1 : 1; the solution was kept at 37°C). The absorbance was measured at 595 nm after 4 min on a plate reader (Sunrise, Tecan Nordic AB, Sweden). Fe^{2+} was used as a standard and L-ascorbic acid was used as a control where one mole of ascorbic acid corresponds approximately to two moles of FRAP (we obtained the value 2.09).

2.6. HPLC Analysis of Ascorbate, Verbascoside, Isoverbascoside, and Iridoids. For ascorbate analysis samples were placed in ultrasonic bath for 10 min and centrifuged for 10 min at 2000 g (Beckham, USA). The supernatant was filtered with a syringe particle filter (glass/nylon 0.45 μm, 30 mm Cameo, Sorbent AB, Sweden) directly into an HPLC-vial. The analysis was made on a Shimadzu HPLC system consisting of a communication bus module (SCL 10A-VP) and a pump (LC 10AD) using an ACE (5 μm) for separation. For detection a variable SPD-10A UV-VIS detector set to 254 nm was used. The mobile phase consisted of a 50 mM sodium phosphate (Fluka, Switzerland) buffer set to pH 2.8. The flow rate was 1 mL min^{-1} and 20 μL sample was injected into the HPLC system. The peak was identified by retention time of an ascorbate standard (Sigma-Aldrich, USA). Quantification was carried by peak area.

Contents of verbascoside, isoverbascoside, and the iridoids acetylacteoside, 8-*O*-p-coumaroyl-harpagide, harpagoside, and pagoside were analyzed in *Harpagophytum* extracts on a Shimadzu HPLC system equipped with a diode-array detector according to a method slightly modified from Karioti et al. [24]. The eluent consisted of solvent A (H_2O at pH 3.2 by formic acid) and solvent B (acetonitrile). The binary gradient was as follows: 95% A (0–5 min), 85% A (5–8 min), 76% A (8–15 min), 75% A (15–19 min), 73% A (19–24 min), 71% A (24–29 min), and 50% A (29 min). A Phenomenex Synergi 4l Hydro-RP 80A column (250 × 4.6 mm) and a guard C18 precolumn were used. Evaluation of data was carried out with Shimadzu Class-VP software (version 6.13 SP2). Retention times and spectral data were obtained and compared with those of the external standards verbascoside, 8-O-p-coumaroyl-harpagide, and harpagoside. The peaks of acetylacteoside, pagoside, and isoverbascoside were verified by HPLC MS. Acetylacteoside and pagoside were quantified against harpagoside, and isoverbascoside was quantified against verbascoside. Detection was carried out at 280 nm with a total run time of 35 minutes. Example chromatograms of accessions are provided as Supplementary Material (Supplementary File, Figure S1, available online at http://dx.doi.org/10.1155/2016/3841803).

2.7. Collection of Venous Blood and Preparation of Neutrophils. West Midlands Research Ethics Committee in Birmingham, UK, in compliance with the Declaration of Helsinki, approved the study (Institutional Review Board approval number 10/H1208/48). The study was based on periodontally and systemically healthy individual volunteers (n = 10; mean age: 29 years, range 21–61 years, all female) who consented to participate in the study. Exclusion criteria included pregnancy, use of nonsteroidal anti-inflammatory drugs, mouth-washes, antimicrobial drugs, or vitamin supplements within the past three months.

Venous blood was drawn from each participant. A discontinuous Percoll gradient (δ = 1.079 : 1.098) was used to isolate neutrophils, followed by erythrocyte lysis using a solution containing 0.83% NH_4Cl, 1% $KHCO_3$, 0.04% EDTA, and 0.25% bovine serum albumin (BSA) for 20 minutes. Isolated cells were then washed and resuspended at 1 × 10^6 cells/mL in solution grade phosphate-buffered saline (GPBS) containing 1 mM glucose and cations (1 mM $MgCl_2$ and 1.5 mM $CaCl_2$). Trypan blue was used to determine cell viability and only samples with more than 98% viability were retained for further analysis.

2.8. Cell Viability Assay. Cell viability was measured using the CellTiter-Glo™ Reagent (Promega). The luciferase present in the reagent uses luciferin, oxygen, and ATP as substrates in a reaction that produces oxyluciferin and releases energy in the form of light. Because the luciferase reaction requires ATP, conditions have been created such that the amount of light produced is proportional to the amount of ATP present, reflecting the number of viable cells [25, 26]. 100 μL of neutrophils in GPBS (1 × 10^5 cells/mL) and 10 μL of PBS, the vehicle control, or the *Harpagophytum* extracts (5%) were added to preblocked (PBS containing 1% BSA overnight, 4°C) white microwells (Microlite 2, VWR, UK). The plate was placed in the microplate reader and incubated at 30°C for 30 min before the addition of 100 μL of CellTiter-Glo® to each well. The contents of the wells were mixed and returned to the plate reader before reading the luminescence levels at 10 min.

2.9. Detection of Reactive Oxygen Species (ROS) by Chemiluminescence Assay. Chemiluminescence assays were performed using luminol to detect total oxygen radical (HOCl and H_2O_2) generation (intra- and extracellular) as described in Matthews et al. [27]. All assays were performed at 37°C using a Berthold microplate luminometer (LB96v). Supplemented PBS (35 μL, PBS supplemented with glucose, Ca^+, and Mg^+) and luminol (30 μL, 3 mM) were added to preblocked (PBS containing 1% BSA overnight, 4°C) white microwells (Microlite 2, VWR, UK). The plate was then placed into the microplate reader and 100 μL of the isolated neutrophils (1 × 10^5) was added to each well. Cells were allowed to settle for 30 min at 37°C prior to priming by addition of the extracts (only 5%) or controls for 30 min at 37°C. Neutrophils were then stimulated with either PMA (Phorbol 12-myristate 13-acetate, 25 nM), *Fusobacterium nucleatum* (MOI 1 : 100), opsonised *S. aureus* (MOI 1 : 300), or PBS (control). *S. aureus* (NCTC 6571) had been grown aerobically on mannitol salt agar and inoculated into tryptone soy broth; opsonised *S. aureus* was prepared according to Bergström and Åsman [28] and stored as cell suspension of 1.2 × 10^9 cells/mL at −80°C. The anaerobic bacteria *F. nucleatum* (Fn; ATCC 10953) were grown at 37°C according to Roberts et al. [29]. The bacteria were washed three times in sterile PBS, heat-treated at 100°C for 10 min, and then diluted to a suspension of 5 × 10^9 cells/mL and stored at −80°C. PMA was

resuspended into DMSO and diluted in PBS. For each subject, all samples were analyzed in triplicate and light emission in relative light units (RLUs) was recorded throughout the experiment.

2.10. Statistical Analysis. Based on the total of 107 polymorphic RAPD and ISSR bands, a matrix of standardized covariates was calculated for the 24 samples (6 samples investigated in this study and 18 control samples for taxonomic classification) and used as input variable in a principal component analysis (PCA) conducted with GenAlEx.

Associations between the content of chemical compounds in the six chemically analyzed samples were similarly investigated with PCA. Based on the scree-plot, three PCA components were selected for illustration of between-sample similarity. This analysis was performed using the Minitab 16 software (Minitab, State College, PA, USA).

Descriptive statistics for mean values and standard deviations were calculated on data for the enhanced chemiluminescence assays, and mean values, standardized to the total relative light units (RLUs) for each test subject, respectively, were compared using the Wilcoxon signed-rank test. SPSS 20 for Windows was used for these calculations.

3. Results and Discussion

3.1. Accession Identification, Diversity, and Selection. The first step in this investigation was to ascertain the taxonomic identity of the selected plant material by DNA analysis of seedlings from the field-collected seed capsules. The clustering of the 24 studied accessions in a DNA marker-based PCA (Figure 2) in general supported the morphology-based species classification. Material from six of these accessions (Table 2) was selected to determine the ability to suppress respiratory burst in human neutrophils and to investigate the antioxidant capacity and phenol content. The selected samples of *H. procumbens* ssp. *transvaalense* (Accession 17; O1APT) and of a putative new variety of *H. procumbens* ssp. *transvaalense* (Accession 3; K1APN) grouped with other *H. procumbens* accessions. Similarly, the two samples of *H. zeyheri* ssp. *zeyheri* (Accession 24; T1AZZ) and *H. zeyheri* ssp. *sublobatum* (Accession 14; MP3AZS), respectively, grouped with other accessions of *H. zeyheri*. One of the two samples of putative interspecific hybrids (Accession 11; MP1APH) took an intermediary position while the other sample (Accession 16; O1APH) showed somewhat stronger affinity to the *H. zeyheri* accessions.

3.2. Content of Total Phenols. Using the Folin-Ciocalteu assay the highest content of total phenols was found in the putative new variety of *H. procumbens* (Accession 3, 28.9 mg GAE/g dw) and in *H. zeyheri* ssp. *sublobatum* (Accession 14, 25.1 mg GAE/g dw) whereas considerably lower content was revealed for the other samples investigated (Table 2). The external standards of harpagide, harpagoside, and verbascoside were also subjected to this analysis. Low phenolic content was identified for the iridoids and high phenolic content for the verbascoside standard (Table 2).

Table 2: Content of total phenols (TP) and antioxidant capacity (FRAP) of *Harpagophytum* extracts, presented as mean with standard deviation per dry weight (dw) of the plant material (GAE: gallic acid equivalents).

Accession	Total phenols (mg GAE/g dw)		FRAP (μmol Fe^{2+}/g dw)	
	Mean	SD	Mean	SD
3	28.9	0.4	596.7	25.2
11	13.5	0.6	204.8	0.1
14	25.1	1.3	444.3	13.0
16	5.1	0.3	80.8	13.2
17	2.1	0.4	33.8	0.2
24	3.5	0.5	54.5	5.6
Standard: harpagide	16.7	1.1	149.2	0.0
Standard: harpagoside	0.0	0.0	612.3	3.2
Standard: verbascoside	359.9	9.8	5854.2	52.7

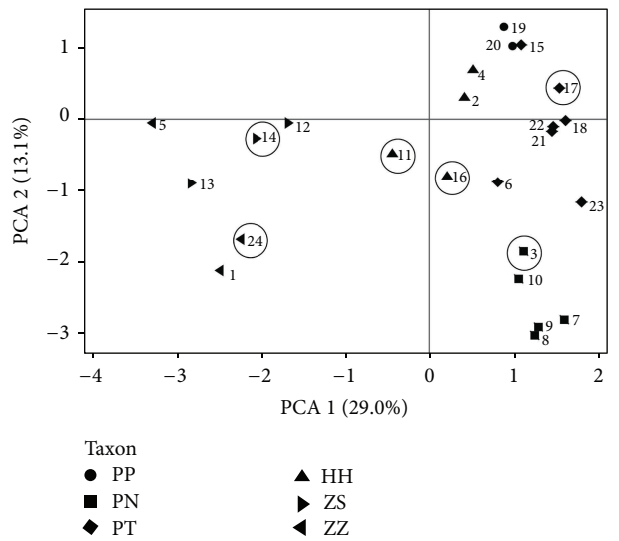

Figure 2: Principal component analysis showing ISSR and RAPD marker-based similarity between 24 *Harpagophytum* accessions used in the DNA and neutrophil study (the 6 accessions within circles). Samples are plotted on the first two components, explaining 29 and 13% of the total variation, respectively. The numbers indicate accession codes, whereas the symbols for the taxa are abbreviated as follows: PP: *H. procumbens* ssp. *procumbens*; PT: *H. procumbens* ssp. *transvaalense*; PN: putative new variety of *H. procumbens* ssp. *transvaalense*; ZS: *H. zeyheri* ssp. *sublobatum*; ZZ: *H. zeyheri* ssp. *zeyheri*; HH: putative interspecific hybrids (between *H. procumbens* and *H. zeyheri*).

3.3. Antioxidant Capacity of Harpagophytum Extracts: Ferric Reducing Activity of Plasma (FRAP). Using the chemical FRAP assay as a measure of antioxidant capacity, Accession 3 had the highest value (596.7 μmol Fe^{2+}/g dw), followed by Accession 14 (444.3 μmol Fe^{2+}/g dw), and more than double that of Accession 11 (204.8 μmol Fe^{2+}/g dw) (Table 2).

The standards harpagide, harpagoside, and verbascoside were also analyzed and verbascoside was the most potent

Table 3: Composition of verbascosides and iridoids in each *Harpagophytum* tuber extract presented as mean value with standard deviation (SD) as mg per g dry weight of the plant material.

Accession	Verbascoside		Isoverbascoside		Acetylacteoside		Pagoside		Harpagoside		8-*O*-p-Coumaroyl-harpagide	
	Mean	SD	Mean	SD	Mean	SD	Mean	SD	Mean	SD	Mean	SD
3	3.04	0.11	21.75	1.16	4.49	0.16	0.11	0.01	4.09	0.34	0.04	0.00
11	1.28	0.11	6.02	0.50	3.30	0.45	0.68	0.08	9.08	0.97	4.04	0.41
14	4.22	0.33	15.62	1.32	1.29	0.15	0.48	0.05	7.07	0.60	3.29	0.35
16	0.64	0.09	2.47	0.27	0.84	0.03	0.17	0.01	0.96	0.15	0.07	0.01
17	0.33	0.05	0.62	0.08	0.23	0.03	0.02	0.00	1.71	0.24	0.09	0.01
24	0.39	0.08	0.64	0.14	0.41	0.11	0.00	0.00	0.16	0.01	0.01	0.00

(5854.2 μmol Fe^{2+}/g dw) with approximately 10 × the capacity of harpagoside and 40 × the capacity of harpagide (Table 2).

Thus, there was a very large difference among samples in antioxidant capacity and also the antioxidant capacity of the different standards varied largely.

3.4. Content of Verbascoside, Isoverbascoside, Iridoids, and Ascorbate. The content of verbascoside was highest in Accession 14 (mean 4.2 mg/g dw) followed by Accession 3 (mean 3.0 mg/g dw) (Table 3). The content of isoverbascoside was highest in Accession 3 (mean 21.8 mg/g dw). Significant amounts of harpagoside and 8-*O*-p-coumaroyl harpagide were identified in Accession 11 as well as in Accession 14 (Table 3). The extracts from Accessions 16, 17, and 24 contained low levels of verbascoside, isoverbascoside, and iridoid compounds. HPLC analysis revealed that there was no ascorbate in the samples (Supplementary File, Figure S2).

Thus, the phytochemical analysis revealed substantial differences in chemical composition between the analyzed taxa but whether these differences are taxon-specific must be ascertained in future studies using a much larger material with several samples of each taxon.

3.5. Cell Viability Assay. There were no significant differences among the effects of different extracts on neutrophil cell viability, and none of the extracts showed lethal/suppressive effects on neutrophils (Supplementary File, Figure S3).

3.6. Effect on Neutrophil Reactive Oxygen Species (ROS) Production. To assess the effects of the extracts on neutrophil ROS production, neutrophils from healthy volunteers were preincubated with extracts (5% solutions, including 2.5% ethanol) or controls (PBS or vehicle control 2.5% ethanol) for 30 min prior to stimulation.

For unstimulated cells (PBS, Figure 3(a)), there were significant differences in response among some of the samples. Accession 3 responded significantly stronger (lower RLUs recorded) than Accessions 16 ($p = 0.028$) and 24 ($p = 0.037$), and Accession 14 was significantly stronger than Accessions 16 ($p = 0.022$), 17 ($p = 0.028$), and 24 ($p = 0.047$) in protecting the cells. However, none of the samples were significantly different from the PBS or vehicle ethanol control.

For stimulated cells, *Staphylococcus aureus* treatment (Figure 3(b)), there was a significant proinflammatory effect of Accession 11 in comparison to Accession 16 ($p = 0.028$). A significant proinflammatory response was also detected for Accession 14 with regard to Accession 17 ($p = 0.017$). However, none of the samples were significantly different from the PBS or vehicle ethanol control.

With the Toll-like receptor ligand *F. nucleatum* treatment (Figure 3(c)), a significant proinflammatory response was detected for Accession 11 in comparison with the vehicle control ($p = 0.037$) and also in comparison with Accession 17 ($p = 0.017$).

With PMA treatment (Figure 3(d)), Accessions 14, 16, and 17 showed significant anti-inflammatory activity in comparison to the PBS control ($p = 0.038$, $p = 0.028$, and $p = 0.049$) but no significant difference was detected in comparison with the vehicle control. There was also a significant difference in anti-inflammatory effects among samples. Accessions 14 ($p = 0.029$) and 17 ($p = 0.037$) had significantly higher activity than Accession 3, and Accessions 14 ($p = 0.015$) and 17 ($p = 0.031$) had significantly higher activity than Accession 11.

Neutrophils were also preincubated with standard solutions (0.5 μg/mL verbascoside and 0.5 μg/mL harpagoside). For unstimulated cells (PBS, Figure 4(a)), significant effects against ROS production were observed for harpagoside and verbascoside in comparison to PBS control ($p = 0.043$ and $p = 0.043$, resp.). Verbascoside was also significantly different to the vehicle control ($p = 0.043$) and to harpagoside ($p = 0.043$). For stimulated cells, *Staphylococcus aureus* and *F. nucleatum* treatments only identified a significant difference between PBS and vehicle control ($p = 0.043$). PMA treatment (Figure 4(b)) revealed a significant difference between PBS and vehicle control ($p = 0.043$) and also between verbascoside and PBS control and harpagoside ($p = 0.043$ and $p = 0.043$, resp.).

Accessions 3 and 14 contained highest levels of verbascoside and isoverbascoside. Accession 11 contained the highest levels of harpagoside, pagoside, and 8-*O*-p-coumaroyl-harpagide. Ouitas and Heard [30] have previously examined

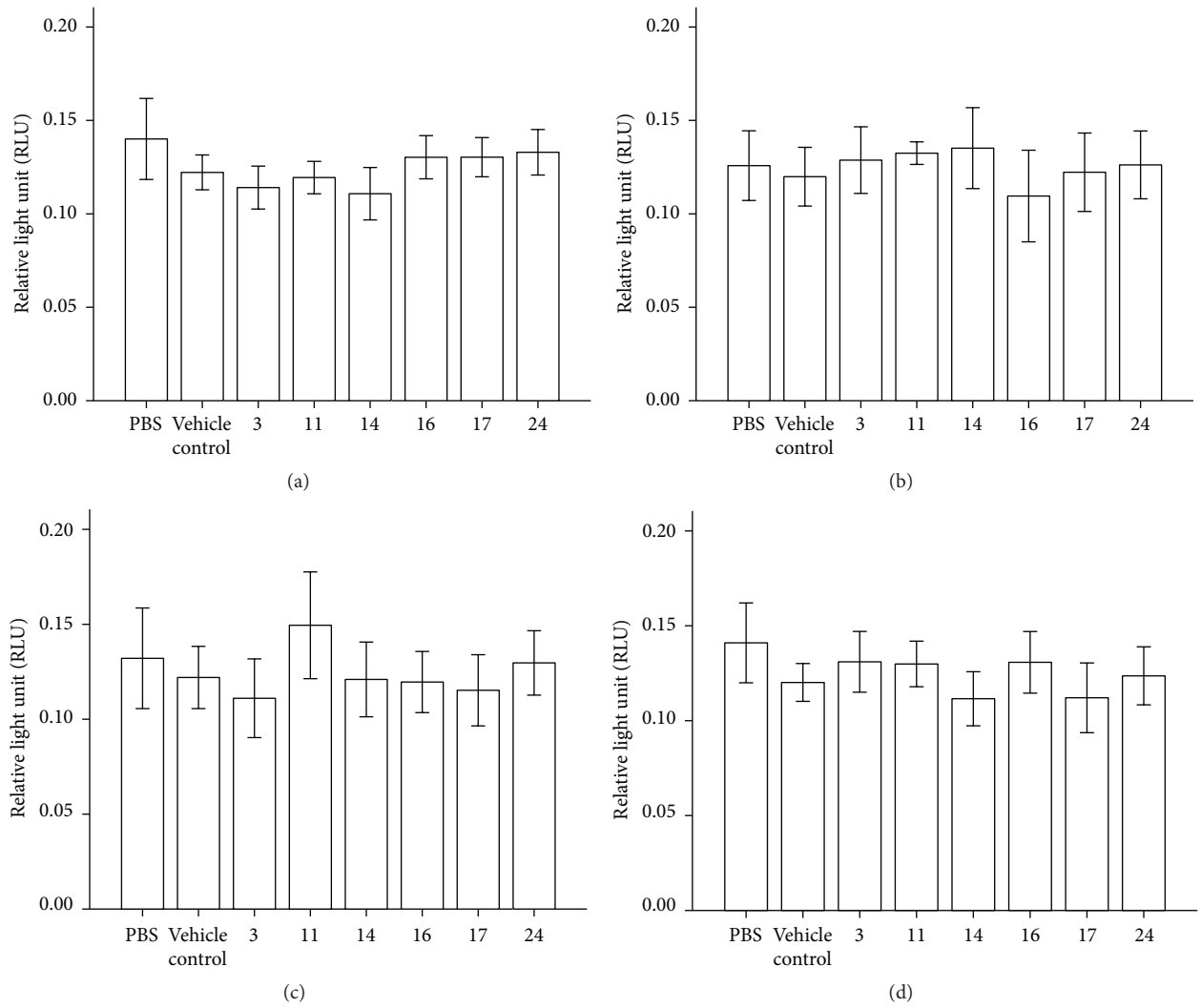

Figure 3: Luminol-detected total ROS production by neutrophils stimulated with (a) PBS (no stimulus), (b) opsonised *Staphylococcus aureus*, (c) *Fusobacterium nucleatum*, and (d) PMA (25 nM) in the presence of PBS, ethanol, and Accessions 3, 11, 14, 16, 17, and 24 ($n = 10$). Error bars: 95% CI. All sample results were compared by Wilcoxon two related samples tests.

a number of *H. procumbens* extracts for anti-inflammatory activity and, in broad agreement with our study, have shown some proinflammatory responses. The reported anti-inflammatory effect by Qi et al. [31] was not replicated in our report, which may be due to cell specific responses and/or the differing properties of the various compounds available in the extracts. In a previous study by Matthews et al. [18] it was demonstrated that ascorbate may significantly decrease the amount of ROS produced by healthy neutrophils stimulated by PMA; however ascorbate was not detected in our samples. Ethanol is known to decrease ROS production by neutrophils [32] and can increase superoxide production during PMA treatment of neutrophils [33]. In our studies the PMA-mediated respiratory burst was clearly affected by ethanol as shown by the vehicle control.

Bivariate Pearson rank correlation analysis identified significant correlations between total phenols and FRAP ($R = 0.991$, $p = 0.000$) as well as between total phenols, FRAP, and PBS control (luminol-detected total ROS production) with verbascoside ($R = 0.934$, $p = 0.006$; $R = 0.903$, $p = 0.014$; $R = -0.931$, $p = 0.007$) and with isoverbascoside ($R = 0.985$, $p = 0.000$; $R = 0.999$, $p = 0.000$; $R = -0.846$, $p = 0.034$). We also noted significant correlation between total phenols and FRAP with PBS control (luminol-detected total ROS production) ($R = -0.888$, $p = 0.018$; $R = -0.847$, $p = 0.033$). The high positive correlations between the content of total phenols and verbascoside as well as with isoverbascoside and the high negative correlation between total phenols and FRAP as well as with the PBS control show that verbascoside really is an important antioxidant phenol in *Harpagophytum* and verifies the antioxidant activity of samples as revealed in the unstimulated cell PBS control treatment.

The present pilot study revealed a tentative anti-inflammatory effect of three *Harpagophytum* taxa using a

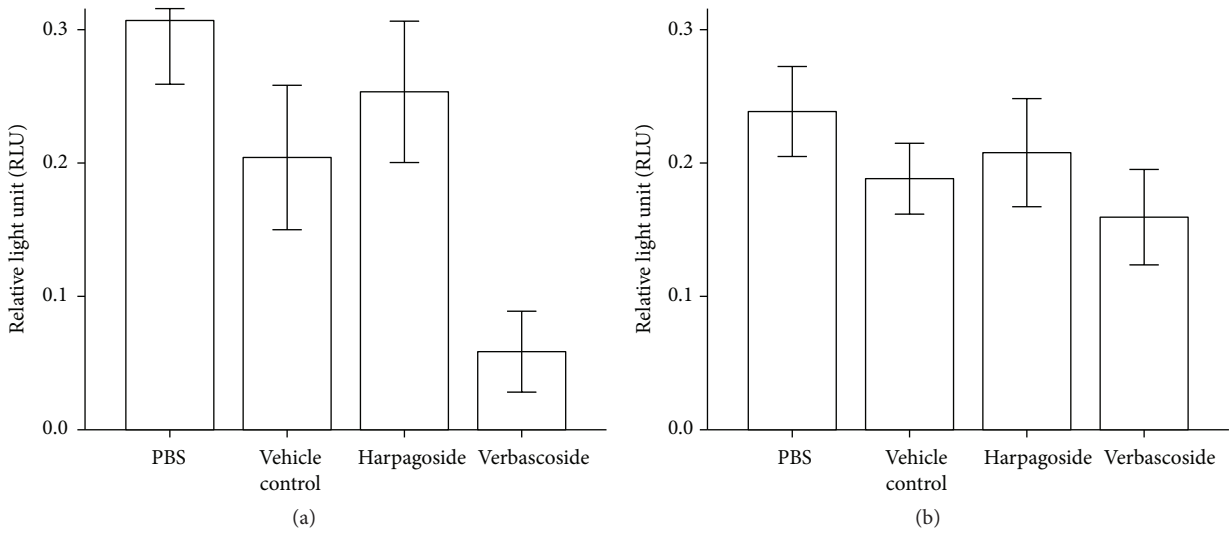

Figure 4: Luminol-detected total ROS production by neutrophils stimulated with (a) PBS or (b) PMA (25 nM) in the presence of PBS, ethanol, harpagoside (0.5 μg/mL), and verbascoside (0.5 μg/mL) ($n = 5$). Error bars: 95% CI. All sample results were compared by Wilcoxon two related samples tests.

modest number of subjects. Future verifying studies using a larger number of subjects should take into account gender and age of volunteers, as well as the impact of single purified constituents of the extracts on respiratory burst process *in vitro*.

4. Conclusions

The accessions of different *Harpagophytum* taxa were shown to be biochemically very variable with regard to content of verbascoside, isoverbascoside, and analyzed iridoids, and some accessions had very high antioxidant capacity. However, we were unable to corroborate a general anti-inflammatory effect for *H. procumbens* with the neutrophil model although evidence of anti-inflammatory activity was noticed for three taxa. In addition, the proinflammatory effect noticed for one taxon needs further verification.

Competing Interests

The authors declare no competing interests.

Authors' Contributions

All authors have contributed to the intellectual content of this paper following these requirements: (1) significant contributions to the conception and design, acquisition of data or analysis, and interpretation of data; (2) drafting or revising the paper for intellectual content; and (3) final approval of the published paper.

Acknowledgments

This study was funded by the NORDIC-SADC Plant Genetic Resources Centre, Lusaka, Zambia.

References

[1] H. D. Ihlenfeldt and H. Hartmann, "Die gattung *Harpagophytum* (Burch.) DC. Ex Meissn. (Monographie der afrikanischen Pedaliaceae II)," *Mitteilungen aus dem Institut für Allgemeine Botanik Hamburg*, vol. 13, pp. 16–69, 1970.

[2] D. W. Lim, J. G. Kim, D. Han, and Y. T. Kim, "Analgesic effect of *Harpagophytum procumbens* on postoperative and neuropathic pain in rats," *Molecules*, vol. 19, no. 1, pp. 1060–1068, 2014.

[3] D. Loew, J. Möllerfeld, A. Schrödter, S. Puttkammer, and M. Kaszkin, "Investigations on the pharmacokinetic properties of *Harpagophytum* extracts and their effects on eicosanoid biosynthesis *in vitro* and *ex vivo*," *Clinical Pharmacology and Therapeutics*, vol. 69, no. 5, pp. 356–364, 2001.

[4] B. Baghdikian, M. C. Lanhers, J. Fleurentin et al., "An analytical study, anti-inflammatory and analgesic effects of *Harpagophytum procumbens* and *Harpagophytum zeyheri*," *Planta Medica*, vol. 63, no. 2, pp. 171–176, 1997.

[5] R. Grahame and B. V. Robinson, "Devil's claw (*Harpagophytum procumbens*): pharmacological and clinical studies," *Annals of the Rheumatic Diseases*, vol. 40, no. 6, p. 632, 1981.

[6] L. W. Whitehouse, M. Znamirowska, and C. J. Paul, "Devil's claw (*Harpagophytum procumbens*): no evidence for anti-inflammatory activity in the treatment of arthritic disease," *Canadian Medical Association Journal*, vol. 129, no. 3, pp. 249–251, 1983.

[7] "*Harpagophytum procumbens* (devil's claw). Monograph," *Alternative Medicine Review*, vol. 13, no. 3, pp. 248–252, 2008.

[8] J. Qi, J.-J. Chen, Z.-H. Cheng, J.-H. Zhou, B.-Y. Yu, and S. X. Qiu, "Iridoid glycosides from *Harpagophytum procumbens* D.C. (devil's claw)," *Phytochemistry*, vol. 67, no. 13, pp. 1372–1377, 2006.

[9] N. Abdelouahab and C. Heard, "Effect of the major glycosides of *Harpagophytum procumbens* (Devil's Claw) on epidermal cyclooxygenase-2 (COX-2) in vitro," *Journal of Natural Products*, vol. 71, no. 5, pp. 746–749, 2008.

[10] T. H. Huang, V. H. Tran, R. K. Duke et al., "Harpagoside suppresses lipopolysaccharide-induced iNOS and COX-2

expression through inhibition of NF-κB activation," *Journal of Ethnopharmacology*, vol. 104, no. 1-2, pp. 149–155, 2006.

[11] M. Kaszkin, K. F. Beck, E. Koch et al., "Downregulation of inos expression in rat mesangial cells by special extracts of *Harpagophytum procumbens* derives from harpagoside-dependent and independent effects," *Phytomedicine*, vol. 11, no. 7-8, pp. 585–595, 2004.

[12] F. Morel, J. Doussiere, and P. V. Vignais, "The superoxide-generating oxidase of phagocytic cells. Physiological, molecular and pathological aspects," *European Journal of Biochemistry*, vol. 201, no. 3, pp. 523–546, 1991.

[13] A. Noguera, S. Batle, C. Miralles et al., "Enhanced neutrophil response in chronic obstructive pulmonary disease," *Thorax*, vol. 56, no. 6, pp. 432–437, 2001.

[14] Y. Zhang, G. L. Mills, and M. G. Nair, "Cyclooxygenase inhibitory and antioxidant compounds from the mycelia of the edible mushroom *Grifola frondosa*," *Journal of Agricultural and Food Chemistry*, vol. 50, no. 26, pp. 7581–7585, 2002.

[15] H. Higuchi, M. Ishizaka, and H. Nagahata, "Complement receptor type 3 (CR3)- and Fc receptor (FcR)-mediated matrix metalloproteinase 9 (MMP-9) secretion and their intracellular signalling of bovine neutrophils," *Veterinary Research Communications*, vol. 31, no. 8, pp. 985–991, 2007.

[16] L. C. Parker, M. K. B. Whyte, S. K. Dower, and I. Sabroe, "The expression and roles of toll-like receptors in the biology of the human neutrophil," *Journal of Leukocyte Biology*, vol. 77, no. 6, pp. 886–892, 2005.

[17] H. Higuchi and H. Nagahata, "Comparison of superoxide production, protein kinase C and tyrosine kinase activities in neutrophils from neonatal calves and cows," *Research in Veterinary Science*, vol. 65, no. 2, pp. 139–143, 1998.

[18] J. B. Matthews, H. J. Wright, A. Roberts, P. R. Cooper, and I. L. Chapple, "Hyperactivity and reactivity of peripheral blood neutrophils in chronic periodontitis," *Clinical and Experimental Immunology*, vol. 147, no. 2, pp. 255–264, 2007.

[19] M. Muzila, G. Werlemark, R. Ortiz et al., "Assessment of diversity in *Harpagophytum* with RAPD and ISSR markers provides evidence of introgression," *Hereditas*, vol. 151, no. 4-5, pp. 91–101, 2014.

[20] M. Muzila, M. P. Setshogo, and S. W. Mpoloka, "Multivariate analysis of *Harpagophytum* DC. Ex meisn (Pedaliaceae) based on fruit characters," *International Journal of Biodiversity and Conservation*, vol. 3, no. 3, pp. 101–109, 2011.

[21] V. L. Singleton, R. Orthofer, and R. M. Lamuela-Raventós, "Analysis of total phenols and other oxidation substrates and antioxidants by means of folin-ciocalteu reagent," *Methods in Enzymology*, vol. 299, pp. 152–178, 1999.

[22] I. F. F. Benzie and J. J. Strain, "The ferric reducing ability of plasma (FRAP) as a measure of "antioxidant power": the FRAP assay," *Analytical Biochemistry*, vol. 239, no. 1, pp. 70–76, 1996.

[23] A. Medina-Remón, A. Barrionuevo-González, R. Zamora-Ros et al., "Rapid Folin-Ciocalteu method using microtiter 96-well plate cartridges for solid phase extraction to assess urinary total phenolic compounds, as a biomarker of total polyphenols intake," *Analytica Chimica Acta*, vol. 634, no. 1, pp. 54–60, 2009.

[24] A. Karioti, E. Fani, F. F. Vincieri, and A. R. Bilia, "Analysis and stability of the constituents of *Curcuma longa* and *Harpagophytum procumbens* tinctures by HPLC-DAD and HPLC-ESI-MS," *Journal of Pharmaceutical and Biomedical Analysis*, vol. 55, no. 3, pp. 479–486, 2011.

[25] B. Ekwall, B. Ekwall, and M. Sjöström, "MEIC evaluation of acute systemic toxicity. Part VIII. Multivariate partial least squares evaluation, including the selection of a battery of cell line tests with a good prediction of human acute lethal peak blood concentration for 50 chemicals," *ATLA*, vol. 28, pp. 201–234, 2000.

[26] N. Sussman, M. Waltersheid, T. Butler, J. Kelly, J. Cali, and T. Riss, "The predictive nature of high-throughput toxicity screening; utilizing a human liver cell line, esearchers are able to identify toxic antihistamines," *Drug Discovery and Development*, vol. 5, pp. 71–72, 2002.

[27] J. B. Matthews, H. J. Wright, A. Roberts, N. Ling-Mountford, P. R. Cooper, and I. L. C. Chapple, "Neutrophil hyper-responsiveness in periodontitis," *Journal of Dental Research*, vol. 86, no. 8, pp. 718–722, 2007.

[28] K. Bergström and B. Åsman, "Luminol enhanced fc-receptor dependent chemiluminescence from peripheral PMN cells. A methodological study," *Scandinavian Journal of Clinical and Laboratory Investigation*, vol. 53, no. 2, pp. 171–177, 1993.

[29] A. Roberts, J. B. Matthews, S. S. Socransky, P. P. E. Freestone, P. H. Williams, and I. L. C. Chapple, "Stress and the periodontal diseases: effects of catecholamines on the growth of periodontal bacteria *in vitro*," *Oral Microbiology and Immunology*, vol. 17, no. 5, pp. 296–303, 2002.

[30] N. A. Ouitas and C. Heard, "Estimation of the relative antiinflammatory efficacies of six commercial preparations of *Harpagophytum procumbens* (Devil's Claw)," *Phytotherapy Research*, vol. 24, no. 3, pp. 333–338, 2010.

[31] J. Qi, N. Li, J.-H. Zhou, B.-Y. Yu, and S. X. Qiu, "Isolation and anti-inflammatory activity evaluation of triterpenoids and a monoterpenoid glycoside from *Harpagophytum procumbens*," *Planta Medica*, vol. 76, no. 16, pp. 1892–1896, 2010.

[32] M. Patel, A. Keshavarzian, V. Kottapalli, B. Badie, D. Winship, and J. Z. Fields, "Human neutrophil functions are inhibited *in vitro* by clinically relevant ethanol concentrations," *Alcoholism: Clinical and Experimental Research*, vol. 20, no. 2, pp. 275–283, 1996.

[33] K. Raddassi and J. J. Murray, "Ethanol increases superoxide anion production stimulated with 4β- phorbol 12-myristate 13-acetate in human polymorphonuclear leukocytes involvement of protein kinase C," *European Journal of Biochemistry*, vol. 267, no. 3, pp. 720–727, 2000.

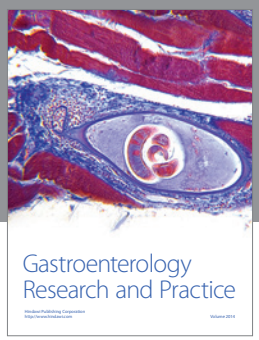

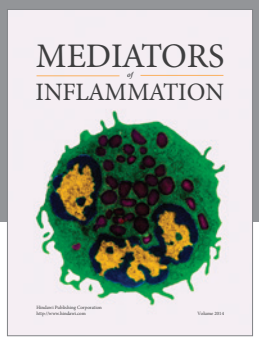

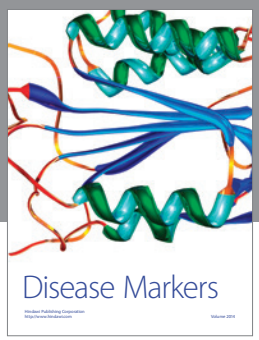

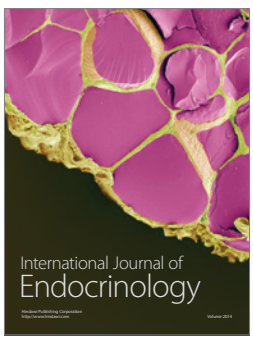

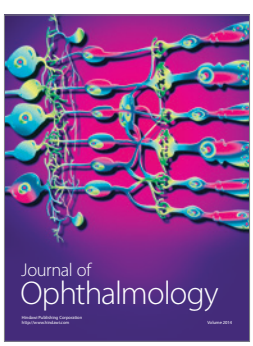

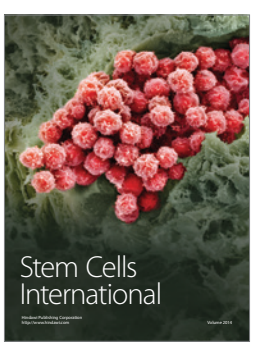

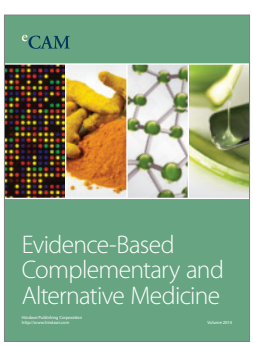

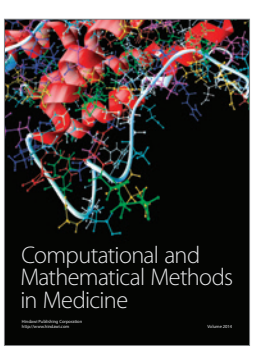

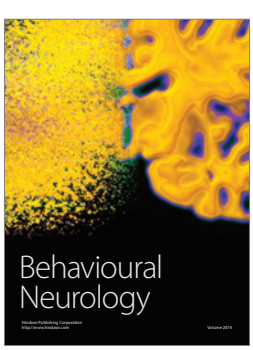

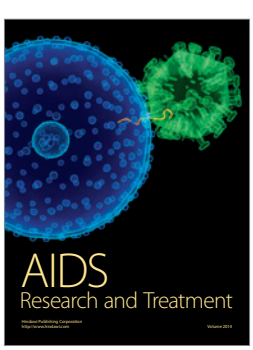

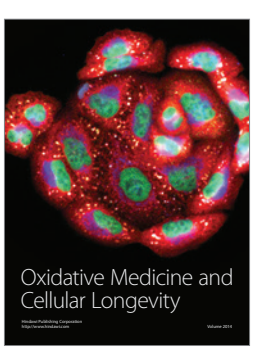

Hindawi

Submit your manuscripts at
http://www.hindawi.com